

A DYNAMIC MODEL OF AMMONIA PRODUCTION  
WITHIN GROW-FINISH SWINE BARNS

A Thesis Submitted to the College of  
Graduate Studies and Research  
In Partial Fulfillment of the Requirements  
For the Degree of Doctor of Philosophy  
In the Department of Agricultural and Bioresource Engineering  
University of Saskatchewan  
Saskatoon

By

ERIN LESLEY CORTUS

Keywords: ammonia, modelling, urine puddles, slurry, convective mass transfer, urease activity,  
urination frequency, model validation.

© Copyright Erin Lesley Cortus, December, 2006. All rights reserved.

## PERMISSION TO USE

In presenting this thesis in partial fulfilment of the requirements for a Postgraduate degree from the University of Saskatchewan, I agree that the Libraries of this University may make it freely available for inspection. I further agree that permission for copying of this thesis in any manner, in whole or in part, for scholarly purposes may be granted by the professor or professors who supervised my thesis work or, in their absence, by the Head of the Department or the Dean of the College in which my thesis work was done. It is understood that any copying or publication or use of this thesis or parts thereof for financial gain shall not be allowed without my written permission. It is also understood that due recognition shall be given to me and to the University of Saskatchewan in any scholarly use which may be made of any material in my thesis.

Requests for permission to copy or to make other use of material in this thesis in whole or part should be addressed to:

Head of the Department of Agricultural and Bioresource Engineering  
University of Saskatchewan  
Saskatoon, Saskatchewan S7N 5A9

## ABSTRACT

Ammonia is a nuisance gas in many swine barns. The overall objective of this research project was to model ammonia formation and transmission processes in a grower-finisher swine barn, by first modelling the ammonia production and emission from urine puddles on the floor surface and the ammonia emission from the slurry pit, and then incorporating these emission rates in a dynamic model that separates the room and slurry pit headspace as two separate, but linked, control volumes. A series of studies were conducted to gather more information about the processes affecting the ammonia emission rate from the floor surface and the slurry that were later included in the overall room model developed. The model was then used to investigate ammonia reducing techniques and technologies based on the understanding of ammonia production and transmission incorporated in the model.

The first step in modelling the ammonia emission rate from the floor surface was to determine the frequency of urinations by grower-finisher pigs. Male and female pigs were observed three times during their finishing phase to determine their urination frequency over the course of a day. The average measured urination frequency was  $0.62 \pm 0.11$  urinations  $\text{pig}^{-1} \text{h}^{-1}$ . A sinusoidal dromedary model was developed to describe the daily variation in urination frequency for male and female pigs between 51 and 78 kg.

In order for the deposited urinations on the floor surface to emit ammonia, the urea in the urine must first be converted to ammonia and the urease enzyme catalyzes this reaction. Two methods, a fixed-time-point method using the indophenol assay for ammonium-nitrogen analysis and a continuous method using the coupled enzyme assay, were used to measure enzyme activity at the floor surface of a swine barn and were compared to reported urease activity levels in the literature. Using both methods, there

appeared to be an ammonia-producing site on the floor surface or within the collected samples that made accurate measurements of urease activity impossible. A review of urease activity levels in the literature from dairy-cow houses suggest that urease activity will be lowest following floor-cleaning and increase quickly following fouling of the floor surface. Based on the literature review, a urease activity value of  $5 \text{ g NH}_3 \text{ m}^{-2} \text{ h}^{-1}$  was suggested for use in ammonia emission modelling of fouled floor surfaces in swine barns until better measurements become available.

The ammonia emissions from 36 simulated urine puddles under a variety of temperature, air velocity and initial urea concentration conditions were measured in a bench-scale experimental set-up. The measurements were used to calibrate and validate a dynamic, mechanistic, urine puddle emission model that considered the processes of evaporation, urea conversion, change in liquid concentration and puddle  $pH$  in order to simulate the amount of ammonia emitted from a puddle. Based on the correlation coefficients ( $R$ ) between measured and simulated values for water volume ( $R=0.99$ ), total ammoniacal nitrogen concentration ( $R=0.90$ ), and total emission ( $R=1.00$ ), along with five other statistical tests for each simulated variable, the model was deemed accurate. The measurements and simulations in this experiment showed the impact of puddle  $pH$ , urease activity and changing environmental conditions on the average puddle emission rate. Puddle emission continued to occur as long as there was still water.

The impact of different slurry compositions on the ammonia emission rate from slurry pits was tested in another bench-scale experimental set-up with emission chambers. The emission chamber concentration data collected was used to calibrate and validate a developed slurry emission model. The collected slurry samples were concentrated

mixtures of urine and feces from individually-housed animals fed different diets. An empirical equation was developed to express the amount of total ammoniacal nitrogen in the slurry that was in the form of ammonia ( $f$ ) and thus volatile to the surroundings. Based on the empirical equation, the simulated value of  $f$  was between 0.03 and 0.08 and did not show the sensitivity to slurry  $pH$  that has been reported by other authors. The slurry emission model with the empirical equation for  $f$  was validated with ammonia emission measurements from eight different slurry samples and simulated hourly concentration measurements within 17% and five-day average concentration measurements within 3%. Further testing was recommended to ensure the model developed for concentrated manure in this study was applicable to the more dilute slurry found in swine barns.

Using the information gained in the previous experiments, a mechanistic model describing the dynamic ammonia concentration in the room and in the slurry channel headspace of grower-finisher swine barns, as well as the ammonia emitted to the surrounding environment was developed. Data was collected from two grower-finisher rooms to use as input data to the model and for calibration and validation purposes. The model calibration procedure determined that the amount of emissions originating from the slurry for the simulated room conditions was generally less than 5% of the total room emissions, the air exchange rate through the slatted floor was approximately 4% of the room ventilation rate, and that in the first two weeks of animal activity in a room the urease activity at the floor surface will increase. The model was validated using separate data from that used in the calibration process. The model simulated hourly room concentration levels within 2.2 ppm and 3-day average concentration levels within 1.6

ppm. The model simulations were more accurate for one room that was fed a typical grower-finisher diet compared to another room fed an experimental diet with lower protein content and sugar-beet pulp inclusion.

The dynamic model was tested for its sensitivity to various input factors in terms of the floor emission rate, slurry emission rate and total emission rate. An interesting aspect of the simulations was that increases in either floor or surface emission rate were compensated to a small extent by decreases in the other emission rate as a result of a reduced concentration gradient for mass transfer. The ammonia emission rate from the floor was most sensitive to changes in urease activity, fouled floor area and puddle area. The ammonia emission rate from slurry was most sensitive to changes in slurry *pH*. The impact of input variables on the total emission rate was dependant on the simulated proportion of the total ammonia emission coming from either the floor surface or slurry channel. Three ammonia reduction techniques were tested and evaluated on their impact to the total ammonia emission rate from a room compared to a given set of control conditions.

The work in this thesis highlighted the importance of ammonia emission from the floor surface. The proportion of ammonia originating from the slurry and from the floor surface respectively will vary on the specific conditions within the barn, and will impact the effect of any ammonia mitigation technique that is investigated or used.

## ACKNOWLEDGMENTS

I am sincerely grateful to the help and encouragement I received from Dr. Stéphane Lemay. He encourages the best in people by demonstrating not only his love of science and engineering, but also his compassion for everyone. I am also thankful for the wisdom and insights from Dr. Ernie Barber who always looked at the big picture. The interest, comments and hours spent reviewing the drafts of this thesis by Dr. Gordon Hill, Dr. Huiqing Guo, Dr. Oon-doo Baik and Dr. Trever Crowe are also appreciated. Thank you to Dr. Arogo for serving as the external examiner during my defence.

I value all the friends I have made in the office and in the barn of the Prairie Swine Centre (PSCI), and the opportunity to participate in research outside the normal engineering realm. I am also indebted to the researchers, technicians and staff of the Research and Development Institute for the Agri-environment (IRDA) in Deschambault, Quebec for making my stay there rewarding. Mr. Rob Fengler was of great assistance in collecting data throughout my research program. My thanks also go to Mr. Michel Payeur, Ms. Laura Smith, Dr. Harold Gonyou and Dr. Bernardo Predicala (PSCI), and Dr. Renato de Freitas (Soil Science Department, University of Saskatchewan) and Dr. Stéphane Godbout (IRDA) for their assistance in the various projects.

Finally, and most importantly, thank you to Scott, Mom, Dad, Deanna, Taryn, Derek, the Cortus', and the rest of my family and friends for encouraging me through this doctorate program and always.

# TABLE OF CONTENTS

	page
PERMISSION TO USE .....	i
ABSTRACT .....	ii
ACKNOWLEDGMENTS .....	vi
LIST OF FIGURES .....	xii
LIST OF TABLES .....	xvi
NOTATION .....	xviii
CHAPTER 1: GENERAL INTRODUCTION .....	1
1.1 Problem Definition.....	1
1.2 Background.....	2
1.2.1 Ammonia.....	2
1.2.2 Ammonia Formation and Emission within Swine Barns.....	4
1.2.2.1 Ammonia formation in urine puddles.....	6
1.2.2.2 Ammonia formation in slurry .....	8
1.2.2.3 Ammonia partitioning in the liquid and gas phases.....	9
1.2.2.4 Ammonia volatilization .....	11
1.2.3 Ammonia Concentration and Emission Measurements .....	15
1.2.3.1 Ammonia emission measurements .....	17
1.2.3.2 Ammonia concentration measurements.....	18
1.2.4 Effects of Ammonia .....	18
1.2.4.1 Human health effects of ammonia .....	18
1.2.4.2 Animal health and productivity .....	20
1.2.4.3 Environmental health and public perception .....	21
1.3 Modelling Ammonia Formation and Emission Within Livestock Buildings .....	22
1.3.1 Modelling in General .....	22
1.3.2 Source Emission Models.....	24
1.3.3 Overall Room Models.....	25
1.3.4 Summary of Developed Models.....	27
1.4 Ammonia Mitigation.....	29
1.4.1 Altered Diet Composition .....	29
1.4.2 Pit Additives.....	31
1.4.3 Floor Area and Floor Type.....	32
1.4.4 Washing and Scraping .....	33
1.4.5 Oil Sprinkling.....	33
1.4.6 Pit Ventilation .....	35
1.5 Current Study .....	35
1.5.1 Hypotheses .....	35
1.5.2 Objectives.....	38
1.5.3 Outline of Thesis .....	39



CHAPTER 2: MEASURING AND SIMULATING THE URINATION FREQUENCY OF GROWER-FINISHER PIGS .....	40
Synopsis .....	40
2.1 Introduction.....	41
2.2 Materials and Method .....	41
2.3 Results and Discussion .....	43
2.4 Summary .....	46
Acknowledgements .....	46
CHAPTER 3: MEASURING UREASE ACTIVITY AND AMMONIA PRODUCTION AT THE FLOOR SURFACE IN A SWINE BARN .....	48
Synopsis .....	48
3.1 Introduction.....	49
3.2 Materials and Method .....	51
3.2.1 Experimental Room and Apparatus .....	51
3.2.2 Sample Collection and Analysis - Fixed-Time-Point Method.....	53
3.2.3 Sample Collection and Analysis - Continuous Method .....	55
3.3 Results.....	58
3.3.1 Fixed-Time-Point Method.....	58
3.3.2 Continuous Method .....	59
3.3.3 Urease Activity Values in the Literature.....	65
3.4 Discussion .....	68
3.4.1 Fixed-Time-Point Assay Method.....	68
3.4.2 Continuous Assay Method .....	69
3.4.3 Effect of Time on Ammonia Production/Urease Activity .....	71
3.4.4 Effect of Location on Ammonia Production/Urease Activity.....	72
3.4.5 Recommendations .....	73
3.5 Summary .....	74
Acknowledgements .....	75
CHAPTER 4: A DYNAMIC, MECHANISTIC MODEL OF AMMONIA EMISSION FROM URINE PUDDLES .....	76
Synopsis .....	76
4.1 Introduction.....	77
4.2 Urine Puddle Model Development .....	79
4.2.1 Water Evaporation .....	79
4.2.2 Urea Degradation .....	81
4.2.3 Ammonia Concentration in the Puddle Solution .....	82
4.2.4 Molar Balance of Emission Chamber .....	84
4.2.5 Calculation Method.....	85
4.3 Materials and Method .....	86
4.3.1 Emission Chambers.....	86
4.3.2 Experimental Procedure .....	87
4.3.3 Calibration and Validation Procedure.....	90
4.4 General Results .....	90
4.4.1 Calibration Results.....	92
4.4.1.1 Water evaporation.....	92

4.4.1.2 Urea conversion .....	92
4.4.1.3 Urease activity .....	93
4.4.1.4 Puddle <i>pH</i> .....	96
4.4.1.5 Calibration summary.....	99
4.4.2 Validation Results .....	99
4.4.2.1 Water evaporation.....	101
4.4.2.2 Puddle <i>pH</i> .....	101
4.4.2.3 Liquid <i>TAN</i> concentration.....	101
4.4.2.4 Total emission.....	103
4.4.3 Model Application .....	103
4.5 Discussion .....	105
4.6 Summary .....	109
Acknowledgements .....	110
CHAPTER 5: MODELLING THE AMMONIA EMISSION FROM SLURRY BASED ON CHEMICAL AND PHYSICAL PROPERTIES .....	111
Synopsis .....	111
5.1 Introduction.....	112
5.2 Model Development.....	113
5.2.1 Convective Mass Transfer Coefficient.....	117
5.2.2 Ammonia Partitioning in the Liquid .....	118
5.2.3 Ammonia Concentration in the Gas Film .....	120
5.2.4 Ammonia Concentration in the Slurry Channel Headspace .....	121
5.2.5 Model Development Summary .....	122
5.3 Materials and Method .....	122
5.3.1 Slurry Collection .....	122
5.3.2 Emission Box Measurements.....	123
5.3.3 Experimental Procedure.....	125
5.3.4 Data Analysis .....	126
5.4 Results.....	127
5.4.1 Slurry Properties .....	127
5.4.2 Emission Box Ammonia Concentration Measurements .....	128
5.4.3 Model Calibration .....	129
5.4.4 Model Validation .....	131
5.4.5 Sensitivity Analysis.....	135
5.5 Discussion .....	136
5.6 Summary .....	138
Acknowledgements .....	139
CHAPTER 6: DYNAMIC SIMULATION OF THE AMMONIA CONCENTRATION WITHIN AND THE AMMONIA EMISSION FROM SWINE BARNS .....	140
Synopsis .....	140
6.1 Introduction.....	141
6.2 Model Development.....	142
6.2.1 Review of Existing Models.....	144
6.2.1.1 Urine puddle emission models.....	144
6.2.1.2 Slurry emission models.....	145

6.2.1.3 Overall room models.....	146
6.2.1.4 Summary of existing models and recommendations .....	147
6.2.2 Control Volume Approach.....	148
6.2.3 Urination Frequency and Location Sub-Model.....	151
6.2.4 Urine Puddle Emission sub-model.....	153
6.2.5 Slurry Emission Sub-Model.....	158
6.2.5.1 Calculating the volatile fraction ( $f_s$ ) of TAN in slurry .....	160
6.2.6 Input Values and Assumptions .....	162
6.2.6.1 Static variables.....	162
6.2.6.2 Dynamic variables .....	163
6.2.6.3 Puddle area and depth .....	163
6.2.6.4 Air velocity over the floor and slurry pit .....	165
6.2.6.5 Air exchange through the slatted floor.....	166
6.2.7 Calculation Method.....	167
6.3 Experimental Materials and Method.....	174
6.3.1 Experimental Rooms.....	174
6.3.2 Data Collection .....	175
6.3.3 Data Analysis Method.....	178
6.4 Results.....	180
6.4.1 Measurements .....	180
6.4.1.1 Environmental conditions .....	180
6.4.1.2 Slurry conditions.....	183
6.4.1.3 Room cleanliness .....	184
6.4.1.4 Ammonia concentration and emission measurements.....	185
6.4.2 Model Behaviour.....	187
6.4.2.1 Random number generators .....	187
6.4.2.2 Steady-state approximation.....	188
6.4.2.3 Slurry emission and pit ventilation rate .....	189
6.4.2.4 Puddle emission factors .....	191
6.4.3 Model Calibration .....	192
6.4.3.1 Modelling the slurry emission/pit ventilation rate .....	192
6.4.3.2 Modelling the emission rate from the floor surface.....	195
6.4.4 Model Validation .....	198
6.5 Discussion.....	204
6.5.1 Model Development.....	204
6.5.2 Measurements .....	204
6.5.3 Slurry Emission.....	206
6.5.4 Pit Ventilation Rate.....	206
6.5.5 Puddle Emission.....	207
6.5.6 Model Accuracy .....	208
6.6 Summary.....	209
Acknowledgments.....	211
 CHAPTER 7: EVALUATING THE IMPACT OF FACTORS ON THE AMMONIA EMISSION RATE FROM SWINE BARNS.....	 212
Synopsis .....	212
7.1 Introduction.....	213

7.2 Calculation Procedure.....	214
7.2.1 ACES Model.....	214
7.2.2 Common Test Conditions .....	218
7.2.3 Reduction Techniques.....	219
7.2.3.1 Scenario 1: Altered diet composition.....	219
7.2.3.2 Scenario 2: Specific dunging area.....	221
7.2.3.3 Scenario 3: Oil layer on the slurry surface.....	221
7.2.4 Method .....	222
7.3 Results.....	222
7.3.1 Mean Simulated Values .....	222
7.3.2 Impact of Input Factors .....	224
7.3.3 Scenarios .....	228
7.4 Discussion.....	229
7.4.1 Factors Affecting Ammonia Emission.....	229
7.4.2 Ammonia Reduction Techniques.....	232
7.5 Summary.....	235
Acknowledgements.....	236
CHAPTER 8: GENERAL DISCUSSION.....	237
Synopsis .....	237
8.1 Introduction.....	238
8.2 Ammonia Production and Emission at the Floor Surface.....	239
8.2.1 Animal Behaviour.....	240
8.2.2 Urease Activity.....	242
8.2.3 Environmental Conditions and Airflow Patterns .....	244
8.2.4 Fecal Matter and Building Materials .....	246
8.3 Ammonia Emission from the Slurry Pit.....	248
8.3.1 Slurry Composition.....	250
8.3.2 Airflow Patterns .....	252
8.4 Modelling Ammonia Production and Emission.....	255
8.5 Promising Ammonia Reduction Techniques and Technologies.....	257
8.6 Future Work .....	261
8.7 Final Conclusions.....	263
REFERENCES .....	265
APPENDIX A: MODEL EVALUATION PARAMETERS .....	275
APPENDIX B: USER MANUAL FOR ACES PROGRAM .....	276

## LIST OF FIGURES

<u>Figure</u>	<u>page</u>
Figure 1.1. Nitrogen chain for fattening pigs in housing with partially slatted floor and surface application of slurry. Percentages represent the distribution of the nitrogen taken in through the feed (adapted from Aarnink (1997)).	5
Figure 1.2. Concentration boundary layer ( $\delta C(L)$ ) development for fluid flow of velocity $v$ over a flat plate of length $L$ (adapted from Incropera and DeWitt, 1996).	12
Figure 1.3. Boundaries for the two-film theory (adapted from Ni, 1999).	13
Figure 1.4. Cross-sectional view of a partially-slatted grower-finisher house, employing a two-control volume approach to modelling the ammonia concentration and emission. Bold arrows represent contributions to the ammonia balance.	37
Figure 2.1. Variation in measured number of urinations per pig per hour over a 24-h period, and the simulated number of urinations per pig per hour using a sinusoidal dromedary model. Vertical bars indicate the SEM ( $0.11 \text{ urinations pig}^{-1} \text{ h}^{-1}$ ) of the average urination frequency for the time of day interval.	46
Figure 3.1. Layout of a partially slatted floor pen. The dashed-line squares indicate the different locations from where samples were collected.	52
Figure 3.2. Sampling apparatus for floor surface sample collection.	53
Figure 3.3. Ammonia production rate in urea solution and water for Locations 1-4. Enzyme activity is the calculated difference between the production rates in urea and water.	59
Figure 3.4. Calculated enzyme activity (based on equation 3.3) compared to the rated activity of standard enzyme solutions containing Jack Bean urease. ( $1 \text{ unit} = 1 \mu\text{mol } NH_3 \text{ min}^{-1}$ )	61
Figure 3.5. Sample absorbance curves as detected by a spectrophotometer, for standard enzyme solutions containing a dilution of Jack Bean urease and an enzyme solution sample collected from the barn floor surface, analysed with and without urea in the reagent mixture.	62
Figure 3.6. Ammonia production rate measurements for enzyme solutions analyzed with and without urea based on the number of days of animal activity. (Vertical bars indicate standard error).	64
Figure 3.7. Ammonia production rate measurements for enzyme solutions analyzed with and without urea based on the sampling location in a pen. (Vertical bars indicate standard error).	64
Figure 4.1. Urine puddle emission model experimental set-up.	85

Figure 4.2. Stainless steel emission chamber, anemometer, plate, balance and sampling tube, used as part of the ammonia emission testing apparatus. ....	87
Figure 4.3. Measured <i>TAN</i> concentration values for three repetitions of Treatment 2. ....	91
Figure 4.4. Fitted urease activity values based on elapsed time and temperature. ....	94
Figure 4.5. Measured and modelled <i>TAN</i> values of all calibration data sets using the developed urease activity model (eq. 4.19; $j = 0.225$ ). ....	96
Figure 4.6. Measured puddle <i>pH</i> over time for six of the twelve treatments. ....	97
Figure 4.7. Simulated and measured puddle characteristics for Treatment 5 (a) and Treatment 7 (b). ....	100
Figure 4.8. <i>NMSE</i> values for <i>TAN</i> simulations, shown based on treatment. ....	102
Figure 5.1. Cross-sectional diagram of a slurry pit showing the contributions of ammonia to the headspace concentration ( $C_H$ ) by incoming air from the room ( $C_R \cdot Q_H$ ) and emission from the slurry ( $E_S$ ), and removal of ammonia by air movement up through the slats ( $C_H \cdot Q_H$ ). .	114
Figure 5.2. Emission box, filled with slurry (a) and inside view (b). ....	123
Figure 5.3. Average ammonia concentration measured in the headspace of the emission boxes during the two trials. Vertical bars indicate the range of measured concentration values.	129
Figure 5.4. Simulated ammonia concentrations compared to measured values for Trial 1-slurry samples. ....	133
Figure 5.5. Fractional bias ( <i>FB</i> ) of the Lin- <i>pH</i> and Exp- <i>pH</i> Model simulations of box concentration as a function of <i>pH</i> . ....	134
Figure 5.6. Fractional bias ( <i>FB</i> ) of the Lin- <i>pH</i> and Exp- <i>pH</i> Model simulations of box concentration as a function of <i>TAN</i> . ....	134
Figure 6.1. Cross-sectional view of a partially-slatted floor room in a swine barn, with bold arrows representing ammonia addition and removal sites to the ammonia contained within Control Volume A (Room airspace) and Control Volume B (Slurry Pit Headspace). ....	149
Figure 6.2. Flowchart for ACES model. ....	169
Figure 6.3. Depth of slurry in the slurry pit based on time in the Control and Treatment (SBP) rooms. ....	183
Figure 6.4. Measured ammonia concentration levels at the exhaust and in the pit headspace over the course of the cycle for the Control and Treatment (SBP) rooms. ....	186
Figure 6.5. Total ammonia emission rates over the course of the cycle for the Control and Treatment (SBP) rooms. ....	187

Figure 6.6. An example of the relationship between slurry emission and pit ventilation rate for the given room emission ( $E_R$ ), slurry emission to pit ventilation rate ratio ( $E_s Q_h^{-1}$ ) and room ventilation rate ( $Q_R$ ). .....	190
Figure 6.7. The impact of initial urea concentration ( $U_0$ ), total volume of urine produced per pig per day ( $V_U$ ), potential urease activity ( $S_m'$ ) and the fouling factors for the slatted ( $r_{slat}$ ) and solid floors ( $r_{solid}$ ) on the total puddle emission rate from the slatted and solid floor areas. (* indicates the mean value) .....	192
Figure 6.8. Fraction values for the calibration data-sets ( $pH_S < 7.5$ ) and projected values ( $pH_S > 7.5$ ) based on slurry $pH$ using the four proposed $f_S$ -equations. ....	193
Figure 6.9. The fractional bias ( $FB$ ) between average simulated and measured puddle emission and room concentration, and bias based on the variance ( $FS$ ) in simulated and measured room concentration based on varying levels of fouled slatted floor area ( $r_{slat}$ ) .....	196
Figure 6.10. The fractional bias ( $FB$ ) between simulated and measured puddle emission for five data-sets using increasing levels of potential urease activity ( $S_m'$ , $g NH_3 m^{-2} h^{-1}$ ) in the puddle emission simulations. ....	198
Figure 6.11. Comparison of the three-day average simulated room and pit headspace ammonia concentration levels compared to the corresponding measured average. ....	201
Figure 6.12. Measured and simulated room and pit concentration values over three days during conditions with clean solid floors (a) and dirty solid floors in two of the six pens (b). ..	202
Figure 6.13. Average measured $E_s Q_h^{-1}$ values for the validation data-sets, and the corresponding simulated average using the input slurry surface $pH \pm 0.2$ units. ....	203
Figure 7.1. Cross-sectional view of a partially-slatted floor room in a swine barn, with bold arrows representing ammonia addition and removal sites to the ammonia contained within Control Volume A (Room airspace) and Control Volume B (Slurry Pit Headspace). ....	215
Figure 7.2. Simulated room concentration and emission levels under low and high ventilation rate situations. ....	223
Figure 7.3. Average floor emission and slurry emission rates for the four sets of conditions tested in winter and summer conditions. ....	228
Figure 8.1. An example graph showing the change in slurry emission (as a proportion of total emission) for varying levels of slurry $pH$ assuming all other variables constant. (Total puddle emission = $23 g NH_3-N d^{-1} AU^{-1}$ ). ....	249
Figure B.1. Simplified flowchart showing the parts of the program visible to the user in solid lines, and the program parts visible only to the designer in dashed lines. ....	277
Figure B.2. Program calculations within the ACES computer program. ....	278

Figure B.3. Main page of the ACES model.....	279
Figure B.4. Geometrical Factors input form.....	280
Figure B.5. Ventilation and room design selection form.....	281
Figure B.6. Environmental Factors input form.....	282
Figure B.7. Nutritional Factors input form.....	283
Figure B.8. Simulation Factors input form.....	284
Figure B.9. Concentration Simulations output form.....	285
Figure B.10. Emission Simulation output form.....	286



## LIST OF TABLES

<u>Table</u>	<u>page</u>
Table 1.1. Ammonia concentrations related to health problems .....	19
Table 2.1. Average urination frequencies for male and female pigs between 51 and 78 kg, based on the time of day. ....	44
Table 3.1. Description of criteria used to assign cleanliness scores to sampling locations in pig pens. ....	54
Table 3.2. Amount of reagents used in the Worthington Enzyme Assay (Worthington, 1995). ....	57
Table 3.3. Floor cleanliness scores for the 12 sampling locations after 0, 11 and 22 days of animal activity. ....	60
Table 3.4. Urease activity levels reported in the literature and their method of determination. ....	66
Table 4.1. Treatment combinations and identification. ....	88
Table 4.2. Comparison of average (n=24) evaluation parameters for $V_P$ , $pH$ , $TAN$ and total emission (mol $NH_3$ ). ....	101
Table 4.3. Urine puddle model results for varying environmental conditions. ....	104
Table 5.1. Slurry emission model comparison.....	116
Table 5.2. Measured slurry properties <sup>Z</sup> on Days 0 and 5 for the respective trials and treatments.....	128
Table 5.3. Average slurry properties and fraction ( $f$ ) values for Data-set 1 slurry samples.....	130
Table 5.4. "Lin- $pH$ Model" evaluation based on Data-set 2 slurry sample measurements. <i>Italicized</i> values are outside of the prescribed evaluation limits (ASTM, 2003).....	132
Table 5.5. "Exp- $pH$ Model" evaluation based on Data-set 2 slurry sample measurements. <i>Italicized</i> values are outside of the prescribed evaluation limits (ASTM, 2003).....	132
Table 5.6. Sensitivity of the Lin- $pH$ and Exp- $pH$ Models to the input variables. ....	135
Table 6.1. Area and depth of urine puddles on slatted floors of different design for pigs between 30 and 100 kg (Adapted from Aarnink et al. (1997) and Aarnink and Elzing (1998)).....	164

Table 6.2. ACES model computing process. ....	170
Table 6.3. Type, collection method and frequency of data collected. ....	177
Table 6.4. Weekly average temperature conditions at various locations within the Control and Treatment (SBP) rooms during the grow-finish cycle. ....	182
Table 6.5. Weekly average relative humidity and ventilation rate conditions during the grow-finish cycle for Control and Treatment (SBP) rooms. ....	182
Table 6.6. Slurry characteristics based on the week of measurement for the Control and Treatment (SBP) rooms. ....	184
Table 6.7. Qualitative solid floor conditions based on the week of measurement for the Control and Treatment (SBP) rooms. ....	185
Table 6.8. The impact of using the four proposed $f_S$ -equations on the range of calculated $f_S$ -values, the estimation of the pit ventilation rate ( $Q_H$ ) and the slurry emission rate ( $E_S$ ). ....	194
Table 6.9. ACES model evaluation for hourly and 3-day average simulated values compared to corresponding measured values, for room concentration, pit headspace concentration and $E_S Q_H^{-1}$ ratio. Bolded values are within the suggested evaluation limits. ( $n$ = number of measured value and simulated value data pairs). ....	200
Table 7.1. The input factors that directly impact the ammonia emission rate calculations for different production sites in a swine barn. ....	217
Table 7.2. Mean input values used in simulations with the ACES Model ....	219
Table 7.3. Simulated emission rates and concentration levels for varying input factors under winter ventilation conditions. ....	225
Table 7.4. Simulated emission rates and concentration levels for varying input factors under summer ventilation conditions. ....	226

## NOTATION

[ ]	Concentration, mol L <sup>-1</sup>
Ø	Diameter
$\rho$	Density, g L <sup>-1</sup>
$\kappa$	Diffusion coefficient through a surface layer film, m s <sup>-1</sup> (unless otherwise stated)
$\Delta$	Timestep, s
$\varphi$	Ion activity
$\nu$	Kinematic viscosity, m <sup>2</sup> s <sup>-1</sup>
$a$	Line of regression intercept
$A$	Area, m <sup>2</sup>
ADP	Adenosine diphosphate
$AN$	Total mass of nitrogen in ammonia form
$\Delta A_{340}$	Change in absorbance of 340 nm light
AU	Animal unit or 500 kg live mass
$b$	Line of regression slope
$C$	Ammonia concentration, mol L <sup>-1</sup> (unless otherwise stated)
$C_5H_6O_5$	$\alpha$ -ketoglutarate
$C_5H_9NO_4$	Glutamate
$CO_2$	Carbon dioxide
$CO_3^{2-}$	Carbonate
$CON_2H_4$	Urea
$COOHNH_2$	Carbamic acid
$d$	Depth, m
$D_{AB}$	Diffusivity of substance A in substance B, m <sup>2</sup> s <sup>-1</sup>
$df$	Degrees of freedom
$E$	Emission, mol s <sup>-1</sup> (unless otherwise stated)
$EC$	Electrical conductivity, mS cm <sup>-1</sup>
Exp- $pH$	Exponential $pH$ model
$f$	Proportion of $TAN$ ( $NH_3 + NH_4^+$ ) in the form of $NH_3$
$F_{A,B}$	Statistic describing the ratio of sample variances where $A$ is the $df$ for the numerator and $B$ is the $df$ for the denominator
$FB$	Bias based on the averages
$FS$	Bias based on the variances
function	Differential equation
$g$	Gravitational constant, m s <sup>-2</sup>
GLDH	Glutamate dehydrogenase enzyme
$h$	Calculation interval for Urine Puddle Emission Model, s
$H$	Henry's Law constant described as the dimensionless ratio of liquid concentration to gas concentration
$H'$	Henry's Law constant described as the ratio of gas partial pressure to liquid concentration, atm L mg <sup>-1</sup>
$H''$	Henry's Law constant described as the dimensionless ratio of gas concentration to liquid concentration

$H'''$	Henry's Law constant described as the ratio of liquid concentration to gas partial pressure
$H^+$	Hydrogen ion
$H_2CO_3$	Carbonic acid
$H_2O$	Water
$H_2SO_4$	Sulphuric acid
$HCO_3^-$	Hydrogen carbonate
HPC	High protein diet
HPSBP	High protein diet with sugar-beet pulp added
IDLH	Immediately dangerous to life and health
$j$	Urease activity regression coefficient
$J$	Jet momentum number
$k$	Convective mass transfer coefficient, $m\ s^{-1}$
$K$	Equilibrium constant for ammonia
$k'$	Convective mass transfer coefficient, units dependant on concentration gradient units
$K_a$	Acid ionization constant or dissociation constant for ammonium
$K_d$	Base ionization constant or association constant for ammonia
$K_m$	Michaelis constant, $mol\ L^{-1}$
$L$	Length, m
Lin- $pH$	Linear $pH$ model
LPC	Low protein diet
LPSBP	Low protein diet with sugar-beet pulp added
$m$	Amplitude of the animal activity curve
$M$	Animal weight, kg
$n$	Number of data points or data pairs used in a statistical analysis
$N$	Number or Nitrogen
$N_L$	Number of urination locations per pen, locations $pen^{-1}$
$N_P$	Number of puddles per floor area
$N_{Pigs}$	Number of pigs per pen, pigs $pen^{-1}$
$N_U$	Number of urinations per pen, urinations $pen^{-1}\ h^{-1}$
$N_{U,Avg}$	Average number of urinations per pig, urinations $pig^{-1}\ h^{-1}$
$N_{U,Obs}$	Number or urinations during an observation period, urinations $pen^{-1}\ (8\ min)^{-1}$
$N_{U,Pig}$	Number of urinations per pig, urinations $pig^{-1}\ h^{-1}$
$NAD^+$	Nicotinamide adenine dinucleotide
$NADH$	Nicotinamide adenine dinucleotide in reduced form
$NH_3$	Ammonia
$NH_3-N$	Total mass of nitrogen in ammonia form
$NH_4^+$	Ammonium
$NH_4-N$	Total mass of nitrogen in ammonia and ammonium forms
NMSE	Normalized mean square error
$OH^-$	Hydroxide ion
$P$	Static pressure, Pa
$P_{CO}$	Proportionality coefficient
$pH$	Negative log of the hydrogen ion concentration

$q$	pH change coefficient
$Q_H$	Air exchange rate between two airspaces, $\text{m}^3 \text{s}^{-1}$ for $Q_R$ and $Q_H$ , $\text{L s}^{-1}$ for $Q_B$
$r$	Portion of floor area covered in manure, %
$R$	Correlation coefficient
$R^2$	Square of the correlation coefficient
$Re$	Reynold's number
$RH$	Relative humidity, %
$RK$	Runge Kutta calculation
SBP	Sugar-beet pulp
$S_m$	Urease activity, $\text{mol U L}^{-1} \text{s}^{-1}$
$S_m'$	Urease activity of a floor surface, $\text{g NH}_3 \text{m}^{-2} \text{h}^{-1}$
$Sc$	Schmidt number
$SEM$	Standard error of the mean
STEL	Short-term exposure limit
$t$	Time, s (unless otherwise stated)
$T$	Temperature, K (except for $T_C$ or unless otherwise stated)
$TA$	Total mass of ammonia and ammonium
$TAN$	Total mass of nitrogen in ammonia and ammonium forms in solution, $\text{mol L}^{-1}$
$Time$	Hour of the day, h
TLV	Threshold limit value
TWA	Time-weighted average
$U$	Urea concentration, $\text{mol L}^{-1}$
$v$	Velocity, $\text{m s}^{-1}$
$V$	Volume, $\text{m}^3$ for $V_R$ and $V_H$ , L for $V_P$ , $V_U$ and $V_B$
$W$	Width, m
$x_{1...7}$	Regression variables
$y$	Height within boundary layer
$Z_{1,2}$	pH change regression coefficients

## Subscripts

$0$	Initial or boundary conditions
$A$	Atmosphere/surroundings
$air$	Air
$atm$	Atmospheric
$B$	Bulk gas above the emitting surface or emission chamber/box
$C$	Temperature expression in $^{\circ}\text{C}$
$cuv$	Reagent volume within a cuvette
$D$	Defecation or fecal material
$E$	Effective surface pH
$F$	Feed
$film$	Film temperature
$G$	Gas film above the liquid surface

<i>H</i>	Slurry pit headspace
<i>H<sup>+</sup></i>	Hydrogen ion
<i>H<sub>2</sub>O</i>	Water
<i>i</i>	Film interface
<i>inlet</i>	Inlet
<i>L</i>	Liquid
<i>M</i>	Building materials
<i>min</i>	Minimum
<i>NH<sub>3</sub></i>	Ammonia
<i>NH<sub>4</sub><sup>+</sup></i>	Ammonium
<i>OH<sup>-</sup></i>	Hydroxide ion
<i>P</i>	Urine Puddle
<i>Pen</i>	Pen of pigs
<i>Pigs</i>	Pigs
<i>Pit</i>	Slurry pit
<i>R</i>	Room airspace
<i>S</i>	Slurry
<i>sat</i>	Saturated air
<i>slat</i>	Slatted floor area per pen
<i>solid</i>	Solid floor area per pen
<i>t</i>	Time
<i>T</i>	Total
<i>U</i>	Urinations
<i>v</i>	Water vapour
<i>y</i>	Height within boundary layer

## CHAPTER 1 GENERAL INTRODUCTION

### 1.1 Problem Definition

Between 1995 and 2005, the Canadian hog industry nearly doubled the number of hogs marketed from 15.6 million to 31.0 million. In that same period, Saskatchewan increased the number of hogs marketed by 1.6 million so that Saskatchewan currently produces approximately 8% of the total hogs marketed in Canada (CPC, 2006). The increase in hogs marketed has been accompanied by an increase in the size of farms, but a decrease in the number of farms, both provincially and nationally (CPC, 2006). An increasing production level is generally indicative of a thriving industry, and the changes in farm size show that swine farming is becoming increasingly intensified and commercialized. Are the increasing production rate and changing production methods sustainable over the long-term provincially and nationally? Global competitiveness, social responsibility and environmental sustainability are commonly accepted as three criteria that production systems must satisfy to be recognized as sustainable. Many political, economical and environmental factors should be considered when discussing sustainability, but one inevitable aspect of swine production systems that currently impedes or threatens each criterion is ammonia ( $NH_3$ ).

Ammonia is a well-known gas in livestock barns that can be detrimental to the health of workers and affect the health and productivity of the animals. In the environment, high amounts of ammonia can lead to disruption of natural ecosystems and ammonia has also been recognised as a constituent of manure odour. The impacts of ammonia affect

the health and safety of workers, the cost of production, the public perception of swine barns, and also the health of the environment.

Therefore, reducing ammonia levels at the animal and worker level and ammonia emissions to the surrounding environment can help the swine industry become more sustainable, but only if the reduction methods are implemented with a positive economic impact. The overall goal of this work is to reduce the impact of ammonia on the health and safety of workers and, at the same time, improve animal health and productivity and reduce the impact of swine production on the surrounding environment by reducing ammonia production in swine barns. By creating a mathematical model to predict ammonia production and emission, potential reduction techniques can be identified, investigated and evaluated before full-scale testing or implementation occurs, resulting in time and cost-savings.

The objective of this chapter is to gather background information from the literature about ammonia gas, ammonia production within swine barns, ammonia emission and concentration levels for swine barns, and the resulting effects of ammonia gas on the workers, animals and surroundings. Existing models are reviewed, as are current ammonia reduction techniques. From the information in the literature, the hypotheses, objectives and contents of the current study are developed.

## **1.2 Background**

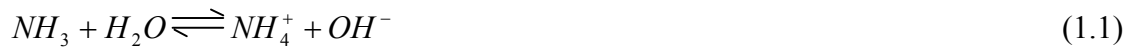
### **1.2.1 Ammonia**

Ammonia compounds consist of one nitrogen atom and three hydrogen atoms arranged in a tetrahedral fashion and with a molecular weight of 17.03 atomic mass units. At room temperature and standard atmospheric pressure, ammonia is a colourless gas with a pungent and irritating odour (CHEMINFO, 2000; Merck, 1983); the Merck Index



(1983) describes the odour as "characteristic of drying urine". The density of ammonia gas at 300 K is  $0.6894 \text{ kg m}^{-3}$ , and the density slowly decreases with increasing temperature (Incropera and DeWitt, 1996).

The nitrogen atom has a lone pair of electrons that makes the ammonia compound a weak base that partially ionizes in solution to form ammonium ( $NH_4^+$ ) and a hydroxide ion ( $OH^-$ ).



Ammonia and ammonium will co-exist in equilibrium in solution, according to the equilibrium constant for ammonia ( $K$ ), which expresses the ratio of activities of the components in the solution (Chang, 1998). The activity of an ion is approximated by the product of the concentration and an activity coefficient ( $\phi$ ; Arogo et al., 2003b).

$$K = \frac{\phi_{NH_4^+} \cdot [NH_4^+] \cdot \phi_{OH^-} \cdot [OH^-]}{\phi_{NH_3} \cdot [NH_3] \cdot [H_2O]} \quad (1.2)$$

Since the concentration of water will remain relatively constant throughout the ionization reaction, equation 1.2 can be modified to express the base ionization constant for ammonia (also referred to as the association constant; eq. 1.3), or the acid ionization constant for ammonium (also referred to as the dissociation constant; eq. 1.4) (Jayaweera and Mikkelsen, 1990). The  $K_b$  and  $K_a$  constants are expressions of the strength of a weak base and weak acid, respectively. For example, larger values of  $K_a$  are associated with stronger acids.

$$K_b = K \cdot [H_2O] = \frac{\phi_{NH_4^+} \cdot [NH_4^+] \cdot \phi_{OH^-} \cdot [OH^-]}{\phi_{NH_3} \cdot [NH_3]} \quad (1.3)$$

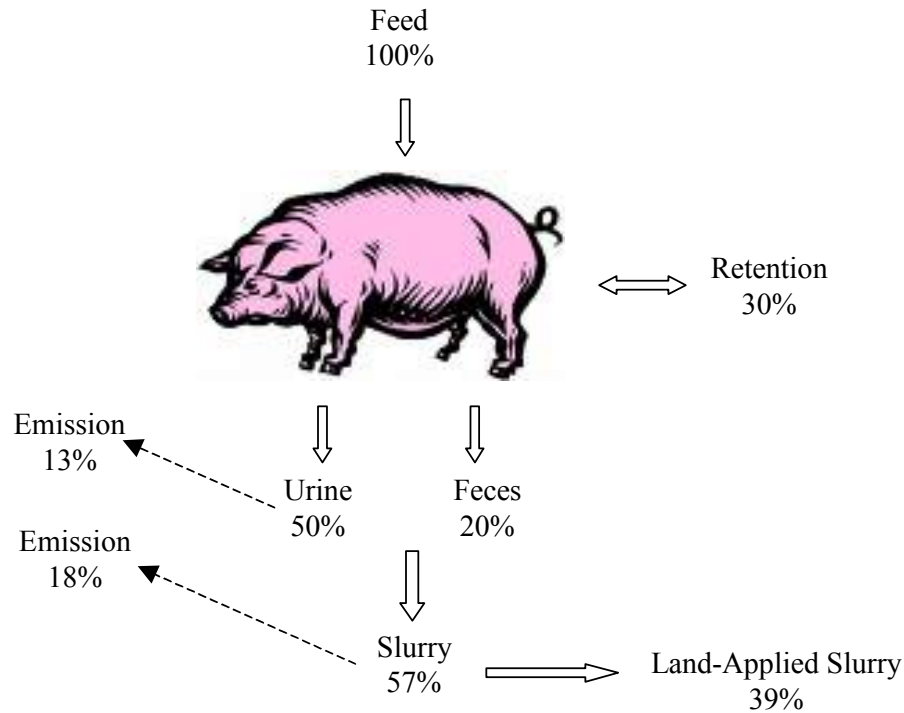
$$K_a = \frac{K}{[H_2O]} = \frac{\phi_{NH_3} \cdot [NH_3] \cdot \phi_{H^+} \cdot [H^+]}{\phi_{NH_4^+} \cdot [NH_4^+]} \quad (1.4)$$

The base ionization constant is  $1.8 \times 10^{-5}$  and the acid ionization constant for the conjugate acid ammonium is  $5.6 \times 10^{-10}$  (Chang, 1998). Activity coefficients are a function of the ionic strength of the solution (Arogo et al., 2003b); in a very dilute solution the activity coefficients are assumed equal to one so that equations 1.3 and 1.4 can be expressed solely in terms of concentration.

Ammonia concentration, in gas and aqueous solution, has been expressed using many different terms in the past. Ammonia, also referred to as free ammonia, is non-ionized ammonia ( $NH_3$ ); total ammonia ( $TA$ ) refers to the sum of the mass of the ammonia and ammonium ( $NH_3 + NH_4^+$ ). Ammoniacal nitrogen is the mass of the nitrogen nuclei of ammonia ( $AN$  or  $NH_3-N$ ), and total ammoniacal nitrogen is the sum of the mass of the nitrogen nuclei in the ammonia and ammonium molecules ( $TAN$  or  $NH_4-N$ ) (Ni, 1999). Conversion between the various forms involves the ratio of molecular weights for nitrogen by itself (14.01 amu) and ammonia (17.03 amu).

### **1.2.2 Ammonia Formation and Emission within Swine Barns**

As a nitrogen compound, ammonia plays an important role in the global nitrogen cycle and livestock facilities represent an anthropogenic (man-made) sink and source in the balance. Figure 1.1, adapted from Aarnink (1997), shows how a pig takes in nitrogen through feed and converts nitrogen to ammoniacal form to be installed back into the soil or air.



*pig image: pig.com.*

**Figure 1.1. Nitrogen chain for fattening pigs in housing with partially slatted floor and surface application of slurry. Percentages represent the distribution of the nitrogen taken in through the feed (adapted from Aarnink (1997)).**

While figure 1.1 only shows emission from urine and slurry, Arogo et al. (2003a) also list decomposing feces and feed on the floor within a barn as ammonia production sites.

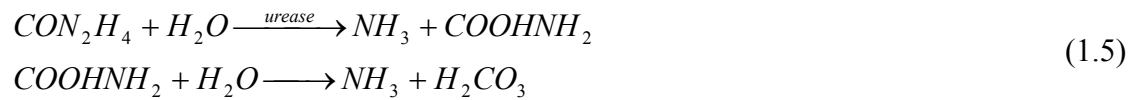
Various authors have examined the formation of ammonia from urine puddles and slurry, the two main ammonia sources identified in figure 1.1; no information on ammonia emission from faecal material was found in the literature. Once ammonia has been formed within a solution (urine or slurry), the process of ammonia volatilization is considered similar to that of any other ammonia solution (Ni, 1999).

Ammonia formation in the urine and slurry within swine buildings has been studied concurrently with ammonia formation in cattle housing. The similar fouling practices of

both types of livestock and similar manure handling methods allow ammonia production mechanisms to be interchanged between species.

### 1.2.2.1 Ammonia formation in urine puddles

Nitrogen released from protein and amino acid degradation is excreted as urea in the urine of mammals (Pond et al., 1990). The enzyme urease catalyzes the hydrolysis of urea ( $CON_2H_4$ ) to ammonia and carbamic acid ( $COOHNH_2$ ), which spontaneously hydrolyzes to form carbonic acid ( $H_2CO_3$ ) and another molecule of ammonia (Mobley and Hausinger, 1989), shown in equation 1.5.



Various bacteria, yeasts, fungi and algae produce urease (Mobley and Hausinger, 1989), including micro-organisms in the feces (Muck, 1982). Braam et al. (1997a) also suggest urease is found in digestive tract salts. Nickel is a cofactor for urease (Mobley and Hausinger, 1989).

Muck (1982) found the urea conversion in a 2.2:1 mixture of feces and urine could be modelled by the Michaelis-Menten equation (eq. 1.6), which was then incorporated by Muck and Steenhuis (1981) in a model to describe ammonia emission from urine puddles in the alley of a free-stall dairy barn. Elzing and Monteny (1997b) also applied equation 1.6 to urine and urine/feces mixtures applied to a fouled slatted floor.

$$\frac{dU}{dt} = -\frac{S_m \cdot U}{K_m + U} \quad (1.6)$$

(NOTE: Urease activity of a floor surface,  $S_m'$  is often expressed on a  $g\ NH_3\ m^{-2}\ h^{-1}$  basis that can be converted to urease activity ( $S_m$ ), with units of  $mol\ U\ L^{-1}\ s^{-1}$ , by division with the solution depth (m) and some unit conversion).

The urease activity,  $S_m$ , is the maximum urea conversion rate at high substrate concentrations. Urease activity can be affected by temperature and  $pH$ , floor surface characteristics and number of days of fouling with feces and urine (Muck, 1982; Braam and Swierstra, 1999; Braam et al., 1997a). Enzyme activity for most enzymes increases with increasing temperature up to a certain limit, but past this limit, enzymes can become denatured (Shuler and Kargi, 2002). Each enzyme has an optimal  $pH$  as well. At other  $pH$  levels, changes can occur in the active site or three-dimensional shape of the enzyme (Shuler and Kargi, 2002). Muck (1982) found urease activity of bovine feces increased up to a temperature of 40°C, and was optimal between  $pH$  levels of 6.8 and 7.6. Aarnink and Elzing (1998) related urease activity to floor surface roughness, but from testing concrete samples with varying surface roughness and coating treatments, Braam and Swierstra (1999) concluded that high levels of urease activity were expected to develop on all floor types within a relatively short "fouling" periods (less than 15 days). Elzing and Monteny (1997a) found that the maximum rate of ammonia emission increased over the first seven days of repeated fouling of a slatted floor with urine and feces. The authors attributed this to increasing urease activity at the floor surface. After seven days, a steady maximum ammonia emission rate indicated that the urease activity or the amount of urease was not limiting to ammonia emission (Elzing and Monteny, 1997a). Braam et al. (1997a) determined that urease activity was limiting up to an activity level of  $2 \text{ g NH}_3 \text{ m}^{-2} \text{ h}^{-1}$ . Above this level of activity, an increase in urease activity resulted in very small increases in ammonia emission from a cubicle house for dairy cows. It is unclear from past research whether urease will develop to non-limiting activity levels on areas of concrete that are fouled intermittently over a growth cycle, such as the solid floor

in a pig pen. No references have been found that describe or account for ammonia contribution to solution by fecal material; the fecal material remains solely the enzyme source in the literature.

The Michaelis constant ( $K_m$ ) in equation 1.6 represents the enzyme's affinity for the substrate (Shuler and Kargi, 2002). A small  $K_m$  value relative to the urea concentration corresponds to a high affinity. Elzing and Monteny (1997b) experimentally determined a  $K_m$  value of 0.002 mol L<sup>-1</sup>.

As ammonia is produced within a urine puddle by urea degradation (2 moles of ammonia are produced for every mole of urea), ammonia is simultaneously emitted from the puddle. The resulting TAN balance of the puddle is represented by the differential equation 1.7 (Elzing and Monteny, 1997b).

$$\frac{dTAN}{dt} = -2 \cdot \left( \frac{-S_m \cdot U}{K_m + U} \right) - \frac{E_p}{V_p} \quad (1.7)$$

#### **1.2.2.2 Ammonia formation in slurry**

In a slurry pit, the environment for ammonia formation is quite different than for a urine puddle. The rate of addition of urine and feces is small compared to the whole slurry volume. The suggested methods of ammonia formation are degradation of fresh urine in the top layers, and anaerobic digestion in the bottom layers of the slurry.

Ammonia produced in the bottom layers could theoretically transfer to the surface layer by diffusion or gas bubbles; Zhang et al. (1994) speculate that the dominant transfer mechanism for ammonia is diffusion because of its high solubility in water. Ammonia formation rates within the slurry have thus far been based on regression equations from experimental data (Zhang et al., 1994). From computer simulations, Zhang et al. (1994) found that in the bottom layers of a slurry channel, the generation of ammonia was faster

than the simulated diffusion so the simulated *TAN* concentration in the slurry increased. In the top layers, the concentration remained more stable, indicating the ammonia production by urea decomposition and ammonia from diffusion were equal or greater than the ammonia emission. Other authors have assumed the total ammoniacal nitrogen homogeneous throughout the slurry (Aarnink and Elzing, 1998).

Many other gases are formed in the slurry during storage including methane, carbon dioxide and hydrogen sulphide. The relationships between these compounds in the solution and at the slurry surface are suspected of affecting one another, most likely by affecting the *pH* of the solution (Sommer and Husted, 1995; Aarnink and Elzing, 1998; Ni et al., 2000b).

### **1.2.2.3 Ammonia partitioning in the liquid and gas phases**

As ammonia is produced within a solution (either urine or slurry), the ammonia will separate into the ammonia and ammonium forms, and the relative concentrations are dependant on the acid or base ionization constants (eq. 1.3 or eq. 1.4). Jayaweera and Mikkelsen (1990) developed equation 1.8 to express the temperature dependency of the acid ionization constant for ammonia in a water solution.

$$K_a = 10^{-\left(0.0897 + \frac{2729}{T+273}\right)} \quad (1.8)$$

The acid ionization constant for ammonium in pig manure with 1% total solids content was found to be one-fifth the  $K_a$ -value for ammonium in water (Zhang et al, 1994), and was one-sixth for concentrated chicken manure slurries with 3.5% to 8.5% total solids (Hashimoto and Ludington, 1971). Further work by Arogo et al. (2003b) showed a variation in the acid dissociation constant for ammonium in slurry based on temperature also. Based on these experiments, a factor is often combined with the known  $K_a$  for

ammonium in water (eq. 1.8) to express the  $K_a$  for ammonium in slurry. The factor could be interpreted as a representation of the relative activities and it is speculated that the factor is related to the solids content of the slurry. The factors that have been used include 0.17 (Hashimoto and Ludington, 1971), 0.2 (Zhang et al., 1994), 0.50 (Liang et al., 2002) and 0.5 to 0.95 (Arogo et al., 2003b).

Ammonia is released as a gas to the surroundings whereas ammonium is not. It is often desirable to express this free ammonia ( $NH_3$ ) as a proportion ( $f$ ) of the total ammonia ( $NH_3 + NH_4^+$ ) since the  $TAN$  concentration of a solution can be measured using various techniques. Zhang et al. (1994) calculated  $f$  by rearranging equation 1.4 and substituting equation 1.8 with a factor of 0.2 to achieve an expression based on  $pH$  and temperature only (eq. 1.9). The denominator in equation 1.9 shows the inverse value of  $K_a$  multiplied by the factor 0.2.

$$f = \frac{10^{pH}}{10^{pH} + 5 \cdot 10^{\left(0.0897 + \frac{2729}{T+273}\right)}} \quad (1.9)$$

Based on equation 1.9 the fraction of ammonia to  $TAN$  will increase exponentially with increasing  $pH$ .

Ammonia in solution will also partition between the liquid and gas phases, and the ratio of concentrations is described using the Henry's Law constant. Treybal (1980) applies Henry's Law to  $TAN$  concentrations in water below  $3.2 \text{ mol L}^{-1}$  at  $10^\circ\text{C}$  and  $2.0 \text{ mol L}^{-1}$  at  $30^\circ\text{C}$ . Outside of this range, Henry's Law and the related constant may not accurately describe the relationship between the gas and liquid phase concentrations because of chemical interaction between ammonia and the liquid or dissociation effects in the solution (Treybal, 1980). As shown by Ni (1999), numerous equations have been



developed to express the Henry's law constant for ammonia, either as the dimensionless ratio of ammonia concentration in the liquid compared to the gas ( $H$ ), the ratio of partial pressure to liquid concentration ( $H'$ ) or the dimensionless ratio of gas concentration to liquid concentration ( $H''$ ). Ni (1999) recommends using a Henry's Law constant that expresses the dimensionless ratio of ammonia concentration in the liquid to the ammonia concentration in the gas layer, similar to the equation developed for swine house slurry emission models by Aarnink and Elzing (1998; eq. 1.10), because the ammonia concentration in the surrounding air is generally expressed as a concentration rather than a partial pressure.

$$H = \frac{C_L}{C_G} = 1431 \cdot 1.053^{(293-T_{film})} \quad (1.10)$$

#### 1.2.2.4 Ammonia volatilization

In both urine puddles and slurry, ammonia at high concentrations in solution will move to an area of lower concentration in order to attain a form of equilibrium. Convective mass transfer is assumed to be the dominant transfer mechanism for most agricultural ammonia sources (Ni, 1999). Equation 1.11 describes the mass transfer process from the concentrated surface of a urine puddle or slurry to the bulk gas phase. The concentration in the gas film immediately above the puddle surface is estimated using the  $f$  variable and Henry constant ( $H$ ), described in the previous section (Zhang et al., 1994).

$$E = A \cdot k \cdot 1000 \cdot (C_G - C_B) = A \cdot k \cdot 1000 \cdot \left( \frac{f \cdot TAN}{H} - C_B \right) \quad (1.11)$$

The convective mass transfer process can be simulated using different assumptions and models. Ni (1999) found that most ammonia emission models employed the

Boundary Layer Theory or the Two-Film Theory in the development of theoretical mass transfer coefficients. Both theories describe the diffusion or conduction of ammonia through the thin liquid and/or gas films at the liquid surface. However, the mathematical representation is different.

The Boundary Layer Theory divides fluid flow past a surface into two regions: the bulk fluid flow region where viscosity can be neglected; and the very thin boundary layer region close to the surface where viscosity effects must be considered (Schlichting and Gersten, 2000). If the fluid flow in this boundary layer is laminar, transport of the solute is by molecular diffusion. As the fluid flow in the boundary layer increases and turbulence increases, packets of solute may be transferred across the streamlines by eddies (Welty et al., 1984). A concentration gradient will form close to the surface and is called the concentration boundary layer (Fig. 1.2).

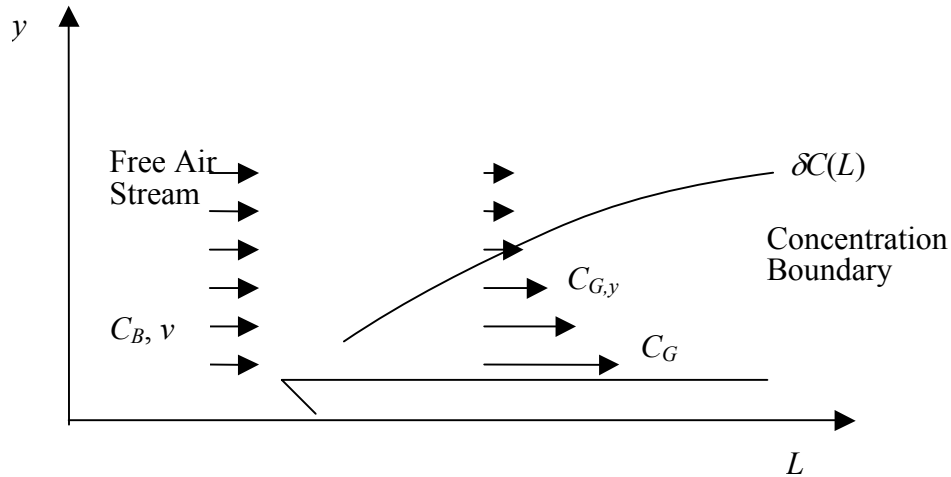


**Figure 1.2. Concentration boundary layer ( $\delta C(L)$ ) development for fluid flow of velocity  $v$  over a flat plate of length  $L$  (adapted from Incropera and DeWitt, 1996).**

At the boundary layer, equation 1.12 is satisfied:

$$\frac{(C_G - C_{G,y})}{(C_G - C_B)} = 0.99 \quad (1.12)$$

Incropera and DeWitt (1996) use numerical techniques to simultaneously solve the governing boundary layer equations describing the hydrodynamic conditions and the species conservation equation. For flow over a horizontal plate,  $k$  can be described by equation 1.13 for laminar flow and equation 1.14 for turbulent flow (Incropera and DeWitt, 1996).

$$k = \frac{D_{AB} \cdot 0.664 \cdot \text{Re}^{1/2} \cdot \text{Sc}^{1/3}}{L} \quad \text{when } \text{Sc} > 0.6. \quad (1.13)$$

$$k = \frac{D_{AB} \cdot 0.037 \cdot \text{Re}^{4/5} \cdot \text{Sc}^{1/3}}{L} \quad (1.14)$$

The second theory is the Two-Film (or two-resistance) Theory developed by Lewis and Whitman (1924). For transfer of material between two phases, there exists an interface between the gas and liquid films (figure 1.3).

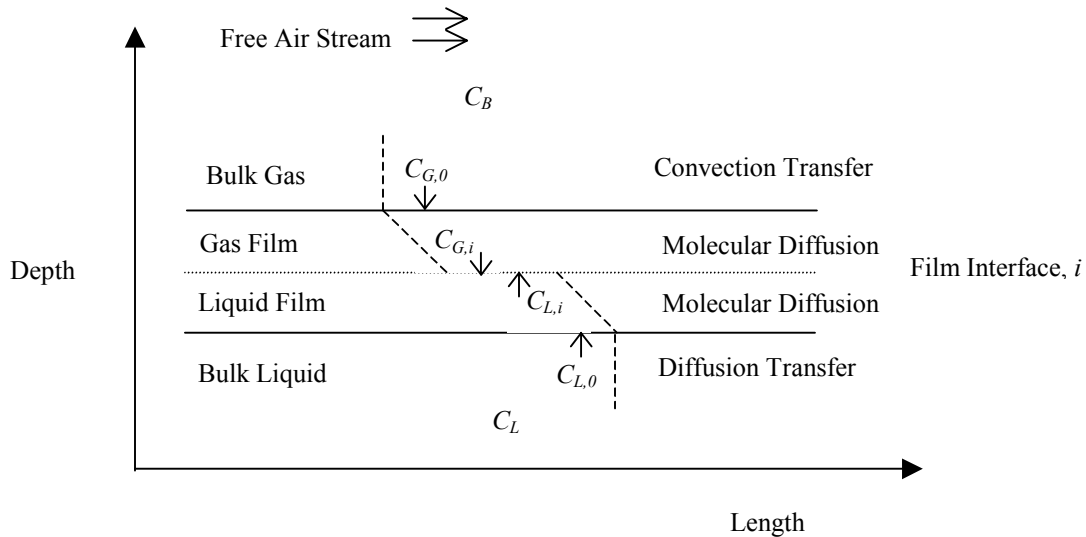


**Figure 1.3. Boundaries for the two-film theory (adapted from Ni, 1999).**

Both films are very thin and close to the surface, therefore they are not subjected to convection currents and the mass transfer across these films is by diffusion only. Each film resists the movement of solute, and the two films may be considered two diffusional

resistances in series (Lewis and Whitman, 1924). It is assumed the interface has no resistance. The overall mass transfer coefficient can be determined from the individual film coefficients ( $\kappa$ ). Equation 1.15 is designed for use with a concentration gradient between the gas and the liquid. The Henry's Law constant ( $H'''$ ) is incorporated in the mass transfer coefficient expression, negating the need for  $H$  in equation 1.11 for the surface gas concentration expression.

$$k' = \frac{\kappa_L \cdot \kappa_G}{H''' \cdot \kappa_L + \kappa_G} \quad (1.15)$$

(NOTE: The units of  $k'$  depend on the units used in the diffusion coefficients and in the concentration gradient. The  $k'$ -variable units can be converted to  $\text{m s}^{-1}$  so that  $k'$  can be used as an expression for  $k$ ).

Haslam et al. (1924) measured the effect of gas velocity and temperature on the rate of ammonia absorption by water. Based on measured mass transfer from gas to the water in a wetted wall type tower with no packing, at different air velocities ( $0.01$  to  $0.46 \text{ m s}^{-1}$ ) and temperatures ( $283$  to  $323 \text{ K}$ ), the following relationships were found for the gas film coefficient (eq. 1.16; units of  $\text{g h}^{-1} \text{ cm}^{-2} \text{ atm}^{-1}$ ) and the liquid film coefficient (eq. 1.17; units of  $\text{cm h}^{-1}$ ).

$$\kappa_G = 5.31 \cdot 10^3 \cdot 3.28 \cdot v^{0.8} T^{-1.4} \quad (1.16)$$

$$\kappa_L = 5.1 \cdot 10^{-7} T^4 \quad (1.17)$$

For gases that are highly soluble, such as ammonia, the liquid film offers very low resistance to solute movement so the mass transfer coefficient can be simplified to the diffusion coefficient through the gas film (Lewis and Whitman, 1924) only.

Ni (1999) reviewed various ammonia emission models for a variety of systems (i.e. swine barns, dairy barns, flooded rice fields) and found that models used a variety of different mass transfer coefficients, some based on calculated values from the theories presented, or experimentally determined mass transfer coefficients. The experimental values of  $k$  varied from  $11.7 \times 10^{-3}$  to  $1.3 \times 10^{-6} \text{ m s}^{-1}$ . From the experimental measurements, the mass transfer coefficient for ammonia was positively related to air velocity and temperature of air or manure. Muck and Steenhuis (1981), Elzing and Monteny (1997b), Aarnink and Elzing (1998) and Monteny et al. (1998) calculated the convective mass transfer coefficient based on the individual gas film diffusivity ( $\kappa_G$ ) from Haslam et al. (1924) (eq. 1.16) within their respective ammonia emission models. The partial pressure based mass transfer coefficient was converted to a concentration-based mass transfer coefficient with units of  $\text{m s}^{-1}$  using the Ideal Gas Law. However, Ni (1999) concluded that using the gas film coefficient as the overall mass transfer coefficient was inappropriate. This mass transfer coefficient has a negative relationship with temperature, which disagrees with measured coefficients (Ni, 1999). Haslam et al. (1924) suggested the negative relationship between the gas film coefficient and temperature was possible if the thickness of the gas film increased because of decreased density and increased viscosity at a faster rate than the specific diffusion rate per unit thickness increased.

### **1.2.3 Ammonia Concentration and Emission Measurements**

Figure 1.1 showed approximately 7% of the nitrogen consumed by a 55-kg pig was emitted to the atmosphere. This number is highly variable depending on many factors, including the size of animals, type of barn and production system, as will be discussed.

There are some key points that are important to consider when reviewing ammonia concentration and ammonia emission data:

1. Ammonia emission and ammonia concentration in the barn are dependant on each other, but each value is important on its own. The emission rate is calculated by multiplying the difference between the room and inlet concentrations by the ventilation rate of the room. Therefore, a room may have a high emission rate, but a low concentration because of a high ventilation rate;
2. Because the emission rate is a product of the concentration and ventilation rates, accurate measurement of both variables is important. Ventilation rate measurements can be especially difficult and there is no standard method to measure airflow rates in naturally-ventilated or mechanically-ventilated barns;
3. The concentration within large enclosed areas is generally considered homogeneous, and the measured ammonia concentration in the exhaust is considered the average room concentration (Aarnink et al., 1995). This assumption can lead to over or under-estimation of the actual ammonia concentration at various locations within an airspace; and
4. Emission rates can be described with various units, including mass per unit time per pig, mass per unit time per 500-kg live mass or animal unit (1 AU = 500 kg live mass), or mass per time per animal place or space (Arogo et al., 2003a).

### 1.2.3.1 Ammonia emission measurements

At least two studies have compiled extensive ammonia emission measurement data. Groot Koerkamp et al. (1998) measured ammonia emissions from 14 housing types for cattle, swine and poultry in England, the Netherlands, Denmark and Germany and found large variations between countries, between commercial houses and between seasons. In the five swine houses used in the study, average ammonia emission rates were between 13.2 and 64 g  $NH_3-N$  d<sup>-1</sup> AU<sup>-1</sup>. Larger emission rates were generally associated with housing for larger animals, such as sows and finisher pigs. Arogo et al. (2003a) reviewed ammonia emissions from swine buildings in the United States and found average emission rates ranging from 34 to 120 g  $NH_3-N$  d<sup>-1</sup> AU<sup>-1</sup> in finishing facilities with deep pit manure collection systems. Emission rates averaged between 4.7 and 19 g  $NH_3-N$  d<sup>-1</sup> AU<sup>-1</sup> for grower-finisher facilities with more frequent manure removal systems (i.e. pull-plug, flushed and pit recharge). The measurement method, climate and length of sampling differed between the various sources of emission data (Arogo et al., 2003a).

Ammonia emission patterns can vary over a cycle of animals, seasonally, and even diurnally. Aarnink et al. (1995) found the mean ammonia emission was 17 g  $NH_3-N$  d<sup>-1</sup> AU<sup>-1</sup> for rearing pigs (based on an average weight of 25 kg) and 26 g  $NH_3-N$  d<sup>-1</sup> AU<sup>-1</sup> (based on an average weight of 110 kg) for fattening pigs, both on partially slatted floors. The same study found a 56% higher emission rate during the summer for rearing pigs, but not for fattening pigs. During the night, ammonia emissions decreased 10% for piglets, and 7% for fatteners (Aarnink et al., 1995).

A wide variety of factors have been correlated with ammonia emission measurements and the variation in emission. Aarnink et al. (1996) and Ni et al. (1999c) found a significant impact of the fouled floor area of partially-slatted floor pens on ammonia

emissions. Aarnink and Wagemans (1997) found animal activity (animal movement) explained 44% of the daily variation in ammonia emission.

### **1.2.3.2 Ammonia concentration measurements**

In the study by Groot Koerkamp et al. (1998), average ammonia concentrations within the swine barns were between 5 and 18 ppm. Lim et al. (2004) measured ammonia concentrations in the room exhaust air based on different manure removal strategies between 5 and 17 ppm. Donham (2000) reported the typical range of ammonia concentrations within swine barns was between 5 and 20 ppm.

Various studies have shown that concentration levels can vary within a room. Wilhelm and McKinney (2001) measured higher ammonia concentration levels at the pit exhaust of a swine barn with pit ventilation compared to the room air. Aarnink and Wagemans (1997) showed that in rooms with partially slatted floors, the concentration above the slatted floor and solid floor areas could differ by over 10 ppm for certain ventilation configurations. Also, the average ammonia concentration in the slurry pit was higher than the concentration over the solid floor area, and similar or slightly lower than the concentration at animal level over the slatted floor.

### **1.2.4 Effects of Ammonia**

As shown in the literature, ammonia does exist in swine barns. The following section describes some of the associated effects of ammonia as an air contaminant in the barn, and in the air emitted to the surrounding environment.

#### **1.2.4.1 Human health effects of ammonia**

The human health effects of exposure to ammonia gas have been quantified with threshold limit values (TLVs) such as the TLV time-weighted average (TLV-TWA), the TLV short-term exposure limit (TLV-STEL) and the TLV immediately dangerous to life



and health (TLV-IDLH). The TLVs shown in Table 1.1 are based on irritation effects (ACGIH, 2000). The nose and throat are often the first organs to experience irritation. Eye tearing can happen at 134 ppm when in contact with the gas for less than 5 min (CHEMINFO, 2000).

**Table 1.1. Ammonia concentrations related to health problems**

<b>Limit</b>	<b>Definition</b>	<b>Concentration (ppm)</b>	<b>Source</b>
Mean Odour Threshold	Concentration at which odour is first detected.	17	CHEMINFO (2000)
TLV-TWA	Time weighted average concentration for a conventional 8-hr per day, 5 days per week work period, to which the worker may be repeatedly exposed with no adverse effects.	25	ACGIH (2000)
TLV-STEL	A 15-min TWA exposure that should not be exceeded at any time during a workday.	35	ACGIH (2000)
TLV-IDLH	Concentration that is immediately dangerous to life and health.	300	CHEMINFO (2000)

Donham et al. (1995) found a correlation between decreases in pulmonary function and increased ammonia levels, among other barn air constituents like total dust, respirable dust, and endotoxins, for swine production facility workers. The symptoms increased with the number of years spent working in the barn environment. Dust and ammonia were the strongest factors related to decreases in pulmonary function over a work period. Because a swine barn environment includes the combined effects of many gases, dust and endotoxins, it is possible the ammonia TLVs for swine barns are affected by other components. Donham (2000) recommended a maximum concentration limit of 7 ppm for swine barn workers.

Mackie et al. (1998) list ammonia and volatile amines as one of the four principal classes of odour compounds. However, odour is a nuisance or annoyance that does not have a universally accepted value for “offensive” or “objectionable” odour. Schiffman (1998) reports that livestock odours can potentially affect mood and memory, but the main health symptoms include eye, nose and throat irritation, headache and drowsiness.

#### **1.2.4.2 Animal health and productivity**

While it is difficult to ask an animal how it feels, different tests and productivity levels have indicated ammonia can negatively impact the health and productivity of a herd.

The common belief is that pigs have a higher tolerance threshold to ammonia than humans. Pigs may become acclimatized to the odour, but they are still affected by the gas. Jones et al. (1997) found that 30 to 100-kg pigs did not avoid areas with ammonia concentrations of 40 ppm, but would initially avoid areas with concentrations of 100 ppm, even with food motivation. Given the choice between 40-ppm compartments and 10-ppm compartments, more time was spent in the 10-ppm compartments, but the aversion to 40 ppm was not immediate which suggests a delayed sense of irritation was experienced. Thermal comfort and companionship were preferred to fresh air. Based on this study, Jones et al. (1997) recommended ammonia levels between 10 and 15 ppm to reduce the risk of infection. Donham (1991) associated cases of pneumonia, pleuritis and arthritis in swine with ammonia levels of 25 ppm, 29 ppm and 23 ppm, respectively. Donham (2000) suggested a maximum concentration of 11 ppm for swine health.

Maintaining low gas concentrations is not only important for the productivity of the animals, but also for the welfare of the animals. Webster (2001) includes "freedom from discomfort" and "freedom from pain, injury and disease" in the list of five freedoms for animal welfare.

#### **1.2.4.3 Environmental health and public perception**

Worldwide, intensive livestock operations and agricultural activities are the major sources for atmospheric ammonia (Krupa, 2003). The Netherlands, where stocking density is very high, have had to enforce strict regulations to reduce ammonia emissions to the environment. Canada has not yet experienced the drastic environmental effects as parts of Europe have (Agriculture and Agri-Food Canada, 1998). In the atmosphere, ammonia is generally removed by diffusion within 4 to 5 km from the source (Krupa, 2003); however, ammonium salt particles formed from atmospheric ammonia and acids such as sulfuric acid, nitric acid and nitrous acid have a longer residence time and can be deposited at greater distances (Krupa, 2003; Aneja et al., 2001).

Consequences of elevated concentrations and increased deposition of nitrogen species in the environment include nitrate contamination of drinking water, eutrophication, harmful algae blooms and decreased surface water quality, and climatic changes associated with nitrous oxide and nitrogen saturation of forest soils (Aneja et al., 2001). Ammonium in the soil may be taken up by the plants or converted to nitrate by nitrification, both processes resulting in soil acidification (Krupa, 2003). While nitrogen can be beneficial to the plant, it can be harmful if in excess. Native vegetation is most sensitive to excessively high ammonia uptake, followed by forests and agricultural crops; the most common effects are foliar injury, alterations in growth and productivity, alterations in drought, frost and pest tolerance and changes to ecosystem biodiversity (Krupa, 2003).

Public perception of the swine industry is generally impacted by the effects of ammonia outside the barn, rather than inside. Aside from the potential environmental impact, there is also a potential health impact on the neighbours of livestock facilities.

Schiffman (1998) suggests livestock odours can potentially cause sensory (eye, ear, nose, throat) irritation and affect mood and memory. Thu et al. (1997) assessed the physical and mental health of 18 people living within a two-mile radius of a 4000-sow swine production facility, compared to rural residents far removed from intensive livestock production. The swine barn neighbours reported significantly higher levels of respiratory symptoms but not a significant increase in mental health problems like depression or anxiety. In this study the health effects were not linked to ammonia in particular, but as a constituent of odour, ammonia could have been a contributor.

### **1.3 Modelling Ammonia Formation and Emission Within Livestock Buildings**

Ammonia can be a definite problem within and around swine barns. Numerous mitigation techniques have been developed to combat ammonia production and emission and these are discussed in the next section. At the core of solving the problem though, is understanding how ammonia is formed and transferred within parts of the barn.

Ammonia formation and emission processes have been identified, but it is when these mathematical descriptions are combined in models that they are more useful for predicting and exploring ammonia generation and transport.

#### **1.3.1 Modelling in General**

France (1988) defines a mathematical model as a set of equations that represent the behaviour of a system and can be classified with the following three criteria:

1. Static or dynamic: A static model does not contain the time variable, whereas a dynamic model includes time-dependency;
2. Deterministic or stochastic: A deterministic model makes definite predictions, whereas a stochastic model considers probability or random elements to predict the expected value and variance of a quantity; and

3. Empirical or mechanistic: An empirical model is designed to describe a result, whereas a mechanistic model is designed to describe the mechanisms leading to a result.

Modelling ammonia emissions from swine barns can provide a valuable tool for scientists, producers and neighbours regarding an intensive livestock operation. Arogo et al. (2003a) could not assign empirical ammonia emission factors to describe the average ammonia emission rate from various barns in the United States because of the wide range of environmental and production conditions affecting emissions, and the lack of long-term measurements. Because of the wide range of production systems, housing design, and manure systems, for example, mechanistic models that consider the processes behind ammonia production and emission are potentially more adaptable than empirical equations or emission factors for swine barn models. With a mechanistic model, scientists are able to describe the phenomenon of mass transport of ammonia, determine the factors that affect overall emission and investigate the effects of changing one or more parameters of a production system (for example, the diet composition or pen design). Also, an ammonia emission model can be used to demonstrate to neighbours and the public the impact a production system may have on them and their environment.

Many authors have investigated the process of ammonia production from the main individual sources (urine puddles and slurry) within swine barns to bring the knowledge to where it is today. The following source emission models and room models are not necessarily an exhaustive list of all models that have been developed, but they represent the development of mechanistic models that the current project has evolved from.

### 1.3.2 Source Emission Models

Muck and Steenhuis (1981) simulated ammonia loss from urine puddles in a free stall dairy barn on a solid floor. The ammonia loss was based on two processes: urea conversion and ammonia volatilization. The urea conversion was based on Michaelis-Menten kinetics as described previously. Validation of the model was completed with urea and ammonia measurements from urine puddles on the floor of a free-stall dairy barn. Chi-squared analysis of the measured and simulated urea and ammonia concentrations indicated the two processes were modelled well by the governing equations. The observed weakness of the model was that it under-predicted ammonia emission rates at low temperatures (5 to 15°C) (Muck and Steenhuis, 1981).

Zhang et al. (1994) developed a computer model for predicting ammonia release from manure pits in a swine building, which couples diffusion and generation within the slurry and ammonia volatilization from the surface. The finite element method was used to calculate the concentration in the various layers of the slurry channel while assuming all transfer within the slurry was by diffusion. Ammonia generation was related to depth of slurry and length of storage period. Ammonia was assumed to be released from the top layer by convective mass transport only. The model was created using measured results for ammonia generation and convective mass transfer, but the simulated results were not validated with measured results.

Elzing and Monteny (1997a, 1997b) measured the ammonia emission from fouled concrete slats in a bench-scale experiment designed to simulate the slatted floor area in a dairy-cow house. Similar to the model developed by Muck and Steenhuis (1981), the model tested in this study was also based on urea conversion to ammonia and convective mass transfer of the ammonia from the puddle surface. Elzing and Monteny (1997a,

1997b) measured and simulated the situations where urine and feces were mixed and applied to the slatted floor surface, and when feces was applied first, followed by urine. The ammonia emission measurements for both situations showed an initial increase in the ammonia emission rate over time, followed by a period of decreasing emission rate. The ammonia emission pattern was simulated "reasonably well" (Elzing and Monteny, 1997b) over a 24-h period, but only by altering the initial urease activity to a higher value than what had been measured.

Liang et al. (2002) followed a similar approach to that of Aarnink and Elzing (1998) when modelling ammonia emissions from a swine anaerobic lagoon and a slurry pit, respectively. The ammonia concentration of the slurry was considered an input to both models, and the emission was based on convective mass transport. The simulations by Liang et al. (2002) generally over-predicted the measured flux from swine anaerobic lagoons and further study into the dissociation constant for anaerobic lagoon liquid was suggested. The slurry pit emission model by Aarnink and Elzing (1998) was compared in conjunction with urine puddle emission calculations to overall room emission measurements.

### **1.3.3 Overall Room Models**

Monteny et al. (1998) and Aarnink and Elzing (1998) modelled ammonia emissions from dairy cow cubicle houses and grower-finisher pig rooms, respectively, but the modelling process was similar. In both models there was a floor module (total emission from all current urine puddles on the solid and slatted floor surface) and a slurry pit module. The emission for each source at each time interval was calculated and summed to create the total ammonia emission rate for the room. Monteny et al. (1998) used a constant urination frequency value found in the literature while Aarnink and Elzing

(1998) used video recordings to determine the number and location of urinations.

Ammonia formation in the urine puddles followed Michaelis-Menten kinetics, the balance of ammonia in the urine solutions was based on equation 1.7, and volatilization was by convective mass transfer. The ammonia concentration of the slurry was considered a measured input to the model (Aarnink and Elzing, 1998) or estimated from literature values (Monteny et al., 1998) and the slurry emission was based on convective mass transfer.

The model by Monteny et al. (1998) was designed for long-term simulations (i.e. one month) and on a monthly basis, estimated the total emission within  $\pm 7\%$  of measured levels. The short-term dynamics of the measured ammonia emission were not well simulated by the model. The model was most sensitive to changes in  $pH$ . Aarnink and Elzing (1998) simulated an ammonia emission rate of  $6.36 \text{ g d}^{-1} \text{ pig}^{-1}$ , with  $1.96 \text{ g d}^{-1} \text{ pig}^{-1}$  emitted from the floor and  $4.40 \text{ g d}^{-1} \text{ pig}^{-1}$  released from the slurry pit. The overall mean measured ammonia emission rate was  $6.84 \text{ g d}^{-1} \text{ pig}^{-1}$ . The percent difference between daily mean simulated and measured emission levels was  $-3.6\%$ , and the relative difference between 10-min simulations and measurements was  $19.1\%$ . The differences between measured and simulated values increased as emission levels increased. This model was also very sensitive to  $pH$ .

Ni et al. (2000c) simulated the ammonia emission from a fattening pig house using a dynamic, mechanistic model that also considered the effect of carbon dioxide release from the slurry. This model was designed for short-term simulations when the floor surface was relatively clean and the emission from puddles could be neglected. For a step-increase in ventilation rate, carbon dioxide emissions from a fattening house



increased immediately, followed by a slower rate of increase in ammonia emissions (Ni et al., 2000b). The hypothesis of the model was that carbon dioxide emission from the slurry increases immediately following an increase in the air velocity over the slurry (which was correlated to the ventilation rate) which results in an increase of the slurry *pH* over time, thus increasing the ammonia concentration at the surface of the slurry and the emission. This concept has been called "Carbon-dioxide Accelerated Ammonia Release" (Ni et al., 2000a, 2000b). Ni et al. (2000c) considered that only the portion of the full room volume where air was fully mixed (better-mixed zone) was involved in the ammonia mass balance, and the estimate of this better-mixed zone was only 20% of the total room volume. Comparisons between measured and simulated ammonia concentration and emission levels over 6 h resulted in  $R^2$  values of 0.861 and 0.947, respectively. A proportionality coefficient was introduced that integrated the dissociation constant, the Henry's Law constant and a *pH* change coefficient.

#### **1.3.4 Summary of Developed Models**

Important similarities and differences between the reviewed models were noted, as well as suggested areas for improvement within each model.

- Ni et al. (2000c) was the only model to consider the dynamic mass balance of ammonia in the room. As part of the dynamic mass balance, there was an estimate of the portion of the room volume involved in the mass balance. Monteny et al. (1998) and Aarnink and Elzing (1998) used steady state mass balances where the total emission was the sum of total puddle emission and total slurry emission. No full-room model considered the concentration of the room and the pit headspace as being significantly different, and therefore, either used the room concentration or neglected the bulk gas concentration in the convective mass transfer gradient for each emission

source. In all three models, the air exchange between the two regions was neglected. Monteny et al. (1998) suggested consideration of air exchange between the slurry pit and the inside air for short-term simulations. Aarnink and Elzing (1998) also suggested that a better understanding of climate and behavioural patterns affecting the air flow could help refine model calculations.

- The convective mass transfer process was used in each model. Monteny et al. (1998), Aarnink and Elzing (1998) and Muck and Steenhuis (1981) used the gas film mass transfer coefficient developed by Haslam et al. (1924). Zhang et al. (1994) and Ni et al. (2000c) used experimentally determined mass transfer coefficients.
- Slurry *pH* was an important factor in each model reviewed because the fraction (*f*) of available *TAN* was exponentially related to *pH*. Ni et al. (2000b, 2000c) concluded that ammonia release from slurry is a function of the dynamic behaviour of the *pH*, which is caused by the co-release of carbon dioxide. Slurry *pH* was not measured to compare with simulated results. Aarnink and Elzing (1998) suggested using an effective *pH* value 1.1 units higher than the *pH* of mixed slurry to account for the difference in carbon dioxide and ammonia emission rates from the surface and diffusion rates through the manure, but suggest further measurements to validate this value.
- Aarnink and Elzing (1998) also suggested determining the depth of urine puddles on the solid floor and for different degrees of fouling to improve model calculations.
- Absorption, adsorption and desorption of ammonia from various materials in the barn present other possible sources and sinks that are difficult to quantify, and were neglected in the ammonia emission models reviewed. Ammonia may absorb into

building materials, skin, hair, water particles or puddles and dust particles in the air, and release under appropriate conditions. Various odorous compounds can be trapped on dust particles (Hammond et al., 1979) and Hammond et al. (1981) conclude that odour is magnified when it is trapped on an aerosol particle.

- Model validation was significantly different in each study and in some cases, not completed. When model validation was performed, the method for evaluating agreement between measured and simulated results varied from a Chi-squared analysis (Muck and Steenhuis, 1981) to a correlation (Ni et al., 2000c) to a descriptive comparison (Elzing and Monteny, 1997b).

#### **1.4 Ammonia Mitigation**

As the understanding of the chemical and physical processes contributing to ammonia production and emission has evolved, many potential mitigation techniques were identified and in some instances tested. Some methods try to reduce ammonia formation from the various sources based on the understanding of ammonia formation, while others attempt to mask or reduce the transport of ammonia gas. A review of many of the current mitigation techniques aimed at reducing the ammonia concentration at the worker level is shown in this section. Methods that reduce ammonia emissions in the exhaust air, such as biofilters, and do not impact the room environment have been excluded. The intent of this section is to review these techniques in order to understand how they were expected to impact emission levels and whether implementing these techniques produced the expected results in terms of ammonia emission reduction.

##### **1.4.1 Altered Diet Composition**

The main entry of nitrogen into the pig house is via the feed. Nitrogen is then excreted as urea in urine, or bacterial proteins and undigested feed in the feces, the

former being more likely to immediately form ammonia. Many studies have examined methods to reduce the amount of urea excreted, including low protein diets and diets containing non-starch polysaccharides. Canh et al. (1998a) found that altering the crude protein level in a pig diet did not significantly affect the faecal nitrogen output. However, when dietary crude protein was reduced from 16.5% to 12.5% the urinary nitrogen was reduced by about 43%, slurry *TAN* concentrations decreased by approximately 43% and slurry *pH* decreased by 1 unit for individually housed pigs. For group-housed animals, the same reduction in crude protein in the diet resulted in a 38% reduction in slurry *TAN* concentration, and a 0.66 unit decrease in slurry *pH*. In both individually-housed animal trials and group-housed animal trials ammonia emission was reduced 10-12.5 for each percent decrease in crude protein level from the slurry and room, respectively.

Canh et al. (1997) found pigs fed diets with higher non-starch polysaccharides excreted less nitrogen in the urine and more in the feces, but the total nitrogen excreted was unchanged. The resulting slurry from these pigs had lower *pH* and ammonia emission levels, attributed to higher volatile fatty acid concentration (Canh et al., 1998b). Payeur (2003) found ammonia emissions from grower-finisher rooms were reduced by 42% when a diet containing both lower crude protein and added sugar-beet pulp was used.

Changes in diet formulation to include less protein and more non-starch polysaccharides can significantly change the cost of the diet and therefore it is important to know the benefits that a change in diet can have before the change is implemented.

### **1.4.2 Pit Additives**

Ammonia generation in the slurry is the result of a series of microbe-assisted reactions. Pit additives may be added to the slurry to reduce gas and odour by different mechanisms that can be grouped in the following categories: 1) masking agents; 2) counteractants; 3) digestive deodorants containing bacteria or enzymes; 4) adsorbents; and 5) chemical deodorants as strong oxidizing agents or germicides (Ritter, 1989, as shown in Zhu et al., 1997). Hendriks et al. (1998) monitored the emission from three grower-finisher compartments, with additive added to the slurry in one compartment. This particular additive was designed to create a matrix for bacteria to grow, feeding on nitrogen and lowering the ammonia release from the manure. This additive showed positive results, lowering ammonia emission by 19% to 57%, and lowering barn air concentrations by 20% to 58.5%. Ni et al. (1999a) tested the effect of a commercial manure additive on the ammonia emission from a large finishing barn. The ammonia emission rate per animal was reduced by 24.2% by using the additive compared to the control. Stinson et al. (1999) tested three additives with claimed biological, chemical and physical effects on slurry. Ammonia measurements showed high variability, but there was no significant difference between the ammonia given off of the control slurry, compared to ammonia emitted from treated manure.

Ni et al. (1999a) mention that the maximum total emission reduction would be governed by the percentage of total emission that originates from the slurry pit. Also, the method for pit additive evaluation differed between these three references. Hendriks et al. (1998) and Ni et al. (1999a) measured the ammonia emission from the room, whereas Stinson et al. (1999) measured the ammonia concentration in a portion of the

slurry channel. Zhu et al. (1997) suggested the development and success of pit additives is hindered by the lack of a standardized procedure for evaluation of different products.

#### **1.4.3 Floor Area and Floor Type**

Slatted floors are designed to remove urine and feces from the room into a storage area under the floor, separating an animal from its excrement and potentially resulting in a cleaner and more hygienic environment (Svennerstedt, 1999). A smaller slurry channel also reduces the surface area for ammonia volatilization. Aarnink et al. (1996) found that by reducing the area of slatted floor from 50% of the pen area to 25% of the pen area, the emission was reduced by 20% in a rearing room and 10% in a fattening room. However, the reduction was only significant in the rearing room, and Aarnink et al. (1996) found that the urine-fouled floor area for a 25% slatted floor was larger than for a 50% slatted floor. This increase in fouling was correlated to a significant increase in ammonia emissions.

The type of floor can affect the drainage properties of the slats. For concrete slats, a V-shape on the underside can reduce the risk of manure collection between the slats (Svennerstedt, 1999). Other materials, such as plastic and cast iron can be used as floor materials and odour and gas absorption may differ between materials as may the behaviour of animals on different flooring types. Pelletier et al. (2005) measured the ammonia emission over 24 h from common swine building materials that had been soaked in manure. The ammonia emission rates from concrete samples were higher than those for plastic, metal and wood materials. Aarnink et al. (1997) observed animals tended to have more difficulty walking on cast iron slatted floor and therefore soiled the solid floor more.

#### **1.4.4 Washing and Scraping**

Braam et al. (1997b) sprayed the solid floor surface of a cubicle dairy cow house with water after the floor had been scraped in an effort to reduce urine puddles on the floor. Ammonia emission was reduced up to 65% by spraying 6 L d<sup>-1</sup> cow<sup>-1</sup>. Washing theoretically increases the drainage of urine into the slurry pit, dilutes the urine present on the floor and also prevents attachment of feces to the floor surface. Braam and Swierstra (1999) suggest cleaning strategies can potentially reduce urease activity by removing or denaturing the enzyme source and thus reduce ammonia emission.

Braam et al. (1997a) found that a 3% floor slope (3-m span) was more effective at reducing ammonia emissions than scraping frequency in a cubicle dairy-cow house. Sloping floors and scraper systems theoretically decrease the puddle thickness, lowering emission, but also increase the puddle area, with the potential to increase emission. Braam et al. (1997a) found the decreased puddle thickness appeared to have a stronger effect than increased puddle area on ammonia emission using sloped floors and/or scrapers.

Many producers will add a layer of water in the bottom of the slurry pits prior to manure collection in order to reduce initial ammonia emissions from the slurry pit (Lim et al., 2004). No experimental verification could be found as to why this method seems to work, but it is suspected that the water layer dilutes the urine and feces that initially fall into the pit, reducing the concentration of ammonia in the slurry and thereby reducing ammonia emission.

#### **1.4.5 Oil Sprinkling**

Creating a barrier to ammonia diffusion and volatilization at the slurry surface has been the focus of research to reduce slurry pit emissions. Derikx and Aarnink (1993)

found that a thin layer of mineral or vegetable oil as a liquid top layer on the slurry inhibited diffusion of ammonia from the slurry to the gas phase, and achieved ammonia emission reductions up to 95%. The results were from a bench scale set-up with little or no airspeed, pig behaviour or building design influence. Pahl et al. (2000) also found ammonia reductions greater than 90% when a layer of oil was placed on the slurry surface in a small-scale set-up. Simulated rain and mixing seemed to increase the effectiveness of the oil layer by evenly distributing the oil. In a full-scale study, Pahl et al. (2000) found a reduced effectiveness of an oil layer applied through the slats when water was added to even the oil layer. The average ammonia reduction was 50%, but the best results occurred when the slurry pit was washed of residual slurry before oil application. If the slurry surface is uneven because of solid material floating on the liquid surface or inadequate liquid to cover the solid material, there is the potential for solid particles to build up on top of the oil, rendering it ineffective. Aarnink and Wagemans (1997) found that a thin layer of mineral oil on the surface of the slurry reduced ammonia emissions by about 31%, but attributed a reduced effect of the oil layer compared to previous research because sawdust mixed in with the oil layer may have affected the ability for urine to pass through the oil film.

Payeur (2003) investigated oil sprinkling on pen surfaces as a method to reduce ammonia concentrations and emissions. The hypothesis was that ammonia release from the slurry pit can be reduced by the thin layer of oil applied on a continuous basis, if the oil layer acts as a barrier to ammonia diffusion. Also, by reducing air-borne dust the ammonia adsorption by dust particles would also be suppressed improving the room air



quality. Payeur (2003) found that although oil sprinkling reduced dust emissions by 76%, ammonia emissions were not significantly reduced with this technique.

#### **1.4.6 Pit Ventilation**

Ventilation fans under the slatted floor have been employed to reduce air contamination in the room space. Pit ventilation is most beneficial in cold weather under minimum ventilation conditions (Wilhelm and McKinney, 2001). Wilhelm and McKinney (2001) found the ammonia levels in a barn with pit ventilation were more than 35% lower than a similar barn without pit ventilation during March and April. Lavoie et al. (1997) also found pit ventilation was able to significantly reduce ammonia concentrations in a farrowing room compared to a neighbouring farrowing room with conventional ventilation. Pit ventilation is a method to remove air contaminants before the gases enter the animal and worker zone, but does not necessarily reduce ammonia emissions to the environment.

### **1.5 Current Study**

#### **1.5.1 Hypotheses**

Ammonia is a well-documented gas that can be produced by the manure in livestock buildings. Knowledge of the ammonia concentration in the bulk room air and the overall ammonia emission from the room to the environment are very important values for the safety of the barn workers, the health and well-being of the pigs and the protection of the environment around the building. Modelling is a preliminary step in trying to understand the factors and processes that contribute to ammonia formation and transmission so that ammonia concentration and emission levels can be estimated based and reduction techniques can be developed with sound, scientifically-based methods.

The process of ammonia formation has been studied quite extensively, as has the ammonia volatilization process. However, ammonia is still one of the most common irritants in swine buildings despite the knowledge gained so far. There appears to be no reduction method or program that reduces ammonia efficiently and cost-effectively, and that is employed by a majority of producers. For modelling to be most effective, further quantification and verification of the individual emission sources is necessary so the relative effects of the floor surface and the slurry pit on the overall emission are better understood.

The hypothesis of this research is that ammonia emissions from a pig-housing unit can be modelled effectively by considering the ammonia emission sites within the room, the ammonia emission sites within the slurry pit and the various air exchanges that occur between the atmosphere, the room and the slurry pit headspace. Following the suggestion by Monteny et al. (1998), a two-control volume approach is proposed and is shown in figure 1.4 listing all possible ammonia emission sites including the slurry ( $E_S$ ), the urine puddles on the floor ( $E_{P,T}$ ), building materials ( $E_M$ ), the pigs ( $E_{Pig}$ ), decomposing feed on the floor ( $E_F$ ) and fecal matter on the floor ( $E_D$ ). From the molar balances of ammonia in each control volume (eqs. 1.18 and 1.19), the concentration and emission from each control volume can be determined with knowledge of the source emission rates and air exchange rates between areas. From the mechanistic model that describes the biological, chemical and physical processes occurring, various methods to reduce ammonia emissions can be investigated.

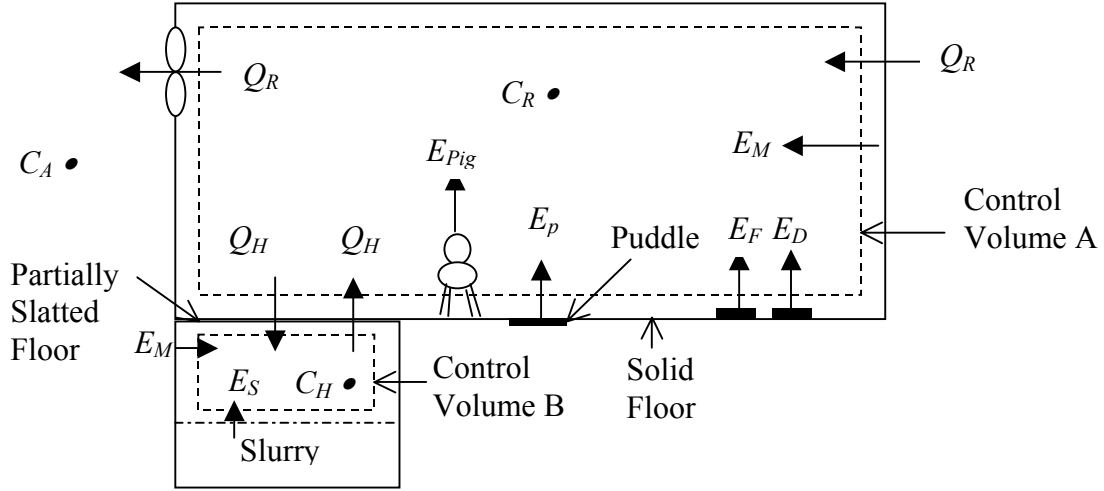


**Figure 1.4. Cross-sectional view of a partially-slatted grower-finisher house, employing a two-control volume approach to modelling the ammonia concentration and emission. Bold arrows represent contributions to the ammonia balance.**

$$V_R \cdot 1000 \cdot \frac{dC_R}{dt} = Q_R \cdot 1000 \cdot (C_A - C_R) + Q_H \cdot 1000 \cdot (C_H - C_R) + E_{P,T} + E_F + E_{Pig} + E_M + E_D \quad (1.18)$$

$$V_H \cdot 1000 \cdot \frac{dC_H}{dt} = Q_H \cdot 1000 \cdot (C_R - C_H) + E_S + E_M \quad (1.19)$$

Based on the literature reviewed, suggestions provided by previous authors and unanswered questions still remaining, certain parameters or estimations within equations 1.18 and 1.19 could be improved from previous models including:

- A prediction equation for the urination frequency of grower-finisher pigs and the location of urinations;
- Measured urease activity values for different floor surfaces within a swine barn, and a correlation with the amount of fouling;
- A puddle emission model that considers the effect of water evaporation;
- Validation of a slurry emission model with slurry of varying composition; and

- A dynamic, overall room model that considers the slurry channel and room area as two separate volumes, with the air exchange through the slatted floor connecting these two volumes.

### **1.5.2 Objectives**

The overall objective for the research project was to model the process of ammonia formation and transmission in a grower-finisher swine unit, considering the individual contributions of the slurry pit and urine puddles, and considering the room and slurry channel as two separate control volumes. The model was then used to test current and potential ammonia reduction techniques based on the factors and processes deemed most important by the model.

To complete the overall objectives, a series of specific objectives were created to solve the problem in parts. The specific objectives were:

- i. to develop a model to predict the urination frequency and location of urinations in a typical grower-finisher pen with a partially slatted floor based on observed behaviour;
- ii. to determine the quantity of urease on the floor surface of a partially-slatted floor swine barn;
- iii. to develop a model to simulate the biological, chemical and physical processes that occur in urine puddles and the resulting effect on ammonia volatilization from the puddles;
- iv. to develop a model to simulate the ammonia volatilization from slurry and validate with variable slurry sample measurements;

- v. to develop a model to predict the overall room and pit headspace ammonia concentrations, and the emission to the environment. This will include creating a computer program to perform the calculations;
- vi. to calibrate and validate the overall room and pit headspace ammonia concentration simulations with measurements from a partially-slatted floor swine barn;
- vii. to understand the impact of environmental factors and production parameters affecting ammonia emission; and
- viii. to investigate the effectiveness and reliability of various ammonia mitigation techniques based on model using simulations.

The developed model was to be dynamic and mechanistic in nature and designed to simulate the hourly emission and concentration levels for three-day periods.

### **1.5.3 Outline of Thesis**

Chapter 2 is a small-scale study of the urination frequency of grower-finisher pigs. Data collected from a grower-finisher room were used to develop a model to predict the diurnal urination frequency for a grower-finisher pig. Chapter 3 outlines measurements taken to assess the urease activity for the model barn used throughout this experiment. A literature review and analysis of reported urease activities is also given. Chapter 4 outlines a bench-scale study on the emission process from individual urine puddles. Chapter 5 focuses on the model development for the slurry emission model. Chapter 6 combines the information from Chapters 1 to 4 in the overall room model, called the Ammonia Concentration and Emission Simulation (ACES) model. Using the ACES model, Chapter 7 discusses different ammonia reduction techniques. Finally, a General Discussion highlights the important results of the entire study.

## CHAPTER 2 MEASURING AND SIMULATING THE URINATION FREQUENCY OF GROWER-FINISHER PIGS

E.L. Cortus<sup>1,2</sup>, H.W. Gonyou<sup>1,3</sup>, S.P. Lemay<sup>1,4</sup>, and E.M. Barber<sup>5</sup>

<sup>1</sup> *Prairie Swine Centre Inc., Saskatoon, SK;*

<sup>2</sup> *Department of Agricultural and Bioresource Engineering, University of Saskatchewan, Saskatoon, SK;*

<sup>3</sup> *Department of Animal and Poultry Science, University of Saskatchewan, Saskatoon, SK;*

<sup>4</sup> *Research and Development Institute in Agri-Environment, Deschambault, QC;*

<sup>5</sup> *College of Agriculture, University of Saskatchewan, Saskatoon, SK.*

Published as a short communication, Canadian Journal of Animal Science (2005) 85: 537-539.

### **Synopsis**

The first step in modelling ammonia production from urine puddles in a swine barn was to determine the number of urinations that were deposited over a 24-h period. Behavioural observations were undertaken and the resulting urination frequency data was incorporated in a dromedary model to enable simulations of the urination frequency for grower-finisher pigs based on the time of day. This chapter has been published as a short communication in the *Canadian Journal of Animal Science*, with the only difference being the notation used and headings added.

## **2.1 Introduction**

Ammonia emission models for swine barns with partially slatted floors depend on the location and frequency of urine puddles (Aarnink and Elzing, 1998). Aarnink et al. (1996) reported a significant positive relationship between urination frequency and ammonia emission for growing and finishing pigs in partially slatted climate-controlled rooms. However, the location and frequency of urine puddle deposition can only be measured by behavioural observations.

Aarnink et al. (1996) attribute 65% of the variation in urinating frequency to animal activity in fattening pigs. Animal activity is defined as moving animals and can be measured by human observations or infrared detectors (Pedersen and Pedersen, 1995). Commission Internationale du Génie Rural (CIGR, 2002) simulates animal activity by sinusoidal dromedary models and sinusoidal camel models for animal houses with one or two periods of maximum activity per day, respectively. Therefore, the objective of this paper is to create a prediction equation to describe urination frequency for male and female grower-finisher pigs, based on observed animal behaviour. Behaviour sampling was performed three times within one cycle of grower-finisher pigs and data were analyzed to examine the effect of gender, observation period and time of day. The urination frequency data were then incorporated in a dromedary model (CIGR, 2002).

## **2.2 Materials and Method**

We observed the urinating behaviour of male and female pigs in a mechanically ventilated room of a commercial barn with partially slatted floors (solid area: 2.4 m x 2.0 m; slatted area: 1.8 m x 2.0 m) during Fall 2001. Males and females were housed separately with three pens for each gender. Each pen started with 12 pigs, but one male and one female pig were removed from the trial before observations occurred, leaving

two pens with 11 animals. The animals had free access to nipple drinkers over the slatted floor portion. Feed was provided ad libitum according to NRC requirements (National Research Council, 1998) with dry feeders in a corner of the solid floor away from the slatted floor. During observation periods, room lighting (71 lx at pen level) was turned on and off at 0700 and 1900, respectively. From 1900h to 0700h, dim lighting (18 lx at pen level) helped observers to see urination events. All animals were weighed within one week of the start and end of the experiment and average pig weights for the measurement days were estimated by linear interpolation. Room temperature was recorded continuously by a datalogger, except for the first observation period when an instrument malfunction limited temperature data to only the final five hours of the period. Animals were otherwise managed according to guidelines provided by the Canadian Council on Animal Care.

The number of acts of urinating in each pen was measured by continuous behaviour sampling for 8 min every hour for 26 h (Martin and Bateson, 1993), starting at 1000h and ending at 1200h the following day. The six pens were observed once per hour, one at a time, by an observer sitting outside the pen at the solid floor end. Five observers were used over each 26-h period and each observer individually collected data over 6 h; the last hour of one observer and the first hour of the next observer coincided to check for differences between observers. We did not include the first two hours of each 26-h data set, which were intended to habituate the animals to the presence of the observers, in the analysis. The number of urinations per hour was calculated as:

$$N_{U,Pig} = \frac{7.5 \cdot N_{U,Obs}}{N_{Pigs}} \quad (2.1)$$



There was good correlation between observers based on the average urination frequencies reported for the four hours during each observation period when there were two observers individually recording the same events ( $n = 12$ ,  $R^2 = 0.93$ ).

The average  $N_{U,Pig}$  for 3-h periods starting at 0700h were determined and used in the statistical analysis. This was repeated during three different observation periods when average pig weight was 51, 64 and 78 kg, respectively. Data were analyzed using the Statistical Analysis System, Release 8.2 (SAS Institute Inc., Cary NC). The effect of gender (male and female), observation period (1, 2 and 3) and time of day starting at 0100h, 0400h, 0700h, 1000h, 1300h, 1600h, 1900h and 2200h, were analyzed using PROC MIXED. The experiment was analysed as a split-split plot design with each pen as an experimental unit. The main plot was the gender, replicated in three pens for each sex. Observation period and time of day were treated as split and split-split plots over time, respectively.

### **2.3 Results and Discussion**

There was no significant difference in overall urination frequency for male and female pigs ( $F_{1,4} = 3.72$ ) and observation period had no significant effect ( $F_{2,8} = 1.53$ ). However, urination frequency was a function of the time of day ( $F_{7,84} = 8.11$ ;  $p < 0.001$ ). Table 2.1 shows the average urination frequencies for this group of male and female pigs between 51 and 78 kg, based on the average of the three observation periods. The minimum urination frequency was  $0.24 \pm 0.11$  urinations  $\text{pig}^{-1} \text{h}^{-1}$  between 0100h and 0400h. The maximum urination frequency was between 1600 and 1900 with a mean value of  $1.06 \pm 0.11$  urinations  $\text{pig}^{-1} \text{h}^{-1}$ . No interactions were significant.

**Table 2.1. Average urination frequencies for male and female pigs between 51 and 78 kg, based on the time of day.**

Time of day	Urination Frequency (urinations pig <sup>-1</sup> h <sup>-1</sup> )			Significant Difference <sup>y</sup>
	Male	Female	SEM <sup>z</sup> (df=84)	
0100h-0400h	0.31	0.16	0.15	**
0400h-0700h	0.29	0.29	0.15	
0700h-1000h	0.83	0.61	0.15	
1000h-1300h	1.19	0.62	0.15	
1300h-1600h	1.05	0.63	0.15	
1600h-1900h	1.12	1.01	0.15	
1900h-2200h	0.45	0.48	0.15	
2200h-0100h	0.37	0.58	0.15	
Mean	0.701	0.547		
SEM <sup>z</sup> (df = 4)	0.056	0.056		

<sup>z</sup>SEM = Standard error of the mean, df = Degrees of freedom

<sup>y</sup> Significant difference between genders for the time of day, P<0.01 (\*\*)

The average number of urinations per day, 14.9 urinations pig<sup>-1</sup> d<sup>-1</sup>, was high compared to 7.1 urinations pig<sup>-1</sup> d<sup>-1</sup> for fattening pigs, reported by Aarnink et al. (1996), which was based on 24-h video recordings of pens of 36 male and female pigs. Video recordings have a fixed view, and it is possible that urinations under males or behind females were not visible. Human observers have the freedom to move around the end of the pen and watch for urinations.

The mean room temperatures were 15.7, 15.8 and 14.8°C (± 0.4°C) for the three observation periods, respectively. With the cool fall weather outside the barn during the experiment the mechanical ventilation system was able to maintain comfortable conditions for the animals. During summer when the outdoor and thus the indoor temperatures rise, animal activity, including urination behaviour would be affected, but this experiment did not test the effect of temperature.

Pig urination occurs from a standing position, so the relationship between urinating activity and animal activity (as defined earlier) seems obvious. The sinusoidal dromedary model for diurnal variation in animal activity predicts relative animal activity, based on

the variation in activity with respect to the average, and the time of day with minimum activity (CIGR, 2002) (eq. 2.2).

$$N_{U,Pig} = N_{U,Avg} \cdot \left( 1 - m \cdot \sin \left( \left( \frac{2\pi}{24} \right) \cdot (Time + 6 - Time_{min}) \right) \right) \quad (2.2)$$

Equation 2.2 was fitted to the measured data by changing values of  $m$  and  $Time_{min}$  to reduce the sum of squares of deviations between the measured data points and the corresponding points calculated using equation 2.2. Figure 2.1 shows a “fitted” curve for urination frequency for pigs between 51 and 78 kg with an average urination frequency of 0.62 urinations  $\text{pig}^{-1} \text{h}^{-1}$ . The midpoint of each 3-h interval was considered the time of day for equation 2.2. The best-fit curve shows minimum urination activity is at 0230h ( $Time_{min} = 2.5$ ) and the variation in frequency over the 24-h period is  $\pm 0.58$  urinations  $\text{pig}^{-1} \text{h}^{-1}$ . The peak, or positive portion, of the sinusoidal curve occurs somewhere between 0700h and 2200h, which is very similar to the lighted period (0700 h to 1900h). The time of day with minimum animal activity and the variation in activity was 0115h and 0.43 urinations  $\text{pig}^{-1} \text{h}^{-1}$ , respectively, for Danish fattening pigs on partially slatted floor (Pedersen and Takai, 1997). The period of illumination was 0600h to 1800h in this previous study. Urination activity follows the same, single peak diurnal pattern associated with drinker use measured by Turner et al. (2000), increasing in late afternoon and decreasing overnight. Drinking behaviour is often linked with feeding behaviour but this behaviour was not measured by Turner et al. (2000) or in this experiment. Animal activity, drinking behaviour and urination activity seem to vary diurnally and are related, but the exact cause and effect relationship in terms of frequency pattern is still not fully understood.

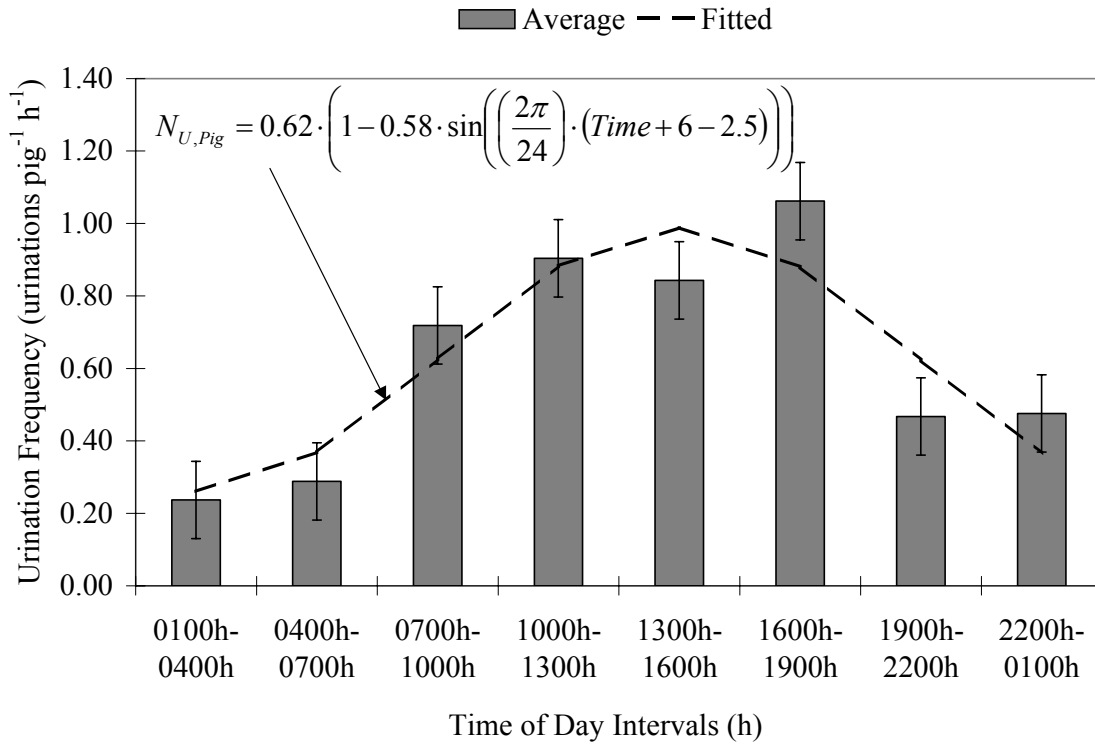


**Figure 2.1. Variation in measured number of urinations per pig per hour over a 24-h period, and the simulated number of urinations per pig per hour using a sinusoidal dromedary model. Vertical bars indicate the SEM (0.11 urinations pig<sup>-1</sup> h<sup>-1</sup>) of the average urination frequency for the time of day interval.**

## 2.4 Summary

The results of this study show that urination frequency is similar for male and female pigs between 51 and 78 kg, and the urination frequency varies diurnally. The urination frequency can be predicted using sinusoidal animal activity model curves, provided the average number of urinations is known.

## Acknowledgements

The authors gratefully acknowledge the funding provided for this project by the Natural Sciences and Engineering Research Council of Canada and Agriculture and Agri-Food Canada. SaskPork, Alberta Pork, Manitoba Pork and Saskatchewan Agriculture and

Food Development Fund provided strategic funding for this project. Special thanks go to the observers.

### CHAPTER 3

#### MEASURING UREASE ACTIVITY AND AMMONIA PRODUCTION AT THE FLOOR SURFACE IN A SWINE BARN

E. L. Cortus<sup>1,2</sup>, S. P. Lemay<sup>3</sup>, E. M. Barber<sup>4</sup>, J. R. de Freitas<sup>5</sup> and B. Z. Predicala<sup>1,2</sup>

<sup>1</sup> *Prairie Swine Centre Inc., Saskatoon, SK*

<sup>2</sup> *Department of Agricultural and Bioresource Engineering, University of Saskatchewan, Saskatoon, SK;*

<sup>3</sup> *Research and Development Institute in Agri-Environment, Deschambault, QC;*

<sup>4</sup> *College of Agriculture, University of Saskatchewan, Saskatoon, SK;*

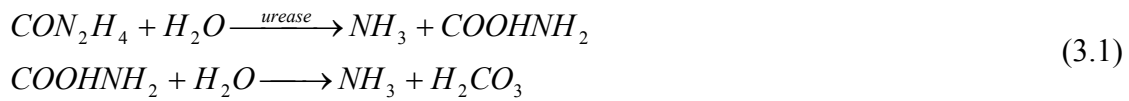
<sup>5</sup> *Department of Soil Science, University of Saskatchewan, Saskatoon, SK.*

#### **Synopsis**

Once urine is deposited on the floor of swine barns, the rate that the urea in the urine is converted to ammonia depends in part on the urease enzyme activity of the floor surface. This chapter outlines two types of measurement methods that were undertaken to measure enzyme activity at the floor surface for different levels of fouling and number of days of animal activity. A literature review of reported enzyme activities was also completed.

### 3.1 Introduction

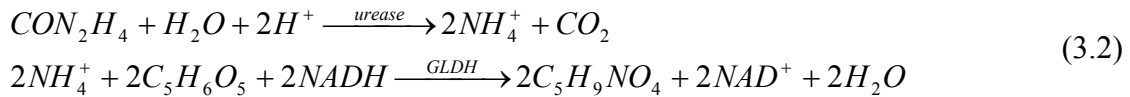
The urine-fouled floor area is considered one of the main sources of ammonia production within a swine barn (Aarnink and Elzing, 1998). Ammonia is produced by the breakdown of urea, the main component of urine, and the reaction is catalyzed by the enzyme urease as shown in equation 3.1 (Mobley and Hausinger, 1989).



Ammonia is a weak base, so once in solution the total ammonia produced will partition itself between ammonia and ammonium. Ammonium will remain in solution, whereas ammonia can volatilize from the liquid surface and become an air contaminant. Thus, understanding the development and prevalence of urease on the barn floor surface is important when trying to determine the ammonia emission from urine puddles on the floor.

Various microorganisms, including many in feces, produce the enzyme urease (Mobley and Hausinger, 1989). The amount of enzyme is quantified by its activity, or maximum forward rate of reaction (Shuler and Kargi, 2002), expressed by the amount of reactant used or product produced per unit time per unit volume. Mobley and Hausinger (1989) list several methods to assay microbial urease that differ in the way ammonia formation is monitored when urea is combined with the enzyme. Some methods are fixed-time-point methods where the ammonia formation in the liquid is monitored at fixed time intervals and the ammonia formation rate is assumed linear between measurements. The methods to measure the ammonia in solution at the fixed time intervals include the indophenol reaction, Nesslerization reaction or the use of *pH*

indicators (Mobley and Hausinger, 1989). The indophenol reaction, also called the Berthelot reaction, is used extensively to measure *TAN* concentration in materials including plant tissue, soil, urine, water and food (Searle, 1984). Other enzyme assay methods are continuous methods where ammonia formation is monitored continuously, generally by measuring the change in colour or absorbance of a sample using a spectrophotometer. The coupled enzyme assay is a continuous method whereby the hydrolysis of urea is coupled to a glutamate dehydrogenase reaction involving  $\alpha$ -ketoglutarate ( $C_5H_6O_5$ ) and nicotinamide adenine dinucleotide in reduced form ( $NADH$ ) to form glutamate ( $C_5H_9NO_4$ ) and nicotinamide adenine dinucleotide ( $NAD^+$ ) Mobley and Hausinger, 1989; eq. 3.2).



The glutamate dehydrogenase enzyme (*GLDH*) is added in excess so that the limiting component to the rate of reaction is the urease. The oxidation of *NADH* results in a loss of absorbance of 340 nm light and the rate of change of absorbance of a sample is indicative of the ammonia production, which is assumed to be from urea degradation catalyzed by the urease enzyme (Worthington, 1995).

Muck (1982), Braam et al. (1997a, 1997b) and Braam and Swierstra (1999) adapted fixed-time-point measurement methods to study urease enzyme activity within the barn environment. The resulting urease activity measurements of fecal material (Muck, 1982), and the urease activity of floor surfaces (Braam et al., 1997a, 1997b; Braam and Swierstra, 1999) have been expressed in various units of measure including mg *N* (g wet feces)<sup>-1</sup> h<sup>-1</sup> and mg *N* (g dry feces)<sup>-1</sup> h<sup>-1</sup> (Muck, 1982), g  $NH_3$  m<sup>-2</sup> h<sup>-1</sup> (Braam et al., 1997a), g  $NH_3$ -*N* m<sup>-2</sup> h<sup>-1</sup> (Braam et al., 1997b) and mg  $NH_3$ -*N* L<sup>-1</sup> (Braam and Swierstra,



1999). Muck (1982) measured ammonia concentration in liquid samples taken 1 h apart using ammonium distillation, while Braam et al. (1997a, 1997b) and Braam and Swierstra (1999) measured ammonia concentration of liquid samples taken 30 min apart with a spectrophotometer.

When measuring the urease activity at the floor surface, there is a concern that the concrete pore structure can trap urine and fecal material, along with all the resulting components like ammonia, urea and nitrogenous compounds, and these compounds may interfere with the enzyme assay method chosen. Also, there is a question about the difference in enzyme activity for floors that are continuously fouled, and those that are relatively clean, except for material transferred by animal movement.

The overall goal of this research was to determine urease activity levels on the solid and slatted floor surfaces of partially slatted floor pens in a swine barn in order to incorporate these enzyme activity levels into an ammonia production model for swine barns. The objectives of this experiment were: (1) to measure the urease activity (or ammonia production) at the floor surface of a grower-finisher room using one fixed-time-point method and one continuous method; (2) to determine if the urease activity (or ammonia production) is a function of the location within a pen (corresponding to the frequency and type of manure application) or number of days of animal activity on the floor surface; and (3) to compare the measured results to values reported in the literature.

## **3.2 Materials and Method**

### **3.2.1 Experimental Room and Apparatus**

The experimental room was a partially-slatted grower-finisher room with six pens. The solid floor of each pen was concrete and measured 2.4 m by 2.0 m, and the slatted floor was pre-cast concrete panels with dimensions of 1.8 and 2.0 m and 18% open area.

The nipple drinker was located on one side of the slatted floor area of each pen. The floor area was divided into three general sampling areas, described in figure 3.1. The slatted floor area was divided in two areas based on observations of floor cleanliness and excreta build-up; the floor area under the drinker was usually wet whereas the area of slatted floor away from the drinker was generally drier, but with a build-up of solid material.

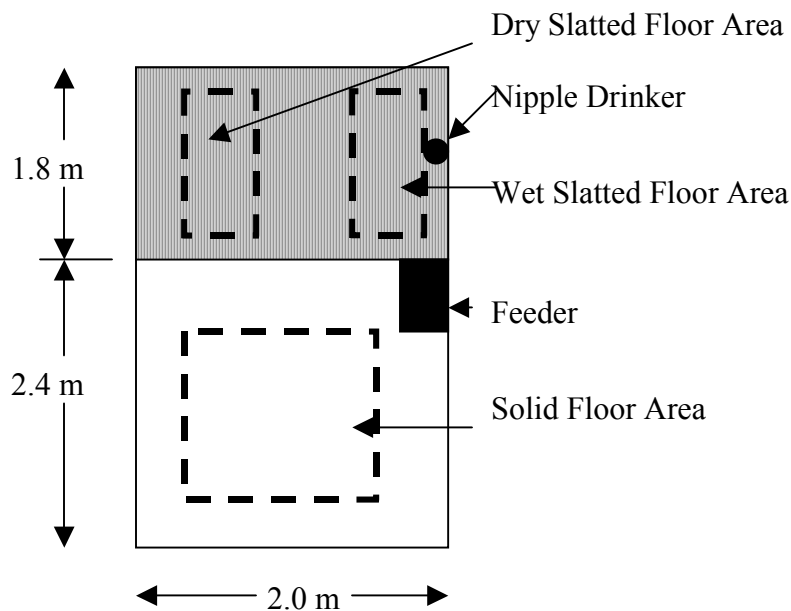


**Figure 3.1. Layout of a partially slatted floor pen. The dashed-line squares indicate the different locations from where samples were collected.**

A sampling apparatus similar to that described in Braam and Swierstra (1999) was used to collect samples of urea solution and water in contact with the barn floor surface (fig. 3.2). The apparatus was a 76-mm-diameter open-ended cylinder, encased in concrete for extra weight. A ring of silicone around the bottom edge of the cylinder was applied to act as a seal so that as liquid was added to the cylinder the liquid was contained

over a specific area of floor surface. The cylinder-opening was sufficiently small to cover only the solid portion between two gaps on the slatted floor.

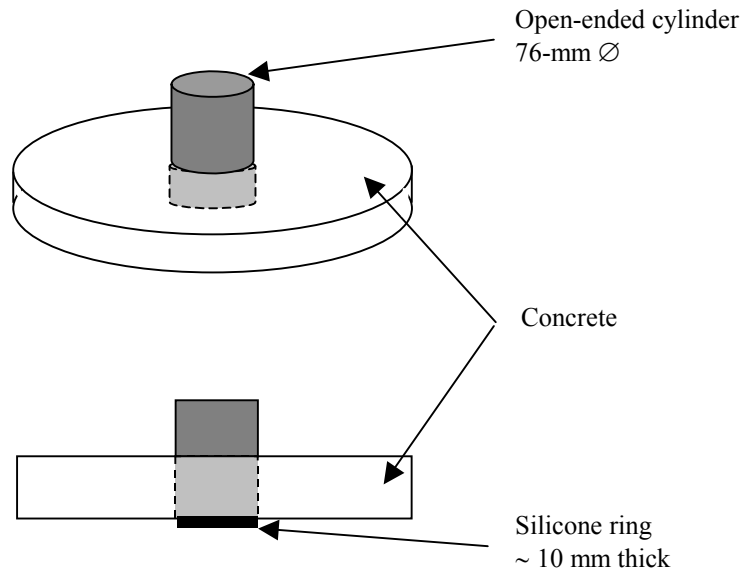


**Figure 3.2. Sampling apparatus for floor surface sample collection.**

The sampling apparatus was immersed in a weak bleach solution and rinsed with tap water between successive uses.

### **3.2.2 Sample Collection and Analysis - Fixed-Time-Point Method**

At a random location on either the solid or slatted floor in each of four pens two sampling apparatuses were placed side by side. Each sampling location was assessed a floor cleanliness score using a scale from zero to six, described in table 3.1. Animals had occupied these pens for different amounts of time, not less than one week, and only one set of samples were collected for this method of urease analysis. Animals were moved out of pens while samples were collected.

**Table 3.1. Description of criteria used to assign cleanliness scores to sampling locations in pig pens.**

Score	Description
0	Dry, clean floor with no presence of dust or fecal material.
1	Dry floor with a thin layer of dust, but no distinguishable fecal material.
2	Dry floor with dust and traces of dry fecal material.
3	Dry floor with dust and over half the area covered in dry fecal material.
4	Dry floor covered in dust and dry fecal material.
5	Partially wet floor, partially covered in wet fecal material.
6	Fully wet floor, fully covered in wet fecal material.

In one cylinder, 90 mL of 0.4 mol L<sup>-1</sup> urea solution (ACS grade, EM Science; distilled water) was added while in the other cylinder 90 mL of distilled water was added, respectively. A 20-mL sample was withdrawn from each cylinder with a sterile syringe within 5 min of contacting the solution with the floor (Initial sample) and approximately 30 min afterwards (Final sample). A 5-mL sub-sample was taken from each 20-mL sample and added to 50 mL of 0.24-N sulfuric acid ( $H_2SO_4$ ) to acidify the sample and thus preserve all of the total ammoniacal nitrogen (*TAN*: a measure of the mass of the nitrogen nuclei of ammonia and ammonium molecules, also referred to as ammonium-N for acidified samples) within the solution in ammonium form. The acidified sample was filtered through Whatman #4 paper and a 0.22- $\mu$ m filter (Fisherbrand syringe filter, Fisher Scientific) to remove any solid material that could potentially break down during storage. The preservation of samples in  $H_2SO_4$  and with pre-filtering was tested in a related experiment to ensure negligible effect of preservation technique on the ammonium analysis of the samples. Samples were stored for 1 d at 4°C prior to analysis.

The samples were analyzed for *TAN* concentration using the automated indophenol reaction in auto-analyzers (Technicon Autoanalyzer II, Technicon Industrial Systems, Tarrytown, NJ). Ammonium-N or *TAN* concentration is determined from the colour

produced by the indophenol reaction when the sample is combined with a buffer solution, sodium hypochlorite solution, and sodium salicylate/sodium nitroprusside solution (Searle, 1984). Test solutions were prepared according to Technicon Method No. 325-74W (Technicon, 1974). Standard solutions were prepared on the day of analysis with 1 to 5 mL of 100-ppm ammonium chloride solution and the appropriate amount of 0.24-N  $H_2SO_4$  to produce solution concentrations of 1 to 5 ppm *TAN*. Samples with concentrations exceeding the detection limits of the auto-analyzers were diluted with 0.24-N  $H_2SO_4$ .

The difference in *TAN* concentration for a given location between the Final and Initial sample taken from the cylinder with urea solution was calculated to determine the ammonia production rate in urea. Similarly, the ammonia production rate in water for the given location was calculated as the difference in *TAN* concentrations for Final and Initial samples taken from the cylinder containing water. Similar to the procedure used by Braam et al. (1997a), cylinders containing water were used to provide a measure of the ammonia production rate by other nitrogenous material on the floor surface. Enzyme activity was assumed to be the difference in ammonia production rate in urea and the ammonia production rate in water. Enzyme activity and ammonia production rates were expressed in  $g\ NH_3\ m^{-2}\ h^{-1}$ .

### **3.2.3 Sample Collection and Analysis - Continuous Method**

The experimental work for the continuous method of urease activity analysis was conducted separate from the experimental work for the fixed-time point method. Samples were collected from three locations in four partially-slatted floor pens after 0, 11 and 22 days of animal activity within the pen. The floor and partitions of each of the pens was washed and disinfected the day before Day 0 and allowed to air-dry over night.

The disinfectant used was Ascend (Ecolab, St. Paul, MN), a quaternary ammonium disinfectant containing 6% n-Alkyldimethylbenzyl ammonium chloride and 9% Didecyldimethyl ammonium chloride. Immediately after samples were collected on Day 0, 12 to 16 female pigs were moved into each pen. Animals were moved out of pens while samples were collected on days 11 and 22. The three sampling locations used are shown in figure 3.1.

For this method, the sampling apparatus was placed on the floor and filled with 75 mL of distilled water. After 5 min the water with the material from the floor, that is hereafter referred to as the enzyme solution, was stirred with a sterile syringe for 1 min before the enzyme solution was withdrawn from the cylinder by the syringe, placed in a storage container and stored at 4°C until analysis. The enzyme solution was filtered using Whatman #4 paper immediately prior to analysis.

The Worthington urease enzyme assay method (Worthington, 1995) was chosen as a continuous method to measure enzyme activity. All reagents in table 3.2 except the enzyme solution were combined in a cuvette (Fisherbrand, Fisher Scientific, Ottawa, ON) and placed in a spectrophotometer (Beckman DU 60, Beckman Coulter Inc., Fullerton, CA) with the light source set at 340 nm. These "blank" samples were monitored for at least 5 min to ensure there was negligible ammonia from any of the reagents. The enzyme solution was then added to the cuvette and the absorbance monitored every 30 s over a 5 to 10 min sampling period. Enzyme solution samples were diluted with buffer solution as required in order to detect the absorbance curve in the time prescribed.

**Table 3.2. Amount of reagents used in the Worthington Enzyme Assay (Worthington, 1995).**

Reagent	Volume (mL)
0.10 mol L <sup>-1</sup> Phosphate buffer, <i>pH</i> 7.6	2.4
0.023 mol L <sup>-1</sup> ADP	0.1
0.0072 mol L <sup>-1</sup> NADH	0.1
0.026 mol L <sup>-1</sup> $\alpha$ -ketoglutarate	0.1
1.8 mol L <sup>-1</sup> Urea	0.1
GLDH (500 units mL <sup>-1</sup> )	0.1
Enzyme solution	0.1

Based on the initial linear slope of the absorbance curve ( $\Delta A_{340} t^{-1}$ ), equation 3.3 can be used to calculate the urease activity of the enzyme solution in g NH<sub>3</sub> m<sup>-2</sup> h<sup>-1</sup>

(Worthington, 1995).

$$S'_m = \frac{\left( \frac{\Delta A_{340}}{t} \right)_{Sample} - \left( \frac{\Delta A_{340}}{t} \right)_{Blank}}{6.22} \cdot \frac{V_{cuv}}{0.1} \cdot 18 \quad (3.3)$$

To ensure the spectrophotometer was working properly and to validate equation 3.3, solutions with standard amounts of urease enzyme (Urease Type IX from Jack Beans, Sigma Aldrich, Oakville, ON) were analyzed at the start of each of the analysis days. The measured rates of change in absorbance of the standard solutions were substituted into equation 3.3 and the calculated urease activity levels were compared to the amount of Jack Bean urease enzyme used in the standard solution. The amount of standard enzyme was assumed to be the true enzyme activity.

Ammonia was assumed to be present in the collected enzyme solutions, but since the *GLDH* was in excess the expectation was that the ammonia would be used up in the reaction immediately resulting in a sharp drop in absorbance, distinguishable from the "urease" curve. However, to be sure that the change in absorbance was caused by urease reacting with the urea in the reagent solution, for every enzyme solution two tests were

conducted with and without urea as part of the reagent solution and the absorbance curves were compared.

The resulting ammonia production rates/enzyme activities were studied to determine if there was an effect of the number of days of animal activity and/or floor location on the samples.

### **3.3 Results**

#### **3.3.1 Fixed-Time-Point Method**

The ammonia production in urea solution and distilled water over 30 min was measured in four random locations, each in a different pen of pigs. Locations 1 to 4 had cleanliness scores of 2, 5, 1 and 6, respectively, at the time of sample collection. Locations 1, 3 and 4 were on the solid floor portion of the individual pens, whereas Location 2 was on the slatted floor portion of one of the pens.

Ammonia production rates in the urea and water cylinders ranged from -0.10 to 5.19 g  $NH_3$  m<sup>-2</sup> h<sup>-1</sup> (fig. 3.3). The ammonia production rates in urea solution were very similar in magnitude to the corresponding ammonia production rates in water for each location and except for Location 2 were lower than the ammonia production rates in water, resulting in negative calculated urease activity values between -1.56 and 0.27 g  $NH_3$  m<sup>-2</sup> h<sup>-1</sup>. A comparison of these results to literature values is discussed in a later section.



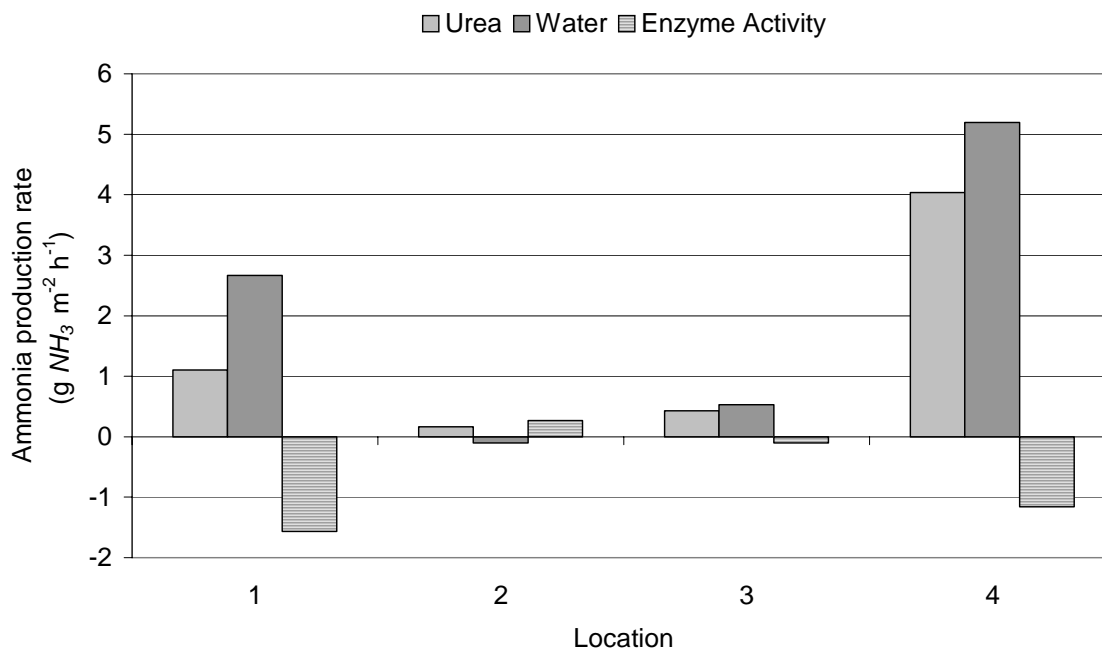


**Figure 3.3. Ammonia production rate in urea solution and water for Locations 1-4. Enzyme activity is the calculated difference between the production rates in urea and water.**

### 3.3.2 Continuous Method

The floor cleanliness scores for the three locations in four pens on Days 0, 11 and 22 are shown in table 3.4 and for each of the 36 points an enzyme solution sample was collected for measurement using the continuous method. Scores did not steadily increase in all locations from 0 to 11 to 22 days, but rather reflected the change in dunging behaviour for each pen of animals over the course of the experiment.

**Table 3.3. Floor cleanliness scores for the 12 sampling locations after 0, 11 and 22 days of animal activity.**

Pen	Location	Cleanliness Score		
		Day 0	Day 11	Day 22
1	Wet Slatted Floor	0	6	6
	Dry Slatted Floor	0	5	4
	Solid Floor	0	6	4
2	Wet Slatted Floor	0	6	6
	Dry Slatted Floor	0	3	4
	Solid Floor	0	2	2
3	Wet Slatted Floor	0	6	6
	Dry Slatted Floor	0	4	4
	Solid Floor	0	3	3
4	Wet Slatted Floor	0	6	6
	Dry Slatted Floor	0	5	2
	Solid Floor	0	3	2

Standard solutions were analyzed each analysis day. The calculated urease activity values for each standard using equation 3.3 (based on the initial, linear portion of the absorbance curve) was determined and compared to the amount of Jack Bean urease in the standard solution. Figure 3.4 shows the comparison between calculated and known amounts of enzyme in the standard solutions used, and also the variation experienced when analyzing similar solutions.

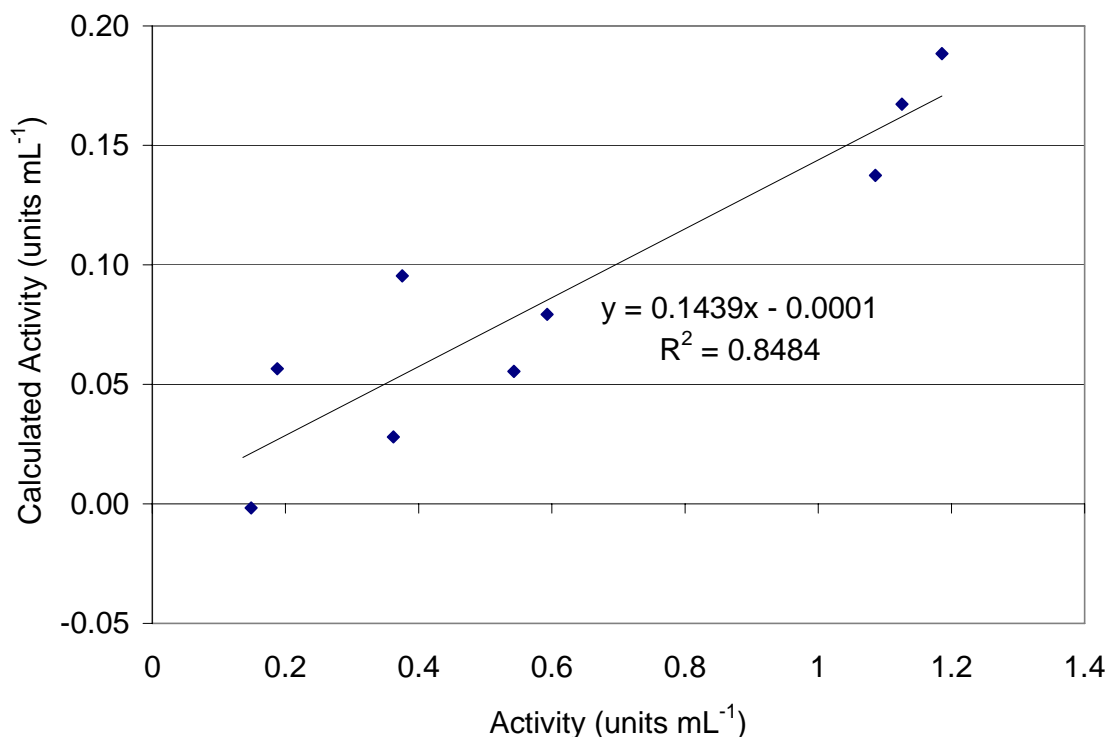


**Figure 3.4. Calculated enzyme activity (based on equation 3.3) compared to the rated activity of standard enzyme solutions containing Jack Bean urease. (1 unit = 1  $\mu\text{mol NH}_3 \text{ min}^{-1}$ )**

Because the calculated activity was lower than the amount of enzyme used in each standard solution (fig. 3.4), the ammonia production rate measurements for all continuous method samples were based on a comparison with the standard enzyme solution curve for the analysis day, rather than equation 3.3.

Figure 3.5 is an example of data collected from samples of standard enzyme solution and a sample collected in the barn analyzed with and without the presence of urea in the reagent mixture. The general absorbance pattern for a standard enzyme solution was a linear slope until the sharp point where the absorbance no longer changed, indicating a reagent had been used up. Based on table 3.2, *NADH* is the limiting reagent. When samples from the barn floor surface were analyzed, there was generally a sharp initial

decrease in absorbance, followed by a gentle curve and a flattened region. This flattened region generally occurred at about 120 s.

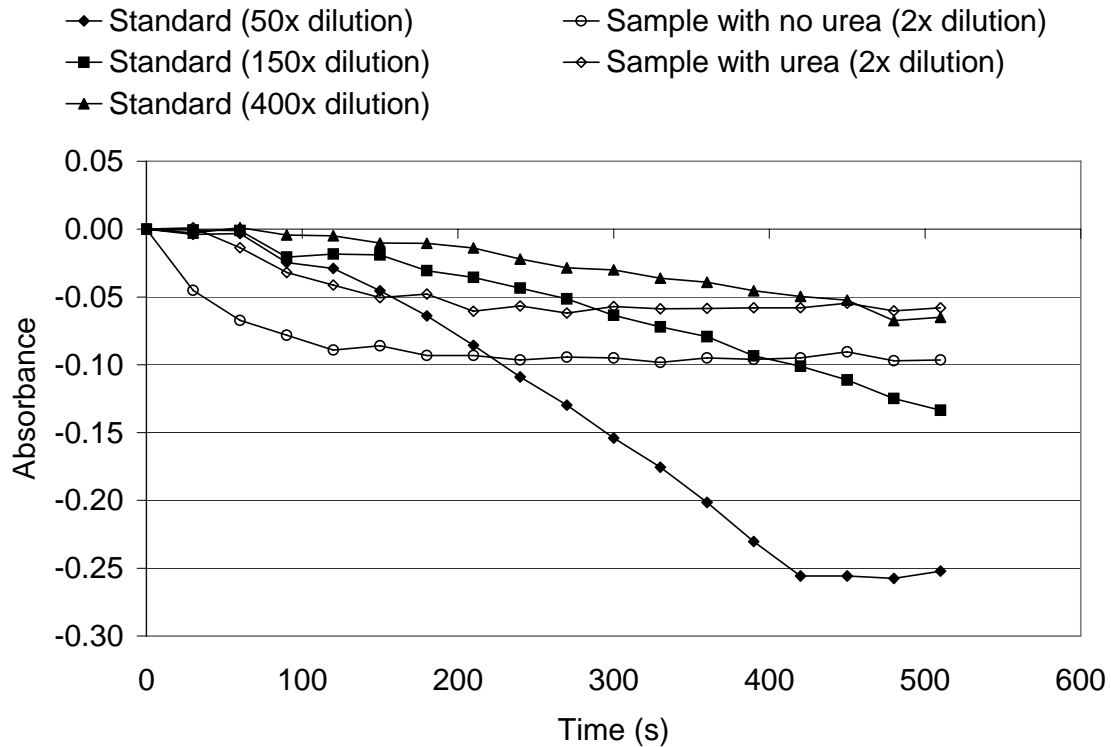


**Figure 3.5. Sample absorbance curves as detected by a spectrophotometer, for standard enzyme solutions containing a dilution of Jack Bean urease and an enzyme solution sample collected from the barn floor surface, analysed with and without urea in the reagent mixture.**

The coupled enzyme method did not appear as specific for the enzyme urease as anticipated for two reasons. First, the "urease" curve was not as distinguishable for the barn floor surface samples compared to the standard enzyme solutions. Second, the absorbance curves for enzyme solutions analyzed without urea in the reagent mixture followed the same pattern and often had larger changes in absorbance compared to the same solutions analyzed with urea in the reagent mixture. Therefore, urease activity values were not calculated. However, the absorbance curves still provided a measure of

the amount of ammonia production over time for each enzyme solution, so the ammonia production rate based on the initial slope over the first 120 s for the absorbance curve from each sample analyzed with and without urea was determined. The ammonia production measurements presented should not be considered definitive, but there are some interesting trends based on the number of days of animal activity (fig. 3.6) and the location in the pen (fig. 3.7).

Figures 3.6 and 3.7 show the similar rate of ammonia production in the enzyme solutions when they were measured with and without urea in the reagent mixture, similar to the fixed-time-point method. Figure 3.6 shows that the ammonia production rate linearly increased in the enzyme solution samples from 0 to 22 days of animal activity in the pen. Figure 3.7 shows that the enzyme solutions with the lowest ammonia production rates were collected from the wet slatted floor area of the pens, and higher ammonia production rates occurred in samples collected from the dry slatted floor area and the solid floor area. The appearance of wet fecal material was therefore not indicative of the ammonia production rate.

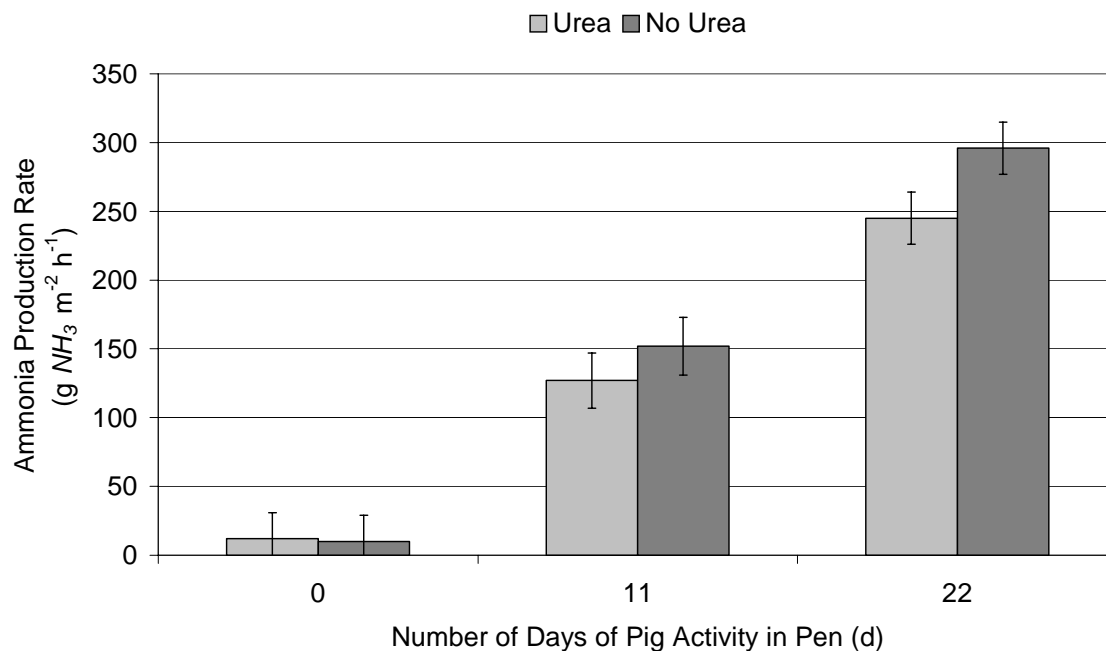


**Figure 3.6. Ammonia production rate measurements for enzyme solutions analyzed with and without urea based on the number of days of animal activity. (Vertical bars indicate standard error).**

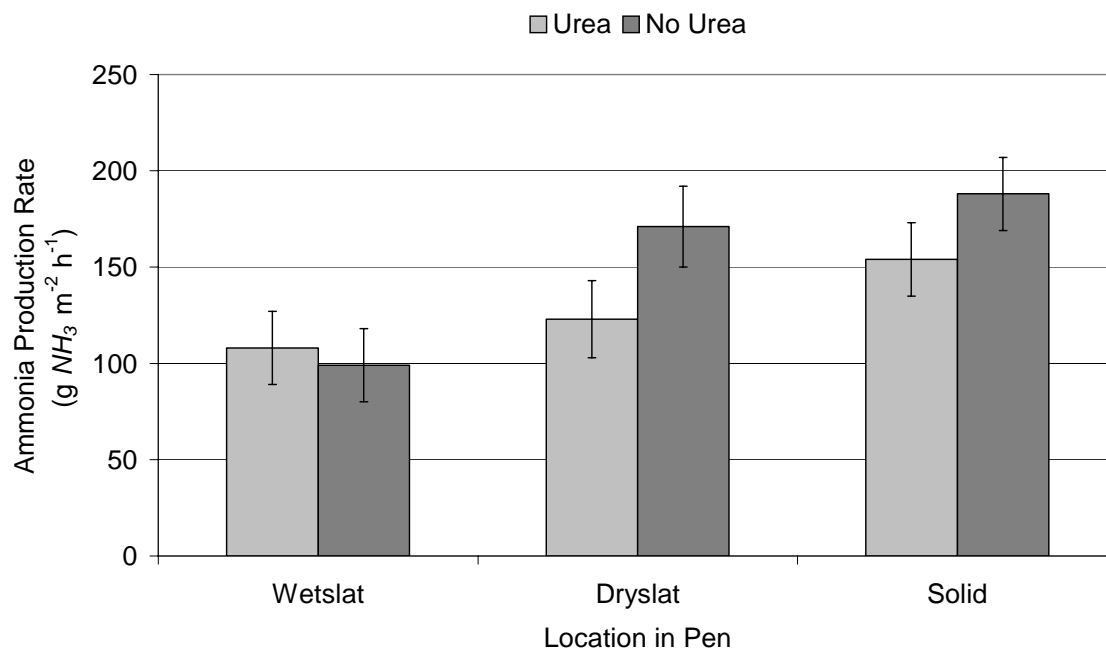


**Figure 3.7. Ammonia production rate measurements for enzyme solutions analyzed with and without urea based on the sampling location in a pen. (Vertical bars indicate standard error).**

### 3.3.3 Urease Activity Values in the Literature

Urease activity levels pertaining to swine and cattle barns found in the literature are presented in table 3.4. Muck (1982) and Elzing and Monteny (1997b) studied the urease activity of bovine feces and bovine feces/urine mixtures, based on the rate of change of the urea concentration in urea solutions mixed with the fecal mixtures. In the studies by Braam et al. (1997a) and Braam et al. (1997b), the urease activity of the floor surfaces of cubicle dairy cow houses were measured for different manure removal strategies. Braam and Swierstra (1999) studied the impacts of concrete strength, treatment of the fresh concrete surface, curing time, treatment of the hardened surface, surface roughness and water penetration depth. The reported values were adjusted to express the urease activity measurements and simulations in common units of  $\text{g NH}_3\text{-N m}^{-2} \text{h}^{-1}$  where possible.

Generally, freshly washed clean surfaces had a very low urease activity as shown by Braam et al. (1997a). As floors became increasingly fouled, minimum urease activities ranged from 0.25 to 5.7  $\text{g NH}_3 \text{ m}^{-2} \text{h}^{-1}$ , based on the floor surface urease activity measurements. The lower range of urease activity levels on the fouled floor surfaces could be attributed to smoother floor surfaces (Aarnink and Elzing, 1998; Braam and Swierstra, 1999) or different manure removal techniques (Braam et al., 1997a, 1997b).

**Table 3.4. Urease activity levels reported in the literature and their method of determination.**

Source (Date) <i>Application</i>	Urease Activity	Method of Determination/Calculation	Urease Activity (Common Units)
Muck (1982) <i>Bovine Feces</i>	0.49 +/- 0.07 to 4.24 +/- 4.09 mg N g wet feces <sup>-1</sup> h <sup>-1</sup> ; 3.4 +/- 0.5 to 27.0 +/- 34.7 mg N g dry feces <sup>-1</sup> h <sup>-1</sup>	- Fixed-time-point method. - Rate of reaction was based on the decrease in urea concentration (measured by jack bean urease and <i>NH<sub>3</sub>-N</i> distillation) over 1 h. - Multiple tests were performed to determine the rate of reaction for solutions with different urea concentrations.	<i>Not enough information</i>
Braam et al. (1997a) <i>Floors of cubicle houses for dairy cows with a manure scraper</i>	Clean <sup>Z</sup> Solid Floor: 0.02 - 0.04 g <i>NH<sub>3</sub></i> m <sup>-2</sup> h <sup>-1</sup> Dirty Solid Floor (15 days of animal activity): 0.25 - 4.58 g <i>NH<sub>3</sub></i> m <sup>-2</sup> h <sup>-1</sup>	- Fixed-time-point method. - Rate of ammonia production in urea solution samples were taken before and after 30 min of contact with the barn floor surface. (Rate of ammonia production in water over 30 min was also measured). - Ammoniacal nitrogen was measured spectrophotometrically.	<i>Clean Solid Floor: 0.02 - 0.04 g NH<sub>3</sub> m<sup>-2</sup>h<sup>-1</sup> Dirty Solid Floor: 0.25 - 4.58 g NH<sub>3</sub> m<sup>-2</sup>h<sup>-1</sup></i>
Braam et al. (1997b) <i>Floors of cubicle houses for dairy cows with a manure scraper, varying number of urine gutters and spraying water</i>	Dirty Solid Floor (8 days of animal activity): 2.7 - 4.7 g <i>NH<sub>3</sub>-N</i> m <sup>-2</sup> h <sup>-1</sup>	- Fixed-time-point method. - Rate of ammonia production in urea solution samples were taken before and after 30 min of contact with the barn floor surface. (Rate of ammonia production in water over 30 min was also measured). - Ammoniacal nitrogen was measured spectrophotometrically.	<i>Dirty Solid Floor: 3.3 - 5.7 g NH<sub>3</sub> m<sup>-2</sup> h<sup>-1</sup></i>



**Table 3.4. (continued)**

Source (Date) <i>Application</i>	Urease Activity	Method of Determination/Calculation	Urease Activity (Common Units)
Elzing and Monteny (1997b) <i>Floors of Cubicle house for dairy cows</i>	Measured: $0.17 \mu\text{mol urea min}^{-1} \text{ g}^{-1}$ Fitted: $0.7 - 4.29 \mu\text{mol min}^{-1} \text{ g}^{-1}$ NOTE: When "Measured" urease activity values were used in simulations, the ammonia production by urine on a fouled floor was underestimated so "Fitted" levels were determined.	- Multiple tests were performed to determine the rate of reaction for urine/feces mixtures in solutions with different urea concentrations. - It is unclear how the rate of reaction was measured.	<i>Fitted: <math>1.6 - 10 \text{ g NH}_3 \text{ m}^{-2} \text{ h}^{-1}</math> (assuming area is <math>2.1 \text{ m}^2</math>)</i>
Aarnink and Elzing (1998) <i>Partially slatted floors of swine barns</i> Based on Braam and van den Hoorn (1996).	Solid Floor: $0.0615 \text{ mmol urea L}^{-1} \text{ s}^{-1}$ Slatted Floor: $0.0026 - 0.0184 \text{ mmol urea L}^{-1} \text{ s}^{-1}$ (depending on floor type)	- Calculated as a function of floor surface roughness (R) and puddle depth (D): $2738 - 2665 * 0.989^R / D$ ( $\text{mg NH}_3\text{-N m}^{-3} \text{ h}^{-1}$ ).	<i>Solid Floor: <math>2.13 \text{ g NH}_3 \text{ m}^{-2} \text{ h}^{-1}</math> Slatted Floor: <math>0.26 - 1.31 \text{ g NH}_3 \text{ m}^{-2} \text{ h}^{-1}</math></i>
Braam and Swierstra (1999) <i>Concrete samples with different surface characteristics</i>	Dirty Solid Floor (15 days of fouling): $1 - 43 \text{ mg NH}_3\text{-N L}^{-1}$ for coated concrete, $25 - 162 \text{ mg NH}_3\text{-N L}^{-1}$ for non-coated concrete	- Fixed-time-point method. - Rate of ammonia production in urea solution samples were taken before and after 30 min of contact with the barn floor surface. - Ammoniacal nitrogen was measured spectrophotometrically (655 nm wavelength light).	<i>Dirty Solid Floor: <math>0.61 - 3.9 \text{ g NH}_3 \text{ m}^{-2} \text{ h}^{-1}</math> (non-coated concrete)</i>

<sup>z</sup> Cleaning procedure involved washing with high pressure water, rinsing with 2-N hydrochloric acid, and washing again with high pressure water after 30 min.

### 3.4 Discussion

#### 3.4.1 Fixed-Time-Point Assay Method

Using the fixed-time-point method, ammonia production rates in urea solutions at the floor surface were very similar to ammonia production rates in water, ranging from 0.2 to 4.0 g  $NH_3$  m<sup>-2</sup> h<sup>-1</sup> and -0.1 to 5.2 g  $NH_3$  m<sup>-2</sup> h<sup>-1</sup>, respectively. The theory behind using both urea and water solutions was that any ammonia produced by compounds on the floor surface would be measured in the water samples so that the ammonia production from urease converting the added urea to ammonia could be separated from any other production mechanisms (Braam et al., 1997a). Based on this assumption, the calculated urease activities from this assay ranged from -1.6 to 0.3 g  $NH_3$  m<sup>-2</sup> h<sup>-1</sup>. Braam et al. (1997a) measured enzyme activity using a similar fixed-time method (*TAN* analysis was different) and also used one water-based sample for every four urea-based samples to account for ammonia production by other sources. There was no indication that there was significant ammonia production in their water samples. It appears that the fixed-time-point method of urease activity analysis used in this study did not produce accurate urease activity values because there was either: (1) significant ammonia production from another source on the floor surface; (2) an interference between something in the sample and the indophenol analysis for ammonia; or (3) there is negligible urease activity on the barn floor surface.

At the floor surface, the quaternary-ammonium disinfectant used to clean the pens before animals were moved in may have interfered with the samples. If the disinfectant remained in the concrete pore structure, it is possible that some disinfectant was flushed out of the pores when the test solutions were added to the cylinders. While the initial sample should have accounted for this background ammonia, if there was a step increase

in ammonia to the samples within the 30-min sample collection period, this would be undistinguishable from any changes over time. The rate of ammonia production by decomposing feed and feces on the floor has not been found in the literature, but feed and fecal material also represent possible ammonia production sites.

The indophenol reaction is subject to interference from compounds commonly found in swine barns including nitrogen compounds, trace metals and sulphur (Searle, 1984). Preliminary tests with different preservation methods were conducted before the experiment to ensure the concentration of a floor surface sample was consistent over time. In the preliminary tests there was no evidence of interference of the preservation method used on the ammonium measurement. There still is, however, a potential interference by something within the sample from the floor surface and this unknown interference would have been present in both the urea solution and water-based samples. Based on the filtering of samples through a 0.22  $\mu\text{m}$  filter as part of the preservation method used, the interfering compound cannot be attributed to any solid matter.

If there were no interferences from compounds on the floor surface or in the sample solutions, the results indicate there was negligible urease activity at the locations tested. The lack of urease activity is difficult to explain based on the bacterial build-up of fouled floor surfaces (De Foy et al., 2004) and the number of urease-associated bacterium in the fecal material of monogastrics such as humans and pigs (Moblely and Hausinger, 1989).

### **3.4.2 Continuous Assay Method**

The expected result of measuring urease enzyme activity by the coupled enzyme assay method was that the impact of ammonia from other sources on the floor would be either recognizable or negligible so that urease activity could be separated out and accurately

measured. The advantage of the coupled enzyme method is that the change in absorbance is monitored continuously throughout the entire process and any changes in the rate of reaction are captured. However, this method appears to be affected as much or more by interference from other ammonia-producing sources compared to the fixed-time-point method used.

The first concern with the continuous method used in this study was that the standard solution activity levels were not accurately predicted using equation 3.3. While it was assumed that the amount of enzyme in the solution was the "accurate" enzyme activity for each standard, there is the possibility that the rated activity was affected by the temperature and *pH* of the reagent solution. The Jack Bean urease rated activity was for *pH* 7.0 and 25°C. The reagent solution *pH* in the method used was 7.6, and there was not temperature control within the spectrophotometer. Based on the less than optimal *pH*, and room temperature conditions during analysis, the lower calculated urease activity values shown in figure 3.4 might not have been as low as initially thought.

The second concern with the continuous method used in this study was that the shapes and slopes of the absorbance curves for the samples analyzed with and without urea were not drastically different. This suggests that an interfering compound was present in the enzyme solution and the source of interference produced or contained more ammonia than urease-degradation of urea could produce. There should have been enough *GLDH* in solution to rapidly convert any ammonia in the enzyme solution, resulting in a sharp drop on the absorbance curve. The absorbance curves generally did show sharp drops, but a gently curved region followed this before the curve flattened. Enzymes act as catalysts and are theoretically not used up in the reaction (Shuler and Kargi, 2002).

Therefore, if urease was present, and assuming none of the other reagents were used up during the initial decrease, there would have been a steady decrease in absorbance over time as the urease helped degrade the urea after the initial drop. This trend in the absorbance curves for the samples was not seen. The similarity between curves with and without urea did help to corroborate the results found using the fixed-time-point method though. The inability of the continuous method to measure urease activity using this method is attributed to the same causes as the fixed-time-point method: (1) an interfering compound on the floor surface; (2) an interfering compound in the enzyme solution; or (3) negligible urease present on the floor surface of the swine barn.

While the enzyme activity could not be determined for the enzyme solutions from the barn floor surface using the continuous method, the ammonia production rates in the enzyme solutions were still calculated.

#### **3.4.3 Effect of Time on Ammonia Production/Urease Activity**

Braam et al. (1997a) found an increase in urease activity based on the number of days of animal activity. Elzing and Monteny (1997a) also speculated that increased ammonia emission from urine on repeatedly fouled floors was caused by an increase in urease activity at the floor surface. The coupled enzyme assay measurements (fig. 3.6) showed that with increasing animal activity, ammonia production at the floor surface increased. The urease activity of floor surfaces has only been measured up to 15 days in the literature, and 22 days in the continuous method in this study. Generally, the increase in urease activity has been linearly related to time, but urease activity measurements were usually stopped after one to two weeks in the studies of cubicle dairy-cow houses because there was not an increase in ammonia emissions associated with increasing urease activity levels past this point in time. In the study by Braam et al. (1997a), only urease

activity levels up to  $2 \text{ g NH}_3 \text{ m}^{-2} \text{ h}^{-1}$  were found to significantly impact ammonia emission. Elzing and Monteny (1997a) reported that repeated fouling of the floor surface only resulted in increased ammonia emission rates for the first seven days of fouling.

Even though urease activity measurements in this experiment were not conclusive, it seems likely based on reported enzyme activity levels from several sources and the bacterium concentration measurement of De Foy et al. (2004) that urease activity will be present on the floor surface of a swine barn after only a few days of animal activity if fecal material is present. It is not known at what level urease activity would be non-limiting to ammonia emissions though.

#### **3.4.4 Effect of Location on Ammonia Production/Urease Activity**

From the coupled enzyme assay measurements, the solid floor and dry slatted floor areas had higher ammonia production levels than the wet slatted floor area. In the fixed-time-point method measurements, Location 2 was located on a wet slatted floor area also, and had lower ammonia production levels than other areas on the solid floor. It is interesting to note that the ammonia production rates measured using the fixed-time-point method were similar in magnitude to reported urease activity levels in the literature. The wet slatted floor area is continually washed by water spilled from the drinker and is also subject to animals standing and walking in that area while drinking. While the floor surface is dark with fecal material and water, the fecal material does not build up in thick layers and is easily washed away or diluted. On the solid and dry slatted floor areas, with increasing animal activity there is, at minimum, an increase of dust and dry fecal material. These areas can be heavily fouled at times, but if animal behaviour changes the floor surface can dry. If this occurs, there is a caked, dry layer of fecal material, sometimes several centimetres thick on top of the concrete. From these results, it appears

that if the solid or dry slatted floor is wetted just with water it becomes an "ammonia producer". The amount of wet, fresh fecal matter was not a strong indicator of ammonia production in this experiment. From the literature, distinctions between urease activity levels for different floor areas were only based on differences in floor surface roughness (Aarnink and Elzing, 1998). Based on this study, the urease activity level cannot be linked to differences in fouling practices or build-up of fecal material over time.

### **3.4.5 Recommendations**

A suitable method to measure urease activity on the swine barn floor surface that is not affected by interference from other ammonia-producing compounds was not found in this study. Until a method is developed, urease activity values found in the literature for cubicle dairy-cow houses provide the best estimates for use in swine barn ammonia emission models. Assuming that urease activity does become a non-limiting factor in swine barns with increased fouling, it appears safer to use the maximum measured urease activity value available to describe the urease activity of fouled floor surfaces. If the non-limiting urease activity level is actually lower there will be little impact of using a higher value. Maximum measured urease activity levels reported for fouled floor surfaces in dairy barns were approximately  $5 \text{ g NH}_3 \text{ m}^{-2} \text{ h}^{-1}$ , and this is the suggested value until more accurate measurements for swine barns are available.

Further work could be conducted using the apparatus described (fig. 3.2) and analysis for  $\text{NH}_4\text{-N}$  using the indophenol method to determine if the interference to the urease activity analysis method was from an interference at the floor surface. By taking more frequent samples of the liquid solution in the apparatus, it may be possible to discern how fast the ammonia is produced and this may help uncover whether significant amounts of

ammonia are coming from the concrete pores or if fecal material is broken down when wetted, for example.

In future urease activity measurements, analysis using  $^{15}\text{N}$ -labeled urea (Mobley and Hausinger, 1989) and mass spectroscopy may help distinguish the urea added as part of the testing method from components derived from the floor.

### **3.5 Summary**

Urease activity on the floor of a swine barn is difficult to measure because the ammonia production from urea decomposition must be distinguishable from the ammonia produced by other unknown sources. A fixed-time-point method and continuous method were used to analyze liquid samples that were in contact with the floor inside pig pens. Both methods detected similar levels of ammonia production in solution that was in contact with the floor surface, with and without the presence of urea, which suggested that there was either interference from something at the floor surface, something within the liquid samples, or negligible urease activity.

In the literature, urease activity was shown to increase with number of days of animal activity or fouling of the floor surface. Ammonia production rates in the enzyme solution samples analyzed using the continuous method supported this trend, but it was not possible to assign urease activity levels based on time in this study. There was a trend in this study that showed pen areas that are frequently wetted with water (i.e. under the drinker) have the lowest ammonia production levels. Urease activity values greater than  $5 \text{ g NH}_3 \text{ m}^{-2} \text{ h}^{-1}$  are recommended in ammonia emission models for urine puddles on the barn floor surface based on literature values until more accurate measurements can be collected.



**Acknowledgements**

The assistance provided by Dr. de Freitas and Mr. Ferhatoglu during sample analysis is greatly appreciated. Funding was provided by the Natural Sciences and Engineering Research Council of Canada, Sask Pork, Alberta Pork, Manitoba Pork and Saskatchewan Agriculture and Food Development Fund.

CHAPTER 4  
A DYNAMIC, MECHANISTIC MODEL OF AMMONIA EMISSION FROM URINE  
PUDDLES

E.L. Cortus<sup>1,2</sup>, S.P. Lemay<sup>3</sup>, E.M. Barber<sup>4</sup>, G.A. Hill<sup>5</sup> and S. Godbout<sup>3</sup>

<sup>1</sup> *Prairie Swine Centre Inc., Saskatoon, SK;*

<sup>2</sup> *Department of Agricultural and Bioresource Engineering, University of Saskatchewan, Saskatoon, SK;*

<sup>3</sup> *Research and Development Institute for the Agri-environment, Deschambault, QC;*

<sup>4</sup> *College of Agriculture, University of Saskatchewan, Saskatoon, SK;*

<sup>5</sup> *Department of Chemical Engineering, University of Saskatchewan, Saskatoon, SK.*

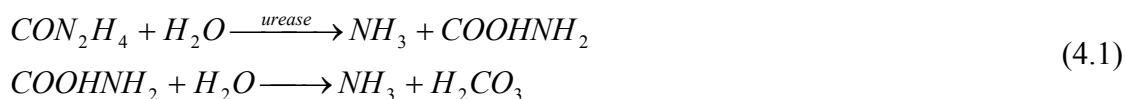
**Synopsis**

Each urination represents an ammonia emission site. In this chapter the ammonia emission rate for an individual puddle is modelled and related to the water evaporation rate. The model is tested and validated using data collected in a bench-scale environmental set-up under monitored environmental conditions.

## 4.1 Introduction

The typical urea ( $CON_2H_4$ ) concentration of swine urine is 0.16 to 0.60 mol L<sup>-1</sup> (Pond and Houpt, 1978), which can degrade to form up to two moles of ammonia ( $NH_3$ ) for every mole of  $CON_2H_4$ . This means that the 5.22-L of urine the average 60-kg pig expels in a day (Lewis and Southern, 2001) can emit up to 6.3 moles  $NH_3$  (107 g  $NH_3$ ). It is no wonder urine puddles on the floor are considered a main source of ammonia emissions in swine buildings, along with the slurry pit (Aarnink and Elzing, 1998).

Urea, the main component of urine, undergoes an enzymatic degradation reaction in the presence of the enzyme urease to form ammonia and carbonic acid ( $H_2CO_3$ ) (Mobley and Hausinger, 1989; eq. 4.1). Urease enzyme is commonly associated with fecal material and is considered abundant on fouled concrete floor surfaces of swine barns (Muck, 1982; Braam and Swierstra, 1999).



Ammonia is a weak base, and carbonic acid is a polyprotic acid; both compounds will ionize in water (eq. 4.2) to form ammonium ( $NH_4^+$ ), hydrogen carbonate ( $HCO_3^-$ ) and carbonate ( $CO_3^{2-}$ ) (Mobley and Hausinger, 1989; Chang, 1998).



The concentrations of  $NH_3$  and  $NH_4^+$  are often summed together in the term total ammoniacal nitrogen ( $TAN$ ), which is a measure of the mass of nitrogen nuclei in  $NH_3$  and  $NH_4^+$  ions present (Ni, 1999). Only  $NH_3$ , the unionized portion of  $TAN$ , will volatilize to the surrounding environment. The volatilization rate depends on the  $TAN$

concentration in the solution, *pH*, surface area, temperature and air velocity over the surface (Ni, 1999). Ammonia emission experiments by Elzing and Monteny (1997a) indicated urea conversion to ammonia and carbon dioxide began immediately when urine was sprinkled on a fouled floor surface. Initially the ammonia emission rate increased with time indicating the formation rate within the solution exceeded the volatilization rate. The ammonia emission rate reached a peak and began to decrease at a slower rate indicating ammonia formation had stopped or was slower than the volatilization rate (Elzing and Monteny, 1997a).

Muck and Steenhuis (1981), Elzing and Monteny (1997b), and Aarnink and Elzing (1998) have modelled the urine puddle emission process for dairy cow and swine urine, considering the enzymatic degradation of urea and the resulting change in liquid *TAN* concentration. One process that has been omitted from these models is water evaporation. Water evaporation can affect the urea and ammonia concentrations within a puddle, depending on the relative rates of urea degradation and ammonia volatilization to water evaporation, which in turn impacts the emission process.

The general goal of the research is to develop a dynamic model to simulate the ammonia concentration within and the emission from swine barns and given the potential emission from a single puddle, a urine puddle ammonia emission model was required. The three specific objectives addressed in developing this urine puddle model were: (1) to develop a model that simulates ammonia production and emission from individual urine puddles based on the known processes occurring within urine puddles including evaporation; (2) to measure the chemical and physical characteristics of individual,

simulated urine puddles in bench-scale emission chambers; and (3) to calibrate and validate the model with the measured results from the bench-scale experiment.

## 4.2 Urine Puddle Model Development

The main hypothesis in the urine puddle model development was that  $NH_3$  emission is a function of three main processes occurring simultaneously: water evaporation, urea degradation and a change in  $TAN$  concentration. The relative rates of these three processes impact the  $NH_3$  emission pattern,  $NH_3$  emission peak, and the puddle "life" (or length of time the puddle emits ammonia). The model development assumed that a single urine puddle was contained within an emission chamber on a solid, non-porous surface, with no drainage. The dependency between the three puddle processes and the emission chamber concentration, as well as the calculation procedure, are described in the following sections as each part of the model development is shown.

### 4.2.1 Water Evaporation

At the floor surface of a barn, ventilation and thermal gradients promote airflow (Randall, 1975). Therefore, convective mass transfer was assumed to be the main mechanism for fluid motion from a liquid phase to a gaseous phase. Equation 4.3 represents the convective mass transfer equation for water, also referred to as the puddle evaporation rate.

$$\frac{dV_P}{dt} = \frac{k_{H_2O} \cdot A_P}{\rho_{H_2O}} \cdot 1000 \cdot (\rho_v - \rho_{v,sat}) \quad (4.3)$$

The convective mass transfer coefficient ( $k$ ) was calculated using the boundary layer approximation (Incropera and DeWitt, 1996) for flow over a flat plate. For laminar flow conditions,  $k$  is approximated using equation 4.4. Laminar conditions are more likely because of low air velocities at the floor surface in the range of 0.2 to 1.0 m s<sup>-1</sup> (Ogilvie et

al., 1990) and small puddle area (resulting in a short puddle length,  $L$ ; Aarnink and Elzing, 1998).

$$k = \frac{D_{AB} \cdot 0.664 \cdot \text{Re}_x^{1/2} \cdot \text{Sc}^{1/3}}{L} \quad \text{when } \text{Re} < 0.5 \times 10^6, \text{ Sc} > 0.6. \quad (4.4)$$

The parameters  $\text{Re}$  and  $\text{Sc}$  depend on the kinematic viscosity ( $\nu$ ) of the bulk fluid, in this case air, whose temperature-dependency is modelled using a regression equation (eq. 4.5) developed from kinematic viscosity versus temperature data from Incropera and DeWitt (1996).

$$\nu = 4 \times 10^{-10} \cdot T^{1.859} \quad (4.5)$$

The parameter  $\text{Sc}$  is also dependant on the diffusivity of water (or any other substance A) in air (substance B). Welty et al. (1984) show that as temperature increases, diffusivity also increases exponentially. Equation 4.6 shows this relationship between the diffusivity at temperature  $T$  relative to diffusivity at a reference temperature of 298 K.

$$D_{AB}(T) = D_{AB}(298 \text{ K}) \cdot \left( \frac{T}{298} \right)^{1.5} \quad (4.6)$$

Based on the temperature dependency of  $\nu$  and  $D_{AB}$ , equation 4.4 was simplified to express the mass transfer coefficient as a function of surface length, temperature, velocity and the diffusivity at 298 K (eq. 4.7).

$$k = 0.0821 \cdot T^{0.7} \cdot \nu^{0.5} \cdot L^{-0.5} \cdot D_{AB}^{0.667}(298 \text{ K}) \quad (4.7)$$

Equation 4.7 is suitable for determining mass transfer coefficients for any gas into air, provided the diffusivity of the substance in air at 298 K is known, and laminar flow conditions exist. The diffusivity of water in air is  $26 \times 10^{-6} \text{ m}^2 \text{ s}^{-1}$  at 298 K (Incropera and DeWitt, 1996). The model calibration process tested the application of equation 4.7 to describe the convective mass transfer coefficient for water.

The saturated vapour density (eq. 4.8) was determined under the assumption that water vapour is a perfect gas and by using prescribed equations for calculating the water vapour saturation partial pressure (Albright, 1990).

$$\rho_{v,sat} = \frac{P_{sat} \cdot 18}{100000 \cdot 0.08315 \cdot T} \quad (4.8)$$

The vapour density of the bulk air above the puddle surface ( $\rho_v$ ) was calculated from the product of the relative humidity ( $RH$ ) and  $\rho_{v,sat}$  (eq. 4.9).

$$\rho_v = \frac{RH}{100} \cdot \rho_{v,sat} \quad (4.9)$$

#### 4.2.2 Urea Degradation

Muck (1982) found the urea conversion in a 2.2:1 mixture of feces and urine followed Michaelis-Menten kinetics. However, water evaporation can also impact the concentration of urea in the puddle. Equation 4.10 was used in this study to describe the change in urea concentration with time.

$$\frac{dU}{dt} = -\frac{S_m \cdot U}{K_m + U} - \frac{U}{V_p} \frac{dV_p}{dt} \quad (4.10)$$

Elzing and Monteny (1997b) and Aarnink and Elzing (1998) used a value of 0.002 mol L<sup>-1</sup> for the Michaelis constant,  $K_m$ , based on experimental results. This value of  $K_m$  is a fraction of the average urea concentration in urine puddles (0.16 to 0.60 M; Pond and Houpt, 1978), which suggests urease has a high affinity for the substrate urea (Shuler and Kargi, 2002).

Theoretically, enzymes are catalysts and are not used up in the reaction. However, changes in  $pH$  and temperature can affect the maximum reaction rate and the stability of the enzyme (Shuler and Kargi, 2002). Muck (1982) found urease activity ( $S_m$ ) of fresh

bovine feces increased with temperature from 10°C to 40°C and was at a maximum between  $pH$  6.8 and 7.6, which was accounted for in the ammonia emission model of Muck and Steenhuis (1981); urease activity was assumed constant throughout the urea degradation process in other models (Aarnink and Elzing, 1998; Elzing and Monteny, 1997b).

The model calibration process tested the assumptions that all the urea in a puddle is converted to ammonia during the emission process, and that urease activity is constant.

#### 4.2.3 Ammonia Concentration in the Puddle Solution

As ammonia concentration in a puddle increases from urea degradation (two moles of ammonia are produced for every mole of urea, eq. 4.1), ammonia will simultaneously be emitted from the puddle. Water evaporation will affect the resulting concentration as well. The relative rates of urea degradation, emission and evaporation were combined to express the dynamic  $TAN$  concentration within the puddle (eq. 4.11).

$$\frac{dTAN}{dt} = -2 \cdot \frac{S_m \cdot U}{K_m + U} - \frac{E_p}{V_p} - \frac{TAN}{V_p} \cdot \frac{dV_p}{dt} \quad (4.11)$$

The ammonia emission process (eq. 4.12) is similar to that of evaporation. In a swine barn environment, the room air concentration constitutes the bulk surrounding air ( $C_B$ ). For the emission chamber that was modelled and tested in this experiment, the concentration of air inside the emission chamber was the bulk surrounding air.

$$E_p = A_p \cdot k_{NH_3} \cdot 1000 \cdot (C_G - C_B) \quad (4.12)$$

The convective mass transfer coefficient for ammonia can also be calculated using the boundary layer approximation (eq. 4.7). Using this approximation, the mass transfer coefficients for water and ammonia differ only in the diffusivity of the given substance in



air at 298 K. Using the  $D_{NH_3,Air}$  value of  $28 \times 10^{-6} \text{ m}^2 \text{ s}^{-1}$  at 298 K (Incropera and DeWitt, 1996),  $k_{NH_3}$  was 1.05 times the value of  $k_{H_2O}$ .

The gas concentration of ammonia at the puddle surface ( $C_G$ ) can only be estimated from the liquid  $TAN$  concentration and theoretical equations to explain ammonia partitioning in solution, and between the liquid and gas phases. Only a fraction ( $f$ ) of the  $TAN$  in solution is in the form of ammonia. The relative concentrations of ammonia and ammonium are estimated using the acid ionization constant (also referred to as the dissociation constant;  $K_a$ ; eq. 4.13). A factor is often combined with  $K_a$  to account for other compounds in the solution affecting the relative concentrations of  $NH_3$ ,  $NH_4^+$  and  $H^+$  (Hashimoto and Ludington, 1971; Zhang et al., 1994; Arogo et al., 2003b).

$$K_a = \frac{\varphi_{NH_3} \cdot [NH_3] \cdot \varphi_{H^+} \cdot [H^+]}{\varphi_{NH_4^+} \cdot [NH_4^+]} \quad (4.13)$$

Rearranging equation 4.13 can provide relative estimates of ammonia and ammonium that can then be used to estimate  $f$ . Based on the estimated value of  $K_a$  that was reported by Jayaweera and Mikkelsen (1990) with the factor of 0.2 from Zhang et al. (1994), and the  $H^+$  concentration of the puddle (determined from the  $pH$ ),  $f$  was calculated using equation 4.14, similar to the urine puddle emission model of Aarnink and Elzing (1998).

$$f = \frac{[NH_3]}{[NH_3 + NH_4^+]} = \frac{10^{pH}}{10^{pH} + \frac{1}{K_a}} = \frac{10^{pH}}{10^{pH} + \frac{1}{0.2 \cdot 10^{-\left(0.0897 + \frac{2729}{T}\right)}}} = \frac{10^{pH}}{10^{pH} + 5 \cdot 10^{\left(0.0897 + \frac{2729}{T}\right)}} \quad (4.14)$$

A factor was used for  $K_a$  in eq. 4.14 because pig urine may typically contain many other ions and compounds including creatine, sodium, potassium and chlorine (Pond and Houpt, 1978).

Henry's Law is used to relate the concentration of ammonia in the gas at the puddle surface ( $C_G$ ) to the concentration in the liquid ( $C_L$ ), and was expressed as a dimensionless ratio of liquid concentration to gas concentration based on temperature, assuming an average temperature of 293 K (Aarnink and Elzing, 1998; eq. 4.15).

$$H = \frac{C_L}{C_G} = 1431 \cdot 1.053^{(293-T)} \quad (4.15)$$

Incorporating equations 4.7, 4.14 and 4.15 into equation 4.12, the ammonia emission from a urine puddle was calculated using equation 4.16:

$$E_P = k_{NH_3} \cdot A_P \cdot 1000 \cdot \left[ \frac{f \cdot TAN}{H} - C_B \right] \quad (4.16)$$

The *TAN* balance of a urine puddle (eq. 4.11) is shown rewritten in equation 4.17, incorporating equation 4.16 that fully describes the factors affecting puddle emission.

$$\frac{dTAN}{dt} = -2 \cdot \frac{S_m \cdot U}{K_m + U} - \frac{k_{NH_3} \cdot A_P \cdot 1000 \cdot \left( \frac{f \cdot TAN}{H} - C_B \right)}{V_P} - \frac{TAN}{V_P} \cdot \frac{dV_P}{dt} \quad (4.17)$$

#### 4.2.4 Molar Balance of Emission Chamber

When a urine puddle is contained within an enclosed emission chamber, as shown in figure 4.1, the puddle emission will contribute to the overall emission chamber concentration, which in turn, affects the puddle emission rate. Air inlets and outlets to the emission chamber, as well as the air exchange rates through these openings, also affect the emission chamber concentration as shown in equation 4.18. The emission chamber and support materials are assumed negligible contributors to the ammonia balance.

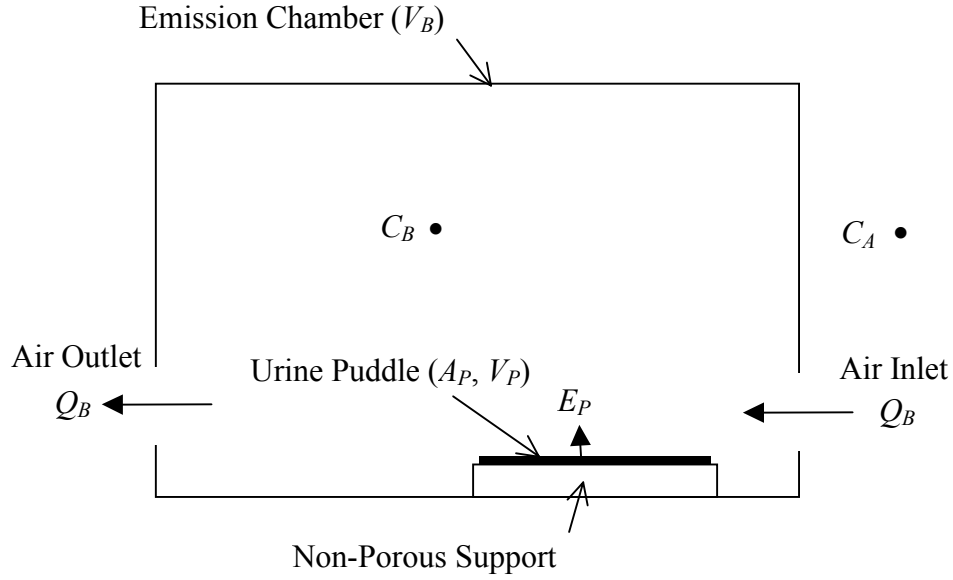


**Figure 4.1. Urine puddle emission model experimental set-up.**

$$\frac{dC_B}{dt} = \frac{Q_B \cdot (C_A - C_B)}{V_B} + \frac{k_{NH_3} \cdot A_P \cdot 1000 \cdot \left( \frac{f \cdot TAN}{H} - C_B \right)}{V_B} \quad (4.18)$$

#### 4.2.5 Calculation Method

The resulting system of differential equations describing the puddle characteristics and chamber concentration over time are equations 4.3, 4.10, 4.17 and 4.18. Fourth-order Runge-Kutta (Rao, 2002) was the explicit method used for solving the system of differential equations. The initial  $V_P$ ,  $U$ ,  $TAN$  and  $C_B$  were used simultaneously to calculate the new value for each variable after a prescribed timestep ( $h$ ). After each step in the Runge-Kutta method, the new value for  $TAN$  was used to calculate the puddle emission rate (eq. 4.16). A stepsize of 300 s was used in the calculations, and was tested during model development to ensure error was not introduced to the results compared with a smaller stepsize (120 s). All calculations were performed using MSExcel®.

### 4.3 Materials and Method

A bench-scale experimental set-up was used to collect data from individual urine puddles in order to calibrate and validate the developed model.

#### 4.3.1 Emission Chambers

Individual urine puddles were monitored within stainless steel emission chambers (900 mm length, 900 mm width, 700 mm height), as described in Pelletier et al. (2005) and shown in figure 4.2. The outlet line from each chamber was connected to a blower and the flowrate out of each chamber was monitored by a rotameter (KSK Flowmeter, Kobald, Point Claire, QC). Air was drawn into the chambers through a 530-mm long by 2-mm high slit in the front of the chamber, just above the puddle surface. Six chambers were contained in six separate rooms with individual temperature control, and supplied by a common incoming air plenum.

In each chamber a 254-mm diameter Corelle® plate was placed atop a balance (Model EK-1200i, A&D Company Ltd., Place; accuracy:  $\pm 0.1$  g) to hold the urine solution. A thin tube (1.67-mm outer diameter) was taped to the middle of the plate and the other end of the tube was led outside of the emission chamber where a syringe could be attached in order to draw liquid samples from the plate.

Sensors (Model CS500, Campbell Scientific (Canada) Corp., Edmonton, AB) monitored the temperature ( $\pm 0.5^{\circ}\text{C}$ ) and relative humidity ( $\pm 3\%$  RH) near the outlet of each emission chamber and in the inlet plenum. A thermal anemometer (TSI Model 8470 Air Velocity Transducer, St. Paul, MN; range: 0 to  $0.5\text{ m s}^{-1}$ ) measured the air velocity above the surface of one puddle each sampling period. The anemometer was placed in a different emission chamber each sampling period. The average air velocities

approximately 2 cm above the plate surface were 0.10 and 0.18 m s<sup>-1</sup> for flowrates of 0.47 and 0.93 L s<sup>-1</sup>, respectively.

The ammonia concentration at the outlet of each emission chamber and in the inlet plenum was measured using photoacoustic infra-red spectroscopy (Model 1312, Innova AirTech Instruments A/S, Ballerup, Denmark). The analyzer accuracy was verified with standard ammonia gas (BOC Canada, Mississauga, ON) once each sampling day. A multiple port valve system cycled between lines connected to each emission chamber, inlet and standard gas (as required). The airflow rate for gas sampling was 0.03 L s<sup>-1</sup>.



**Figure 4.2. Stainless steel emission chamber, anemometer, plate, balance and sampling tube, used as part of the ammonia emission testing apparatus.**

#### **4.3.2 Experimental Procedure**

To create a variety of puddle emission conditions the air temperature, air velocity and urea concentration factors were combined in a 3×2×2 factorial treatment design,

respectively, as shown in table 4.1 with assigned Treatment names. Six simulated urine puddles were used during each 44-h sampling period. During each sampling period, the same airflow rate of either 0.47 or 0.93 L s<sup>-1</sup> was maintained through each chamber to create air velocity conditions of 0.10 or 0.18 m s<sup>-1</sup>, respectively. Each temperature and urea concentration combination was represented in each sampling period. Each treatment was replicated three times for a total of 36 data-sets collected over six sampling periods.

**Table 4.1. Treatment combinations and identification.**

Treatment	Airspeed (m s <sup>-1</sup> )	Urea Concentration (mol L <sup>-1</sup> )	Temperature <sup>z</sup> (K)
1	0.10	0.4	289
2	0.10	0.4	294
3	0.10	0.4	299
4	0.10	0.2	289
5	0.10	0.2	294
6	0.10	0.2	299
7	0.18	0.4	289
8	0.18	0.4	294
9	0.18	0.4	299
10	0.18	0.2	289
11	0.18	0.2	294
12	0.18	0.2	299

<sup>z</sup> Temperature set-point values are shown; the measured temperature values for each puddle with respect to elapsed time were used in the model calculations.

Before each sampling period, the plates were washed and dried, placed on the scales and the liquid sampling lines were attached. Urea solutions (ACS grade urea, EM Science, Germany; and distilled water) were prepared fresh daily and a sample was taken for *TAN* analysis by automated colorimetry. At the start of each sampling period, a measured mass of Jack Bean urease enzyme (Type IX from Jack Beans, Sigma Chemical Company, St. Louis, MO; 0.69×10<sup>-3</sup> mol U s<sup>-1</sup> g<sup>-1</sup> rated activity at 298 K and *pH* 7.0) was mixed thoroughly with 250 ml of urea solution in a beaker and gently poured onto the plate in one of the emission chambers. The cover of the emission chamber was replaced

and was not opened until the end of the sampling period. This was repeated for each sample.

The plate and solution mass, temperature, relative humidity and air velocity measurements were recorded every 10 min electronically throughout the sampling periods. The gas analyzer collected concentration readings at 45-s intervals over a span of 10 min for each sampling location, but only the data from the last four minutes were averaged to generate the concentration level for the chamber (or inlet).

Liquid samples of the puddle solution were withdrawn by syringe approximately 1, 5, 11, 17, 24, 34 and 44 h after the start of each sampling period. Before sampling, the tube was purged by pushing air through with the syringe. Approximately 6 mL of puddle solution was drawn each sample: 3 mL were stabilized in 0.24 N sulphuric acid solution and analyzed for total ammonium-*N* concentration by automated colorimetry; the *pH* of the remaining sample was measured with *pH* test strips (Sigma Chemical Company, St. Louis, MO; range: 4.5-10.0; accuracy:  $\pm 0.5$ ). Some *pH* measurements were repeated with a *pH* meter (Oakton Economy *pH* Benchtop Meter; accuracy:  $\pm 0.01$ ), to increase accuracy and verify the *pH* strip measurements.

The surface area of the puddle solution on the Corelle® plates decreased as the water evaporated. An equation was developed to describe the puddle area based on measured surface areas for known amounts of water on each plate. The solution surface area decreased from 0.036 to 0.024 m<sup>2</sup> as the volume of water decreased from 0.250 to 0.015 L.

#### 4.3.3 Calibration and Validation Procedure

The temperature, relative humidity, air velocity, initial urea concentration, urease activity and initial puddle mass were used as input variables to the puddle emission model. In the calibration process, the hypotheses regarding the mass transfer coefficient of water, the percentage of urea conversion and constant urease activity, and constant *pH* were tested by comparing model simulations to measured values for water mass, liquid *TAN* concentration and total emission and making adjustments to the model as required. The model was validated by comparing water mass, liquid *TAN* concentration, total emission and ultimately *pH* simulations for individual puddles to corresponding measurements. Twelve data sets that included a random sample of each treatment combination were used in the calibration process, and the other two data sets for each combination were used for validation. Of the 12 calibration data sets, six sets included *pH* meter measurements, while the remaining six sets had only *pH* strip measurements. Six of the validation data sets also had *pH* meter measurements.

The standard prepared by ASTM (2003) was used as a guideline for evaluating model accuracy during the calibration and validation processes. The statistical calculations and suggested evaluation limits are shown in Appendix A.

#### 4.4 General Results

The carefully controlled conditions of this experiment resulted in very similar results between trials for a given treatment. Figure 4.3 shows the similarity between repetitions using the *TAN* concentration measurements taken from Treatment 2 samples as an example. The *TAN* concentration of each puddle initially increased sharply, followed by a slightly slower rate of decrease. The decrease in concentration presumably occurred once the urea was used up. The *TAN* concentration pattern (fast increase and slower



decrease) was echoed in the emission chamber  $NH_3$  concentration measurements indicating the puddle emission pattern was similar to the pattern described by Elzing and Monteny (1997a).

These general results validated two of the main processes, urea degradation and change in *TAN* concentration, were occurring. Balance measurements and the lack of water on the plates after each trial validated water evaporation also occurred. The main hypothesis that ammonia emission is a function of water evaporation, urea degradation and change in *TAN* concentration was therefore accepted and the model calibration process continued.

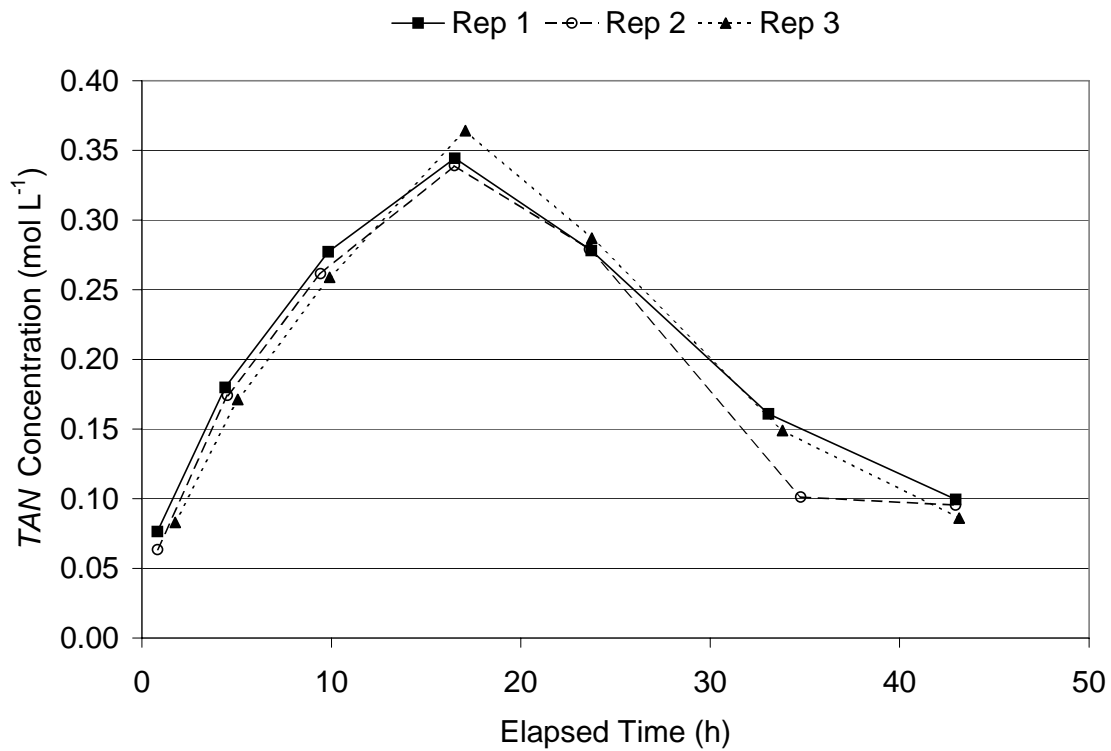


**Figure 4.3. Measured *TAN* concentration values for three repetitions of Treatment 2.**

#### 4.4.1 Calibration Results

Model calibration was an iterative procedure because of the inter-relations between water volume, urea conversion, *TAN* concentration, and as found in the calibration procedure, urease activity and *pH*. Therefore, fitting procedures for some variables were completed simultaneously.

##### 4.4.1.1 Water evaporation

Using the balance data for the twelve calibration data sets, the measured water mass values were compared to the predicted volume values assuming the density of the simulated urine puddles was constant and equal to  $1 \text{ kg L}^{-1}$ . The resulting correlation coefficient (*R*) values for each data-set (each representing a different treatment) were at least 0.99. The fractional bias values ranged from -0.01 to 0.01, which means the average predicted water volume was within  $\pm 1\%$  of the measured water mass. All other evaluation parameters prescribed by ASTM (2003) were well within the suggested limits.

Since the boundary layer theory approximation (eq. 4.7) proved accurate for modelling  $k_{H_2O}$  and the resulting evaporation, equation 4.7 was used to calculate  $k_{NH_3}$  as well.

##### 4.4.1.2 Urea conversion

If all the urea was used up during the emission process, the total amount of ammonia emitted by the end of the emission process should have been twice the initial number of moles of urea in solution. For each calibration data-set, the measured total puddle emission plus any ammonia remaining in the puddle solution at the end of the sampling period, minus an approximation of the urea and ammonia removed when liquid samples were taken, was calculated. The percentage of urea converted to ammonia ranged from 84% to 100%. Treatments 1 to 6 ( $0.10 \text{ m s}^{-1}$  airspeed) resulted in urea conversion

percentages between 84% and 93%, and Treatments 7 to 12 ( $0.18 \text{ m s}^{-1}$  airspeed) had urea conversion percentages between 92% and 100%.

The measurements supported the hypothesis that all the urea in the puddle solutions can be converted to ammonia. In the model calculations however, it was necessary to account for urea removed with the samples in order to prevent the total emission from being over-predicted.

#### **4.4.1.3 Urease activity**

The average rated activity for the Jack Bean urease used in the experiment was  $58.5 \times 10^{-6} \text{ mol U L}^{-1} \text{ s}^{-1}$  (range  $20.2 \times 10^{-6}$  to  $75.2 \times 10^{-6} \text{ mol U L}^{-1} \text{ s}^{-1}$ ) at a  $pH$  of 7.0 and a temperature of 298 K. These urease activity values and the estimate of  $0.002 \text{ mol L}^{-1}$  for  $K_m$  (Elzing and Monteny, 1997b) were used in initial model simulations. The simulated ammonia production rate resulted in higher  $TAN$  concentrations of the puddles compared to the measured  $TAN$  concentrations. The literature value for  $K_m$  was considerably smaller than the initial urea concentration levels so there was theoretically little impact of this variable. The error was attributed to temperature and  $pH$  effects on the enzyme activity (Shuler and Kargi, 2002; Muck, 1982), resulting in lower urease activities than the rated levels.

An initial test was performed to detect the level and general pattern of the urease activity within the puddle solutions by individually fitting two urease activity values to each sample, representing the average activity for the first two to four hours of urea conversion and the remaining time of urea conversion, respectively. The initial urease activity ( $S_{m,0}$ ) was assumed constant for all samples and the best-fit between simulated and measured  $TAN$  concentration values occurred for a value of  $8 \times 10^{-6} \text{ mol U L}^{-1} \text{ s}^{-1}$ .

With a value for  $S_{m,0}$ , the secondary  $S_m$  value producing the best fit between measured and simulated  $TAN$  concentration values for each of the twelve calibration samples was determined individually for each puddle. This was completed after the initial  $pH$  model was developed, as shown in the next section. The fitted urease activity values decreased over time, and at a faster rate for cooler temperatures (fig. 4.4).

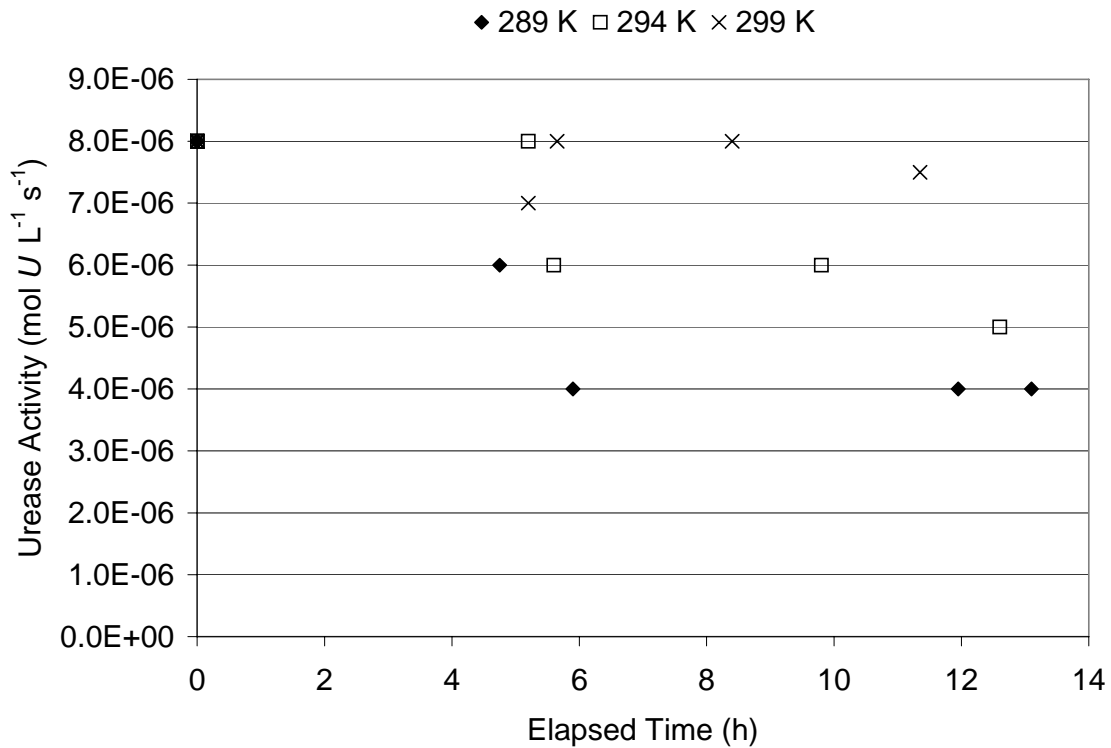


**Figure 4.4. Fitted urease activity values based on elapsed time and temperature.**

The effect of elevated  $pH$  during the urea degradation process (see following section on Urine puddle  $pH$ ) was assumed consistent between treatments and the main reason behind the drop in the initial urease activity to  $8 \times 10^{-6} \text{ mol U L}^{-1} \text{ s}^{-1}$ . Further perceived changes in the urease activity level were attributed to temperature effects. The temperature effect on enzyme activity is generally expressed by an Arrhenius relationship (Muck, 1982; Shuler and Kargi, 2002), but because the enzyme was at similar conditions

before being added to the puddle solutions at different temperatures, there was a perceived time delay for the temperature impact as well. Equation 4.19 was developed to express the change in urease activity over time based on the difference from the optimal temperature for the Jack Bean urease enzyme used in this experiment. From figure 4.4, the optimal temperature appeared to be close to the Jack Bean Urease prescribed temperature of 298 K; therefore, 298 K was incorporated in equation 4.19 as the point from which  $S_m$  decreased with decreasing temperature. The rate at which  $S_m$  decreased with decreasing temperature and increasing time was described with the variable  $j$ .

$$S_m = S_{m,0} \cdot e^{-j \cdot \left( \frac{1}{T} - \frac{1}{298} \right) \cdot t} \quad (4.19)$$

Equation 4.19 was applied in the simulations for the twelve calibration samples and the value of  $j$  was varied from 0.050 to 0.300 in 0.025 increments to determine the best fit between measured and modelled values of  $TAN$ , for measurements taken when the  $TAN$  concentration of each puddle was increasing with time. A  $j$ -value of 0.225 produced the lowest  $NMSE$  (0.027) and  $FB$  value closest to zero (-0.0027). As shown in figure 4.5, the regression line between 36 measured and simulated  $TAN$  concentration pairs (representing two to five sampling points from each of the twelve data-sets) had a slope near 1 and an intercept less than 7% of the average measured mean  $TAN$  concentration. Figure 4.5 also shows that at low concentration values, the data pairs are in better agreement, indicating the use of a common  $S_{m,0}$  was justified.

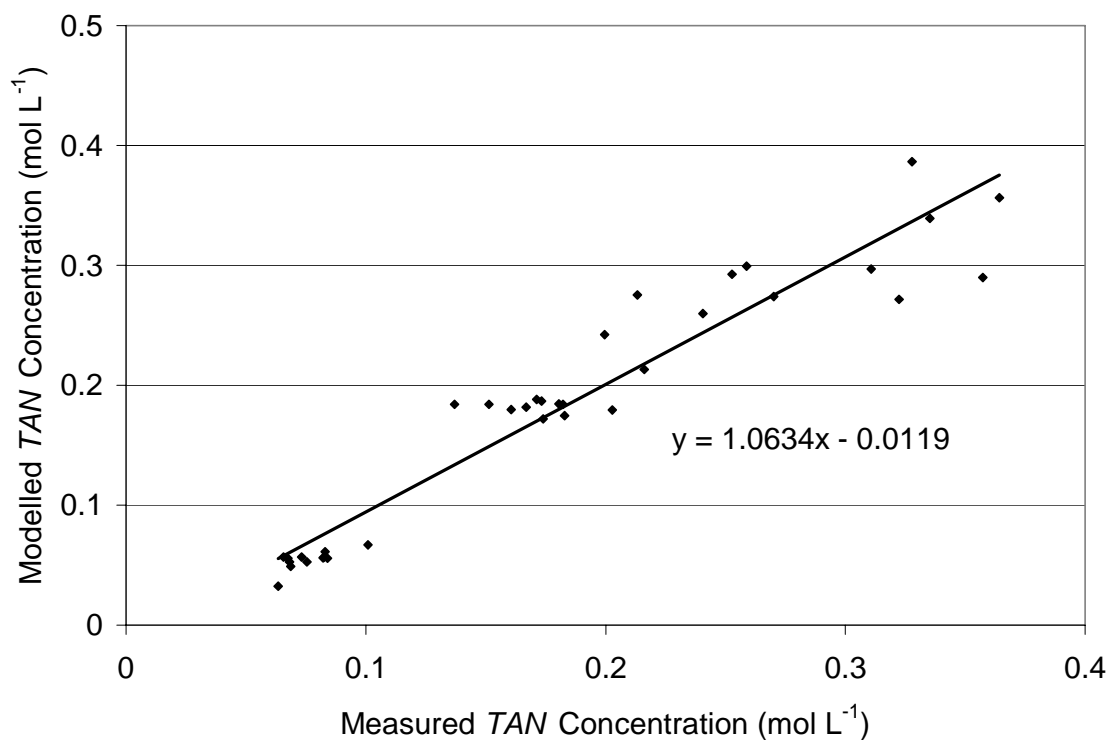


**Figure 4.5. Measured and modelled *TAN* values of all calibration data sets using the developed urease activity model (eq. 4.19;  $j = 0.225$ ).**

#### **4.4.1.4 Puddle *pH***

The urine puddle *pH* levels were between 9.1 and 9.3 at the one-hour sampling point, and decreased over the life of the puddle (figure 4.6). The initial rate of decrease was slow, and this corresponded to when the measured *TAN* concentrations of the puddles were increasing. Towards the end of the sampling period, the *pH* levels stabilized.

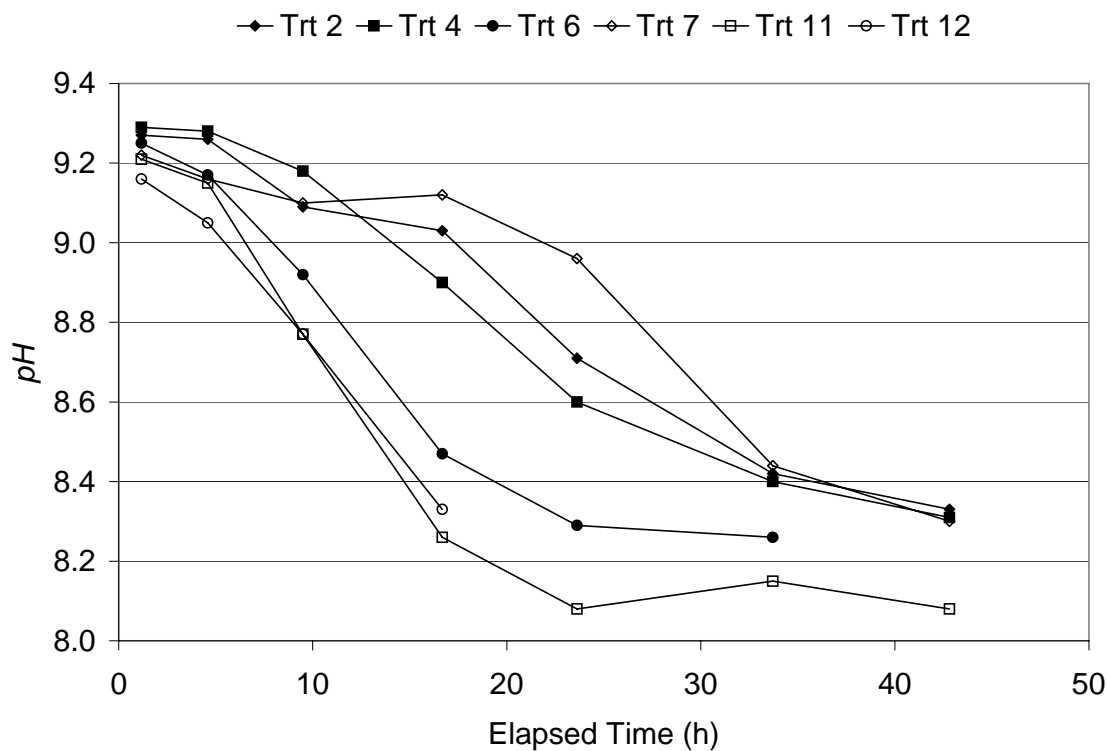


**Figure 4.6. Measured puddle  $pH$  over time for six of the twelve treatments.**

During initial simulations, the urine puddle  $pH$  was assumed constant at a value of 8.8 (Aarnink and Elzing, 1998). The resulting  $E_{P,T}$  and  $TAN$  simulations were significantly different from measured values. Using measured  $pH$  values greatly improved the model's accuracy up to the point where the  $pH$  measurements started to stabilize. Subsequent to this point, using the measured  $pH$  level in the calculation of  $f$  (eq. 4.14) seemed to underestimate the amount of ammonia available; the simulated  $TAN$  concentration would begin to increase and the total emission was lower than the measured emission indicating that ammonia was being retained in the puddle in the simulations. The hypothesis that a constant  $pH$  could be used in the model was shown to be false.

As urea breaks down, carbonic acid is created in conjunction with ammonia, so the puddle  $pH$  was likely the result of the combined  $TAN$  and  $H_2CO_3/HCO_3^-/CO_3^{2-}$  content of the puddles. A mechanistic equation to describe the change in  $H_2CO_3/HCO_3^-/CO_3^{2-}$  was therefore investigated, but measurements were not available to properly validate the equation. Instead, a two-part empirical model was developed to simulate the change in  $pH$  over time, based on the change in  $TAN$  (eqs. 4.20 and 4.21). Two regression coefficients,  $Z_1$  and  $Z_2$  were used because the relationship between the change in  $pH$  and change in  $TAN$  should be different depending on whether there was both urea degradation and emission occurring (i.e.  $d(TAN)/dt > 0$ ) or only emission occurring ( $d(TAN)/dt < 0$ ). Also, equation 4.14 was modified so that  $f$  had a minimum value (eq. 4.22). An estimated value for the initial puddle  $pH$  was required by the model.

$$\frac{d(pH)}{dt} = Z_1 \cdot \frac{d(TAN)}{dt} \quad \text{for } \frac{d(TAN)}{dt} > 0 \quad (4.20)$$

$$\frac{d(pH)}{dt} = Z_2 \cdot \frac{d(TAN)}{dt} \quad \text{for } \frac{d(TAN)}{dt} < 0 \quad (4.21)$$

$$f = \text{MAXIMUM} \left( \frac{10^{pH}}{10^{pH} + 5 \cdot 10^{\left(0.0897 + \frac{2729}{T}\right)}}, f_{\min} \right) \quad (4.22)$$

The initial slope,  $Z_1$ , was tested with the six calibration data sets with  $pH$  meter measurements and the corresponding  $TAN$  measurements. The value of  $Z_1$  was fit by varying the value of  $Z_1$  from -0.5 to -1.0 in increments of 0.05 and multiplying  $Z_1$  with the measured change in  $TAN$  with time to produce different patterns in the change of  $pH$ . The best fit between modelled and measured  $pH$  values was obtained for a slope ( $Z_1$ ) of -0.75.



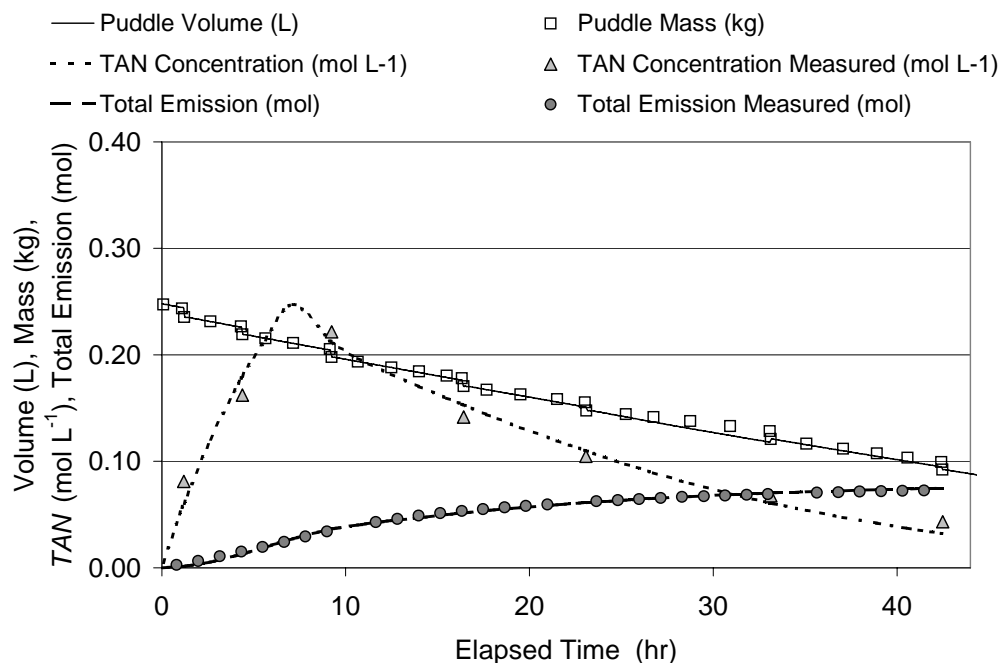
The secondary slope,  $Z_2$ , was fit in conjunction with the minimum  $f$ -value by comparing the measured and simulated values for both  $TAN$  concentration and  $pH$ . The value of  $Z_2$  was varied between 3 and 7 in increments of 1, and  $f_{min}$  was varied between 0 and 1.0 in increments of 0.25. For both  $TAN$  concentration and  $pH$  simulations, a  $Z_2$  value of 6.0 was optimal when used in conjunction with a  $f_{min}$  value of 0.05.

#### **4.4.1.5 Calibration summary**

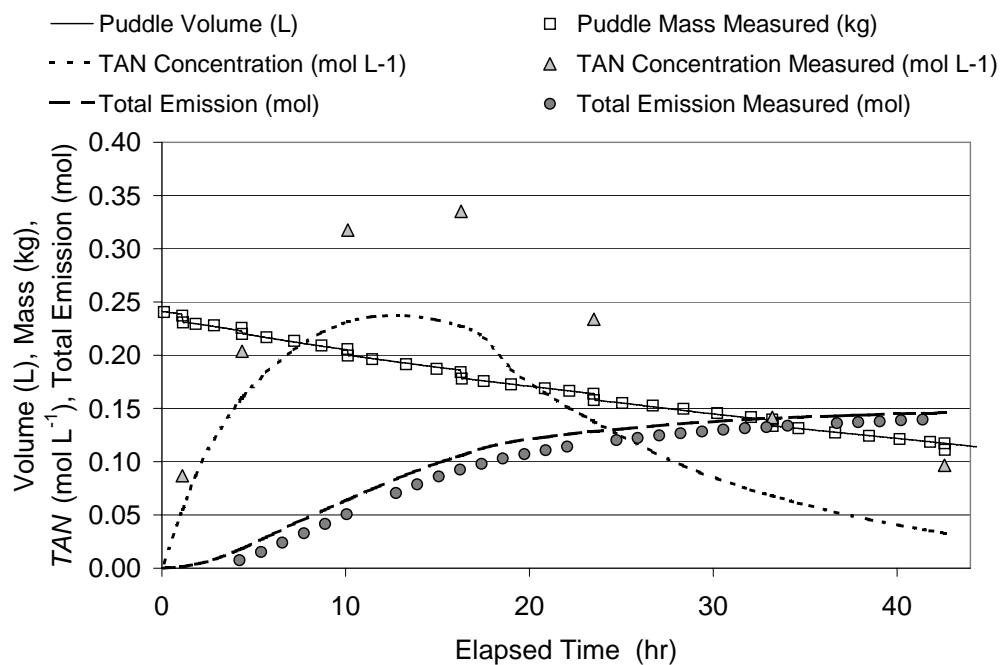
The model to simulate ammonia emissions and liquid  $TAN$  concentration was made more complex, but also more accurate based on the calibration procedure. Equations 4.19, 4.20, 4.21 and 4.22 were added to the system of equations describing the puddle, along with the fitted values for  $j$ ,  $Z_1$ ,  $Z_2$  and  $f_{min}$ , and also solved explicitly in time.

#### **4.4.2 Validation Results**

Using the calibrated model the simulations for water volume,  $pH$ ,  $TAN$  and total ammonia emission ( $E_{P,Tot}$ ) for the validation sub-sets (24 sub-sets in total) were compared to the respective measured values. Figure 4.7 displays the measured and simulated results for one repetition each of Treatments 5 and 7 as examples of the model simulations compared to measurements. The overall results of all validation simulations are shown in table 4.2, and explained in further detail in the following sections.



(a)



(b)

**Figure 4.7. Simulated and measured puddle characteristics for Treatment 5 (a) and Treatment 7 (b).**

**Table 4.2. Comparison of average (n=24) evaluation parameters for  $V_P$ ,  $pH$ ,  $TAN$  and total emission (mol  $NH_3$ ).**

Parameter	Average evaluation parameter							
	$V_P$		$pH$		$TAN$		<i>Total Emission</i>	
	Mean	(SD) <sup>z</sup>	Mean	(SD)	Mean	(SD)	Mean	(SD)
General Agreement								
<i>R</i>	0.99	(<0.01)	0.89	(0.29)	0.90	(0.20)	1.00	(0.01)
<i>a</i>	1.00	(0.02)	1.10	(0.50)	0.99	(0.25)	1.01	(0.07)
<i>b</i>	-0.001	(0.005)	-1.20	(4.61)	-0.019	(0.033)	0.0001	(0.007)
<i>NMSE</i>	<0.001	(<0.001)	0.002	(0.002)	0.096	(0.112)	0.012	(0.012)
Bias								
<i>FB</i>	-0.005	(0.010)	-0.027	(0.024)	-0.157	(0.13)	0.003	(0.10)
<i>FS</i>	0.007	(0.053)	0.134	(0.76)	0.169	(0.29)	0.020	(0.13)

<sup>z</sup> SD: Standard deviation.

#### 4.4.2.1 Water evaporation

No changes were made to the water evaporation model based on the calibration results. During validation with the evaporation data for 24 urine puddles, equation 4.3 with equation 4.7 to describe  $k_{H_2O}$  again proved very accurate (table 4.2) for modelling the change in water mass. The evaluation parameters were all very low, with an average bias less than 1%, based on the mean measured and simulated values for each puddle.

#### 4.4.2.2 Puddle $pH$

Based on the comparison of simulated  $pH$  values to  $pH$  values measured using both  $pH$  strips and a  $pH$  meter, the model simulated the puddle  $pH$  well. The average simulated  $pH$  for all puddles was about 3% lower than the average measured  $pH$  value, and all other evaluation parameters, with the exception of *R*, were within suggested limits set by ASTM (2003).

#### 4.4.2.3 Liquid $TAN$ concentration

Figure 4.8 shows the normalized mean square error (NMSE) between measured and simulated  $TAN$  values for the validation data sets, based on treatment. The largest *NMSE* value occurred with Rep 2 of Treatment 11. It was noted during data collection that some

enzyme was lost before it was added to the solution for this particular puddle, resulting in this sample having the lowest potential  $S_m$  ( $2.02 \times 10^{-6} \text{ mol } U \text{ L}^{-1} \text{ s}^{-1}$ ) based on the mass of enzyme added to the solution; since the model assumed constant urease activity between all samples, the *TAN* concentration was likely over-predicted.

For the majority of the other samples, *NMSE* values below 0.1 show that the simulated values for *TAN* concentration over the life cycle of each puddle were within  $\pm 0.05 \text{ mol L}^{-1}$  of the measured values. In general, the average *TAN* concentration for each puddle was under-predicted 16% by the model (*FB*: -0.157) and larger bias values were associated with treatments 7 to 12 with the higher air velocity, compared to treatments 1 to 6 with a lower air velocity. The average values of all evaluation parameters (table 4.2) were within the values suggested by ASTM (2003) for adequate model performance.

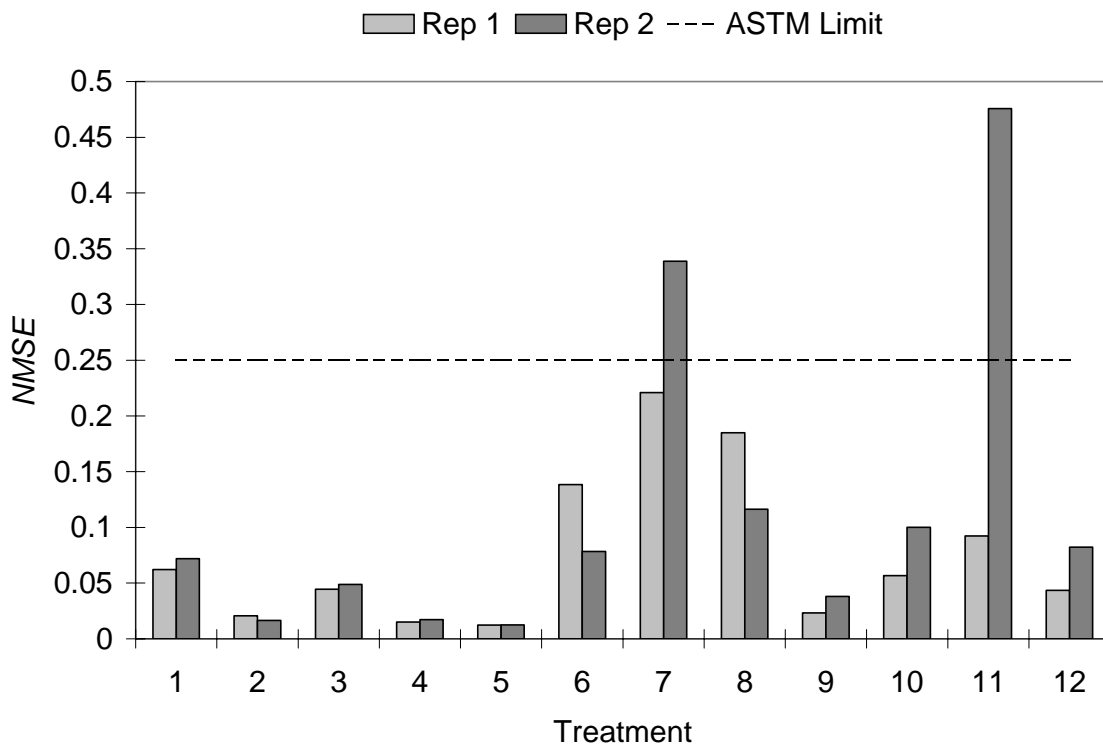


**Figure 4.8. *NMSE* values for *TAN* simulations, shown based on treatment.**

#### 4.4.2.4 Total emission

Based on the average *NMSE* value for all validation data-sets (table 4.2), the simulated total emission values over time for the validation data sets were  $\pm 11\%$  of the measured emission levels (based on the measured inlet and outlet ammonia concentrations and the air exchange rate of the emission chambers). Table 4.2 displays the averages for the remaining evaluation parameters that were well within the ASTM (2003) suggested limits.

#### 4.4.3 Model Application

When the urine puddle emission model is applied to a real-life situation of a urine puddle on the floor of a barn, certain conditions will be different, and inconsistent variables like temperature, air velocity, relative humidity and urease activity can potentially affect the rate the ammonia is given off from the puddle, the "life" of the puddle, and the total emission. In the following analysis, the following assumptions were made when testing the effect of varying environmental conditions: an initial urea concentration of  $0.4 \text{ mol L}^{-1}$ ; all of the urea was converted to ammonia; the surrounding air concentration ( $C_B$ ) was negligible; no drainage or absorption of solution by the floor surface; puddle area and depth were consistent with the puddle shape on a Corelle® plate; and urease activity was constant over the life of the puddle and not temperature-dependent.

Table 4.3 shows the resulting puddle emission and puddle life expectancy when the value of one variable is changed from the mean value, with the other variables remaining at the mean value.

**Table 4.3. Urine puddle model results for varying environmental conditions.**

Variable (Mean Value)	Value	Average Emission Rate (g $NH_3$ d <sup>-1</sup> )	Puddle life (d)	Total Emission (g $NH_3$ )
Mean		0.83	4.1	3.4
Temperature (293 K)	283	0.44	7.7	3.4
	303	1.50	2.3	3.4
Velocity (0.1 m s <sup>-1</sup> )	0.05	0.58	5.8	3.4
	0.40	1.65	2.1	3.4
Relative Humidity (50%)	20	1.32	2.6	3.4
	80	0.33	>10	3.4
Urease Activity ( $6 \times 10^{-6}$ mol $U$ L <sup>-1</sup> s <sup>-1</sup> )	$1 \times 10^{-6}$	0.35	4.1	1.4
	$2 \times 10^{-6}$	0.69	4.1	2.9
	$3 \times 10^{-6}$	0.82	4.1	3.4
	$4 \times 10^{-6}$	0.82	4.1	3.4
	$5 \times 10^{-6}$	0.82	4.1	3.4
	$6 \times 10^{-6}$	0.83	4.1	3.4
	$7 \times 10^{-6}$	0.82	4.1	3.4
	$8 \times 10^{-6}$	0.82	4.1	3.4
	$9 \times 10^{-6}$	0.83	4.1	3.4
	$1 \times 10^{-5}$	0.82	4.1	3.4

The total emission, equal to the average emission rate multiplied by the puddle life, was equal for nearly all situations tested. As was determined from the measurements, ammonia emission will occur over the length of the puddle life, since some *TAN* will always be present as ammonium in solution. Therefore, increasing temperature, velocity, or decreasing the relative humidity rate will not only decrease the puddle life, but increase the average emission rate as well. For urine puddles with the same initial urea concentration and volume, a low urease activity can reduce the total ammonia emitted from a puddle if the urease activity is sufficiently smaller than the emission rate. Above a certain urease activity ( $3 \times 10^{-6}$  mol  $U$  L<sup>-1</sup> s<sup>-1</sup> for the simulated urine puddle), urease activity has a negligible effect on the average emission, puddle life or total emission.

## 4.5 Discussion

Urine puddles are an important consideration in ammonia emission models for rooms with partially and fully-slatted floors. Ni et al. (1999c) found a high correlation ( $R = 0.852$ ) between ammonia emission rate and floor contamination. This experiment reinforces the initial calculations made of the potential emission from a single pig, just from the urine, if all the urea in a puddle is converted to ammonia.

These bench-scale measurements provided valuable data to calibrate and validate equations predicting the physical, chemical and biological processes occurring within a urine puddle. With carefully controlled and/or monitored temperature, airspeed, chemical composition, and absorption by extraneous sites, fewer assumptions were needed than in a real-world situation of a puddle on the floor of a barn. While the puddle emission model has been made more complex by considering water evaporation, urease activity inhibition and puddle  $pH$  changes over time, the relative weight of factors affecting ammonia emission are now better understood. The potential differences between the environmentally-controlled conditions used in this experiment and the "real-world" situation of a urine puddle on the solid or slatted floor of a barn are addressed in this section where possible.

Overall, the model provided accurate estimations of the water evaporation, puddle  $pH$ , liquid concentration and total emission for simulated urine puddles, based on the guideline values prescribed by ASTM (2003). By using various statistical analyses to calibrate the model and also validate the resulting system of equations, the model was capable of providing not only reasonable average values, but also simulated the changing values over time well compared to the measurements.

By using the boundary layer approximation to calculate the mass transfer coefficient for water and ammonia, the  $k_{NH_3}$  value was 1.05 times higher than  $k_{H_2O}$ , meaning the resistance to transport of water through the boundary layer film over the liquid surface was higher than that of ammonia. While water evaporation did impact the resulting concentrations, the major processes affecting the rate of ammonia emission in this experiment were urea degradation and ammonia concentration of the liquid.

Under experimental conditions, the majority (if not all) of the urea was converted to ammonia and all of this ammonia was released as the puddle evaporated. Since ammonia ionizes in water, some ammonia will exist in the puddle as long as there is water. In the real-world, from casual observations, urine puddles on the floor are not perfect circles with a consistent depth that last over 44 h. Ammonia emission from a mixture of 2 kg of cow urine and 3 kg of cow feces on a bench-scale slatted floor surface fell to near zero after 24 hr (Elzing and Monteny, 1997a), a time-scale that seems more typical on the floor surface. A concrete slatted floor will allow some urine to drain into the pit, and some liquid may also enter the pores of the concrete. If some drainage or absorption occurs before all of the urea is converted by enzyme present on the floor surface, the potential emission may be less than seen in these measurements. As well, absorption of ammonia-containing solution by the floor may delay the emission process.

Enzyme activity is not a direct measurement; instead the rate of formation of enzyme/substrate-specific products is usually measured using various substrate concentrations, and the resulting rates are analyzed using one of numerous methods (Shuler and Kargi, 2002). In this experiment, urease activity was initially based on the provided rated activity and amount of enzyme used, but finally the enzyme activities



were estimated based on the measured *TAN* concentration over time, which also relied on accurate estimations of emission, *pH* and evaporation. A common enzyme was added to all puddles in one sampling period from a common temperature state, so the assumption of a common  $S_{m,0}$  seemed valid and fit well with the experimental data. A similar *pH* level for all puddles during the initial ammonia formation period (figure 4.7) supported the decision to assume temperature and time had the largest effects on enzyme activity. A decrease in activity at a lower temperature resembles data found in the literature (Muck, 1982; Shuler and Kargi, 2002), although elapsed time was not considered in these models. In the real-world situation, the enzyme source will likely be fecal matter and more variable than the Jack Bean source used in this experiment, although the specific differences between the enzyme sources are not known. Also, the urease (from faecal material) temperature will likely be at equilibrium with the floor surface. Even though a urine puddle will be body temperature when excreted, the puddle will likely assume the temperature of the floor and enzyme source relatively quickly, and the temperature effect over time will be less important. While simulating the change in urease activity was beneficial in modelling the ammonia emission from the simulated urine puddles in this experiment, in the case of urease activity on the barn floor surface it may be safe to assume a constant value of  $S_m$ .

Urease activity has been shown to depend on the amount of fouling and floor surface characteristics, but after 7 to 15 days of repeated fouling, the increasing urease activity appeared to have a negligible effect on the ammonia emission rate (Elzing and Monteny, 1997b; Braam et al., 1997a). This was reiterated in the Model Application section that shows urease activity will have a negligible impact on the ammonia emission rate past a

certain value. The value where urease activity becomes negligible will depend on the other puddle emission factors though, so the non-limiting urease activity value simulated in the Model Application section cannot necessarily be applied for all puddle emission simulations.

An increase in ammonia concentration in a pure ammonia and water solution would result in a  $pH$  increase but this was not seen in the simulated urine puddles after the first  $pH$  measurement. This was attributed to the buffering effect of the carbonic acid, and the theory is as follows. In the absence of any volatilization from the solution, the  $TAN$  would increase at twice the rate of the  $H_2CO_3/HCO_3^-/CO_3^{2-}$  concentration. Carbonic acid produced by the breakdown of urea lowers the overall  $pH$  of the system by contributing  $H^+$  ions to solution. Carbonic acid,  $HCO_3^-$  and  $CO_3^{2-}$  will exist in equilibrium, similar to  $NH_3$  and  $NH_4^+$ . While higher  $pH$  levels promote  $NH_3$  concentration and thus more  $TAN$  available for emission, lower  $pH$  levels promote  $H_2CO_3$  concentration, the volatile portion of this system. The decrease in puddle  $pH$  shows that the ratio of  $TAN$  to  $H_2CO_3/HCO_3^-/CO_3^{2-}$  decreases from the start, and that the ammonia is removed from the urine puddle faster than the carbonic acid. At an optimal  $pH$  both substances could achieve a steady emission rate. This may explain why the  $pH$  stabilizes toward the end of the puddle life, even when  $dTAN dt^{-1}$  is still decreasing.

In this experiment, the average total emission for 0.25-L puddles of 0.2 and 0.4 mol  $L^{-1}$  initial urea concentrations were 1.4 and 2.9 g  $NH_3$ , respectively. Within the temperature and velocity conditions tested, the total amount of ammonia emitted depended on the initial amount of urea present. Changes in temperature, relative humidity and velocity conditions can result in changes to the average puddle emission

rate, and the resulting puddle life. In general, changes in the rate of ammonia emission are similar to changes in evaporation. Even if there is some urea left unconverted, all of the ammonia produced will be emitted.

#### 4.6 Summary

Urine puddle emission is the end result of a series of physical, chemical and biological processes occurring within a urine puddle, including evaporation, enzymatic degradation of urea, *pH* change, and ammonia emission. Even the enzyme within the puddle can be affected by environmental parameters and change over time. A system of equations was developed to model these processes simultaneously in order to determine the change in *TAN* of the puddle and the total emission from the urine puddle. The main components, assumptions and considerations in this model are:

- using a convective mass transfer coefficient calculated using the boundary layer theory can accurately describe the evaporation of water from a puddle and this theory is assumed applicable for ammonia transport as well;
- urease activity will decrease over time at less than ideal temperature conditions;
- the *pH* of a urine puddle will rapidly increase following contact with urease enzyme, but the ammonia in the solution will be buffered by carbonic acid, resulting in a lower *pH* than a pure ammonia solution. The faster volatilization rate of ammonia compared to carbonic acid will promote a decrease in *pH* over time;
- at low *pH* levels, 5% of the *TAN* will consistently be in the volatile form of  $NH_3$ ;
- the total amount of ammonia emitted from a urine puddle will depend more on the initial amount of urea present in solution and less on the environmental conditions,

assuming urease is present and abundant. Environmental conditions will affect the evaporation rate, average  $NH_3$  emission rate and puddle life.

Based on the percent difference between the average of the simulated values to the average of the measured values for each puddle, the bias associated with the model calculations for water volume,  $pH$ ,  $TAN$  and total emission were 0.5% (std dev 1.0%), -2.8% (std dev 2.4%), -15.3% (std dev 13%) and 0.5% (std dev 10%), respectively. The developed model can be incorporated in overall room ammonia emission models to simulate the ammonia production and emission from individual urine puddles on the floor surface.

### **Acknowledgements**

The authors gratefully acknowledge the use of the facilities at Research and Development Institute for the Agri-environment, Deschambault station, and the help provided by M. Larouche and other technicians. Funding was provided by Natural Sciences and Engineering Research Council of Canada, Sask Pork, Alberta Pork, Manitoba Pork and Saskatchewan Agriculture and Food Development Fund.

## CHAPTER 5

### MODELLING THE AMMONIA EMISSION FROM SLURRY BASED ON CHEMICAL AND PHYSICAL PROPERTIES

E.L. Cortus<sup>1,2</sup>, S.P. Lemay<sup>3</sup>, E.M. Barber<sup>4</sup>, and G.A. Hill<sup>5</sup>

<sup>1</sup> *Department of Agricultural and Bioresource Engineering, University of Saskatchewan, Saskatoon, SK;*

<sup>2</sup> *Prairie Swine Centre Inc., Saskatoon, SK;*

<sup>3</sup> *Research and Development Institute for the Agri-environment, Deschambault, QC;*

<sup>4</sup> *College of Agriculture, University of Saskatchewan, Saskatoon, SK;*

<sup>5</sup> *Department of Chemical Engineering, University of Saskatchewan, Saskatoon, SK.*

#### **Synopsis**

Besides the floor surface, the slurry pit is recognized as the other main source of ammonia emissions in swine barns. However, the variable composition of slurry can make estimation of certain emission parameters difficult. In this experiment, the manure from individually-housed pigs fed different diets was collected, and a slurry emission model was developed to express the amount of ammonia given off.

## 5.1 Introduction

The under-floor manure storage area, often referred to as the slurry pit, is recognized as one of the main sources of ammonia within swine and cattle barns. With the steady addition of urine, feces, drinking water and spilled feed to the slurry pit, ammonia and other gases are continually formed by the breakdown of urea and other nitrogenous material such as proteins (Anderson et al., 1987). Given the highly variable nature of slurry composition and storage length, models that simulate the ammonia production rate within slurry are still developing (Ni, 1999). However, measurements of physical and chemical slurry properties that facilitate predicting the rate of ammonia release from the slurry surface are possible. By developing a model that simulates the ammonia emission from slurry based on measurable variables, the livestock industry will be better able to address the impact the slurry emission has on human and animal health.

The flow of nitrogen in a pig is like any control volume; what goes in, minus the retention by the animal, equals what comes out. Therefore, diet composition is a large determinant in slurry composition. For example, reducing dietary crude protein can lower the amount of nitrogen excreted in the urine and can also result in lower slurry *pH* and ammonia emissions (Canh et al., 1998a). Adding sugar-beet pulp to a pig's diet was found to lower the *pH* and ammonia emissions from slurry by increasing the volatile fatty acid concentration of the slurry (Canh et al. 1998b).

Numerous models have been developed to simulate the ammonia emission from slurry surfaces. The models of Zhang et al. (1994), Aarnink and Elzing (1998), Ni et al. (2000c) and Liang et al. (2002) are all based on convective mass transfer, but differences exist among the models in mass transfer coefficients and ammonia partitioning in the solution. All four models are very sensitive to the slurry *pH*, which can vary greatly between

manure sources (Paul and Beauchamp, 1989) and even within the depths of a manure channel (Zhang et al., 1994; Aarnink and Elzing, 1998; Ni et al., 2000c). Of the slurry emission models developed, validation and calibration have been completed with either full-scale room measurements (Aarnink and Elzing, 1998; Ni et al., 2000c) that do not necessarily separate slurry emission from emission by other sources, or with lagoon storage emission data (Liang et al., 2002). Model calibration has introduced factors relating the mixed slurry *pH* and the emission rate of carbon dioxide to the *pH* at the manure surface in models by Aarnink and Elzing (1998) and Ni et al. (2000c), respectively. However, changes in surface *pH* and differences between mixed and surface *pH* have not been validated with measured data in conjunction with the model testing.

The overall objective of this experiment was to develop a slurry emission model to simulate the ammonia emission rate from slurry pits within swine barns that is suitable for a range of slurry properties. In order to do this, the specific objectives were: (1) to build on pre-existing models and develop a model to simulate the ammonia emission from slurry; (2) collect emission measurements from slurry samples varying in composition in a bench-scale slurry pit experiment; and (3) calibrate and validate the model using the bench-scale measurements. The calibration process focused on determining the fraction of total ammoniacal nitrogen in ammonia form, based on accessible slurry properties.

## **5.2 Model Development**

A schematic diagram of a slurry pit in relation to the slatted and solid floors is shown in figure 5.1. Urine, fecal matter, spilled feed and water drain through the slatted floor and mix to become slurry. Ammonia is produced within the slurry from the breakdown

of urea and other nitrogenous material. Once in solution, the ammonia exists in two forms, ammonia ( $NH_3$ ) and ammonium ( $NH_4^+$ ). The total amount of nitrogen contained within the ammonia and ammonium molecules in a solution is referred to as the total ammoniacal nitrogen concentration, or *TAN*. The non-ionized portion of *TAN*, ammonia, is volatile and can be transferred to the slurry pit headspace air whereas the ammonium will stay in the solution. Air is added and removed from the slurry pit headspace through the slatted floor. Ammonia absorption or desorption by the walls and slatted floor is neglected.

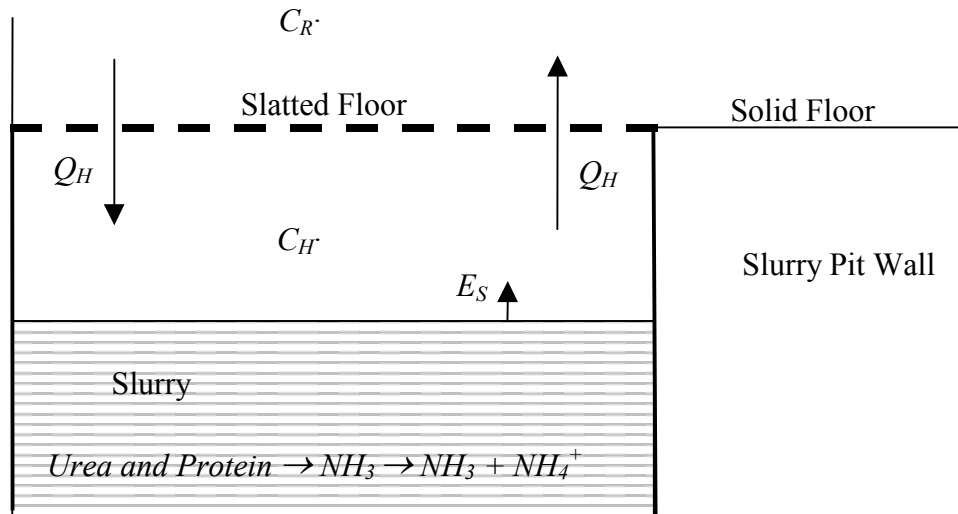


**Figure 5.1. Cross-sectional diagram of a slurry pit showing the contributions of ammonia to the headspace concentration ( $C_H$ ) by incoming air from the room ( $C_R \cdot Q_H$ ) and emission from the slurry ( $E_S$ ), and removal of ammonia by air movement up through the slats ( $C_H \cdot Q_H$ ).**

Ni (1999) showed that the core model for ammonia emission from slurry surfaces in past models was that of convective mass transfer (eq. 5.1), with sub-models to determine the convective mass transfer coefficient ( $k$ ) and the ammonia concentration in the gas film ( $C_G$ ). In determining  $C_G$ , most models have determined the relative amount of ammonia to *TAN* ( $f$ ) in the liquid and then estimated the ammonia concentration in the



gas film relative to the liquid based on the Henry's Law constant ( $H$ ). The concentration gradient for ammonia emission is dependant on the concentration of ammonia in the surrounding bulk air. In the model of Aarnink and Elzing (1998), the room air ( $C_R$ ) was considered the surrounding air and was ignored in the mass transfer calculation. In developing this slurry emission model,  $C_H$  will be retained in the mass transfer equation as the concentration of the surrounding air.

$$E_s = k \cdot A \cdot 1000 \cdot (C_G - C_H) = k \cdot A \cdot 1000 \cdot \left( \frac{f \cdot TAN}{H} - C_H \right) \quad (5.1)$$

In developing the slurry emission model to determine  $k$ ,  $f$  and  $H$ , in order to solve equation 5.1, the models developed by Zhang et al. (1994), Aarnink and Elzing (1998) and Ni et al. (2000c) for under-floor slurry storages and Liang et al. (2002) for lagoon storage were compared and are presented in table 5.1. There were differences between models, not only in the calculations, but also in the units of measure. The equations were converted to similar units when possible. The temperature variable refers to the temperature of the slurry, except where the film temperature is specified.

**Table 5.1. Slurry emission model comparison.**

Calculated Variable	Variable calculations specific to each model			
	Zhang et al. (1994)	Aarnink and Elzing (1998)	Ni et al. (2000c)	Liang et al. (2002)
Mass transfer coefficient ( $k$ )	$k = 5.3 \times 10^{-3} - 1.3 \times 10^{-2} \cdot v$ $+ 8.5 \times 10^{-4} \cdot v \cdot T_C$ $+ 2.3 \times 10^{-2} \cdot v^2$	$k = 50.1 \cdot v^{0.8} \cdot T_{film}^{-1.4}$	$k = 4.78 \times 10^{-7} \cdot T_C^{0.8} \cdot v^{0.7}$	$k = \left( \frac{1}{k_L} + \frac{1}{H'' \cdot k_G} \right)^{-1}$ where $k_L = 2.229 \times 10^{-6} \cdot e^{0.236 \cdot v}$ $k_G = 5.317 \times 10^{-5} + 2.012 \times 10^{-3} \cdot v$
Fraction of TAN in unionized form ( $f$ ) or Proportionality coefficient ( $P_{CO}$ )	(A1) $f = \frac{10^{pH}}{10^{pH} + \frac{1}{K_a}}$ where $K_a = 0.2 \cdot 10^{-\left(0.0897 + \frac{2729}{T}\right)}$	(B1) $f = \frac{10^{pH_E}}{10^{pH_E} + \frac{1}{K_a}}$ where $pH_E = pH + 1.1$ $K_a = 0.2 \cdot 10^{-\left(0.0897 + \frac{2729}{T_{film}}\right)}$	(C1) $P_{CO} = \frac{K_a}{(q \cdot 10^{-pH_i} + K_a) \cdot H}$ where $K_a = 10^{-0.0897 - \frac{2729}{T}}$	(D1) $f = \frac{K_a}{K_a + 10^{-pH}}$ where $K_a = 0.5 \cdot 10^{-\left(0.0897 + \frac{2729}{T}\right)}$
Henry Constant ( $H$ )	(A2) $H' = \frac{P_G}{C_L}$ $H' = 1.1561 \cdot e^{-\frac{4151}{T}}$	(B2) $H = \frac{C_L}{C_G}$ $H = 1431 \cdot 1.053^{(293 - T_{film})}$	(C2) $H = \frac{C_L}{C_G}$ $H = 10^{\frac{1478}{T} - 1.69}$	(D2) $H'' = \frac{C_G}{C_L}$ $H'' = \frac{2.395 \times 10^5}{T} \cdot e^{\left(-\frac{4151}{T}\right)}$
Overall Emission ( $E_S$ ) <sup>z</sup>	(A3) $E_S = k \cdot A \cdot \left( \frac{f \cdot TAN}{H'} - C_B \right)$	(B3) $E_S = \frac{k \cdot A \cdot f \cdot TAN}{H}$	(C3) $E_S = k \cdot A \cdot \left( \frac{17}{18} \cdot P_{CO} \cdot TAN - C_B \right)$	(D3) $E_S = k \cdot A \cdot f \cdot TAN$
	(A4)	(B4)	(C4)	(D4)

NOTE: Care has been taken to convert all models to similar variables, and it is not the authors' intention to misrepresent previous models.

<sup>z</sup> Unit conversion may be necessary to properly solve  $E_S$ .

### 5.2.1 Convective Mass Transfer Coefficient

Ni (1999) showed the wide range of convective mass transfer coefficients used for agricultural ammonia sources. The experimental values ranged from  $1.3 \times 10^{-6}$  to  $11.7 \times 10^{-3} \text{ m s}^{-1}$ , and there was a positive relationship for the coefficient with temperature and air velocity. Zhang et al. (1994) and Ni et al. (2000c) used experimental mass transfer coefficients in their respective models, shown as equations A1 and C1 in table 5.1, respectively. For theoretical calculations of the mass transfer coefficient, two main theories are used (Ni, 1999). Aarnink and Elzing (1998) and Liang et al. (2002) base the mass transfer coefficient calculation on the Two-Film Theory proposed by Lewis and Whitman (1924). For this theory, the conductivities of the liquid ( $k_L$ ) and gas ( $k_G$ ) films at the emission surface are combined in the overall coefficient (see equation D1 in table 5.1 as an example). The individual film coefficients used by Liang et al. (2002) were derived by Liss and Slater (1974) (eq. D1 in table 5.1). Aarnink and Elzing (1998) use the gas film coefficient ( $k_G$ ) measured by Haslam et al. (1924) as the overall mass transfer coefficient (eq. B1 in table 5.1).

The other theory that has been applied is the Boundary Layer Theory (Ni, 1999), which is described in Incropera and DeWitt (1996). The mass transfer coefficient is based on the properties of the gas flowing over a flat surface of length  $L$  for laminar ( $Re < 5 \times 10^5$ ; eq. 5.2) or transitional/turbulent flow ( $Re > 5 \times 10^5$ ; eq. 5.3).

$$k = \frac{0.664 \cdot Re^{0.5} \cdot Sc^{0.333} \cdot D_{A,B}}{L}, \quad Sc \geq 0.6 \quad (5.2)$$

$$k = \frac{0.0296 \cdot Re^{0.8} \cdot Sc^{0.333} \cdot D_{A,B}}{L}, \quad 0.6 < Sc < 3000 \quad (5.3)$$

The  $Re$  and  $Sc$  parameters (dimensionless) are functions of surface length, velocity, kinematic viscosity and diffusivity. Kinematic viscosity of air can be expressed as a function of film temperature, using the regression equation shown in equation 5.4. Film temperature is assumed to be equal to the average temperature of the solution and surrounding air (Incropera and DeWitt, 1996).

$$\nu = 4 \times 10^{-10} \cdot T_{film}^{1.859} \quad (5.4)$$

Diffusivity also exhibits an exponential relationship with temperature, shown in equation 5.5, adapted from Welty et al. (1984), assuming the collision interval effects at different temperatures are negligible.

$$D_{A,B}(T_2) = D_{A,B}(T_1) \cdot \left( \frac{T_2}{T_1} \right)^{1.5} \quad (5.5)$$

Diffusivity of ammonia in air at 298 K is  $0.28 \times 10^{-4} \text{ m}^2 \text{ s}^{-1}$  (Incropera and DeWitt, 1996) and this temperature and respective diffusivity can replace  $T_1$  and  $D_{A,B}(T_1)$  in equation 5.5.

Incorporating equations 5.4 and 5.5 into equation 5.2, an equation to express  $k$  as a function of velocity, temperature, length and diffusivity was developed. Equation 5.6 is applicable for the transfer of a substance A, from a liquid surface to the surrounding air (substance B), provided there are laminar flow conditions, the  $Sc$  value is approximately equal to or greater than 0.6, and the diffusivity of substance A in air at 298 K is known.

$$k = 0.0821 \cdot T_{film}^{0.70} \cdot \nu^{0.5} \cdot D_{A,B}^{0.66} \cdot L^{-0.5} \quad (5.6)$$

### 5.2.2 Ammonia Partitioning in the Liquid

The ammonia produced within the slurry will separate and exist in two forms, ammonia and ammonium. Ammonia concentration measurements of liquid samples,

however, provide a measure of *TAN*. Because only the ammonia fraction of the *TAN* is volatile, Zhang et al. (1994) introduced a variable (*f*) to relate the amount of ammonia relative to *TAN*.

$$f = \frac{[NH_3]}{[NH_3 + NH_4^+]} = \frac{[NH_3]}{TAN} \quad (5.7)$$

Theoretically, the amount of ammonia and ammonium in solution are in equilibrium according to equation 5.8 (Arogo et al., 2003b), where  $K_a$  represents the acid ionization constant for ammonium, also referred to as the dissociation constant.

$$K_a = \frac{\varphi_{NH_3} \cdot [NH_3] \cdot \varphi_{H^+} \cdot [H^+]}{\varphi_{NH_4^+} \cdot [NH_4^+]} \quad (5.8)$$

The temperature-dependency of  $K_a$  for ammonium in water was modelled by Jayaweera and Mikkelsen (1990) (eq. 5.9).

$$K_a = 10^{-\left(0.0897 + \frac{2729}{T_{film}}\right)} \quad (5.9)$$

The activity coefficients ( $\varphi$ ) are a function of the ionic strength of the solution, and normally assumed equal to one for dilute solutions (Arogo et al., 2003b). However, a factor that theoretically represents the combination of activity values has been combined with the  $K_a$  for ammonium in water to estimate  $K_a$  for ammonium in manure. Zhang et al. (1994) and Aarnink and Elzing (1998) used a factor of 0.2, Liang et al., (2002) used a factor of 0.5, while Arogo et al. (2003b) suggested factors between 0.50 and 0.94 based on the temperature of the slurry solution. Arogo et al. (2003b) concluded that more studies are required to determine  $K_a$  values for slurry with different *TAN* concentrations and solid contents.

In the models of Zhang et al. (1994), Aarnink and Elzing (1998) and Liang et al. (2002), the  $f$  variable was calculated by rearranging Eq. 5.8 to express the ammonium concentration as a function of the ammonia concentration,  $H^+$  concentration and  $K_a$ , and substituting the expression into Eq. 5.7. The resulting equation for  $f$  was then expressed as a function of  $pH$  (negative logarithm of  $H^+$ ) and  $K_a$  with the corresponding factor. The resulting  $f$  variables have an exponential relationship with  $pH$  and, as shown in Aarnink and Elzing (1998), a small increase in slurry  $pH$  (0.1 unit) resulted in a large increase (9%) in the simulated ammonia emission from a barn because of the higher amount of ammonia available.

A  $K_a$ -factor less than one reduces the impact of  $pH$  on the partitioning of ammonia in the liquid and the resulting emission but, as shown by Arogo et al. (2003b), this factor can be highly variable depending on the physical and chemical properties of the slurry. Therefore, this model will assume that  $f$  is better estimated from measured chemical and physical properties. While there are numerous measurable properties, this paper will focus on  $TAN$ ,  $pH$ , electrical conductivity ( $EC$ ) and  $T_{film}$  measurements. Electrical conductivity can provide an estimation on the amount of dissolved ions in a solution (Sawyer and McCarty, 1978). A regression equation (eq. 5.10) was proposed that estimates the fraction,  $f$ , based on  $TAN$ ,  $pH$ ,  $EC$  and  $T_{film}$ , with the coefficients  $x_{1...5}$  determined in the model calibration process.

$$f = x_1 \cdot TAN + x_2 \cdot pH + x_3 \cdot EC + x_4 \cdot T_{film} + x_5 \quad (5.10)$$

### 5.2.3 Ammonia Concentration in the Gas Film

Another estimation in slurry emission models is the amount of ammonia in the gas layer at the surface of the manure. Treybal (1980) recommended applying the Henry's

Law constant for *TAN* concentrations in water below 3.2 mol L<sup>-1</sup> at 10°C and 2.0 mol L<sup>-1</sup> at 30°C. Similar to the mass transfer coefficient, numerous equations have been developed to express the Henry constant (Ni, 1999), either as the dimensionless ratio of ammonia in the liquid compared to the gas ( $H$ , eqs. B3 and C3 in table 5.1), the dimensionless ratio of ammonia in the gas compared to the liquid ( $H''$ , eq. D3 in table 5.1) or the ratio of partial pressure to liquid concentration ( $H'$ , eq. A3 in table 5.1). Ni (1999) recommended using  $H$  for slurry emission models because the ammonia concentration in the surrounding air is generally expressed as a concentration, rather than a partial pressure. Based on this recommendation, the  $H$ -calculation from Aarnink and Elzing (1998) was used in this slurry emission model (eq. 5.11).

$$H = \frac{C_L}{C_G} = 1431 \cdot 1.053^{(293 - T_{film})} \quad (5.11)$$

#### 5.2.4 Ammonia Concentration in the Slurry Channel Headspace

If high enough, the ammonia concentration in the slurry channel headspace ( $C_H$ ) can impact the concentration gradient for slurry emission. Assuming the slatted floor above the slurry channel acts as a conduit for incoming air to the headspace and for outgoing air, the dynamic concentration of the headspace is shown in equation 5.12.

$$\frac{dC_H}{dt} = \frac{Q_H \cdot C_R - Q_H \cdot C_H + E_S}{V_H} = \frac{Q_H \cdot C_R - Q_H \cdot C_H + k \cdot A \cdot 1000 \cdot \left( \frac{f \cdot TAN}{H} - C_H \right)}{V_H} \quad (5.12)$$

If the channel concentration can be considered a steady state variable, and assuming the incoming air has a negligible ammonia concentration, equation 5.12 can be simplified to the static model shown in equation 5.13.

$$C_H = \frac{k \cdot A \cdot 1000 \cdot f \cdot TAN}{H \cdot (Q_H + k \cdot A \cdot 1000)} \quad (5.13)$$

### 5.2.5 Model Development Summary

With input values for  $T_{film}$ ,  $v$ ,  $TAN$ ,  $pH$ ,  $EC$  and  $A$ , the emission from slurry can be calculated using equation 5.6 to determine the mass transfer coefficient, equation 5.10 to estimate  $f$ , equation 5.11 to calculate the Henry's Law constant, all incorporated in equation 5.1 to simulate the ammonia emission rate. For slurry contained within an airspace like a slurry pit, the concentration of the slurry pit headspace can be estimated using the most recent measurement or simulated value, and the air exchange rate  $Q_H$ .

## 5.3 Materials and Method

Data for input, calibration and validation of the developed slurry emission model were collected from slurry produced by individual pigs in conjunction with another experiment (Smith et al., 2004). The slurry was placed in emission boxes designed to simulate a slurry pit environment with low airspeed and a low air exchange rate, where the ammonia concentration in the emission box headspace ( $C_B$ ) was analogous to the slurry channel headspace concentration ( $C_H$ ), and the air exchange rate through the emission box ( $Q_B$ ) was analogous to the air exchange rate through the slatted floor ( $Q_H$ ). Measurements collected from the slurry and from within the emission boxes provided the data needed for input to the model, and for calibration and validation of the model.

### 5.3.1 Slurry Collection

Two metabolism trials were performed with average pig weights of 58 (Trial 1, Data-set 2) and 94 kg (Trial 2, Data-set 1), respectively. For each trial, four different diet formulations were prepared and are explained in greater detail in Smith et al. (2004). Two pigs in each trial were given the same diet treatment. The four treatments were low



protein, with and without sugar beet pulp added as a form of fermentable carbohydrates (LPSBP and LPC, respectively), and high protein, with and without sugar-beet pulp (HPSBP and HPC, respectively). An 18-day acclimation period was provided for the animals to adjust to the experimental diets before slurry collection.

Pigs were housed individually in metabolism crates with a cone-shaped metal tray under the slatted floor of each pen. The cone of the tray was plugged with a rubber stopper and all urine and feces were collected together for two (Trial 2) to four days (Trial 1). Water spillage from the drinker was collected separately, so the slurry samples were highly concentrated mixtures of urine and feces only. After the collection period for each trial, the slurry from one pen was emptied into a bucket and mixed with a paint stirrer. From the mixed slurry, an 8-L sample was taken and put into an emission box. This was repeated for all eight pigs during each of the two trials.

### 5.3.2 Emission Box Measurements

The slurry samples were placed in emission boxes constructed from 17-L Rubbermaid containers (Wooster, OH) lined with Tedlar bags to prevent gas and odour absorption as shown in figure 5.2. The lid was sealed to the box before measurements were taken.



(a)

(b)

**Figure 5.2. Emission box, filled with slurry (a) and inside view (b).**

The air inlet to each emission box was a series of 7 holes (13.5-mm diameter) on one end of the box, 12.7 mm above the slurry surface. Teflon tubing from the outlet on the other end of each chamber was connected to the ammonia measurement system. Ambient ammonia concentration was also measured. The ammonia measurement system consisted of a sampling pump that drew air through one sampling line at an average rate of  $0.05 \text{ L s}^{-1}$  into the ammonia analyzer (Chillgard RT refrigerant monitor, MSA Canada, Edmonton, AB; range 0 to 1000 ppm; accuracy  $\pm 2 \text{ ppm}$ ), while a second pump continually purged the remaining eight lines at a similar flowrate. A programmable logic controller (Septre Controls Ltd., Regina, SK) coordinated the sampling of different emission boxes by switching the sampling lines every ten minutes; only data from the last four minutes of the ten-minute sampling period were saved and used to compute an average concentration. A dust filter was installed at the inlet to each line in the box to prevent particulate contamination of the line or analyzers.

Temperatures of the slurry surface and airspace in the box were continuously measured (Type T Thermocouple, temperature accuracy:  $\pm 0.5^\circ\text{C}$ ) and averaged to determine the film temperature.

Air velocity measurements within the boxes were taken after the emission trials were completed, 5 mm above the liquid surface, with a thermal anemometer (TSI Model 8470 Air Velocity Transducer, St. Paul, MN). The range of the anemometer was 0 to  $0.5 \text{ m s}^{-1}$  and the instrument was calibrated in a bench-top wind tunnel (Model 8390, TSI Incorporated, St. Paul, MN). The velocity was measured at nine locations in each box. For each box, the velocity measurement at the nine locations did not differ more than 10% from the average box velocity measurement. The range of average velocity

measurements for all boxes was 0.019 to 0.041 m s<sup>-1</sup>. An average velocity of 0.025 m s<sup>-1</sup> was used in all calculations. A sensitivity analysis (shown in the Results section) showed that the average velocity under- or over-predicted the concentration by less than 10% based on the range measured.

Before each trial the boxes were rinsed with bleach solution and water and fumigated. The empty boxes were measured for any ammonia absorption using the same method as the experiments over 24 h, and it was found that the ammonia concentration in the boxes was less than 1 ppm different from the ambient concentration.

### **5.3.3 Experimental Procedure**

Eight slurry samples were used in each of two trials, with four treatments replicated twice in each trial. The animal diets are considered the treatments, and will be referred to as HPC, HPSBP, LPC and LPSBP.

The slurry collected from the eight pigs during each slurry collection period was placed in emission boxes, which were stored in an instrumentation room. The measured headspace concentrations exceeded the limit of the ammonia analyser (1000 ppm) when first measured. The experimental procedure was altered slightly to accommodate this. For each slurry sample in both trials, the ammonia was allowed to volatilize from the slurry samples for a few days until the ammonia concentration levels for all boxes were below 1000 ppm. The slurry was emptied into a bucket and remixed with the paint stirrer before being placed back in the box. A 1-L slurry sample was taken at this time, referred to as the Day 0 sample, and analyzed for *TAN*, *pH* and *EC*. After measuring the ammonia emission for another five days, the emission trials were considered complete and another slurry sample was taken, referred to as the Day 5 sample, and analyzed for *TAN*, *pH* and

*EC*. Slurry samples were analysed by Enviro-Test Laboratories (Saskatoon, SK).

Chemical properties between day 0 and day 5 for each sample were linearly interpolated.

The data from the HPC (Rep 2) sample in Data-set 2 was discarded because of a hole discovered in the gas sampling line. Power outages occurred in both trials, resulting in the loss of some ammonia concentration measurements.

#### **5.3.4 Data Analysis**

Concentration data were used in the data analysis. Data-set 1 samples were used for calibration, and Data-set 2 samples were used for validation. The emission boxes were designed to simulate the slurry channel environment, so  $C_H$ ,  $V_H$  and  $Q_H$  in equation 5.12 and 5.13 of the slurry emission model were replaced with the emission box concentration ( $C_B$ ), emission box volume ( $V_B$ ), and emission box air exchange rate ( $Q_B$ ), respectively. Preliminary calculations using equations 5.12 and 5.13 to simulate the emission box concentration levels with input values collected in Data-set 1 were similar in magnitude for calculation intervals less than 2 h, prompting the use of the simpler, steady state equation (eq. 5.13).

The calibration process using Data-set 1 samples was as follows: (1) equation 5.13 was rearranged to solve for  $f$ , based on the measured airspace ( $C_B$ ) and  $TAN$  values for a slurry sample; (2) an average value for  $f$  was obtained for each of the samples based on the measured air and  $TAN$  values throughout the trial; (3) single and multi-variable regression was then performed to express  $f$  as a function of different combinations of measured slurry property values (eq. 5.10); and finally, (4) regression equations were evaluated based on their statistical significance to determine the appropriate expression for  $f$ . All calculations were performed using MSExcel®.

During the validation process, the calibrated equation for  $f$  was incorporated in eq. 5.13 (hereafter referred to as the Linear- $pH$  (Lin- $pH$ ) Model), and the simulated air concentration values for each Data-set 2 sample were compared to measured air concentration values over time. The two largest changes to the Lin- $pH$  Model compared to previous models were a different  $k$  estimation and a linear relationship between  $pH$  and  $f$ . To evaluate the improvement these two changes made to the simulation process, the Lin- $pH$  Model was compared to a second model that also used equation 5.13 to calculate the emission box concentration, but estimated  $k$  and  $f$  using equation A2 and B1 (from table 5.1), respectively. The second model was referred to as the Exponential- $pH$  (Exp- $pH$ ) Model. Both the Lin- $pH$  and Exp- $pH$  Models were evaluated following the Standard Guide for Statistical Evaluation of Indoor Air Quality Models (ASTM, 2003) that uses six parameters to judge model performance (Appendix A).

A sensitivity analysis was performed using both models to investigate the effects of different input variables on the simulated slurry emission using equation 5.1. Each input variable was changed from 80% to 120% of its mean value in 10% increments while retaining the other input variables at their mean values.

## 5.4 Results

### 5.4.1 Slurry Properties

Table 5.2 shows the measured  $TAN$ ,  $pH$  and  $EC$  measurements on Days 0 and 5 for the sixteen slurry samples. There was not a discernable relationship between  $TAN$  and  $pH$ , as one would expect in a pure ammonia and water solution, likely because other components in the manure were biasing the  $pH$ . In a pure ammonia solution, the  $pH$  increases as  $TAN$  concentration increases because ammonia is a weak base.

**Table 5.2. Measured slurry properties<sup>Z</sup> on Days 0 and 5 for the respective trials and treatments.**

Data-set	Treatment <sup>Y</sup>	Rep	TAN (mol L <sup>-1</sup> )		pH		EC (mS cm <sup>-1</sup> )	
			Day 0	Day 5	Day 0	Day 5	Day 0	Day 5
1	HPC	1	0.66	0.59	9.1	8.9	39.8	34.1
	HPC	2	0.81	0.74	9.1	9.0	43.6	38.4
	HPSBP	1	0.62	0.55	8.8	8.7	31.2	31.7
	HPSBP	2	0.41	0.38	8.5	8.5	26.3	24.8
	LPC	1	0.55	1.05	8.7	8.1	21.9	33.0
	LPC	2	1.11	1.08	8.6	8.4	42.3	39.4
	LPSBP	1	0.32	0.28	8.7	8.7	18.1	20.7
	LPSBP	2	1.11	1.10	8.5	8.0	40.5	34.9
2	HPC	1	0.37	0.32	8.8	9.1	26.8	22.8
	HPC	2	0.49	0.47	8.7	9.2	33.4	30.4
	HPSBP	1	0.47	0.42	8.0	8.5	27.0	32.8
	HPSBP	2	1.10	1.04	8.8	9.1	44.7	46.8
	LPC	1	1.01	0.98	7.7	8.0	43.8	43.3
	LPC	2	0.64	0.54	8.4	8.6	44.3	37.9
	LPSBP	1	0.66	0.56	8.4	8.7	33.8	35.4
	LPSBP	2	1.17	1.07	8.4	8.6	40.2	44.4

<sup>Z</sup> TAN: Total ammoniacal nitrogen; EC: Electrical conductivity

<sup>Y</sup> HPC: high protein; HPSBP: high protein with sugar-beet pulp; LPC: low protein; and LPSBP: low protein with sugar-beet pulp

#### 5.4.2 Emission Box Ammonia Concentration Measurements

The airspace concentrations in the emission boxes were high, even after the slurry was allowed to volatilize for a number of days. The air concentrations were on average between 250 and 820 ppm, with no discernable difference between Data-sets 1 and 2 (fig. 5.3).

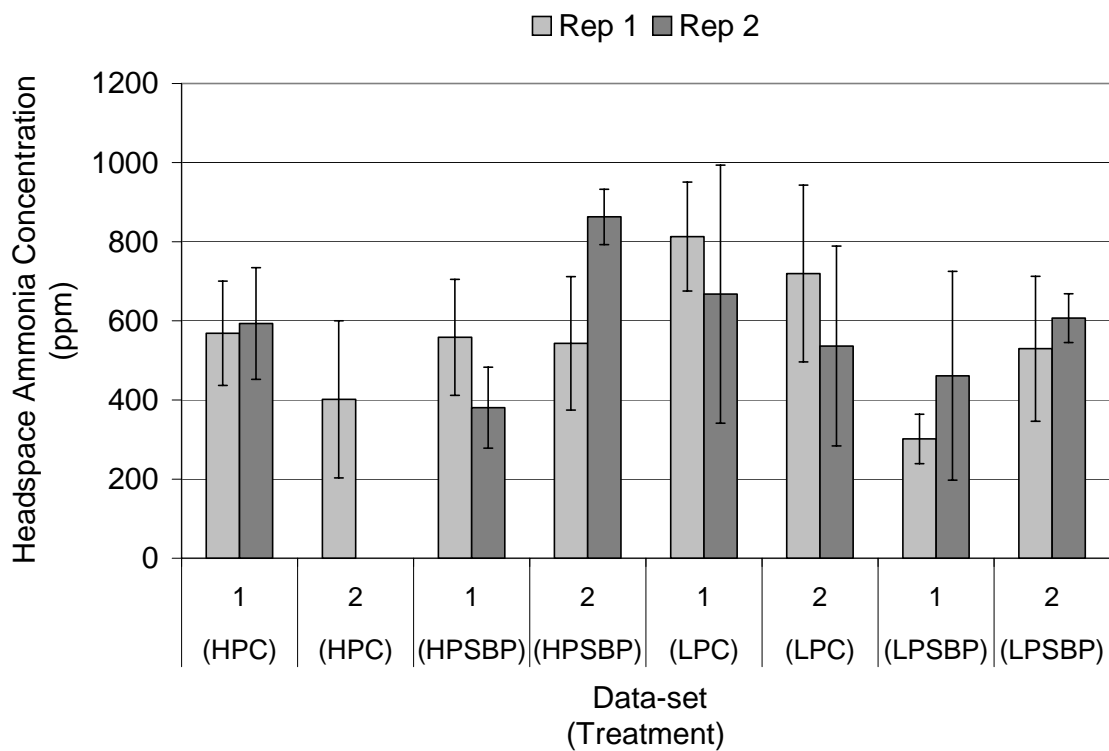


**Figure 5.3. Average ammonia concentration measured in the headspace of the emission boxes during the two trials. Vertical bars indicate the range of measured concentration values.**

#### 5.4.3 Model Calibration

The fraction ( $f$ ) of total ammoniacal nitrogen in ammonia form for each slurry sample in Data-set 1 was calculated and the average value is shown in table 5.3 with the corresponding average slurry properties.

**Table 5.3. Average slurry properties and fraction ( $f$ ) values for Data-set 1 slurry samples.**

Diet	Rep	$n^z$	$T_{film}$ (K)	$TAN$ (mol l <sup>-1</sup> )	$pH$	$EC$ (mS cm <sup>-1</sup> )	$f$	
							Mean	SD <sup>y</sup>
HPC	(1)	45	297.7	0.63	9.0	37.1	0.068	0.008
HPC	(2)	44	297.3	0.78	9.1	41.2	0.058	0.007
HPSBP	(1)	42	298.5	0.59	8.8	31.4	0.068	0.006
HPSBP	(2)	43	297.5	0.40	8.5	25.6	0.073	0.009
LPC	(1)	43	297.5	0.78	8.4	27.0	0.084	0.024
LPC	(2)	45	297.3	1.10	8.5	40.9	0.047	0.011
LPSBP	(1)	45	297.3	0.30	8.7	19.3	0.077	0.006
LPSBP	(2)	45	296.9	1.10	8.3	37.9	0.033	0.009

<sup>z</sup>  $n$ : number of simulated values

<sup>y</sup> Std Dev: standard deviation

Single variable linear regression was performed for the  $f$  values shown in table 5.3 as a function of  $TAN$ ,  $pH$ ,  $EC$  and  $T_{film}$ , respectively. There was a very large difference between Day 0 and Day 5  $TAN$  concentration and  $pH$  measurements for the LPC (1) sample. Since the majority of other slurry samples did not exhibit this drastic change within five days, this slurry sample appeared to be an outlier or anomaly. All regressions were performed with and without the LPC (1) sample, and removing the sample provided a better fit for most models. The single variable  $TAN$  best modelled the variable  $f$  ( $R = 0.95$ ,  $F_{1,5} < 0.001$ ).

Multiple regression was then performed with combinations of  $TAN$  and  $pH$ ,  $EC$  and/or  $T_{film}$ . By incorporating  $TAN$  and  $pH$  in the regression equation 5.10, the intercept ( $x_5$ ) was no longer significantly different from zero and was set to zero ( $R = 0.974$ ,  $F_{2,5} = 0.002$ ). Similarly, adding the variable temperature to the regression equation negated the need for the intercept in the regression equation ( $R = 0.968$ ,  $F_{2,5} = 0.003$ ). The regression equation incorporating  $TAN$  and  $pH$  (eq. 5.14) was chosen as the model to predict  $f$  considering the higher  $R$ -value.

$$f = -0.0444 \cdot TAN + 0.00105 \cdot pH \quad (5.14)$$



#### 5.4.4 Model Validation

The box concentration for each of the Data-set 2 samples was calculated using equation 5.14 in equation 5.13 (Lin-*pH* Model) for the same instances that measured concentration values were available. A second set of model calculations were performed for the same instances using the Exp-*pH* Model. Sample HPC (2) could not be used because ammonia concentration data was not collected. The corresponding measured and simulated concentration values were compared and evaluated for both the Lin-*pH* Model and Exp-*pH* Model, shown in tables 5.4 and 5.5, respectively.

The correlation coefficient ( $R$ ), normalized mean square error ( $NMSE$ ) and fractional bias ( $FB$ ) were within the prescribed evaluation limits for the majority of slurry samples using the Lin-*pH* Model (table 5.4). The  $FB$  values show the average simulated concentration for each sample was between 23% lower and 11% higher than the average measured concentration. The Lin-*pH* Model shows improvement compared to the Exp-*pH* Model (table 5.5), where the average simulated concentration was over 100% lower and higher than the measured concentration in some cases.

Each set of box concentration measurements showed some diurnal variation that generally decreased in magnitude over the trial. The diurnal variation was attributed to changing temperature patterns over each 24-h period since the instrumentation room where the emission boxes were stored did not have constant temperature control. The change in concentration over each day and over the length of the trial was not as well simulated as the overall average concentration based on the  $b$  and  $a$ -values in table 5.4 and as shown in figure 5.4.

**Table 5.4. "Lin-*pH* Model" evaluation based on Data-set 2 slurry sample measurements. *Italicized* values are outside of the prescribed evaluation limits (ASTM, 2003).**

Diet	Rep	<i>n</i>	Average Concentration (ppm)		Statistical Values for Overall Agreement				Statistical Values for Bias	
			Measured	Simulated	<i>R</i>	<i>b</i>	<i>a</i>	<i>NMSE</i>	<i>FB</i>	<i>FS</i>
HPC	(1)	31	401	424	0.985	<i>0.471</i>	235	0.0324	0.06	<i>-1.26</i>
HPSBP	(1)	29	534	499	0.899	<i>0.595</i>	176	0.0146	-0.08	<i>-0.78</i>
HPSBP	(2)	13	863	685	<i>0.784</i>	<i>0.383</i>	354	0.0556	-0.23	<i>-1.23</i>
LPC	(1)	21	720	596	0.956	<i>0.328</i>	360	0.0544	-0.19	<i>-1.58</i>
LPC	(2)	28	537	600	0.992	<i>0.540</i>	311	0.0297	0.11	<i>-1.09</i>
LPSBP	(1)	29	530	590	0.981	<i>0.672</i>	234	0.0179	0.11	<i>-0.72</i>
LPSBP	(2)	13	607	613	0.959	<i>0.833</i>	108	0.0007	0.01	<i>-0.28</i>
Average					0.937	<i>0.546</i>	254	0.0293	-0.03	<i>-0.99</i>

**Table 5.5. "Exp-*pH* Model" evaluation based on Data-set 2 slurry sample measurements. *Italicized* values are outside of the prescribed evaluation limits (ASTM, 2003).**

Diet	Rep	<i>n</i>	Average Concentration (ppm)		Statistical Values for Overall Agreement				Statistical Values for Bias	
			Measured	Simulated	<i>R</i>	<i>b</i>	<i>a</i>	<i>NMSE</i>	<i>FB</i>	<i>FS</i>
HPC	(1)	31	401	489	<i>0.807</i>	<i>0.281</i>	376	0.0888	0.20	<i>-1.57</i>
HPSBP	(1)	29	543	162	<i>-0.677</i>	<i>-0.213</i>	277	<i>1.7959</i>	<i>-1.08</i>	<i>-1.64</i>
HPSBP	(2)	13	863	1400	<i>0.661</i>	<i>1.267</i>	307	0.2432	<i>0.48</i>	<i>1.14</i>
LPC	(1)	21	720	135	<i>-0.082</i>	<i>-0.007</i>	139	<i>3.7253</i>	<i>-1.37</i>	<i>-1.97</i>
LPC	(2)	28	537	345	0.978	<i>0.341</i>	162	<i>0.2591</i>	<i>-0.44</i>	<i>-1.57</i>
LPSBP	(1)	29	530	359	<i>0.749</i>	<i>0.232</i>	237	0.2035	<i>-0.38</i>	<i>-1.65</i>
LPSBP	(2)	13	607	513	0.948	<i>1.431</i>	<i>-356</i>	0.0319	-0.17	<i>0.78</i>
Average					<i>0.483</i>	<i>0.476</i>	163	<i>0.9068</i>	<i>-0.39</i>	<i>-0.93</i>

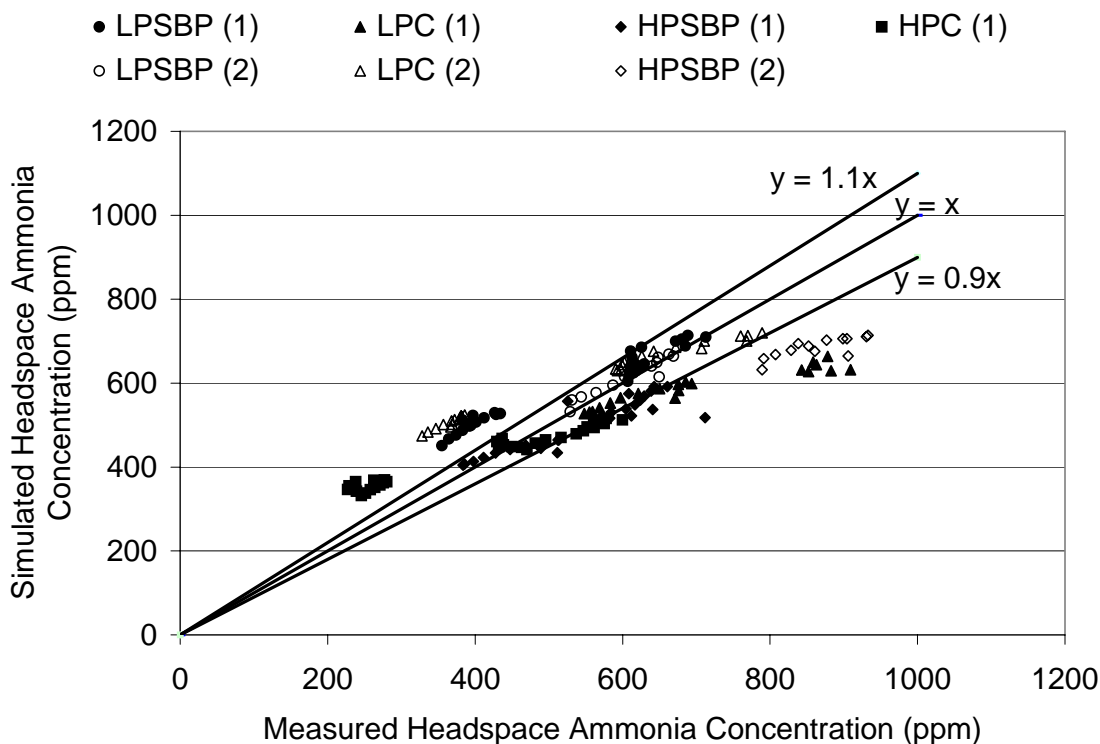


**Figure 5.4. Simulated ammonia concentrations compared to measured values for Trial 1-slurry samples.**

The main differences between the Lin-*pH* Model and all previous models studied (table 5.1) lie in the choice of mass transfer coefficient and the determination of available ammonia in the liquid. The fractional bias in simulating the emission box concentration appears improved by using the Lin-*pH* Model, especially at lower *pH* values compared to the Exp-*pH* Model that was also tested (figs. 5.5 and 5.6). Figures 5.5 and 5.6 also show that the largest error in model simulations with the Lin-*pH* Model occurred in samples with the extreme measured values of *TAN* ( $>1.0 \text{ mol L}^{-1}$ ) and *pH* ( $< 8$  and  $>9$ ).

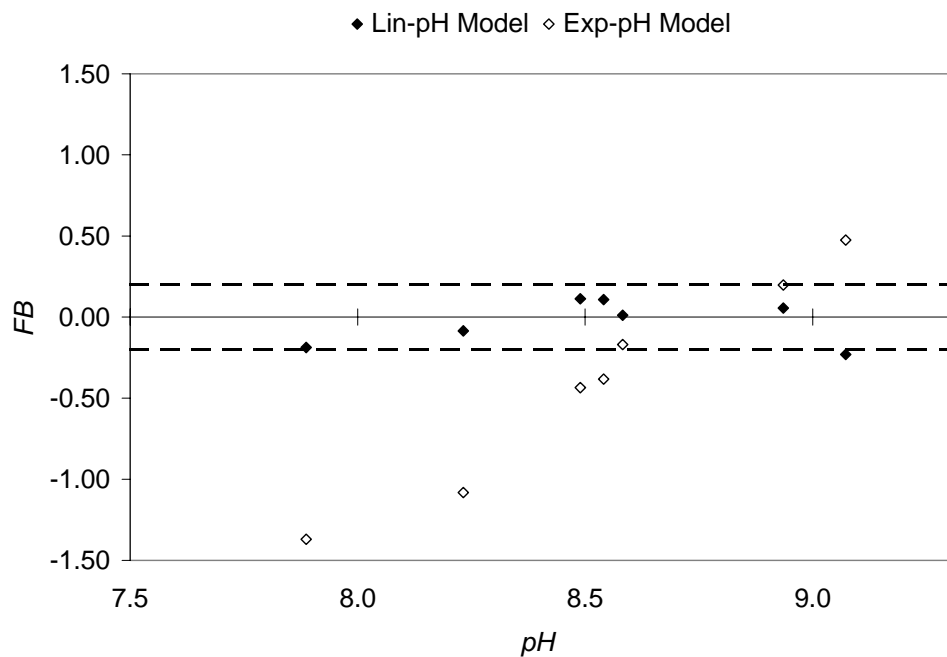


**Figure 5.5. Fractional bias (*FB*) of the Lin-*pH* and Exp-*pH* Model simulations of box concentration as a function of *pH*.**

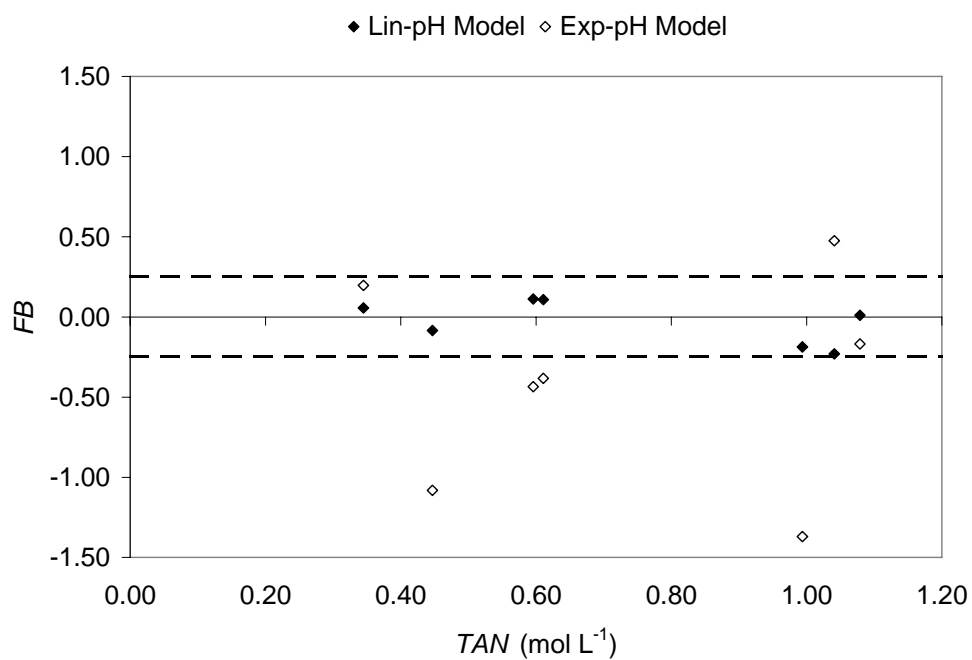


**Figure 5.6. Fractional bias (*FB*) of the Lin-*pH* and Exp-*pH* Model simulations of box concentration as a function of *TAN*.**

### 5.4.5 Sensitivity Analysis

The sensitivity of the emission rate calculation (eq. 5.1) to the input variables  $T_{film}$ ,  $\nu$ ,  $TAN$  and  $pH$  by both the Lin- $pH$  and Exp- $pH$  Models is shown in table 5.6. For the same input variable values, the average emission rate was lower using the Exp- $pH$  model compared to the Lin- $pH$  model.

**Table 5.6. Sensitivity of the Lin- $pH$  and Exp- $pH$  Models to the input variables.**

Variable (Mean)	Value	Value Relative to Mean (%)	Lin- $pH$ Model Sensitivity		Exp- $pH$ Model Sensitivity	
			$E_s$ (g h <sup>-1</sup> )	% Change	$E_s$ (g h <sup>-1</sup> )	% Change
Average		100	0.158		0.115	
$T_{film}$ (298 K)	293	80	0.121	-24	0.065	-44
	296	90	0.138	31	0.086	-25
	301	110	0.181	14	0.152	32
	303	120	0.207	31	0.200	74
$\nu$ (0.025 m s <sup>-1</sup> )	0.020	80	0.141	-11	0.096	-16
	0.023	90	0.150	-5	0.105	-8
	0.028	110	0.166	5	0.124	8
	0.030	120	0.173	10	0.133	16
$TAN$ (0.5 mol L <sup>-1</sup> )	0.40	80	0.134	-15	0.092	-20
	0.45	90	0.155	-2	0.115	1
	0.55	110	0.188	19	0.158	38
	0.60	120	0.209	32	0.192	68
$pH$ (8.8)	7.0	80	0.117	-26	0.002	-98
	7.9	90	0.137	-13	0.016	-86
	9.7	110	0.179	13	0.602	426
	10.6	120	0.199	26	1.372	1098

Temperature has a large impact on the emission rate calculations for both the Lin- $pH$  and Exp- $pH$  models. In the Lin- $pH$  model, an increase in temperature results in a higher mass transfer coefficient and thus a higher emission rate. In the Exp- $pH$  model, an increase in temperature decreases the mass transfer coefficient (eq. A1), but the emission rate still increases because of the strong positive relationship between  $f$  and  $T$  shown in eq. B1.

Changing the variable  $v$  had the smallest impact in both models compared to other variables, and again, the effect was smaller with the Lin- $pH$  Model because of the differences in mass transfer coefficient determination for the Lin- $pH$  model (eq. 5.6) and the Exp- $pH$  model (eq. B1).

The Lin- $pH$  Model shows a reduced sensitivity to  $TAN$  compared to the Exp- $pH$  Model, and this is attributed to the negative relationship between  $f$  and  $TAN$ , as shown in eq. 5.14.

The relative effect of  $pH$  is significantly larger on the emission rate calculations with the Exp- $pH$  model. For every 0.1 unit increase in  $pH$  from 8.8, the Lin- $pH$  model estimates a 48% increase in emission whereas the Exp- $pH$  model estimates a 1% increase in emission.

The Lin- $pH$  model is most sensitive to changes in  $T_{film}$  and  $pH$ . The Exp- $pH$  model is most sensitive to  $pH$ .

## 5.5 Discussion

The concentration of the slurry samples were higher than reported slurry concentration levels from several sources in the literature, likely because the urine and feces were combined with no dilution. Based on the slurry analysis results (table 5.2), lowering the crude protein and adding sugar-beet pulp to the diet composition did not result in the expected changes to  $TAN$  and  $pH$ , as was reported by Canh et al. (1998a; 1998b). The slurry emission measurements and developed slurry emission model may not truly reflect the slurry conditions in a slurry channel, but the model development does still have some important implications for slurry emission models for slurry pits in swine barns.

By changing the diet composition, there was a large variability in the slurry composition, enabling calibration of the model equations with variable sets of data.

Using an empirical equation to determine  $f$  based on measurable properties appears justified for the concentrated manure used in this study, since the unknown components and high variability limited the application of  $K_a$ . Rather than developing an empirical equation for  $f$ , the other option in the calibration process was to determine an appropriate factor that could be combined with the acid ionization constant for ammonium. Solving for the  $K_a$ -factor would not have been suitable with this data, as was done by Arogo et al. (2003b), since there was not a strong exponential relationship of the average  $f$  values with  $pH$ .

The reduced sensitivity of the Lin- $pH$  Model to  $pH$  shown in table 5.6 is explained by the linear relationship of  $f$  with  $pH$ . During the model calibration, it was interesting to note the amount of available nitrogen was consistently between 3% and 9%, even with the elevated  $pH$  levels of the slurry samples tested. There is an interesting coincidence in terms of the level of  $f$  with the model simulations by Aarnink and Elzing (1998) and Ni et al. (2000c). In the model developed by Aarnink and Elzing (1998), the effective slurry  $pH$  was adjusted from the measured slurry  $pH$  in order to increase agreement between measured and simulated ammonia emission values. The mean slurry  $pH$  used in this model was 7.5, which produces an effective  $pH$  of 8.6. Ni et al. (2000c) estimated the  $pH$  of the surface manure to be 8.8 at equilibrium. It is in this range (8.6 - 8.8) that the exponential equations for  $f$  ( $K_a$ -factor = 0.2), such as equation A2, resulted in  $f$ -values between 0.03 and 0.05 (3-5%), for a film temperature of 293 K. It may be possible that the fraction of available ammonia at the slurry surface is less dependent on  $pH$  even at lower  $pH$  levels in the range of 7 to 8, if the results in this study using concentrated manure reflect what also happens in diluted slurry.

Harper et al. (2000) found the ammonia emission rate from an anaerobic lagoon system for a swine facility to exhibit a positive, *linear* relationship with air velocity, temperature, *pH* and ammonium concentration. The sensitivity analysis of the Lin-*pH* model as shown in table 5.6 shows the slurry emission calculations using equation 5.14 for *f* also resulted in positive, linear relationships between emission and temperature, air velocity and *pH*. Harper et al. (2000) found slurry concentration and *pH* had lower statistical influence on the ammonia emission rate compared to air speed and temperature, whereas temperature and *pH* had the largest relative effects on emission using the Lin-*pH* model.

It will be useful to repeat these measurements over a wider temperature range, and with diluted slurry to see if there is a minimum value for the amount of *TAN* available as ammonia. In doing so, it may be possible to replace the empirical equation for *f* (eq. 5.14) with a mechanistic equation that better explains the effect of the physical and chemical properties of the slurry on the ammonia partitioning within the slurry. In the meantime, equation 5.14 provides a simple equation to determine *f*, based on obtainable measurements that can be used when predicting emission from urine/feces mixtures. With further understanding of how ammonia emission occurs, we will better understand the contribution of the slurry channel to over all barn emissions, and we will be better able to identify ammonia control technologies.

## **5.6 Summary**

A model was developed to simulate the emission from pig slurry and the model was compared to previous models in terms of the development and results. The model was calibrated and validated with manure collected from grower-finisher pigs fed various



diets that resulted in slurry samples with a range of *TAN* concentrations and *pH* measurements.

During model calibration, the amount of ammonia relative to *TAN* was between 3% and 9%. A linear regression equation was developed to relate the fraction of ammonia relative to the total ammoniacal nitrogen concentration (*TAN*) of the slurry to the slurry *TAN* concentration and mixed slurry *pH*. The average emission box concentration simulated with the model was less than 25% different from the average measured box concentration, a significant improvement over simulations using previous model equations. There was increased lack of fit between measured and simulated concentration levels when the slurry exhibited extreme *TAN* or *pH* values. More measurements with diluted slurry will help uncover the minimum amount of ammonia in a slurry sample that is in volatile form.

### **Acknowledgements**

The assistance provided by Ms. Laura Smith, Ms. Karen Stewart and Mr. Rob Fengler during data collection is appreciated. The authors acknowledge the financial support provided by NSERC. Also, SaskPork, Alberta Pork, Manitoba Pork and Saskatchewan Agriculture and Food Development Fund provided strategic funding for the Prairie Swine Centre Inc.

CHAPTER 6  
DYNAMIC SIMULATION OF THE AMMONIA CONCENTRATION WITHIN AND  
THE AMMONIA EMISSION FROM SWINE BARNS

E.L. Cortus<sup>1,2</sup>, S.P. Lemay<sup>3</sup> and E.M. Barber<sup>4</sup>

<sup>1</sup> *Prairie Swine Centre Inc., Saskatoon, SK;*

<sup>2</sup> *Department of Agricultural and Bioresource Engineering, University of Saskatchewan, Saskatoon, SK;*

<sup>3</sup> *Research and Development Institute in Agri-Environment, Deschambault, QC;*

<sup>4</sup> *College of Agriculture, University of Saskatchewan, Saskatoon, SK.*

**Synopsis**

The objective of this chapter is to build an ammonia emission model to simulate the hourly and daily ammonia concentration and emission patterns for grow-finish swine barns. This chapter incorporates experimental work from the preceding four chapters in the model development. The model is calibrated and validated using data collected from two grower-finisher swine rooms and is shown to predict the average room and slurry pit headspace concentration within 1% and 10% of measured values, respectively.

## **6.1 Introduction**

Intensive livestock operations provide many benefits to the communities that they are situated in, including supporting local businesses and farmers, and providing employment opportunities for local residents. However, like all businesses, intensive livestock operations need to be aware and take responsibility for the health of their workers and the barn's impact on the surrounding environment. Manure gases produced within barns can degrade the air quality for workers and animals and negatively impact the air, soil and water outside the barn. Continued attention to the issue of manure gases will help to ensure the sustainability of the industry.

Ammonia is a well-documented manure gas produced in livestock buildings and in manure storages. While the health effects specific to ammonia on animals and workers are often difficult to separate from the combined effect of ammonia, dust, endotoxins and other gases, exposure to ammonia has been correlated with decreases in pulmonary function in swine production facility workers (Donham et al., 1995). In swine production, ammonia is one of several air contaminants correlated with animal health problems like pneumonia and pleuritis (Donham, 1991). Once emitted to the atmosphere, excess ammonia can contribute to foliar injury of vegetation (Krupa, 2003), eutrophication of water systems and acidification of soil systems (Sutton et al., 1993).

Ammonia concentrations within barns vary, as do the resulting emissions to the environment. Some of the factors associated with emission levels include the manure collection system (Arogo et al., 2003a), ventilation system design (Aarnink and Wagemans, 1997), diet (Canh et al., 1998a, 1998b, 1998c), and room cleanliness (Ni et al., 1999c; Aarnink et al., 1996). Because of the numerous variables affecting emission rates, average empirical emission factors used to estimate ammonia emissions from

animal feeding operations are often misleading (Arogo et al., 2003a) and do not give an accurate estimate of the emissions for specific barns. At the same time though, the understanding of the emission process within swine barns has increased over the past twenty-five years, resulting in mechanistic models of ammonia production and emission. Mechanistic models of ammonia release continue to evolve to promote further understanding of the production and emission processes and to allow cost- and time-effective investigation of ammonia reduction techniques.

The objectives of this paper are: (1) to develop an "Ammonia Concentration and Emission Simulation" model, hereafter referred to as the ACES model, to predict hourly and daily ammonia concentration and emission patterns for swine barns; and (2) to calibrate and validate the model using measured concentration and emission data from a grower-finisher barn. The model development follows a two-control-volume approach, with sub-models to simulate the urination frequency and location, urine puddle emission and slurry emission. The model is calibrated and validated with data collected for a specific partially-slatted grow-finish room and is limited to mechanically ventilated facilities. For future applications of the ACES model to test ammonia reduction techniques, the model is adaptable to a variety of building designs and production parameters.

## **6.2 Model Development**

In a swine barn environment, nitrogen enters the system through the feed consumed by the animals. Fattening pigs retain approximately 30% of the nitrogen for growth (Aarnink, 1997) and the rest is excreted in the urine (in the form of urea) or feces (mainly in the form of protein) (Canh et al., 1997). The partitioning of nitrogen in the urine or feces is related to feed composition (Canh et al., 1997). In the urine, one mole of urea is

readily converted to two moles of ammonia and one mole of carbon dioxide in the presence of the enzyme urease that is attributed to bacteria in fecal material (Elzing and Monteny, 1997a). Fecal material is generally considered a negligible ammonia source by itself (Aarnink and Elzing, 1998) since the nitrogen is mainly in the form of bacterial protein that takes longer to convert to ammonia than urea. The exact rate and conditions for breakdown of proteins are not well understood. Therefore, when determining the amount of ammonia produced in a swine barn, knowledge of where urinations and defecations occur, as well as the amount and compositions, are important parameters to the ammonia emission process.

Urinations and defecations can occur anywhere within a pen, even on the walls. However, from an early age, pigs like to maintain their dunging area separate from their sleeping area (Watson, 1985). Producers have used partially slatted floors to provide separate dunging and sleeping areas, and to reduce the surface area of the slurry pit and urine-fouled floor area (Aarnink et al., 1996). When a urination occurs on the solid floor of a partially-slatted floor room, some of the urine may drain towards the slatted floor (and slurry storage area under the slatted floor) if the floor is sloped in that direction (Aarnink and Elzing, 1998); otherwise, the urine remains in a puddle on the floor surface. When a urination or defecation occurs on a slatted floor, a portion of the excrement remains on the slats, and the rest falls into the slurry storage under the floor. The slurry storage area under the slatted floor stores urine, feces, spilled water and spilled feed for one day up to many months depending on the barn design and manure removal technology. The liquid slurry mixture contains ammonia as a result of the breakdown of urea and from the microbial breakdown of proteins within the slurry over time (Zhang et

al., 1994). The result is two potential sites where ammonia production and emission needs to be determined: the urine-fouled floor area and the slurry storage under the slatted floor. In a partially slatted floor room, the urine-fouled floor area may be on the slatted floor, solid floor or both.

### **6.2.1 Review of Existing Models**

Ammonia emission models for dairy cattle and swine houses have developed simultaneously, given the similarities in urine and feces composition, and the method of manure storage and handling.

Convective mass transfer is used to describe ammonia volatilization from most agricultural sources, including urine puddles and stored slurry (Ni, 1999). However, Ni (1999) found a wide variation in the model equations used to determine the convective mass transfer coefficient and the partitioning of ammonia in the gas film above a liquid source. Determination of the ammonia partitioning is important for two reasons. First, ammonia is a weak base and will dissociate in solution to exist in both ammonia and ammonium forms. Liquid ammonia concentration measurements provide the total amount of the nitrogen in ammonia and ammonium forms in solution, referred to as *TAN* (Ni, 1999). Only the ammonia form is volatile and emitted from the solution under the proper conditions. Second, convective mass transfer equations require the concentration gradient of a substance between the gas phase at the liquid surface, and the surrounding air. Henry's law (and developed Henry's constants) is used to relate the partitioning of a substance between the liquid and the gas film surrounding the liquid.

#### **6.2.1.1 Urine puddle emission models**

Muck and Steenhuis (1981) modelled ammonia loss from dairy cow urine puddles based on two processes: urea to ammonia conversion following Michaelis-Menten

kinetics and ammonia volatilization by convective mass transfer. Elzing and Monteny (1997b) further developed and tested a similar model, using urine and urine/feces mixtures on a slatted floor in a scale model of a dairy cow house. This two-process model for urine puddles has also been adapted and used by Monteny et al. (1998) for free stall cubicle dairy cow houses and Aarnink and Elzing (1998) for fattening swine barns with partially-slatted floors. The resulting ammonia emission mechanism and pattern for urine puddles is described by Elzing and Monteny (1997a) as follows: ammonia generation (from urea decomposition) initially exceeds ammonia volatilization until a point where the ammonia concentration in the puddle and ammonia volatilization rate are at a maximum; after this point, volatilization exceeds ammonia formation resulting in a decrease in both ammonia concentration and emission.

#### **6.2.1.2 Slurry emission models**

Many models have been developed for slurry emission, since slurry storage is an important source of ammonia inside and outside of swine and cattle barns. No models have been identified that describe the mechanics behind ammonia generation within the slurry, but some empirical models of ammonia generation do exist (Zhang et al., 1994). Most models rely on knowledge of the slurry composition and  $pH$  to determine the ammonia concentration at the slurry surface before the emission is modelled by a convective mass transfer equation.

Similar to models for urine puddle emission, the volatile proportion of  $TAN$  at the slurry surface ( $f$ ) has usually been calculated using a relationship with the slurry  $pH$  and the acid dissociation constant ( $K_a$ ) for ammonium in water. However, the acid dissociation constant has been adjusted by multiplying  $K_a$  with factors ranging from 0.17 to 0.94 depending on the type and temperature of the solution (Hashimoto and Ludington,

1971; Zhang et al., 1994; Arogo et al., 2003b). These factors are based on experimental work with slurry solutions in the  $pH$  range of 9 to 12. Aarnink and Elzing (1998) and Ni et al. (2000b, 2000c) suggest the surface  $pH$  of the slurry is higher than  $pH$  of the mixed slurry, resulting in a higher value for  $f$  and thus a higher ammonia emission rate. This surface  $pH$  effect has not been validated with measurements and was applied in slurry emission model calculations where the average slurry  $pH$  was between 7.5 and 9.0. The expression for  $f$  as a function of the  $pH$  and  $K_a$  results in ammonia emission models that are very sensitive to slurry  $pH$ .

### **6.2.1.3 Overall room models**

The contributions of each emission site to the total emission are combined in overall "room" or "house" models. Monteny et al. (1998) combined the ammonia emission from urine puddles on the floor and the ammonia emission from the slurry channel in a conceptual model to simulate monthly ammonia emissions from dairy-cow houses. Total emission was determined as the sum of puddle and slurry emission. Aarnink and Elzing (1998) followed a similar approach to model the daily ammonia emission from fattening pig barns with partially-slatted floors. The model by Ni et al. (2000c) assumed the bulk of emissions in a pig house to come from the slurry, since this model was designed for short time periods with clean floors.

The three room models were designed for and validated with different types of measurements. Monteny et al. (1998) validated the dairy-cow house model by comparing simulated and measured monthly ammonia emissions and found an average relative difference between measured and simulated values of 3.8%. Aarnink and Elzing (1998) validated their ammonia emission model for fattening pig barns using 10-min and daily ammonia emission rates (Aarnink and Elzing, 1998). The average relative difference



between 10-min measurements and simulations was 19.1%, and the average daily simulated ammonia emission was 3.6% lower than the measured mean. The model by Ni et al. (2000c) was designed for short-term use and validated with ammonia concentration and emission levels for a period spanning about six hours. The correlation ( $R^2$ ) values between simulated and measured concentration and emission levels were 0.86 and 0.95, respectively, for the single validation data-set.

#### **6.2.1.4 Summary of existing models and recommendations**

The existing literature identifies three main processes that contribute to the daily ammonia emission pattern: urine puddle deposition, floor emission and slurry emission. Few models have been developed to incorporate these three processes in an overall room model, and in these cases, long-term simulations have been more accurate than short-term simulations. As well, the general approach has been to sum together the emission from urine puddles with the emission from slurry without taking into account the air exchange rate through the slatted floor and the potential for different concentrations in these two main areas. Monteny et al. (1998) recommended consideration of air exchange between the slurry pit and the inside air to improve ammonia modelling, which was incorporated in the following model development.

Other suggestions from the literature for improving ammonia modelling were noted. For daily simulations, Monteny et al. (1998) recommended frequent measurement and incorporation of time-dependant parameters in the model. Aarnink and Elzing (1998) recommended finding a better estimation for the  $pH$  of the top layer of slurry to improve model simulations, which would validate the suggestion by Aarnink and Elzing (1998) and Ni et al. (2000b, 2000c) that there is a significant change or difference in the slurry surface  $pH$  compared to the mixed slurry  $pH$  on the ammonia emission rate from slurry..

Both of these recommendations were addressed by the method of data collection in the following work.

Within the puddle and slurry emission models reviewed, the concentration gradient between the solution surface and bulk air has been neglected (with the exception of Ni et al., 2000c) and the evaporation rate of urine puddles has been ignored. In the following model development, the bulk gas concentration in the concentration gradient for urine puddles and slurry is retained, and water evaporation is included in the urine puddle emission calculations.

Aarnink and Elzing (1998) recommended determining the depth of urine puddles on the solid floor and for different degrees of fouling. This recommendation was not addressed in the following model development; instead, data was taken from the literature to estimate these parameters.

### **6.2.2 Control Volume Approach**

The model of Aarnink and Elzing (1998), that considers the contribution of urine puddles and the slurry pit to ammonia production, provides a starting point in developing the ACES model to simulate indoor air concentrations and emission rates. Feces and urine generally co-exist on the floor surface but only the urine portion will be considered volatile, similar to Elzing and Monteny (1997b). Absorption or desorption of ammonia by building materials or animals is also neglected because for a room that has been used extensively, the rate of absorption will be low and the rate of desorption will also be low compared to slurry or urine puddles. The ammonia generation mechanism within the slurry will not be modelled either; instead, slurry properties need to be measured or estimated and input into the model in order to calculate the slurry emission based on the surface conditions.

The main difference between the ACES model and previous models is the designation of the room as having two airspaces separated by the slatted floor. A control-volume depiction of a partially slatted floor room with a shallow slurry channel was constructed as shown in figure 6.1. Two control volumes A and B represent the room airspace and the slurry pit headspace, respectively. All incoming air is assumed to enter through planned inlets in the building structure with a concentration  $C_A$ . Hereafter the pit ventilation rate term ( $Q_H$ ) is applied to the air movement through the slatted floors. Air removal by exhaust fans in the slurry channel has been omitted in this study. Both control volumes are assumed completely mixed.

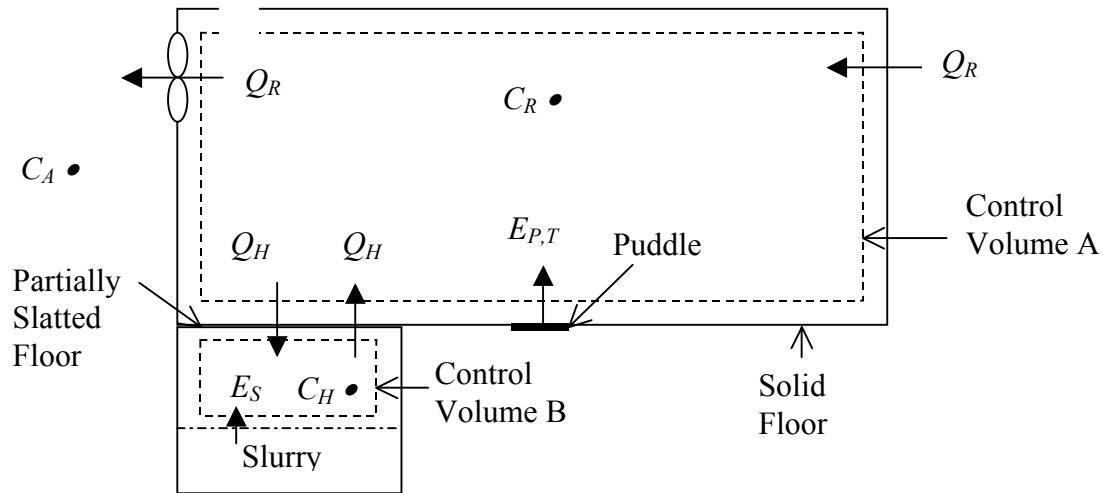


**Figure 6.1. Cross-sectional view of a partially-slatted floor room in a swine barn, with bold arrows representing ammonia addition and removal sites to the ammonia contained within Control Volume A (Room airspace) and Control Volume B (Slurry Pit Headspace).**

The ammonia sources for Control Volume A are incoming air through the inlets from the surroundings ( $Q_R \cdot C_A$ ) and through the slatted floor from the slurry channel ( $Q_H \cdot C_H$ ), as well as ammonia produced by all existing urine puddles ( $E_{P,T}$ ). Ammonia is removed from the room through the exhaust fans ( $Q_R \cdot C_R$ ), and by air movement down through the

slatted floor into the slurry channel ( $Q_H \cdot C_R$ ). Within the slurry channel, the incoming air from the room ( $Q_H \cdot C_R$ ) and the slurry emission ( $E_S$ ) are the sources of ammonia, and the outgoing air to the room is the only removal site ( $Q_H \cdot C_H$ ). Equations 6.1 and 6.2 show the contribution of ammonia sources and removal sites in the respective molar balance equations for control volumes A and B, respectively.

$$V_R \cdot 1000 \cdot \frac{dC_R}{dt} = Q_R \cdot 1000 \cdot C_A - Q_R \cdot 1000 \cdot C_R + Q_H \cdot 1000 \cdot C_H - Q_H \cdot 1000 \cdot C_R + E_{P,T} \quad (6.1)$$

$$V_H \cdot 1000 \cdot \frac{dC_H}{dt} = Q_H \cdot 1000 \cdot C_R - Q_H \cdot 1000 \cdot C_H + E_S \quad (6.2)$$

The molar balance equations can be rearranged to express the change in room and headspace concentration as a system of two differential equations (eqs. 6.3 and 6.4), providing the core of the ACES model.

$$\frac{dC_R}{dt} = \frac{Q_R \cdot (C_A - C_R)}{V_R} + \frac{Q_H \cdot (C_H - C_R)}{V_R} + \frac{E_{P,T}}{V_R \cdot 1000} \quad (6.3)$$

$$\frac{dC_H}{dt} = \frac{Q_H \cdot (C_R - C_H)}{V_H} + \frac{E_S}{V_H \cdot 1000} \quad (6.4)$$

By solving the differential equations 6.3 and 6.4, the room and headspace concentration can be determined. Based on the concentrations and ventilation rates, the emissions from the room to the surroundings and from the slurry channel into the room airspace can also be determined as shown in equations 6.5 and 6.6, respectively.

$$E_R = Q_R \cdot 1000 \cdot (C_R - C_A) \quad (6.5)$$

$$E_H = Q_H \cdot 1000 \cdot (C_H - C_R) \quad (6.6)$$

In building the ACES model to solve equations 6.3 through 6.6, it was necessary to determine the number and location of urine puddles, the rate of ammonia emission from each puddle and the rate of emission from the slurry. Three sub-models are incorporated

in the overall model to mechanistically describe these processes. The concept behind using sub-models is that as changes to each sub-model are made through further testing, they can be altered and re-incorporated in the overall model without large changes to the calculation procedure. The basic structures of the three sub-models are explained in the next three sections, followed by an explanation of the input variables required for the model and the calculation procedure.

### **6.2.3 Urination Frequency and Location Sub-Model**

The objective of the urination frequency and location sub-model is to determine the number of urinations that occur every hour and the distribution of puddles in the pen. Given the variable nature of both urination frequency and location, this sub-model combines model equations and random number generators to simulate the animal behaviour. The general assumption by this sub-model is that urinations only occur at the start of every hour (to simplify the computing process). The input values required for this sub-model are the number of animals per pen ( $N_{pigs}$ ), the slatted ( $A_{slat}$ , m<sup>2</sup>) and solid floor ( $A_{solid}$ , m<sup>2</sup>) areas, and the relative amount ( $r$ , expressed as a %) of floor area in the solid ( $r_{solid}$ ) and slatted ( $r_{slat}$ ) floor regions covered in manure.

Cortus et al. (2005) determined that urination frequency could be successfully modelled using a dromedary animal activity curve, and that a single equation was suitable for male and female pigs between 51 and 78 kg (eq. 6.7). Cortus et al. (2005) measured an average urination frequency of 0.62 urinations pig<sup>-1</sup> h<sup>-1</sup>, with a variation of  $\pm 0.58$  urinations pig<sup>-1</sup> h<sup>-1</sup> over 24 h. The time of minimum activity (2h30, expressed as 2.5 in eq. 6.7) corresponded to the middle of the darkened period in a 12 h lighted, 12 h darkened system. On a per pen basis, the average number of urinations per pen can be determined with knowledge of the number of pigs.

$$N_U = N_{Pigs} \cdot 0.62 \cdot \left( 1 - 0.58 \cdot \sin \left( \left( \frac{2\pi}{24} \right) \cdot (Time + 6 - 2.5) \right) \right) \quad (6.7)$$

To account for some random behaviour by the animals, a Poisson random number generator program (Ruckdeschel, 1981) was incorporated in the sub-model to simulate a "randomized" number of urinations using  $N_U$  from equation 6.7 as an input value to the program. The Poisson random number generator generates a value for  $N_U$ , based on the principle that for an infinite number of generations, the mean generated number would be equal to  $N_U$  generated using eq. 6.7 for a given time of day (*Time*).

Animals develop dunging areas within their pens, so the distribution of urine puddles is often limited to certain areas (Watson, 1985). However, certain factors like temperature and animal weight can cause the animals to change areas or promote dunging on the solid floor (Aarnink and Elzing, 1998; Ni et al., 1999c). Urinations and defecations occur in the same area so if fecal material is present, urine likely was or is still present as well. Equations 6.8 and 6.9 were developed to simulate the number of urinations that occur on both portions of the floor based on the relative cleanliness scores. The values for  $N_{P,slat}$  and  $N_{P,solid}$  are rounded to the nearest integer following calculation.

$$N_{P,slat} = N_U \cdot \frac{r_{slat} \cdot A_{slat}}{r_{solid} \cdot A_{solid} + r_{slat} \cdot A_{slat}} \quad (6.8)$$

$$N_{P,solid} = N_U \cdot \frac{r_{solid} \cdot A_{solid}}{r_{solid} \cdot A_{solid} + r_{slat} \cdot A_{slat}} \quad (6.9)$$

The total number of urinations occurring on the solid or slatted floor are randomly distributed within the fouled area using the following process: the manure covered area is determined from the product of the respective floor area and fouling factor ( $r$ ); the manure-covered area is divided by the puddle area to generate  $N_L$  discrete locations (eqs.

6.10 and 6.11) where urinations can occur; a random number generator generates  $N_P$  discrete locations between 1 and  $N_L$  using a uniform distribution; within locations generated, the puddle properties are set to initial values (as discussed in the puddle emission sub-model). Multiple puddles may be deposited on one location, but each new puddle is assumed to replace the previous one. Again,  $N_{L,slat}$  and  $N_{L,solid}$  are integer values, and are rounded to the nearest integer following calculation.

$$N_{L,slat} = \frac{r_{slat}}{100} \cdot \frac{A_{slat}}{A_{P,slat}} \quad (6.10)$$

$$N_{L,solid} = \frac{r_{solid}}{100} \cdot \frac{A_{solid}}{A_{P,solid}} \quad (6.11)$$

An array system is used to keep track of where urine puddles are located and their present status and properties (discussed in the Urine Puddle Emission sub-model). Each area of floor (slatted and solid) is expressed as an array within the ACES model, composed of  $N_L$  rows of data, with each row corresponding to one location.

#### 6.2.4 Urine Puddle Emission sub-model

The objective of the urine puddle emission sub-model is to calculate the physical and chemical characteristics of a single urine puddle after a user-specified time interval ( $\Delta$ ) based on initial conditions, and then to calculate the resulting puddle emission. The study shown in Chapter 4 found that water volume, urea concentration, *TAN* concentration and puddle *pH* were all necessary considerations in determining puddle emission and, therefore, a system of equations was developed to describe the urine puddle emission process when urine puddles are on a non-porous surface. General assumptions in this sub-model are: there is negligible liquid and gas absorption by the floor surface underneath or immediately surrounding the puddle; the puddle temperature is the same as the room

temperature (thus, the film temperature is equal to the room temperature); the puddle area is constant (only depth changes as volume decreases); the initial urea concentration of all urinations is the same; and urease is always present and at consistent activity levels.

Input values required by this sub-model are the puddle area ( $A_p$ , m<sup>2</sup>), room temperature ( $T_R$ , K), air velocity over the puddle surface ( $v_R$ , m s<sup>-1</sup>), relative humidity ( $RH$ , %) and initial urea concentration of the urine ( $U_0$ , mol l<sup>-1</sup>). The general equations and order of calculations used will be discussed in this section. For more background and validation of the sub-model development, refer to Chapter 4.

When a puddle is first deposited on the floor, certain initial conditions are assumed in the model. The initial puddle volume depends on the puddle location (slatted verses solid) and floor type and calculated as the product of the puddle area and puddle depth. The initial urea concentration of the puddle is an input to the model and the initial *TAN* concentration is assumed zero. The initial puddle *pH* of simulated urine puddles with initial urea concentrations of 0.2 or 0.4 mol L<sup>-1</sup> was between 9.1 and 9.3 in Chapter 4 so the ACES model assumes the initial puddle *pH* of all urine puddles is 9.2.

The puddle volume will change over time because of evaporation, modelled in equations 6.12 through 6.15, assuming that the puddle is a perfect circle, that water vapour behaves as an ideal gas, and that the density of the liquid in the urine puddle ( $\rho_p$ ) is 1 kg m<sup>-3</sup> (1 g L<sup>-1</sup>). The mass transfer coefficient is based on the boundary layer theory and was developed in Chapter 4. The diffusivity of ammonia in air at 298 K is 0.28E-04 m<sup>2</sup> s<sup>-1</sup> (Incropera and DeWitt, 1996). The assumption of laminar flow (i.e.  $Re < 5 \times 10^5$ ) in eq. 6.14 was tested and found valid for air velocities ranging from 0.2 to 2 m s<sup>-1</sup> and temperatures ranging from 283 to 303 K, for characteristic lengths up to 3.5 m.



$$L_P = \sqrt{\frac{4 \cdot A_P}{\pi}} \quad (6.12)$$

$$\rho_{v,sat} = \frac{P_{sat} \cdot 18}{100000 \cdot 0.08315 \cdot T_R} \quad (6.13)$$

$$k_{H_2O} = 0.0821 \cdot T_R^{0.7} \cdot \nu_R^{0.5} \cdot L_P^{-0.5} \cdot D_{H_2O,Air}^{0.666} \quad (6.14)$$

$$\frac{dV_P}{dt} = \frac{k_{H_2O} \cdot A_P}{\rho_P} \cdot 1000 \cdot \left( \rho_{v,sat} \cdot \left( \frac{RH}{100} - 1 \right) \right) \quad (6.15)$$

The urea concentration of the puddle will change over time as the urea breaks down into ammonia and carbon dioxide (carbonic acid) catalyzed by the enzyme urease. The change in urea concentration over time is calculated using equation 6.16, which is based on the Michaelis Menten equation for enzyme kinetics and also incorporates the effect of evaporation (Chapter 4).

$$\frac{dU}{dt} = - \left( \frac{S_m \cdot U}{K_m + U} \right) - \frac{U}{V_P} \cdot \frac{dV_P}{dt} \quad (6.16)$$

Elzing and Monteny (1997b) determined a Michaelis constant ( $K_m$ ) value of 0.002 mol L<sup>-1</sup> in a laboratory analysis of urease activity in a urine/feces mixture that will be applied in the ACES model.

Urease activity has been expressed using many different units in the literature. Many of the reported urease activities represent the urease activity associated with the surface area of the floor in contact with solution. This type of urease activity measurement will hereafter be referred to as the potential urease activity ( $S_m'$ ) and have units of g NH<sub>3</sub> m<sup>-2</sup> s<sup>-1</sup>. Dividing  $S_m'$  by the puddle depth and correcting for the proper units results in the urease activity ( $S_m$ ) with units of mol U L<sup>-1</sup> s<sup>-1</sup>.

The  $S_m'$  of the floor surface has been linked to fecal material and amount of fouling (Braam et al., 1997a; Braam et al., 1997b; Braam and Swierstra, 1999). Based on the literature review conducted in Chapter 3, and since urinations and defecations occur in the same general areas, all urinations are assumed to occur on dirty floors with an average potential urease activity of  $5 \text{ g } NH_3 \text{ m}^{-2} \text{ s}^{-1}$ .

After urea has started decomposing, ammonia is produced and the volatile portion of the *TAN* will volatilize to the surroundings. The concentration of *TAN* will also be related to the rate of water disappearance. Equations 6.17 through 6.20 describe the modelling process for the change in *TAN* with time. Equation 6.17 determines the convective mass transfer coefficient for ammonia based on the boundary layer theory (Chapter 4). Equation 6.18, from Aarnink and Elzing (1998) determines the fraction of *TAN* (which includes ammonia and ammonium) in ammonia form based on the puddle *pH* and temperature down to a minimum value of 0.05 (Chapter 4). Equation 6.19, also from Aarnink and Elzing (1998), calculates the dimensionless Henry constant for ammonia, relating the ammonia concentration in the liquid to the ammonia concentration in the gas film above the solution. Equation 6.20 sums the effects of urea degradation, ammonia volatilization and water evaporation on *TAN* concentration.

$$k_{NH_3,P} = 0.0821 \cdot T_R^{0.7} \cdot \nu_R^{0.5} \cdot L_P^{-0.5} \cdot D_{NH_3,Air}^{0.666} \quad (6.17)$$

$$f_P = MAX \left( \frac{10^{pH_P}}{10^{pH_P} + 5 \cdot 10^{(0.0897 + \frac{2729}{T_R})}}, 0.05 \right) \quad (6.18)$$

$$H_P = 1431 \cdot 1.053^{(293 - T_R)} \quad (6.19)$$

$$\frac{dTAN_P}{dt} = -2 \cdot \left( \frac{S_m \cdot U}{K_m + U} \right) - \frac{k_{NH3,P} \cdot A_P \cdot 1000 \cdot \left( \frac{f_P \cdot TAN}{H_P} - C_R \right)}{V_P} - \frac{TAN_P}{V_P} \cdot \frac{dV_P}{dt} \quad (6.20)$$

Urine puddle  $pH$  can have a large impact on the rate of ammonia emission from a urine puddle, since the fraction of  $TAN$  in ammonia form is exponentially related to  $pH$  (eq. 6.18). Urine puddle  $pH$  was linked to the change in  $TAN$  within the puddle, and the relationship depends if  $TAN$  is increasing or decreasing (Chapter 4) (eq. 6.21).

$$\begin{aligned} \frac{dpH_P}{dt} &= -0.75 \cdot \frac{dTAN_P}{dt} \text{ for } \frac{dTAN_P}{dt} > 0 \text{ or} \\ \frac{dpH_P}{dt} &= 6 \cdot \frac{dTAN_P}{dt} \text{ for } \frac{dTAN_P}{dt} < 0 \end{aligned} \quad (6.21)$$

Using the array system generated by the Urination Frequency and Location sub-model, current values for puddle age,  $V_P$ ,  $U$ ,  $TAN_P$  and  $pH_P$  are stored in separate columns for each possible puddle location (array row). The current values are used as initial values and the differential equations 6.15, 6.16, 6.20 and 6.21 are solved together using the fourth-order Runge Kutta method (Rao, 2002) to determine the new values for  $V_P$ ,  $U$ ,  $TAN_P$  and  $pH_P$  after an interval ( $h$ ) of 150 s (Chapter 4). To calculate  $TAN_{P,t+h}$  for example, equations 6.22 through 6.25 are solved, followed by equation 6.26. In equations 6.22 through 6.25, *function* represents the differential equation that is being solved (eq. 6.20 in this example).

$$RK_1 = function(t, V_{P,t}, U_t, TAN_{P,t}, pH_{P,t}) \quad (6.22)$$

$$RK_2 = function(t + 0.5 \cdot h, V_{P,t}, U_t, TAN_{P,t} + 0.5 \cdot h \cdot RK_1, pH_{P,t}) \quad (6.23)$$

$$RK_3 = function(t + 0.5 \cdot h, V_{P,t}, U_t, TAN_{P,t} + 0.5 \cdot h \cdot RK_2, pH_{P,t}) \quad (6.24)$$

$$RK_4 = function(t + h, V_{P,t}, U_t, TAN_{P,t} + RK_3, pH_{P,t}) \quad (6.25)$$

$$TAN_{P,t+h} = TAN_{P,t} + \frac{h}{6} \cdot (RK_1 + 2 \cdot RK_2 + 2 \cdot RK_3 + RK_4) \quad (6.26)$$

When solving for  $V_{P,t+h}$ ,  $U_{t+h}$  or  $pH_{P,t+h}$ , the respective variable is incrementally changed as  $TAN$  was in the example, while the remaining variables retain their current values for time  $t$ . The new values,  $V_{P,t+h}$ ,  $U_{t+h}$ ,  $TAN_{P,t+h}$  and  $pH_{P,t+h}$  replace the old values in the array to become the current values, and solution of equations 6.12 through 6.26 is repeated until the user-specified time interval ( $\Delta$ ) has elapsed. At the end of the calculation interval the volatile fraction of  $TAN_{P,t+\Delta}$  is re-calculated using the new puddle  $pH$  ( $pH_{P,t+\Delta}$ ) (eq. 6.27), and the puddle emission is determined using equation 6.28.

$$f_{P,t+\Delta} = MAX \left( \frac{10^{pH_{P,t+\Delta}}}{10^{pH_{P,t+\Delta}} + 5 \cdot 10^{(0.0897 + \frac{2729}{T_R})}}, 0.04 \right) \quad (6.27)$$

$$E_P = k_{NH3,P} \cdot A_P \cdot 1000 \cdot \left( \frac{f_{P,t+\Delta} \cdot TAN_{P,t+\Delta}}{H_P} - C_{R,t} \right) \quad (6.28)$$

The emissions from each puddle in a pen at time  $t + \Delta$  are summed together to determine the total puddle emission from a pen (eq. 6.29), and the total puddle emission is the sum of emissions from all pens (eq. 6.30).

$$E_{P, Pen} = E_{P, Pen} + E_P \quad (6.29)$$

$$E_{P,T} = N_{Pen} \cdot E_{P, Pen} \quad (6.30)$$

### 6.2.5 Slurry Emission Sub-Model

The objective of the slurry emission model is to simulate the rate of ammonia release from the slurry surface after a user-specified time interval ( $\Delta$ ), based on measured chemical and physical characteristics. In Chapter 5 a model for slurry emission from concentrated manure was tested and various parts of that model are incorporated in this

sub-model. Important assumptions for this sub-model are that slurry properties are constant throughout the slurry pit and the air flow over the slurry is directional to the pen length (i.e. the emitting length for convective mass transfer is equal to the length of the slatted floor in a pen). The slurry emission sub-model requires input values for slurry temperature ( $T_S$ , K), slurry pit headspace temperature ( $T_H$ , K), air velocity over the slurry surface ( $v_H$ ,  $\text{m s}^{-1}$ ), length of the slatted floor ( $L_{slat}$ , m), slurry  $TAN$  ( $TAN_S$ ,  $\text{mol l}^{-1}$ ), slurry  $pH$  ( $pH_S$ ) and the number of pens ( $N_{Pen}$ ).

The slurry emission sub-model, shown in equations 6.31 through 6.35, is based on convective mass transfer of ammonia from the slurry surface to the surrounding air. In this model, the surrounding air is the slurry pit headspace air at time  $t$ . The film temperature can be determined from input values for slurry temperature and headspace temperature (eq. 6.31). This model utilizes an ammonia mass transfer coefficient based on the boundary layer theory (Incropera and DeWitt, 1996) assuming laminar flow over the slurry surface (eq. 6.32). The assumption of laminar flow (i.e.  $Re < 5 \times 10^5$ ) was tested and validated for air velocities ranging from 0.02 to 0.12  $\text{m s}^{-1}$  and temperatures ranging from 283 K to 303 K, for an emitting length up to 12 m.

$$T_{film} = \frac{T_H + T_S}{2} \quad (6.31)$$

$$k_{NH_3,S} = 0.0821 \cdot T_{film}^{0.7} \cdot v_H^{0.5} \cdot L_{slat}^{-0.5} \cdot D_{NH_3,Air}^{0.666} \quad (6.32)$$

There are four proposed methods to determine the fraction of  $TAN$  in the slurry that is in ammonia form and thus volatile (eq. 6.33). The development of these methods is discussed in greater detail in the following sub-section. Selection of the appropriate method is discussed in the Model Calibration section.

$$f_s = \frac{[NH_3]}{[NH_3 + NH_4^+]} \quad (6.33)$$

Once the volatile fraction of  $TAN_s$  is calculated using one of the four suggested methods, the concentration of the gas layer at the slurry surface is approximated using the dimensionless Henry constant calculation from Aarnink and Elzing (1998) (eq. 6.34).

$$H_s = 1431 \cdot 1.053^{(293 - T_{film})} \quad (6.34)$$

The slurry emission rate for the whole slurry channel is calculated using equation 6.35 based on the slat area for one pen and the number of pens.

$$E_s = N_{Pen} \cdot k_{NH_3, S} \cdot A_{slat} \cdot 1000 \cdot \left( \frac{f_s \cdot TAN_s}{H_s} - C_H \right) \quad (6.35)$$

#### 6.2.5.1 Calculating the volatile fraction ( $f_s$ ) of TAN in slurry

The review of slurry emission models in Chapter 5 showed that the majority of previous slurry emission models determined the fraction of  $TAN_s$  in ammonia form by considering the acid dissociation constant for ammonium in water ( $K_a$ ) and the slurry  $pH$ . The relationship between  $K_a$  and temperature was derived by Jayaweera and Mikkelsen (1990) and is shown in equation 6.36.

$$K_a = \frac{[NH_3] \cdot [H^+]}{[NH_4^+]} = 10^{-\left(0.0897 + \frac{2729}{T_{film}}\right)} \quad (6.36)$$

Equation 6.36 can be re-arranged and substituted into equation 6.33 so that  $f_s$  is calculated as a function of  $pH_s$  and  $K_a$  only.

Various authors have suggested that the  $K_a$  value for ammonium in water shown in equation 6.36 will be affected by other components in a slurry mixture such as solids content and have experimentally determined factors for  $K_a$  to account for this impact. For example, Zhang et al. (1994) used a factor of 0.2 for diluted pig manure that

effectively decreases the relative amount of ammonia compared to ammonium for a given  $pH_S$  level. The  $f_S$ -equation from the slurry emission model by Zhang et al. (1994) is the first proposed method for determining  $f_S$  as shown in equation 6.37 ( $f_{S1}$ ).

$$f_{S1} = \frac{10^{pH}}{10^{pH} + \frac{1}{0.2 \cdot K_a}} \quad (6.37)$$

The second proposed method for determining  $f_S$  is similar to equation 6.37, except that the acid dissociation constant for ammonium in slurry is considered the same as for ammonium in water, shown in equation 6.38 ( $f_{S2}$ ).

$$f_{S2} = \frac{10^{pH}}{10^{pH} + \frac{1}{K_a}} \quad (6.38)$$

The third method is based on the suggested equation for  $f_S$  from the model by Aarnink and Elzing (1998). Based on simulations Aarnink and Elzing (1998) made the suggestion that there was a slurry surface effect on the emission process, and that the surface  $pH_S$  was 1.1 units higher than the mixed slurry  $pH$ . The effect of elevated  $pH_S$  at the slurry surface could also be attributed to a higher dissociation constant for ammonium in slurry compared to water. For example, a surface effect of 1.1 units is equivalent in the  $pH_S$  range of 5 to 8 of a factor of 2.5. Equation 6.39 is the third proposed method for determining  $f_S$ .

$$f_{S3} = \frac{10^{pH+1.1}}{10^{pH+1.1} + 5 \cdot 10^{\left(0.0897 + \frac{2729}{T}\right)}} \approx \frac{10^{pH}}{10^{pH} + \frac{1}{2.5 \cdot 10^{\left(0.0897 + \frac{2729}{T}\right)}}} \quad (6.39)$$

As shown in Chapter 5, slurry emission tests with concentrated manure showed a less-sensitive relationship between  $f_S$  and  $pH_S$  than equations 6.37 to 6.39 would predict.

There was also a negative effect of increasing ammonia on the  $f_S$ -value. The fourth proposed method for determining  $f_S$  is based on the study demonstrated in Chapter 5 and is shown in equation 6.40.

$$f_{S4} = -0.0444 \cdot TAN_S + 0.0105 \cdot pH_S \quad (6.40)$$

The appropriate method for calculating  $f_S$  is tested and discussed in the Model Calibration section.

## 6.2.6 Input Values and Assumptions

Following the development of the sub-models, variables were identified as inputs to the various functions. Many of these variables are easily obtained or measured within a barn and have been included as input values. Other variables such as puddle area, air velocity over the floor and pit surfaces, and the air exchange between the slurry channel and room are determined based on literature values and the input room design and environmental factors.

### 6.2.6.1 Static variables

Static variables related to room design, nutrition and simulation parameters are input to the ACES model. The listing of the numerous variables is shown in table 6.2 at the end of the Model Development section. From the room design variables, the slatted floor area per pen, the solid floor area per pen, room volume and slurry pit headspace volume can be determined (eqs. 6.41 to 6.44, respectively). Equation 6.44 assumes the room is 15% wider than the total width of the pens in a room, the room is 20% longer than the total length of the pens in a room, and the ceiling height is 3.0 m.

$$A_{slat} = L_{slat} \cdot W_{pen} \quad (6.41)$$

$$A_{solid} = (L_{Pen} - L_{slat}) \cdot W_{pen} \quad (6.42)$$



$$V_R = N_{Pen} \cdot (W_{Pen} \cdot 1.15 \cdot L_{Pen} \cdot 1.20 \cdot 3.0) \quad (6.43)$$

$$V_H = N_{Pen} \cdot L_{Slat} \cdot W_{Pen} \cdot (d_{Pit} - d_S) \quad (6.44)$$

#### 6.2.6.2 Dynamic variables

As suggested by Monteny et al. (1998), frequent measurement of time-dependant parameters is important in short-term ammonia modelling. The ACES model is designed to incorporate changing environmental conditions and requires values for room temperature, slurry temperature, pit temperature, relative humidity, room ventilation rate, static pressure difference between the room and surroundings and ammonia concentration of the inlet air, based on time.

#### 6.2.6.3 Puddle area and depth

Aarnink et al. (1997) measured the urine puddle area of grower-finisher pigs within grow-finish pig buildings on slatted floors of different materials and designs and found the slatted floor puddle area increased by 0.0096 m<sup>2</sup> every three-week period. Aarnink and Elzing (1998) translated this data to express slatted floor puddle area based on slatted floor type and animal weight. The data was further developed into a best-fit linear equation (eq. 6.45) with coefficients depending on the floor type (table 6.1) for the ACES model. The mean depth of urine puddles on clean and fouled slatted floor surfaces were measured by Aarnink and Elzing (1998). The puddle depth measurements for fouled floor surfaces shown in table 6.1 are used in the ACES model.

$$A_{P,slat} = x_1 + x_2 \cdot M_{Pig} \quad (6.45)$$

**Table 6.1. Area and depth of urine puddles on slatted floors of different design for pigs between 30 and 100 kg (Adapted from Aarnink et al. (1997) and Aarink and Elzing (1998)).**

Floor Design	Slatted Floor Puddle Area Coefficients for eq. 6.45		Puddle Depth <sup>z</sup> (m)
	$x_1$	$x_2$	
Concrete slatted floor, 15% open area (10-cm wide slats with 2-cm gaps)	0.057	0.00055	0.00136
Concrete slatted floor, 18% open area (7-cm wide slats with 1.8-cm gaps)	0.031	0.00054	0.00161
Cast iron slatted floor, 32% open area (2.5-cm wide slats with 1.5-cm gaps)	0.020	0.00055	0.00166
Metal slatted floor, 50% open area (1-cm wide slats with 1-cm gaps)	-0.002	0.00055	0.00225

<sup>z</sup> Puddle depth assumes fouled floor surface.

Assuming a pig urinates 15 times per day (Cortus et al. 2005), and the volume of each urination is the same, the volume of urine deposited per urination is calculated in equation 6.46. Aarnink and Elzing (1998) measured the puddle area for a known volume of urine deposited on the solid floor and known distance from the slatted floor. This has been adapted for use in the ACES model, assuming all urinations on the solid floor occur at the midpoint on the solid floor (eq. 6.47).

$$V_U = \frac{V_{U,T}}{15} \quad (6.46)$$

$$A_{P,solid} = 0.038 + 0.162 \cdot V_U + 0.043 \cdot \frac{(L_{Pen} - L_{Slat})}{2} \quad (6.47)$$

The measured mean depth of 0.5-l urine puddles on a clean, dry concrete floor was 0.282 mm (Aarnink and Elzing, 1998). On concrete slatted floors the puddle depth on fouled floors was 2.3 times the depth on clean concrete floors. Applying this relationship to solid floors results in an average puddle depth of 0.6 mm that is used in the ACES model.

#### 6.2.6.4 Air velocity over the floor and slurry pit

Air speed over the floor is a difficult measurement. Randall (1980) found minimum airspeeds at animal level (0.3 m above the floor) ranging from 0.15 to 0.28 m s<sup>-1</sup> at minimum ventilation levels (0.1 m<sup>3</sup> s<sup>-1</sup>), and 0.2 to 1.8 m s<sup>-1</sup> at maximum ventilation levels (1.0 m<sup>3</sup> s<sup>-1</sup>), in swine barns of numerous ventilation and room designs. The average airspeed levels incorporate measurements from 10 locations within a pen. Ogilvie et al. (1990) present best-fit equations for floor air speed as a function of either jet momentum number or the ratio of air flow to floor area, for a variety of locations and types of air inlets, as well as the penning layout. The ACES model assumes a constant airflow over the entire pen surface, and uses the regression equation variables in Ogilvie et al. (1990) to simulate the floor air speed based on the jet momentum number. The process for floor airspeed calculation involves: determining the saturation vapour partial pressure for the inlet temperature; determining the air density at the inlet (eq. 6.48; Albright, 1990) assuming the air mixture is a perfect gas; determining the resulting inlet velocity (eq. 6.49) (Albright, 1990); calculating the jet momentum number (eq. 6.50) (Ogilvie et al., 1990); and using the jet momentum number and regression variables ( $x_{3..5}$ ) from Ogilvie et al. (1990) to calculate the average air speed at animal level (eq. 6.51).

$$\rho_{air,inlet} = \frac{\left( \left( \frac{1}{P_{atm} + \Delta P_R} \right) \cdot 287.0 \cdot T_{inlet} \cdot \left( 1 + 1.6078 \cdot \frac{0.62198 \cdot \frac{RH}{100} \cdot P_{sat}}{P_{atm} + \Delta P_R - \frac{RH}{100} \cdot P_{sat}} \right) \right)}{1 + \left( \frac{0.62198 \cdot \frac{RH}{100} \cdot P_{sat}}{P_{atm} + \Delta P_R - \frac{RH}{100} \cdot P_{sat}} \right)} \quad (6.48)$$

$$v_{inlet} = \left( \frac{2 \cdot \Delta P_R}{\rho_{air,inlet}} \right)^{0.5} \quad (6.49)$$

$$J = \frac{Q_R \cdot v_{inlet}}{g \cdot V_R} \quad (6.50)$$

$$v_R = x_3 + x_4 \cdot J^{x_5} \quad (6.51)$$

Air velocity over the slurry surface was predicted by Aarnink and Elzing (1998) using a linear relationship with ventilation rate per floor area. Equation 6.52 is an adaptation of the equation to account for changes to pen design and room area that is incorporated in the ACES model.

$$v_H = \frac{2.3 \cdot Q_R}{(N_{Pen} \cdot 1.15 \cdot L_{Pen} \cdot 1.20 \cdot W_{Pen})} + 0.02 \quad (6.52)$$

#### 6.2.6.5 Air exchange through the slatted floor

Quantifying the air exchange through slatted floors is difficult since it may be related to thermal buoyancy, forced ventilation or natural ventilation (Monteny and Overbeek, 1997). Air exchange measurements between the room and slurry channel have been attempted in a scale model swine house (Yu et al., 1991) and in cubicle dairy-cow houses (Monteny and Overbeek, 1997) using tracer gas methods, but the air exchange rate is still difficult to estimate for most designs and ventilation rates. Yu et al. (1991) found inlet jet speed and direction, ventilation rate and direction of airflow at floor level affected the rate of air exchange through the slatted floor. For a ceiling inlet in the wall opposite the slatted floor, with air flowing across the ceiling and down the wall toward the slatted floor, the air exchange rate through the slatted floor expressed as air changes per hour ranged from 1% to 21% of the total ventilation rate also expressed as air changes per hour. Monteny and Overbeek (1997) found the measured pit ventilation rate showed an

exponential relationship with the temperature difference between the slurry pit air and the incoming air. The basis behind this relationship was cold incoming air from the inlets would sink down through the slatted floor, forcing the warmer slurry pit air upwards. From a zero to 3°C temperature difference, the minimum air exchange rate was 2000 m<sup>3</sup> h<sup>-1</sup>. The pit ventilation rate increased exponentially to 5000 m<sup>3</sup> h<sup>-1</sup> and 7500 m<sup>3</sup> h<sup>-1</sup> for a temperature difference of 10°C and room air exchange rates of 12000 m<sup>3</sup> h<sup>-1</sup> and 18000 m<sup>3</sup> h<sup>-1</sup>, respectively. In the ACES model, equation 6.53 is applied as the pit ventilation rate, and the constants  $x_6$  and  $x_7$  are determined and discussed in the Results Section.

$$Q_H = x_6 \cdot (T_H - T_R) + x_7 \cdot Q_R \quad (6.53)$$

### 6.2.7 Calculation Method

The sub-model results, input values and calculated values for puddle area, air velocity and air exchange through the slatted floor are incorporated in the core model equations (eqs. 6.3 and 6.4) based on their values at time  $t + \Delta$ . Using initial values for  $C_R$  and  $C_H$  (initially input by the user and thereafter based on the last simulation), equations 6.3 and 6.4 are solved together using the fourth-order Runge-Kutta method (Rao, 2002) to determine values for room and headspace concentration at time  $t + \Delta$ , and the new emission rates accordingly.

Figure 6.2 shows the computing process proposed for the ACES model to simulate  $C_R$ ,  $C_H$ ,  $E_R$  and  $E_H$  over a specified period of time, at user-defined timestep intervals ( $\Delta$ ). The model assumes that the slurry properties are constant throughout the slurry pit. The model also considers every pen to have the same dimensions, floor type and slatted floor area. Pens are separated based on their cleanliness as either clean pens (no fouling of the solid floor) or dirty pens (some fouling of the solid floor). All dirty pens are assumed to

have the same level of fouling. These assumptions allow puddle emission calculations on a per pen basis and multiplication by the number of clean pens and dirty pens, respectively, to determine total emission rates from the floor and slurry channel.

A computer program has been developed using Visual Basic 6.0 programming language to instruct the user on what input variables are required and to perform all the necessary calculations. Table 6.2 provides the overall procedure for the ACES model to complete all the necessary calculations between the user-defined start and end times.

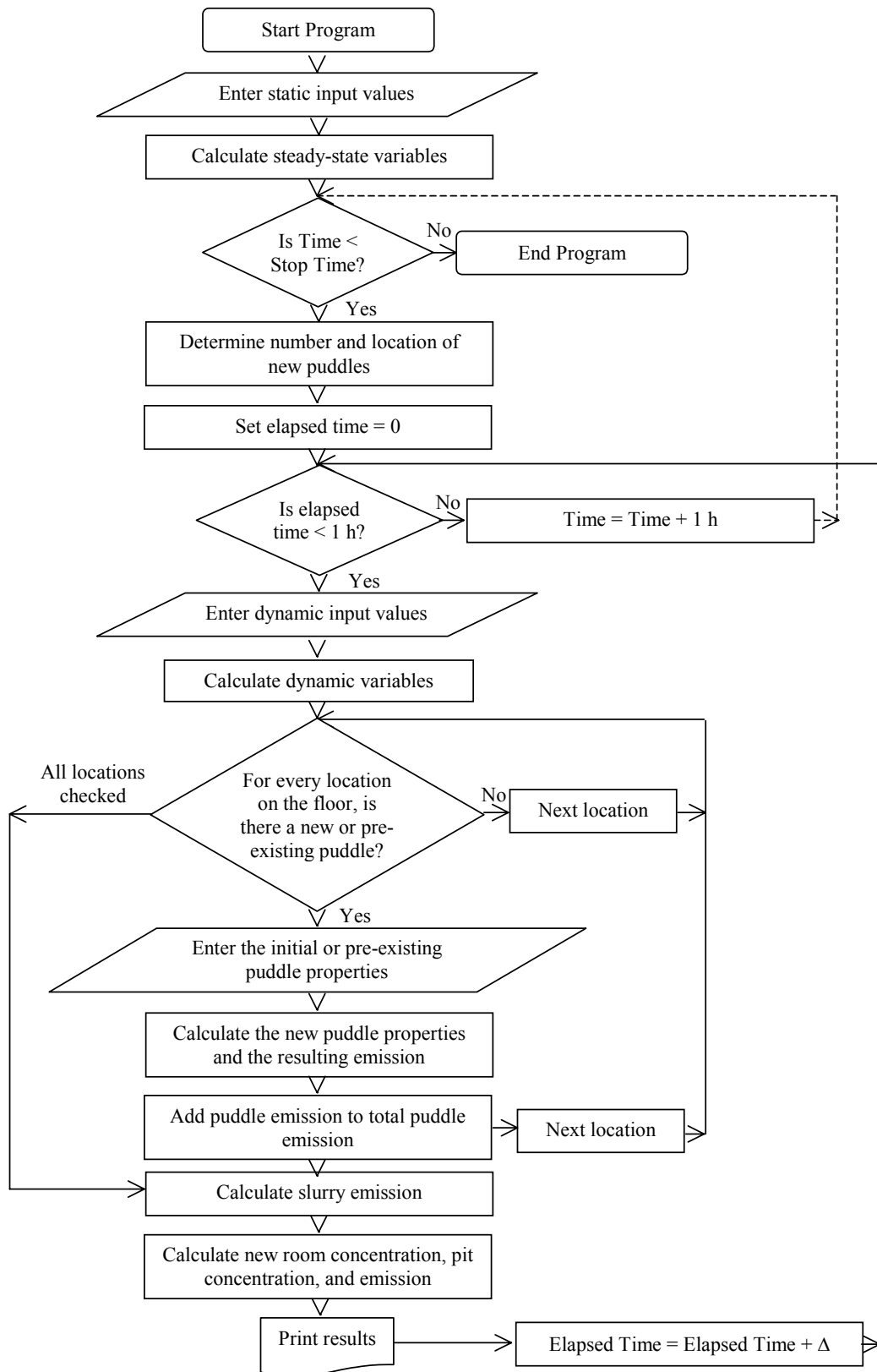


**Figure 6.2. Flowchart for ACES model.**

**Table 6.2. ACES model computing process.**

Process	Variable	Calculation	Eq.
<b>START</b>			
Enter input values	<b>Building Design Factors</b>	<b>Nutrition Factors</b>	<b>Simulation Factors</b>
	Pen Length ( $L_{Pen}$ )	Initial Urea Concentration ( $U_0$ )	Start Date and Time
	Pen Width ( $W_{Pen}$ )	Average Pig Weight ( $M_{pig}$ )	Stop Date and Time
	Slatted Floor Length ( $L_{slat}$ )	Urine Volume per Pig per Day ( $V_{U,T}$ )	Initial Room Concentration ( $C_R$ )
	Slatted Floor Type	Slurry TAN ( $TAN_S$ )	Initial Headspace Concentration ( $C_H$ )
	Number of Pens ( $N_{Pens}$ )	Slurry pH ( $pH_S$ )	Slatted Floor Fouling Factor ( $r_{slat}$ )
	Number of Dirty Pens ( $N_{DirtyPens}$ )		Solid Floor Fouling Factor ( $r_{solid}$ )
	Number of Pigs per Pen ( $N_{Pig}$ )		Timestep ( $\Delta$ )
	Ventilation/Room Design		
	Slurry Depth ( $d_S$ )		
	Pit Depth ( $d_{Pit}$ )		
Calculate steady state variables	$A_{slat}$	$A_{slat} = L_{slat} \cdot W_{pen}$	6.41
	$A_{solid}$	$A_{solid} = (L_{Pen} - L_{slat}) \cdot W_{pen}$	6.42
	$V_R$	$V_R = N_{Pen} \cdot (W_{Pen} \cdot 1.15 \cdot L_{Pen} \cdot 1.20 \cdot 3.0)$	6.43
	$V_H$	$V_H = N_{Pen} \cdot L_{slat} \cdot W_{Pen} \cdot (d_{Pit} - d_S)$	6.44
	$A_{P,slat}$	$A_{P,slat} = x_1 + x_2 \cdot M_{Pig}$ where $x_{1,2}$ are dependant on slatted floor type (table 6.1) (Adapted from Aarnink et al., 1997 and Aarnink and Elzing, 1998)	6.45
	$V_U$	$V_U = \frac{V_{U,T}}{15}$	6.46
	$A_{P,solid}$	$A_{P,solid} = 0.038 + 0.162 \cdot V_U + 0.043 \cdot \frac{(L_{Pen} - L_{slat})}{2}$ (Adapted from Aarnink and Elzing, 1998)	6.47
<b>Loop 1</b> From start date and time to stop date and time, in 1 h increments			
Urine Puddle Frequency and Location sub-model (assuming all pens have the same fouled floor areas)	$N_U$	$N_U = N_{Pigs} \cdot 0.62 \cdot \left( 1 - 0.58 \cdot \sin \left( \left( \frac{2\pi}{24} \right) \cdot (Time + 6 - 2.5) \right) \right)$ (Cortus et al., 2005) Use a random number generator (using a Poisson distribution), to generate a random number of urinations based on a mean of $N_U$	6.7
	$N_{P,slat}$	$N_{P,slat} = N_U \cdot \frac{r_{slat} \cdot A_{slat}}{r_{solid} \cdot A_{solid} + r_{slat} \cdot A_{slat}}$	6.8
	$N_{P,solid}$	$N_{P,solid} = N_U \cdot \frac{r_{solid} \cdot A_{solid}}{r_{solid} \cdot A_{solid} + r_{slat} \cdot A_{slat}}$	6.9
	$N_{L,slat}$	$N_{L,slat} = \frac{r_{slat}}{100} \cdot \frac{A_{slat}}{A_{P,slat}}$	6.10
	$N_{L,solid}$	$N_{L,solid} = \frac{r_{solid}}{100} \cdot \frac{A_{solid}}{A_{P,solid}}$	6.11
		Randomly distribute puddles within the grids	



**Table 6.2 (continued)**

Loop 2		From 0 to 60 min, in $\Delta$ increments	
Enter current environ- mental conditions	<b>Environmental Factors</b>		
	room temperature ( $T_R$ )		
	slurry temperature ( $T_S$ )		
	slurry pit headspace temperature ( $T_H$ )		
	relative humidity ( $RH$ )		
	ventilation rate ( $Q_R$ )		
	static pressure ( $\Delta P_R$ )		
	inlet concentration ( $C_A$ )		
Calculate dynamic variables	$\rho_{air,inlet}$	$\rho_{air,inlet} = \left( \frac{\left( \frac{1}{P_{atm} + \Delta P_R} \right) \cdot 287.0 \cdot T_{inlet} \cdot \left( 1 + 1.6078 \cdot \frac{0.62198 \cdot \frac{RH}{100} \cdot P_{sat}}{P_{atm} + \Delta P_R - \frac{RH}{100} \cdot P_{sat}} \right)}{1 + \left( \frac{0.62198 \cdot \frac{RH}{100} \cdot P_{sat}}{P_{atm} + \Delta P_R - \frac{RH}{100} \cdot P_{sat}} \right)} \right)^{-1}$	6.48
	$v_{inlet}$	(Albright, 1990) $v_{inlet} = \left( \frac{2 \cdot \Delta P_R}{\rho_{air,inlet}} \right)^{0.5}$	6.49
	$J$	(Albright, 1990) $J = \frac{Q_R \cdot v_{inlet}}{g \cdot V_R}$	6.50
	$v_R$	(Ogilvie et al. 1990) $v_R = x_3 + x_4 \cdot J^{x_5}$ where $a_{3...5}$ are dependant on ventilation design (Ogilvie et al., 1990)	6.51
	$v_H$	$v_H = 2.3 \cdot \frac{V_R}{N_{Pen} \cdot (L_{Pen} \cdot 1.15 \cdot W \cdot 1.20)} + 0.02$	6.52
	$Q_H$	(Aarnink and Elzing, 1998) $Q_H = x_6 \cdot (T_H - T_R) + x_7 \cdot Q_R$ where $x_{6,7}$ are regression coefficients	6.53
Loop 3		For each possible puddle location on the slatted and solid floor areas in a pen, what kind of urine puddle exists?	
Set puddle properties for the current loop	No Puddle Exists: <b>Repeat Loop 3</b>	A New Puddle Exists: $V_{P,0} = A_P \cdot d_P \cdot 1000$ $U_0 = U_0$ $TAN_{P,0} = 0$ $pH_{P,0} = 9.2$	An Old Puddle Exists: Use conditions determined from the previous cycle of Loop 2.

**Table 6.2 (continued)**

Urine Puddle Emission sub-model	$L_P$	$L_P = \sqrt{\frac{4 \cdot A_P}{\pi}}$	6.12
	$\rho_{v,sat}$	$\rho_{v,sat} = \frac{P_{sat} \cdot 18}{100000 \cdot 0.08315 \cdot T_R}$ where $P_{sat}$ is determined for $T_R$	6.13
	$k_{H_2O,P}$	$k_{H_2O} = 0.0821 \cdot T_R^{0.7} \cdot v_R^{0.5} \cdot L_P^{-0.5} \cdot D_{H_2O,Air}^{0.666}$ (Chapter 4)	6.14
	$V_{P,t+h}$	$\frac{dV_P}{dt} = \frac{k_{H_2O} \cdot A_P}{\rho_P} \cdot 1000 \cdot \left( \rho_{v,sat} \cdot \left( \frac{RH}{100} - 1 \right) \right)$ (Chapter 4)	6.15
	$U_{t+h}$	$\frac{dU}{dt} = - \left( \frac{S_m \cdot U}{K_m + U} \right) - \frac{U}{V_P} \cdot \frac{dV_P}{dt}$ (Chapter 4)	6.16
	$k_{NH_3,P}$	$k_{NH_3,P} = 0.0821 \cdot T_R^{0.7} \cdot v_R^{0.5} \cdot L_P^{-0.5} \cdot D_{NH_3,Air}^{0.666}$ (Chapter 4)	6.17
	$f_{P,t}$	$f_P = MAX \left( \frac{10^{pH_P}}{10^{pH_P} + 5 \cdot 10^{\left( \frac{0.0897 + 2729}{T_R} \right)}}, 0.05 \right)$ (Adapted from Aarnink and Elzing, 1998 and Chapter 4)	6.18
	$H_P$	$H_P = 1431 \cdot 1.053^{(293 - T_R)}$ (Adapted from Aarnink and Elzing, 1998)	6.19
	$TAN_{P,t+h}$	$\frac{dTAN_P}{dt} = -2 \cdot \left( \frac{S_m \cdot U}{K_m + U} \right) - \frac{k_{NH_3,P} \cdot A_P \cdot 1000 \cdot \left( \frac{f_P \cdot TAN}{H_P} - C_R \right)}{V_P} - \frac{TAN_P}{V_P} \cdot \frac{dV_P}{dt}$ (Chapter 4)	6.20
	$pH_{P,T+h}$	$\frac{dpH_P}{dt} = -0.7 \cdot \frac{dTAN_P}{dt}$ for $\frac{dTAN_P}{dt} > 0$ and $\frac{dpH_P}{dt} = 6.0 \cdot \frac{dTAN_P}{dt}$ for $\frac{dTAN_P}{dt} < 0$ (Chapter 4)	6.21
		Determine $V_{P,t+\Delta}$ , $U_{t+\Delta}$ , $TAN_{P,t+\Delta}$ and $pH_{P,t+\Delta}$ use fourth order Runge Kutta, and a calculation interval ( $h$ ) of 150 s.	6.22 to 6.26
	$f_{P,t+\Delta}$	$f_P = MAX \left( \frac{10^{pH_P}}{10^{pH_P} + 5 \cdot 10^{\left( \frac{0.0897 + 2729}{T_R} \right)}}, 0.05 \right)$ (Adapted from Aarnink and Elzing, 1998 and Chapter 4)	6.27
	$E_P$	$E_P = k_{NH_3,P} \cdot A_P \cdot 1000 \cdot \left( \frac{f_{P,t+\Delta} \cdot TAN_{P,t+\Delta}}{H_P} - C_R \right)$ (Chapter 4)	6.28
	$E_{P,Pen}$	$E_{P,Pen} = E_{P,Pen} + E_P$	6.29
	<b>Repeat Loop 3</b>		
	$E_{P,T}$	$E_{P,T} = N_{Pen} \cdot E_{P,Pen}$	6.30

**Table 6.2. (continued)**

Slurry Emission sub-model	$T_{film}$	$T_{film} = \frac{T_H + T_S}{2}$	6.31
	$k_{NH3,S}$	$k_{NH3,S} = 0.0821 \cdot T_{film}^{0.7} \cdot v_H^{0.5} \cdot L_{Slat}^{-0.5} \cdot D_{NH3,Air}^{0.666}$ (Chapter 5)	6.32
	$f_S$	To be determined	6.33
	$H_S$	$H_S = 1431 \cdot 1.053^{(293 - T_{film})}$ (Adapted from Aarnink and Elzing, 1998)	6.34
	$E_S$	$E_S = N_{Pen} \cdot k_{NH3,S} \cdot A_{slat} \cdot 1000 \cdot \left( \frac{f_S \cdot TAN_S}{H_S} - C_H \right)$	6.35
Core model equations	$C_{R,t+\Delta}$	$\frac{dC_R}{dt} = \frac{Q_R \cdot (C_A - C_R)}{V_R} + \frac{Q_H \cdot (C_H - C_R)}{V_R} + \frac{E_{P,T}}{V_R \cdot 1000}$	6.3
	$C_{H,t+\Delta}$	$\frac{dC_H}{dt} = \frac{Q_H \cdot (C_R - C_H)}{V_H} + \frac{E_S}{V_H \cdot 1000}$	6.4
		Determine $C_{R,t+\Delta}$ and $C_{H,t+\Delta}$ using fourth order Runge Kutta	6.22 to
	$E_R$	$E_R = Q_R \cdot 1000 \cdot (C_R - C_A)$	6.26
	$E_H$	$E_H = Q_H \cdot 1000 \cdot (C_H - C_R)$	6.5 6.6
Print Results		Print the results	
		<b>Repeat Loop 2</b>	
		<b>Repeat Loop 1</b>	
<b>END</b>			

### **6.3 Experimental Materials and Method**

With the ACES model developed, data from two rooms in a production facility were collected to calibrate and validate the model and test some of the assumptions. Data collection measurements were in conjunction with one trial of the study by Payeur (2003).

#### **6.3.1 Experimental Rooms**

Experimental data was collected in two mechanically ventilated grower-finisher rooms of a pork production research facility over the course of one cycle (12 weeks) of animals. Each room measured 14.2 m by 5.3 m with 3.0-m ceilings and contained six partially slatted floor pens measuring 4.2 m by 2.0 m. The slatted floor portion of each pen was 2.4 m in length and made of concrete slats. The solid floor portion was concrete and gently sloped toward the slatted floor. The 0.6-m deep slurry channel was located under the slatted floor portion of the room. Manure was drained from the rooms every one to three weeks by pulling a drain plug at one end of the manure channel. The plug-pulling event lasted approximately 15 min, and the plug was replaced. A 10-cm layer of slurry was left in the channel following each plug-pulling event to help maintain slurry concentration consistency.

In each room, negative pressure pulled outside air into the attic and then into the room through six air inlets located on the ceiling, opposite to the slatted floor side of the room. Each inlet was situated over one pen. The inlet air was directed across the ceiling, toward the slatted floor side of the room. A natural gas heater provided supplemental heat in cold weather. Three fans (stages 1 and 2 were variable-speed fans, stage 3 was a single speed fan) in each room provided the ventilation requirements.

One room was fed a typical grower-finisher diet with 19.2% protein content during weeks one to five and 18.6% protein content during weeks six to twelve and will be referred to as the Control room. The second room was fed a diet lower in protein content (17.2% weeks one to five, 16.6% weeks six to twelve) with sugar-beet pulp added as a source of fermentable carbohydrates at levels of 5% (week one), 10% (week 2), 15% (weeks three to twelve), and will be referred to as the SBP room. Food was provided to meet the pigs' appetite (*ab libitum*). Water was delivered to each pen through nipple drinkers located over the slatted floor.

Each room was filled with 72 animals at the start of the cycle with an average weight of 22.2 kg. Each pen contained six males and six females. Two animals were removed from the Control room, and five animals were removed from the SBP room before the end of the cycle for health reasons.

### **6.3.2 Data Collection**

Various types of data were collected to provide input data for the model, and resulting ammonia concentration and emission data to compare the model simulations against. Table 6.3 shows the method and frequency of each of the measured variables. All temperature, humidity, static pressure and fan speed measurements were recorded by a datalogger (Datataker DT 100, Data Electronics, Rowville, Australia) every 15 min.

Ammonia and carbon dioxide gas concentrations were measured at the inlet, exhaust and approximately 10 cm below the slatted floor in the centre of the room. Air was drawn continuously through the sampling lines from each location, and analyzed sequentially by a photo-acoustic infrared ammonia analyzer (Chillgard RT, MSA, Edmonton, AB;  $\pm 2$  ppm).

The  $pH$  of the top 30 mm of slurry was collected using a scoop and measured in three locations across the width of the slurry channel on a weekly basis. The average was calculated and expressed as the slurry surface  $pH$  ( $pH_S$ ). Composite samples of mixed slurry from the same three locations (slurry throughout the depth was combined and mixed *in situ* with a paint mixer) were then collected and sent to an independent lab for  $pH$ , electrical conductivity, ammonium-nitrogen ( $TAN$ ), sodium, phosphorus, potassium, sulphur, total Kjeldahl nitrogen and total solids analysis. Only the measurements of surface  $pH$ , mixed  $pH_S$  and  $TAN_S$  are reported.

Ventilation rates were determined from the static pressure and fan speeds, in conjunction with regression equations of the fan curves for the fans used.

**Table 6.3. Type, collection method and frequency of data collected.**

Measured Variable	Measurement Method and/or Instrument	Frequency of Measurement
Temperature		
Center of room	Type T Thermocouple; $\pm 0.5^{\circ}\text{C}$	15 min
Inlet	Type T Thermocouple; $\pm 0.5^{\circ}\text{C}$	15 min
Slurry pit headspace	Type T Thermocouple; $\pm 0.5^{\circ}\text{C}$	15 min
Slurry surface	Type T Thermocouple; $\pm 0.5^{\circ}\text{C}$	15 min
Floor of slurry pit	Type T Thermocouple; $\pm 0.5^{\circ}\text{C}$	15 min
Relative Humidity (center of room)	Model F22H-65, Rotronic Instrument Corp., Huntington, NY; $\pm 1.5\%$	15 min
Fan Speed	Proximity Sensor; Model SR3, Microswitch, Freeport, IL	15 min
Static Pressure	Static Pressure Transducer; Model 264, Setra, Boxborough, MA; $\pm 0.62$ Pa	15 min
Water intake per room	Water meters; Model C700, ABB Water Meters, Inc., Florida; $\pm 5\%$	daily
Feed intake per pen <sup>z</sup>	Feed added to feeders weighed	daily
Pen cleanliness	Daily scraping activities for the solid floor reported	daily
Slurry depth	Meter stick	3 times/week (min)
Slurry surface <i>pH</i>	<i>pH</i> meter; Orion Model 250A, Orion Research, Boston, MA; $\pm 0.01$ Mean of measurements at three locations along the length of the channel	2 wks
Mixed slurry <i>TAN</i>	Independant lab analysis Sample was a mixture of three samples taken along the length of the channel	2 wks
Mixed slurry <i>pH</i>	Independant lab analysis Sample was a mixture of three samples taken along the length of the channel	2 wks
Animal weight	Scale	5 times/cycle
Ammonia Concentration		
Exhaust	Chillgard RT, MSA, Edmonton, AB; $\pm 2$ ppm	80 min
Inlet	(Continuous concentration readings over 10 min intervals for each sampling location; only data from last four minutes used to calculate average concentration value)	80 min
10-cm below slatted floor		80 min

<sup>z</sup> Variable is not currently used in ACES model.

The nitrogen content of urine from grower-finisher swine fed diets ranging in crude protein and sugar-beet pulp content was measured in a separate metabolism study, described in Smith et al. (2004). The diet compositions in the study by Smith et al. (2004) were not identical to those used in Payeur (2003), but do show an effect of reducing the crude protein content by 2 percentage units and adding 15% sugar-beet pulp on the nitrogen excretion patterns by both grower (average weight: 42.8 kg) and finisher

pigs (average weight: 78.9 kg). The low protein diet with sugar-beet pulp added decreased the nitrogen excretion in the urine by 30% in grower pigs and 25% in finisher pigs. Since the majority of the nitrogen in urine is urea, and the range of urea concentration measurements was from 0.417 to 0.518 mol l<sup>-1</sup> (unpublished results from the trial by Smith et al. (2004)), the initial urea concentration for this experiment was approximated as 0.46 mol l<sup>-1</sup> for the animals in the Control room, and a 25% reduction to 0.35 mol l<sup>-1</sup> for animals in the SBP room.

The volume of urine excreted per day per pig ( $V_{U,T}$ ) was approximated as half of the average water intake per pig per day, as measured by the water meters. This approximation is based on water intake and urine excretion measurements from individually housed grower-finisher pigs in the studies by Smith et al. (2004) (unpublished results) and Shaw (2003).

### **6.3.3 Data Analysis Method**

The collected measurements were compiled on a daily or weekly basis and reviewed to determine the similarity of the rooms in terms of environmental conditions and also for an effect of diet treatment on slurry properties and measured concentration and emission levels.

The collected data was divided into four-day data sets to be used in the calibration and validation processes. Four-day subsets were chosen so that the number of urine puddles on the floor could stabilize in the first day and only the last three days of each data set were compared to measured values. A third of the subsets from both rooms were randomly chosen and used in model calibration. The remaining subsets were used in model validation. For measurements collected periodically, like animal weight and slurry properties, average values for the start date and time of each subset were estimated by



linear interpolation. There were 14 data-sets for the Control room and 16 for the SBP room.

Using the range of input data measured, the behaviour and sensitivity of the model related to the random number generators, steady-state approximations, the combined effect of slurry emission and pit ventilation rate, and puddle emission parameters were reviewed.

Model calibration used measurements of room concentration, pit headspace concentration, the difference between room and pit headspace concentration, and total emission (as determined from the room and inlet concentrations and the room ventilation rate) to compare to simulated results. The slurry emission/pit ventilation rate parameters were first calibrated by testing various models of volatile fraction of ammonia. Second, the simulated puddle emission was calibrated by testing various degrees of floor contamination and potential urease activity levels. Measured and simulated averages for the dependant variable were compared using the fractional bias (*FB*) and bias based on the variance parameters (*FS*) as shown in Appendix A.

Validation of the model was performed using separate data-sets than those used in the calibration process. The agreement between hourly data and three-day average values was evaluated for all data, and based on diet treatment (Control vs. SBP). Measured and simulated concentration values were compared and the accuracy associated with the concentration simulations was assumed transferable to emission simulations based on the dependency of the concentration calculations on the ventilation rate. Concentration values were chosen as the tested variable because the measurement error associated with the concentration measurements was considered less than the measurement error

associated with both the concentration and ventilation rate measurements used to determine the emission rate. The model performance was evaluated using all of the suggested parameters in the Standard Guide for Statistical Evaluation of Indoor Air Quality Models (ASTM, 2003), shown in Appendix A.

## **6.4 Results**

### **6.4.1 Measurements**

Data was collected during approximately 8 weeks of the 12-week grow-finish cycle from both the Control and SBP room. Instrument malfunctions prevented collection of ammonia concentration measurements during weeks 3 through 6 and ventilation rate measurements during week 1 in the Control room.

#### **6.4.1.1 Environmental conditions**

The temperature data collected from the inlet, room, under the slatted floor and on the slurry surface is shown in table 6.4. There was less than 1°C difference between the Control and SBP rooms at the inlet and room levels. The decreasing inlet temperature is reflective of the seasonal change from September to November. The decreasing room temperature over the trial is reflective of decreased set-point temperatures as the pigs grew larger. The difference between rooms was up to 2.5°C for the pit headspace and slurry surface temperatures. The larger differences tended to occur towards the end of the trial, and the Control room tended to have higher temperatures at all locations than the SBP room.

The relative humidity and ventilation rate measurements were well matched between rooms throughout the trial (table 6.5). The Stage 3 fan was not used in either room after Week 1 because lower heat production by the small animals initially, followed by cooler inlet air temperatures as the fall season progressed, negated the need for increased

ventilation. The ventilation rates within both rooms fluctuated diurnally between approximately  $0.4 \text{ m}^3 \text{ s}^{-1}$  and  $1.5 \text{ m}^3 \text{ s}^{-1}$  using only the Stage 1 and Stage 2 fans.

While there were differences between rooms for slurry and pit headspace temperatures, the difference was generally less than  $2^\circ\text{C}$ . The similar RH and ventilation rate measurements also support the assumption that the rooms had similar airflow patterns. The low temperature differences between room and slurry pit headspace temperatures did not support studying the impact of a temperature difference for the pit ventilation rate (variable  $x_6$  in eq. 6.53) based on measurements by Monteny and Overbeek (1997) so further estimates of the pit ventilation rate were made by estimating the value of  $x_7$  only. Estimation of  $x_7$  is discussed in more detail in the Model Calibration section.

**Table 6.4. Weekly average temperature conditions at various locations within the Control and Treatment (SBP) rooms during the grow-finish cycle.**

Week	Average Temperature (Standard Deviation) (°C)													
	Inlet		Room				Pit Headspace				Slurry Surface			
	Control	SBP	Control	SBP	Control	SBP	Control	SBP	Control	SBP	Control	SBP	Control	SBP
1	18.1 (7.7)	18.2 (7.8)	22.5 (3.3)	22.4 (4.0)	24.9 (2.0)	24.9 (2.4)	21.5 (1.0)	21.7 (0.8)						
2	11.5 (7.0)	11.1 (7.3)	19.6 (2.0)	19.9 (2.0)	22.4 (1.4)	21.6 (1.3)	20.0 (1.2)	19.5 (0.9)						
3 to 6	data not available													
7	4.6 (5.7)	4.0 (5.9)	16.2 (1.6)	16.0 (1.6)	14.7 (1.2)	15.2 (1.3)	15.2 (1.1)	14.2 (0.8)						
8	0.9 (4.2)	0.1 (4.1)	15.6 (1.0)	15.0 (1.4)	15.2 (1.0)	14.6 (1.1)	15.1 (1.2)	13.8 (0.8)						
9	-1.0 (6.1)	-1.7 (5.9)	15.5 (0.6)	15.2 (0.5)	16.0 (1.7)	14.4 (0.7)	15.3 (1.0)	13.8 (0.7)						
10	3.2 (5.2)	2.5 (5.1)	15.4 (1.6)	15.0 (1.5)	16.4 (1.5)	15.2 (1.2)	15.5 (1.2)	14.1 (1.0)						
11	0.6 (4.5)	0.4 (4.5)	15.5 (1.0)	15.3 (1.0)	17.8 (1.5)	15.8 (1.1)	16.1 (1.3)	14.5 (0.8)						
12	2.3 (5.7)	2.1 (5.8)	15.5 (1.8)	15.2 (1.7)	18.3 (2.4)	15.5 (1.7)	16.0 (1.4)	14.0 (1.6)						

**Table 6.5. Weekly average relative humidity and ventilation rate conditions during the grow-finish cycle for Control and Treatment (SBP) rooms.**

Week	Relative Humidity (Standard Deviation) (%)				Ventilation Rate (Standard Deviation) (m <sup>3</sup> s <sup>-1</sup> )			
	Control		SBP		Control		SBP	
1	45 (10)	41 (14)			n/a	2.11 (1.07)		
2	51 (7)	51 (7)			0.87 (0.53)	0.99 (0.44)		
3 to 6	data not available							
7	47 (7)	48 (7)			0.98 (0.43)	0.95 (0.43)		
8	51 (4)	52 (4)			0.81 (0.37)	0.82 (0.37)		
9	53 (3)	55 (3)			0.83 (0.42)	0.77 (0.41)		
10	53 (4)	52 (5)			1.10 (0.38)	1.05 (0.39)		
11	57 (3)	56 (3)			0.92 (0.39)	0.93 (0.37)		
12	56 (4)	53 (4)			1.13 (0.41)	1.12 (0.39)		

#### 6.4.1.2 Slurry conditions

Water intake and feed intake increased over the course of the grow-finish cycle. Following the increase in feed and water intake, there was a corresponding increase in the amount of slurry produced. Figure 6.3 shows the depth of the slurry throughout the trial, as well as the instances where the slurry was drained from the room by pulling the plug in the bottom of the slurry channel. When the slurry was drained, a 10-cm layer was left in the bottom of the slurry channel to avoid drastic changes in the slurry properties.

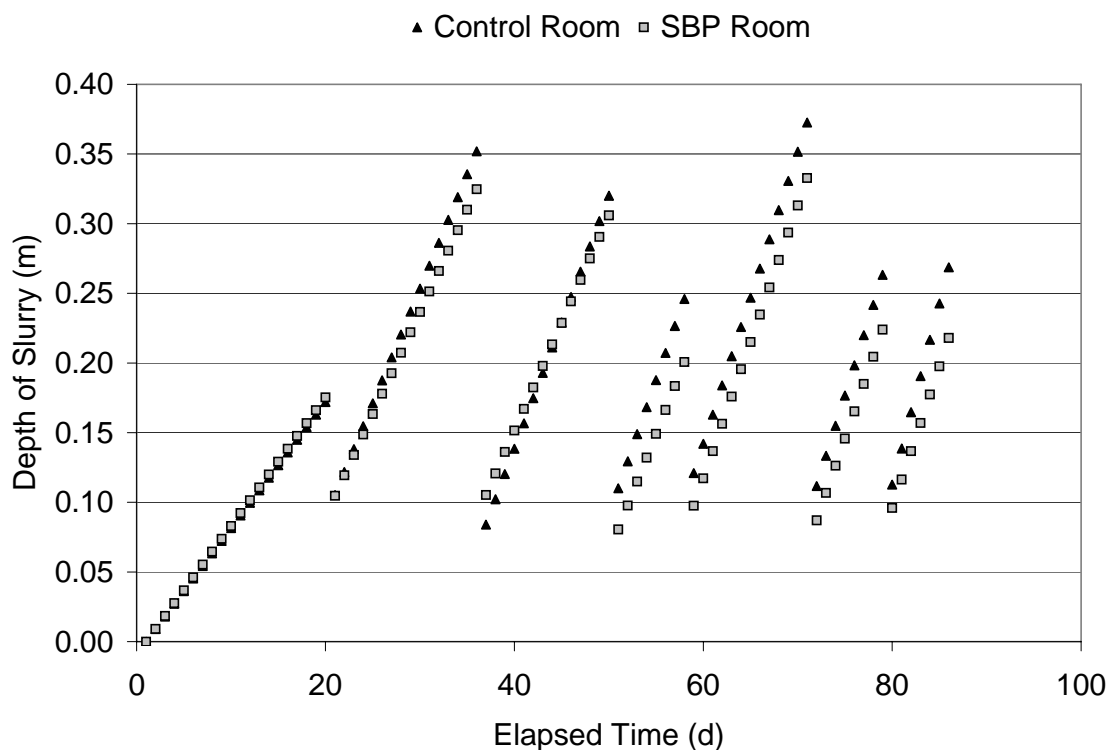


**Figure 6.3. Depth of slurry in the slurry pit based on time in the Control and Treatment (SBP) rooms.**

Table 6.6 shows the slurry properties measured during the trial based on diet treatment. The SBP pulp diet resulted in a lower surface  $pH_S$ , mixed  $pH_S$  and  $TAN_S$  towards the end of the trial, as was expected. The surface  $pH_S$  measurements were

initially higher than the mixed  $pH_S$  measurement in both rooms, but in general, the results do not support the suggestion of a higher surface  $pH_S$  compared to the mixed slurry  $pH_S$  by Aarnink and Elzing (1998) and Ni et al. (2000c). Mean surface  $pH_S$  measurements were used in the model because they were taken *in situ*.

**Table 6.6. Slurry characteristics based on the week of measurement for the Control and Treatment (SBP) rooms.**

Week	Mean Surface $pH_S$ (Std Dev)		Mixed $pH_S$		$TAN_S$ (mol L <sup>-1</sup> )	
	Control	SBP	Control	SBP	Control	SBP
1	data not available					
2	6.8 (0.11)	6.7 (0.15)	6.3	6.5	0.18	0.24
3 to 5	data not available					
6	7.0 (0.17)	6.3 (0.18)	6.9	6	0.33	0.29
7	6.9 (0.08)	6.3 (0.18)	7.1	6.7	0.36	0.33
8	7.1 (0.03)	6.7 (0.12)	7.2	7.2	0.39	0.34
9	6.9 (0.12)	6.8 (0.09)	7.6	6.8	0.45	0.32
10	7.1 (0.03)	6.6 (0.14)	7.4	7.2	0.42	0.38
11	7.0 (0.05)	6.8 (0.12)	7.2	7.2	0.48	0.40
12	7.1 (0.02)	6.8 (0.17)	7.5	7	0.51	0.43

#### 6.4.1.3 Room cleanliness

Cleanliness of the solid floor areas in each of the pens was qualitatively described throughout the trial by recording whether the pen required scraping as part of the daily barn procedures. When a solid floor was "scraped", the manure on the solid floor surface was manually removed and placed on the slatted floor so that the bulk of the manure fell into the slurry channel below. Table 6.7 shows the change in solid floor cleanliness over the course of the trial. The cleanliness of the slatted floor in each pen was not recorded.

**Table 6.7. Qualitative solid floor conditions based on the week of measurement for the Control and Treatment (SBP) rooms.**

Week	Description of Floor Condition (Total of Six Pens Per Room)	
	Control	SBP
1	six pens dirty	six pens dirty
2	six pens dirty	five pens dirty
3	four pens dirty	two pens dirty
4	six pens dirty	four pens dirty
5	one pen dirty	one pen dirty
6	all pens clean and dry	all pens clean and dry
7	all pens clean and dry	all pens clean and dry
8	two pens partially dirty	all pens clean and dry
9	two pens partially dirty	all pens clean and dry
10	three pens dirty	all pens clean and dry
11	three pens dirty	all pens clean and dry
12	three pens dirty	all pens clean and dry

Initially all pens were dirty in the solid floor area. This is a common occurrence when animals are moved into a room and dunging areas are being established. This initial presence of fecal matter in all pens helps to establish the fact that urease could be present on all surfaces from actual fecal material, as well as any fecal material transferred by animal movement throughout the rest of the trial.

#### **6.4.1.4 Ammonia concentration and emission measurements**

The measured ammonia concentrations in the room and pit headspace areas for both rooms are shown in figure 6.4. In general, the room and pit headspace concentrations in the Control room are higher than the corresponding concentrations in the SBP room. Also, the difference between the pit headspace concentration and room concentration increases dramatically over the course of the cycle in the Control room, whereas the difference is negligible in the SBP room, especially towards the end of the cycle. There are instances where the room concentration is higher than the slurry pit headspace concentration in the SBP room.

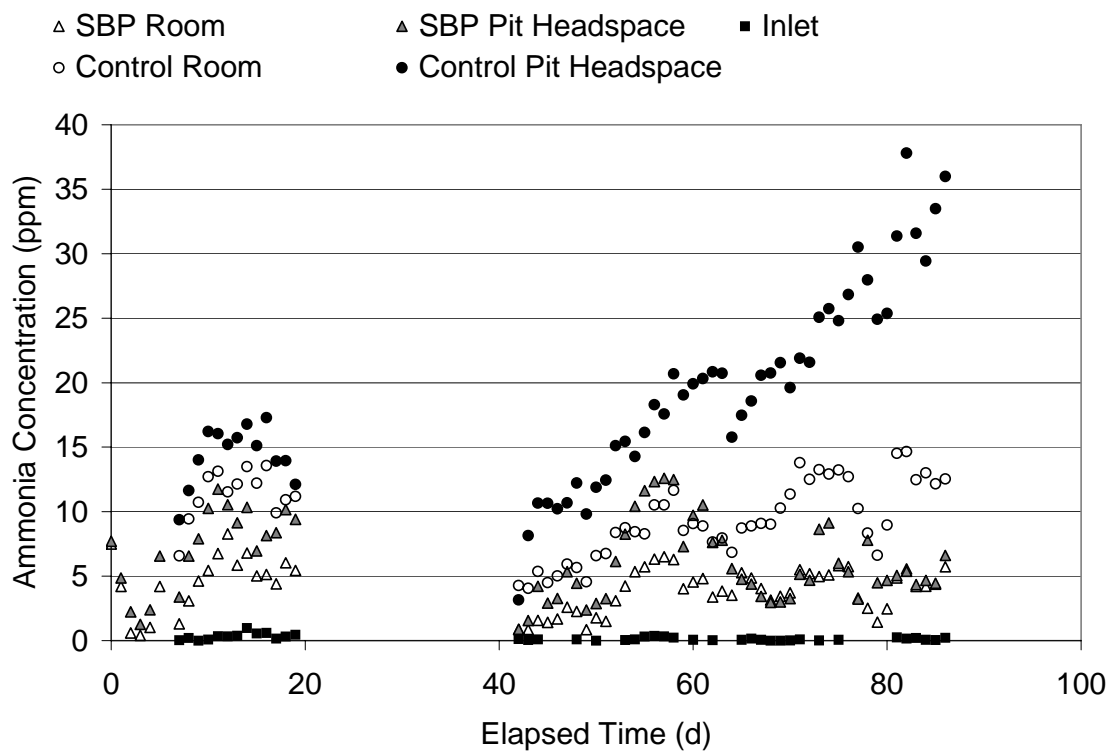


**Figure 6.4. Measured ammonia concentration levels at the exhaust and in the pit headspace over the course of the cycle for the Control and Treatment (SBP) rooms.**

The total emission from each room, based on the measured concentration and corresponding ventilation rates, is shown in figure 6.5. When expressed using a  $\text{g NH}_3\text{-N d}^{-1} \text{ AU}^{-1}$  basis, the total emission rate is very high when the animals are smaller. In general, the control room had a higher emission rate than the SBP room.



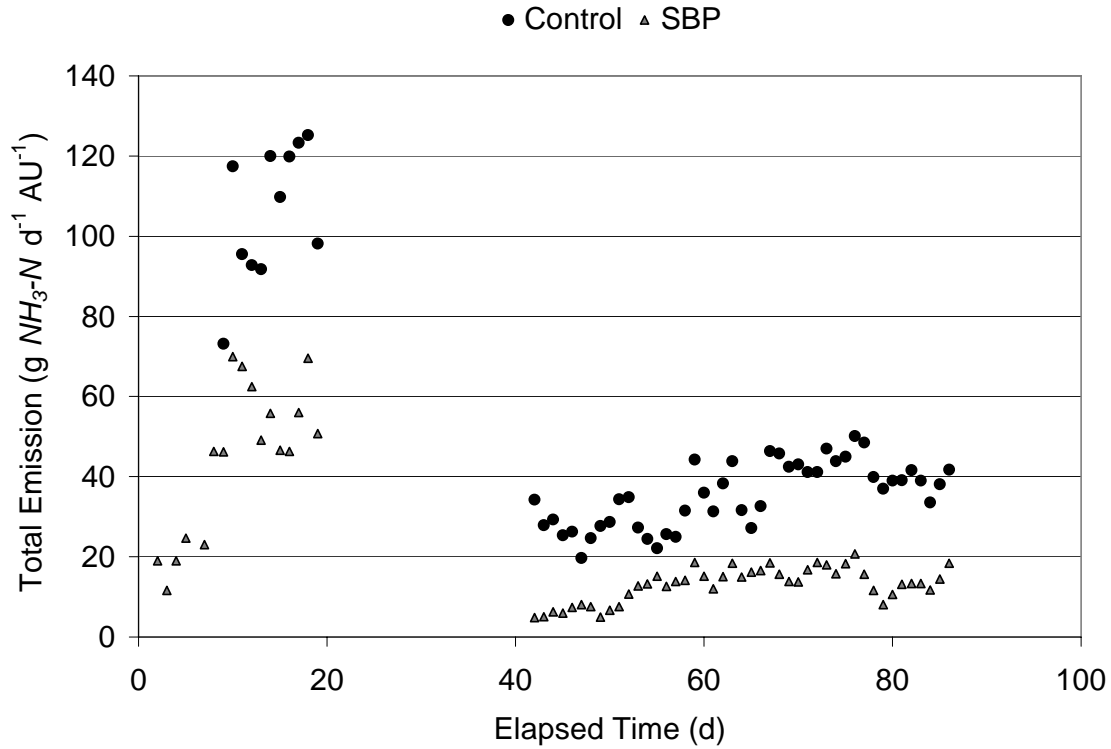


**Figure 6.5. Total ammonia emission rates over the course of the cycle for the Control and Treatment (SBP) rooms.**

#### 6.4.2 Model Behaviour

Several operations and relationships within the model were studied in greater detail to understand the implications on the model results before the model was calibrated.

##### 6.4.2.1 Random number generators

During model testing the Poisson random number generator for  $N_U$  and the random number generator for the puddle distribution were removed in order to remove the variability associated with them. When the Poisson random number generator was removed  $N_U$  was solely based on equation 6.7.

By removing the random number generator for puddle location, the urine puddles were distributed by allotting a puddle to each location in order and restarting the distribution at

the first location after the last location ( $N_L$ ) was reached. This fixed pattern resulted in the maximum number of emitting locations on the floor and this resulted in a 25% larger total puddle emission rate from the dirty pens compared to the average puddle emission rate calculated from three simulations using a random distribution. The small proportion of the slatted floor fouled in clean pens (as discovered in the Model Calibration Section) resulted in a negligible impact of random verses fixed puddle location on the total puddle emission. The total puddle emission rate simulations using a random puddle distribution were considered a better representation of reality. Therefore, in order to use the fixed puddle distribution pattern but still simulate the total puddle emission rate that the random puddle distribution pattern predicted, the total puddle emission rate from the dirty pens using a fixed puddle distribution was reduced by 25% in the ACES model.

#### **6.4.2.2 Steady-state approximation**

There was no indication in the concentration measurements suggesting that the impact of time was significant on the concentration following a change in a variable such as ventilation rate. Therefore, steady-state approximations of equations 6.3 and 6.4 were made and helped to establish two important relationships. First, the total emission from a room will be approximately equal to the sum of the total puddle emission and total slurry emission (eq. 6.54). This relationship was the basis for the room models by Aarnink and Elzing (1998) and Monteny et al. (1998). Second, the difference in concentration between the room and pit headspace level will be approximately equal to the slurry emission rate divided by the pit ventilation rate, hereafter described by the notation  $E_s Q_h^{-1}$  (eq. 6.55).

$$E_S + E_{P,T} = Q_R \cdot 1000 \cdot (C_R - C_A) = E_R \quad (6.54)$$

$$\frac{E_s}{Q_H} = 1000 \cdot (C_H - C_R) \quad (6.55)$$

With measurements of  $C_R$ ,  $C_H$ ,  $C_A$  and  $Q_R$  it is possible to calculate  $E_R$  and estimate the average  $E_s Q_h^{-1}$ . With an estimate of  $Q_H$ , slurry emission can be approximated from equation 6.55, and then total puddle emission can also be approximated from equation 6.54. The ability to separate the slurry emission or puddle emission from the total measured room emission allows the slurry emission simulations and total puddle emission simulations to be calibrated separately.

#### 6.4.2.3 Slurry emission and pit ventilation rate

Following the steady-state relationship shown in equation 6.55, the ratio of slurry emission to pit ventilation rate is estimated from the difference in pit and room concentration. Slurry emission can be estimated using developed equations as shown in the model development but the estimate will affect the simulated pit ventilation rate and vice versa. The following data from one of the calibration data-sets were used to illustrate the relationship between slurry emission and pit ventilation rate:

- the solid floor areas of all six pens were clean;
- the average measured total emission rate was  $0.00013 \text{ mol s}^{-1}$ ;
- the average measured value of  $E_s Q_h^{-1}$  was  $0.000195 \text{ mol m}^{-3}$ ; and
- the average room ventilation rate was  $0.94 \text{ m}^3 \text{ s}^{-1}$ .

The slurry emission was set at values ranging from 0 to 100% of the total emission rate and then divided by the average measured value of  $E_s Q_h^{-1}$  to estimate  $Q_H$ .

Figure 6.6 shows that as the pit ventilation rate decreases, there is a corresponding decrease in slurry emission. As slurry emission decreases as well, slurry emission represents a lower proportion of the total emission.

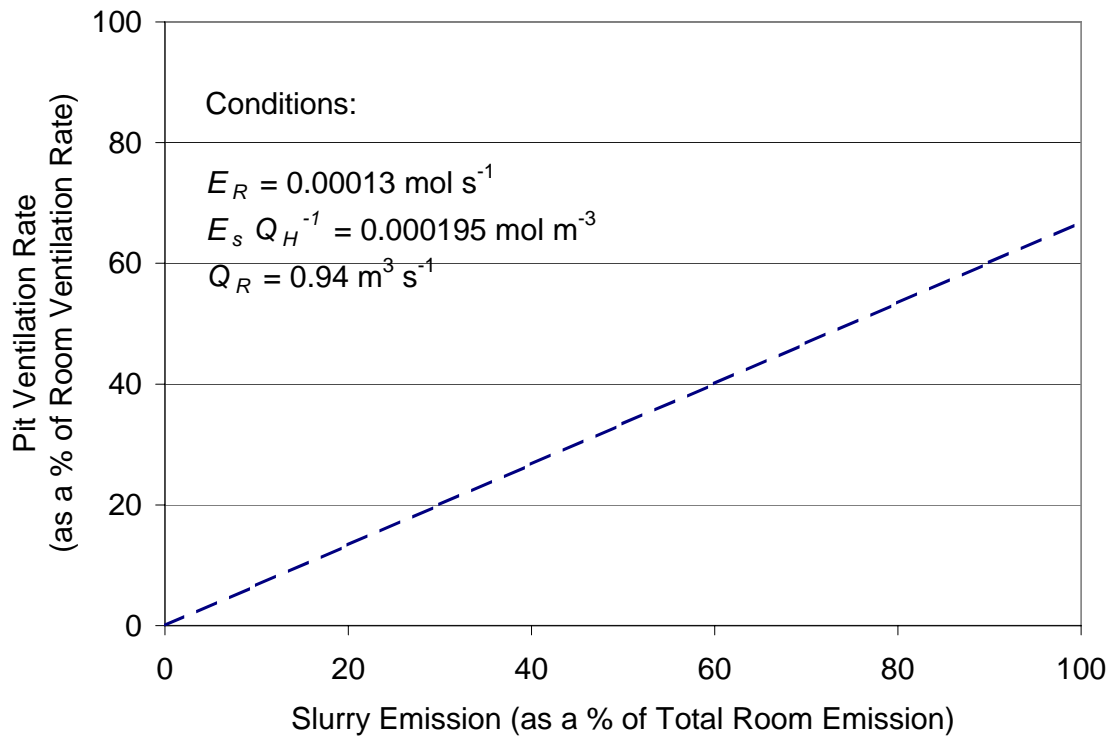


**Figure 6.6. An example of the relationship between slurry emission and pit ventilation rate for the given room emission ( $E_R$ ), slurry emission to pit ventilation rate ratio ( $E_s Q_H^{-1}$ ) and room ventilation rate ( $Q_R$ ).**

While the pit ventilation rate is not a well-understood variable, the pit ventilation rate should be a small fraction (<25%) of the room ventilation rate (Yu et al., 1991; Monteny and Overbeek, 1997). In the example shown in figure 6.6, the slurry emission will be less than 40% of the total emission for a pit ventilation rate that is 25% of the room ventilation rate. If, however, the slurry emission was estimated as a larger proportion of the total emission, such as 70% (Aarnink and Elzing, 1998), the pit ventilation rate would need to be approximately 50% of the room ventilation rate in order to maintain the same ratio of  $E_s Q_h^{-1}$ .

#### 6.4.2.4 Puddle emission factors

The chemical and physical characteristics of every individual urine puddle on the solid and slatted floor areas were not measured during the experiment but there are estimates for the various factors associated with the emission process. For many of these factors there are either measured data or data from the literature to support a range of possible values, and the impact of these variables over the possible range was tested through a series of simulations. There is only limited data for puddle area, puddle depth and air velocity over the floor surface so these factors were not tested here. The impact of the other puddle emission factors was determined by setting mean values for initial urea concentration ( $0.4 \text{ mol L}^{-1}$ ), urine volume per pig per day ( $4 \text{ L pig}^{-1} \text{ d}^{-1}$ ), potential urease activity ( $5 \text{ g NH}_3 \text{ m}^{-2} \text{ h}^{-1}$ ) and fouling of the solid and slatted floors (20%) and performing a series of simulations, varying one factor at a time over the expected range of that variable for each simulation.

Figure 6.7 shows the effect of changing initial urea concentration and the total volume of urine over the expected or measured range of input values is small compared to the effect of urease activity or fouled floor factor. Also, figure 6.7 shows that as potential urease activity and fouled floor factors increase the puddle emission rate begins to level off. This indicates that this factor is becoming non-limiting to the puddle emission process by either ensuring either the majority of urea in a puddle is converted in the case of increasing  $S_m'$  values, or that each puddle is allowed enough time to emit the bulk of the ammonia produced within that puddle in the case increasing  $r_{slat}/r_{solid}$  values.

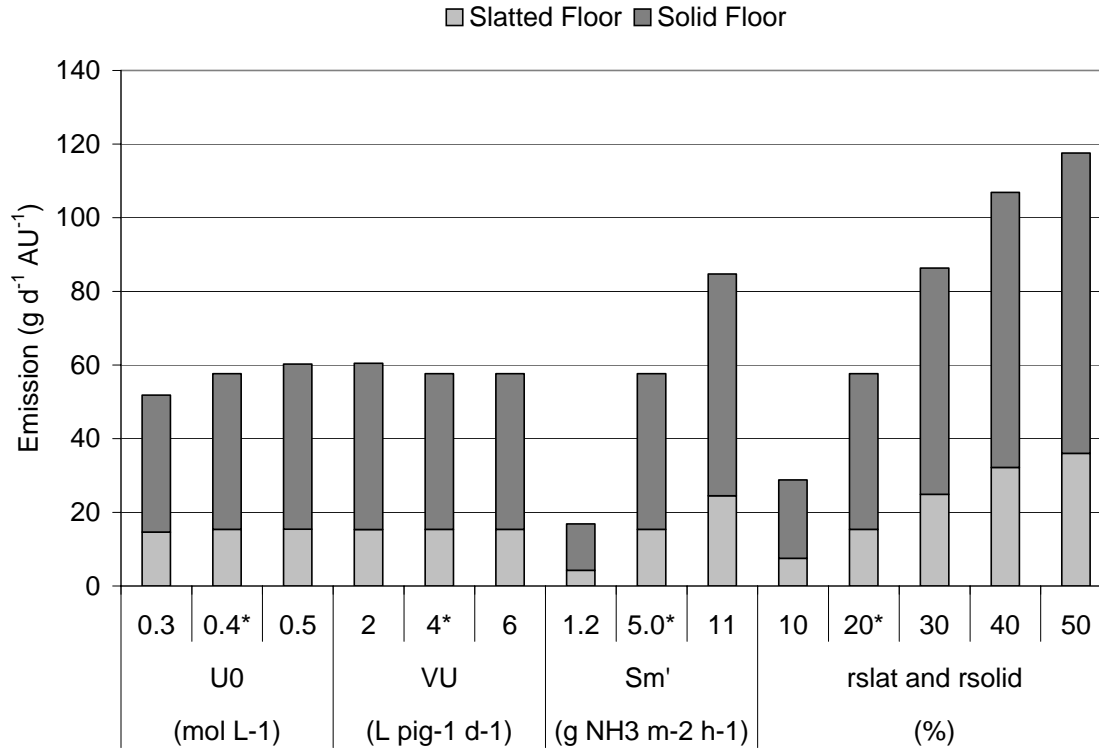


**Figure 6.7. The impact of initial urea concentration ( $U_0$ ), total volume of urine produced per pig per day ( $V_U$ ), potential urease activity ( $S_m'$ ) and the fouling factors for the slatted ( $r_{slat}$ ) and solid floors ( $r_{solid}$ ) on the total puddle emission rate from the slatted and solid floor areas. (\* indicates the mean value)**

### 6.4.3 Model Calibration

#### 6.4.3.1 Modelling the slurry emission/pit ventilation rate

As explained in the Model Development Section, there are four proposed equations to calculate the volatile fraction of  $TAN$  in the slurry. Figure 6.8 shows the simulated  $f_S$ -values for the calibration sub-sets using the mean surface  $pH$  measurements. A projection of  $f_S$ -values at  $pH_S$  levels above 7.5 is also shown to illustrate the possible connection between  $f_{S1}$  to  $f_{S3}$  with  $f_{S4}$ . The projected values for using the  $f_{S4}$  equation assume a  $TAN_S$  concentration of  $0.5 \text{ mol L}^{-1}$ .

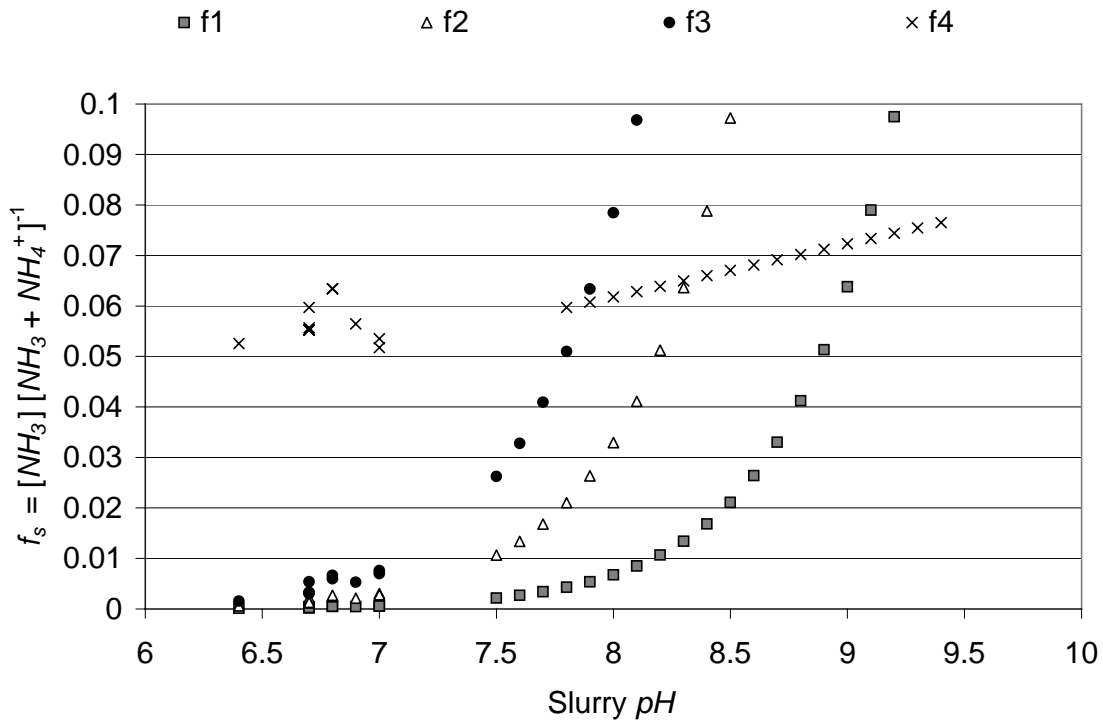


**Figure 6.8. Fraction values for the calibration data-sets ( $pH_s < 7.5$ ) and projected values ( $pH_s > 7.5$ ) based on slurry pH using the four proposed  $f_s$ -equations.**

There is a significant difference in  $f_s$ -values calculated using  $f_{s4}$  compared to values calculated using  $f_{s1}$  to  $f_{s3}$ . As shown in the Model Behaviour section, a lower simulated slurry emission necessitates a lower pit ventilation rate, and also results in a lower proportion of the total emission emanating from the slurry. The average slurry emission for each of the ten calibration data-sets was calculated four times incorporating a different  $f_s$ -equation each time. The slurry emission rates were then divided by a range of pit ventilation rates from 0.01 to 0.55 times the average measured room ventilation rate. The range of simulated  $E_s Q_h^{-1}$  ratios for one  $f_s$ -equation was compared to the measured average  $E_s Q_h^{-1}$  for each data-set and the pit ventilation rate that resulted in the lowest overall fractional bias for all datasets was chosen and the process was repeated with the

simulated ratios using the other  $f_S$ -equations. Table 6.8 shows the best-fit pit ventilation rate and the resulting slurry emission rate expressed as a proportion of the total emission rate.

**Table 6.8. The impact of using the four proposed  $f_S$ -equations on the range of calculated  $f_S$ -values, the estimation of the pit ventilation rate ( $Q_H$ ) and the slurry emission rate ( $E_S$ ).**

Method of $f_S$ determination	Range of calculated $f_S$ -values	Estimated $Q_H$ (expressed as a % of $Q_R$ )	Mean $E_S$ (Range) (expressed as a % of $E_R$ )
$f_{S1}$ ; $0.2 \cdot K_a$	0.000124 - 0.000612	<1	-1 (-3 to -1)
$f_{S2}$ ; $K_a$	0.00062 - 0.003055	1	1 (-1 to 3)
$f_{S3}$ ; $2.5 \cdot K_a$	0.00155 - 0.00760	4	4 (1 to 14)
$f_{S4}$ ; Linear regression eqn	0.0517 - 0.0634	55	82 (30 to 193)

It appears that using  $f_{S1}$  and  $f_{S2}$  underestimates slurry emission. Using  $f_{S3}$  results in slightly higher slurry emission levels and, based on these levels, the pit ventilation rate should be approximately 4% of the room ventilation rate. Using  $f_{S4}$ , the slurry emission accounts for anywhere from 30% to over 100% of the total emission from the room. It does seem likely that for conditions where the solid floor of every pen is clean, the majority of the emission would be coming from the slurry channel; however, for this to occur, the pit ventilation rate would need to be approximately 55% of the room ventilation rate. The equation for  $f_{S4}$  was developed in Chapter 5 for concentrated slurry samples with  $pH$  levels between 7.7 and 9.2. The considerably different slurry properties between the samples tested in Chapter 5 and the room slurry conditions may explain why equation 6.40 is not applicable in the ACES model.

The actual pit ventilation rate and slurry emission rate may be in between Models 3 and 4. The measurements from this experiment do not facilitate a more accurate approximation of either a factor for  $K_a$  or a new equation for  $f_S$ . However, there is an indication from the  $E_S Q_H^{-1}$  measurements that slurry emission can be negative and this



would result from a low  $f_S$ -value. Within the ACES model, the volatile fraction of *TAN* in the slurry was estimated using  $f_{S3}$  and the pit ventilation rate was estimated using equation 6.53 with the coefficients  $x_6$  and  $x_7$  set at 0 and 0.04, respectively.

#### 6.4.3.2 Modelling the emission rate from the floor surface

Based on the analysis in the Model Behaviour section, the ACES model is sensitive to changes in input values for floor cleanliness and urease activity when calculating total puddle emission. Using the average measurement of  $E_R$ ,  $E_s Q_h^{-1}$  and  $Q_R$  for each data set, and the estimate of  $Q_H$  ( $=0.04 \cdot Q_R$ ), the average puddle emission rate was calculated by the difference between total emission rate and slurry emission rate. The average simulated puddle emission rates from the various tests run were compared to the estimated total puddle emission rates using the *FB* evaluation parameter. Room concentration simulations and measurements were also compared. The *FB* value shows the relative difference between the simulated and measured average puddle emission rates, compared to the measured emission rate.

Floor cleanliness (table 6.7) was only assessed based on the amount of solid floor fouled so it was first necessary to approximate the percentage of slatted floor that was fouled in the pens with no solid-floor fouling. During collection of the five of the calibration data-sets (1 data-set from the Control room and 4 data-sets from the SBP room) between weeks 6 and 10 there was no reported fouling of the solid floor in any of the pens. Potential urease activity was left at a constant level of  $5 \text{ g } NH_3 \text{ m}^{-2} \text{ h}^{-1}$  and values of  $r_{slat}$  between 10% and 40% were applied to all five data-sets. The minimum average difference between the average simulated puddle emission to the measured puddle emission occurred when the  $r_{slat}$  value was 29% (figure 6.9). The puddle emission has a large impact on the level and variation of the room concentration so the average *FB*

and  $FS$  values for simulated and measured average room concentration values were also compared for different  $r_{slat}$  values. The  $FS$  value shows the relative difference between the simulated and measured puddle emission rate variations, compared to the variation of the measured emission rate. When the  $r_{slat}$  value approached 30% the level and variation in room concentration were over-predicted. The results in figure 6.9 suggest an  $r_{slat}$  value of 25% will slightly under-predict puddle emission and room concentration but this effect will be compensated by a better simulation of the variability in room concentration. An  $r_{slat}$  value of 25% is reasonable based on research that animals are more likely to urinate along walls and pen partitions (Baxter, 1982).

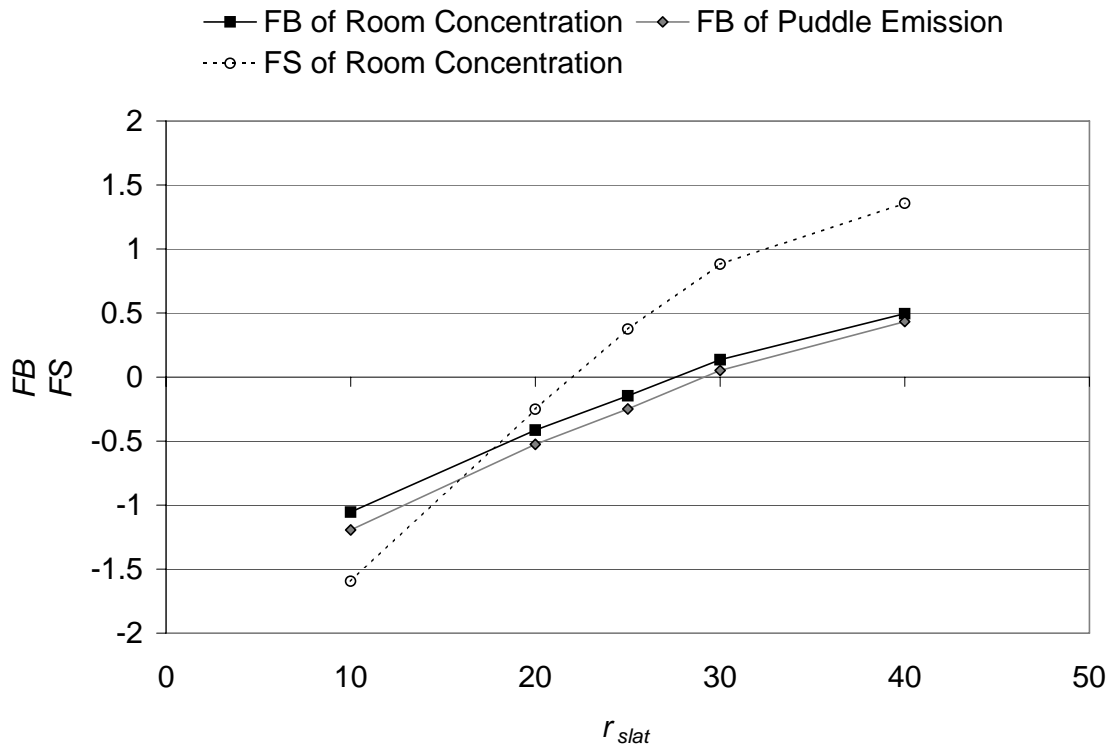


**Figure 6.9. The fractional bias ( $FB$ ) between average simulated and measured puddle emission and room concentration, and bias based on the variance ( $FS$ ) in simulated and measured room concentration based on varying levels of fouled slatted floor area ( $r_{slav}$ ).**

The remaining five calibration data-sets were collected during weeks 1, 2, 11 and 12 when there was fouling on the solid floor for at least three of the pens. Similar to the test for the  $r_{slat}$  value with clean pens, the  $r_{solid}$  and  $r_{slat}$  values for the dirty pens were changed simultaneously in 10% intervals from 10% to 60%. In this comparison the results showed that for data-sets collected near the beginning of the cycle, a smaller  $r_{slat}/r_{solid}$  value was required compared to datasets from later in the cycle in order to minimize the error between measured and simulated puddle emission. Logbook descriptions of the pen cleanliness did not support a lower value for fouled area near the start of the trial.

A second test was used that involved setting the  $r_{slat}/r_{solid}$  values at 50% for the dirty pens and testing various urease activity levels for each data-set (figure 6.10). For the first data-set shown in figure 6.10, a potential urease activity of  $0.00012 \text{ mol } U \text{ m } L^{-1} \text{ s}^{-1}$  in the ACES model shows great improvement in simulating the puddle emission compared to the mean input level. Similarly, smaller but increasing potential urease activity levels for the second and third data-set also help improve the model simulations. These small and increasing urease activity levels agree with the measurements by Braam et al. (1997a) who measured linearly increasing  $S_m'$  levels over the first 15 days of fouling from  $1.6E-7$  to between  $2.5E-05$  and  $4.1E-05 \text{ mol } U \text{ m}^{-2} \text{ s}^{-1}$ .

As a result of this calibration process for the floor emission rate the  $r_{slat}$  value for slatted floor surfaces in clean pens was set at 25%. When pens became dirtier, the suggested input values for  $r_{slat}$  and  $r_{solid}$  values are both 50%. As the solid floor cleanliness increased from clean to dirty, the input values for  $r_{slat}$  and  $r_{solid}$  should increase simultaneously from 25% to 50%. In the first two weeks of the cycle, the input potential urease activity should also linearly increase from 0 to  $5 \text{ g } NH_3 \text{ m}^{-2} \text{ h}^{-1}$ .

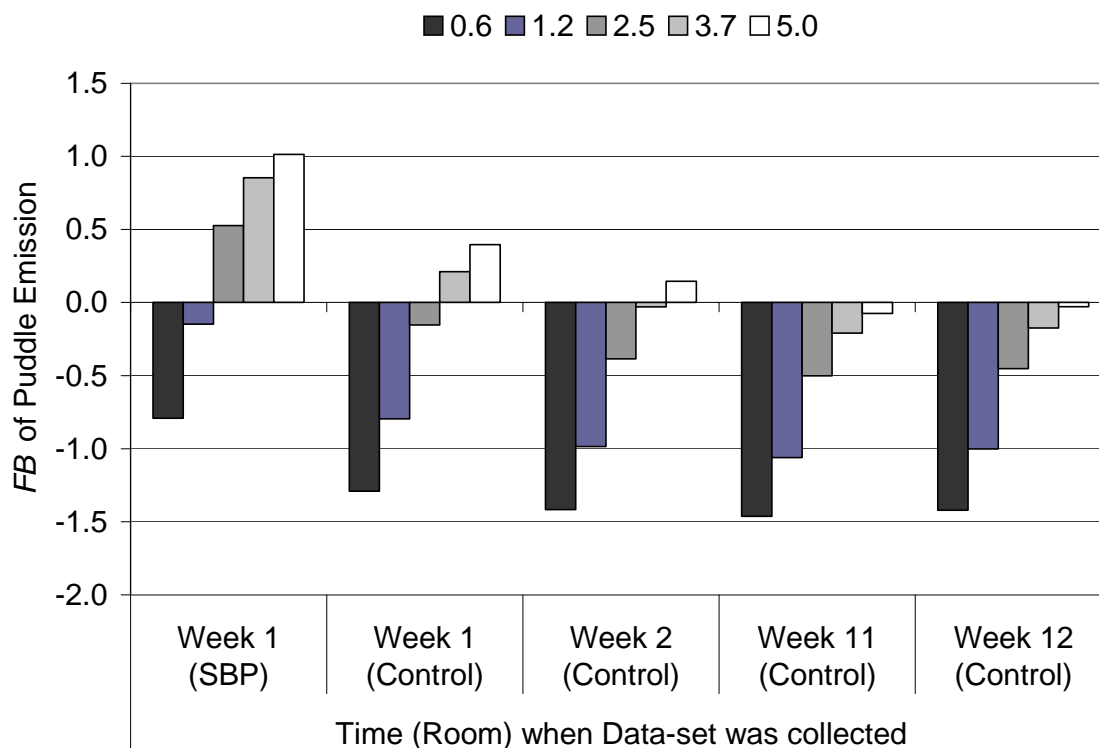


**Figure 6.10. The fractional bias (*FB*) between simulated and measured puddle emission for five data-sets using increasing levels of potential urease activity ( $S_m'$ ,  $\text{g NH}_3 \text{ m}^{-2} \text{ h}^{-1}$ ) in the puddle emission simulations.**

#### 6.4.4 Model Validation

The calibrated model was used to simulate the ammonia concentration and emission levels for the twenty validation data-sets and these results were compared to measured results. General model behaviour was evaluated using the ASTM standard, with emphasis on the *FB* and *FS* values. Table 6.9 shows all evaluation parameters.

The average measured and simulated room concentrations were 6.0 and 5.9 ppm, respectively. The regression line parameters (*a* and *b*) show that over the range of concentration variables the average simulated variable was close to the measured level. The *R*-value is lower than the suggested limit of 0.9 (ASTM, 2003) because there was

increased variation between the measured and simulated values at higher concentration levels and the variation was mainly from over-predictions in the room concentration for data from the SBP room. The average simulated pit headspace concentration was 1.2 ppm higher than the measured concentration. Again, the evaluation parameters  $R$  and  $a$  were outside of the suggested limits because of over-predicted values for the SBP room.

Comparison of the three-day average measured and simulated values for room concentration and pit headspace concentration show that, similar to the overall data evaluation, the model was more accurate in simulating the conditions inside the Control room compared to the SBP room. The regression intercepts for overall and room-based comparisons of the average data were generally higher than 25% of the measured mean (ASTM, 2003) resulting from over-predictions of measured values at low levels.

The  $NMSE$  values provide estimates of how well each simulated concentration value compared to the corresponding measured value. For hourly data this provides a measure of how well the model simulated the dynamics of the concentration values over time. For the room concentration data the ACES model accuracy was  $\pm 2.2$  ppm for hourly simulations, and  $\pm 1.6$  ppm for 3-day averages. For the pit headspace concentration, the ACES model accuracy was  $\pm 4.3$  ppm and  $\pm 2.9$  ppm for hourly and 3-day average simulations, respectively.

The  $FB$  parameter expresses the difference in averages on a percent basis, making a nominal difference much higher on a percent difference basis at lower levels. The ACES model tended to over-predict concentration values less than 5 ppm. As shown in figure 6.11, 25 out of 40 of the three-day average simulated concentration values were within  $\pm 2$  ppm of the measured averages.

**Table 6.9. ACES model evaluation for hourly and 3-day average simulated values compared to corresponding measured values, for room concentration, pit headspace concentration and  $E_S Q_H^{-1}$  ratio. Bolded values are within the suggested evaluation limits. ( $n$  = number of measured value and simulated value data pairs)**

Evaluation Parameter	Parameter Values for Hourly Data			Parameter Values for 3-Day Average Data		
	Overall ( $n^L=1061$ )	Control ( $n=472$ )	SBP ( $n=590$ )	Overall ( $n=20$ )	Control ( $n=9$ )	SBP ( $n=11$ )
<b>Room Concentration</b>						
Mean (Measured; ppm)	6.0	8.7	3.8	5.9	8.5	3.7
Mean (Simulated; ppm)	5.9	8.2	4.2	6.0	7.9	4.3
$R$	0.83	0.82	0.65	0.88	<b>0.91</b>	0.58
$b$	<b>0.83</b>	<b>0.97</b>	0.65	<b>0.75</b>	<b>0.96</b>	0.48
$a$	<b>0.96</b>	<b>-0.23</b>	1.66	1.57	<b>-0.17</b>	2.55
NMSE	<b>0.14</b>	<b>0.07</b>	0.29	<b>0.07</b>	<b>0.02</b>	<b>0.19</b>
FB	<b>-0.01</b>	<b>-0.06</b>	<b>0.08</b>	<b>0.02</b>	<b>-0.07</b>	<b>0.15</b>
FS	<b>0.01</b>	<b>0.32</b>	<b>&lt;0.01</b>	<b>-0.32</b>	<b>0.09</b>	<b>-0.38</b>
<b>Pit Headspace Concentration</b>						
Mean (Measured; ppm)	11.3	18.8	5.3	11.1	18.1	5.3
Mean (Simulated; ppm)	12.5	18.6	7.7	12.3	18.1	7.6
$R$	0.87	0.68	0.69	<b>0.93</b>	0.78	0.74
$b$	<b>0.75</b>	0.67	0.64	<b>0.79</b>	0.71	<b>0.80</b>
$a$	4.02	6.04	4.32	3.53	5.31	3.36
NMSE	<b>0.13</b>	<b>0.07</b>	0.30	<b>0.06</b>	<b>0.03</b>	<b>0.21</b>
FB	<b>0.10</b>	<b>-0.01</b>	0.37	<b>0.11</b>	<b>&lt;-0.01</b>	0.35
FS	<b>-0.29</b>	<b>-0.05</b>	<b>-0.15</b>	<b>-0.32</b>	<b>-0.22</b>	<b>0.17</b>
<b><math>E_S Q_H^{-1}</math></b>						
Mean (Measured; mol m <sup>-3</sup> )				0.00021	0.00039	0.00007
Mean (Simulated; mol m <sup>-3</sup> )				0.00026	0.00041	0.00013
$R$				0.79	0.47	-0.03
$b$				0.67	0.30	-0.04
$a$				0.00011	0.00029	0.00014
NMSE				0.30	<b>0.11</b>	1.74
FB				<b>0.20</b>	<b>0.05</b>	0.68
FS				<b>-0.32</b>	-0.84	0.88

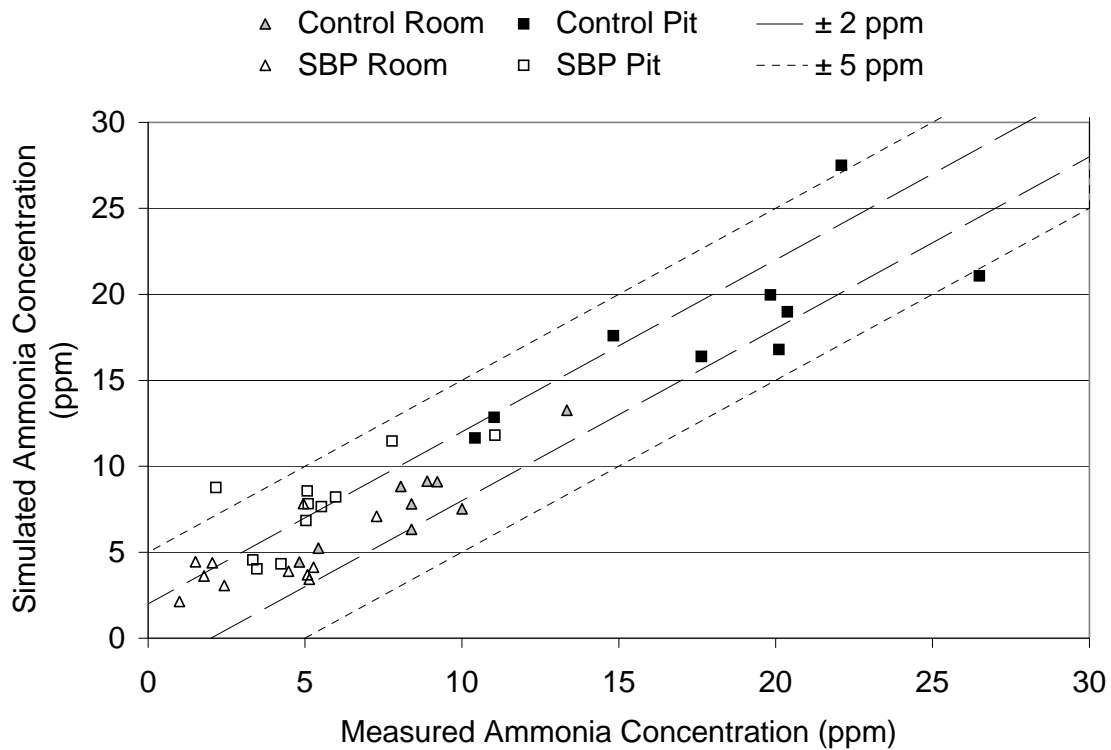
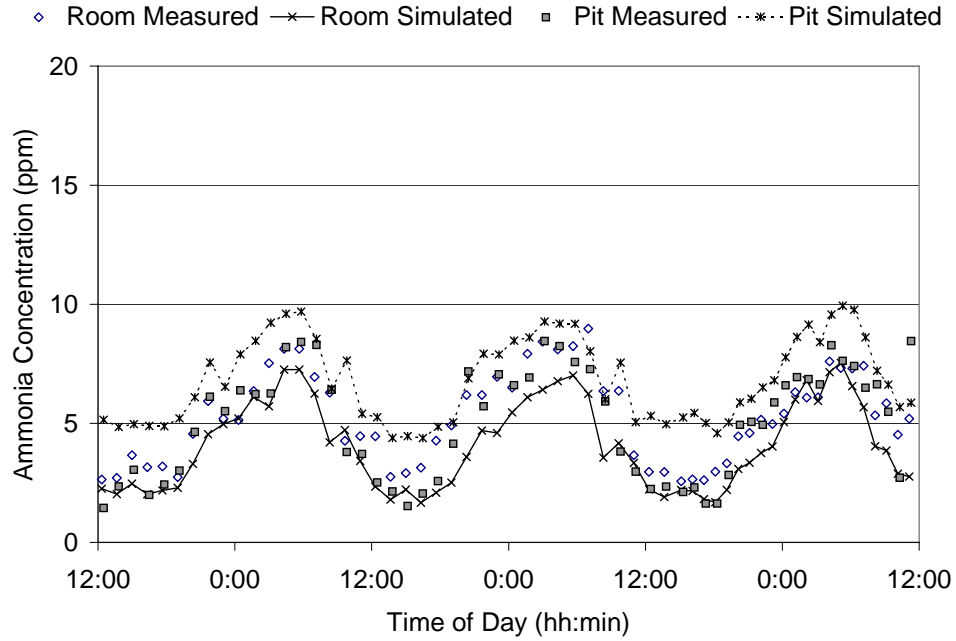
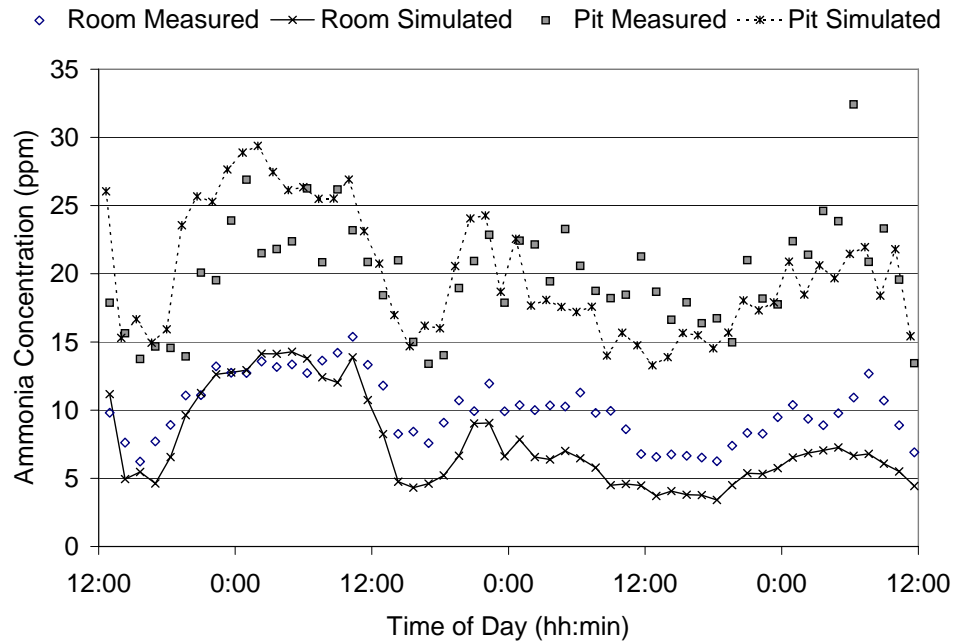


**Figure 6.11. Comparison of the three-day average simulated room and pit headspace ammonia concentration levels compared to the corresponding measured average.**

Figure 6.12 shows there was increased variation in the measured and simulated concentration levels with an increased amount of fouling of the solid floor and this variability lowered the calculated  $R$ -value. The regression line parameters ( $b$  and  $a$ ) indicate that even with the increased variability at higher concentration levels the average simulated values were still close to the average measured values. On an hourly basis, the simulations are better when there are clean floors compared to dirty floors.



(a)



(b)

**Figure 6.12. Measured and simulated room and pit concentration values over three days during conditions with clean solid floors (a) and dirty solid floors in two of the six pens (b).**



The slurry emission calculation was exponentially related to  $pH_S$  and therefore, similar to previous models that also used an exponential relationship for  $f_s$  with  $pH_S$ , the slurry emission is very sensitive to variability in  $pH_S$ . The surface  $pH_S$  measurements often differed by as much as 0.4 units across the width of the slurry channel. As shown in figure 6.13, if the input value for surface  $pH_S$  in the model was  $\pm 0.2$  units, the range of values would account for most  $E_s Q_h^{-1}$  measurements except for the very low ones.

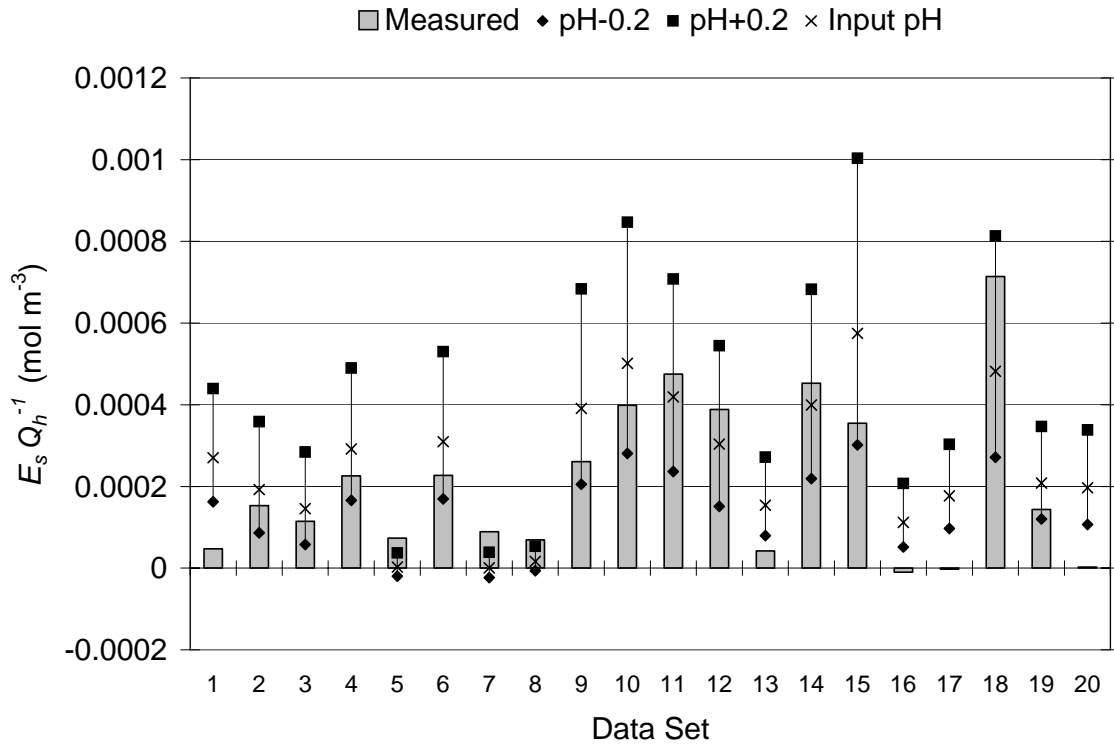


**Figure 6.13. Average measured  $E_s Q_h^{-1}$  values for the validation data-sets, and the corresponding simulated average using the input slurry surface  $pH \pm 0.2$  units.**

Based on the average simulated values of slurry emission, total puddle emission and total room emission for the twenty validation data-sets, the total puddle emission accounted for 95% of the total room emission. For simulated situations when the solid floor area of the pens were clean (based on observations), the floor emission originated

from urine puddles on the slatted floor. For data-sets based on the Control room conditions, total puddle emission was 94% of the total room emission with a range of 92% to 96%. For the SBP room simulations, the average was 95% with a range of 82% near the beginning of the trial when lower urease activity values were used in the simulations to 100% when the slurry *pH* was low.

## **6.5 Discussion**

### **6.5.1 Model Development**

The ACES model is a series of over 50 equations combined to simulate four variables: room concentration, pit headspace concentration, room emission rate and slurry emission rate. Many of these equations are incorporated in sub-models that have been tested independently of the data used in the overall model calibration. The use of sub-models facilitates further development of individual parts of the model.

The developed urination frequency and location sub-model is an attempt to model behaviour and the randomness associated with it. While animal behaviour patterns are often recognizable there will always be some variability. As shown in figure 6.12, as urination location becomes more random, room concentration levels also become less predictable.

The computation time for the ACES program is minimal and additional programming with Visual Basic can perform a number of simulations within a period of about one minute. This short calculation time allows extensive model testing in a short time period and demonstrates the time-savings that models can provide.

### **6.5.2 Measurements**

Monteny et al. (1998) suggested frequent measurement of time-dependent variables in order to improve short-term simulations. Ventilation, temperature and humidity

measurements were collected every 15 min for this experiment. This frequency captured the changes in ventilation rate that are significant in the room concentration simulations.

In the companion study by Payeur (2003), the SBP treatment significantly reduced ammonia emissions by 42% compared to a control diet based on measurements through three cycles of grower-finisher swine. In this study, the slurry emission was lower in the SBP room compared to the Control room. The lower  $TAN_S$  and  $pH_S$  measurements in the SBP room slurry support the expected impact of the low protein sugar-beet pulp diet used in the SBP room. If the assumption of the lower initial urea concentration in the swine urine for the SBP room was exhibited in this study as it was in Smith et al. (2004), then the puddle emission rate would be impacted by diet as well. Based on figure 6.7 it appears the amount of fouled floor had a larger impact on the total puddle emission than the initial urea concentration for this study.

The difference between room and pit headspace concentration was an important relationship derived from the measurements in this study. This parameter can be incorporated in future studies for similar barn designs with no exhaust fans in the slurry channel. This parameter makes it possible to compare slurry emission rates between rooms that have similar airflow patterns and hypothetically similar pit ventilation rates. There was a 10-min time lag between the concentration measurements for the room and pit headspace so instantaneous differences were not possible; therefore, in this study, only the 3-day average measured difference was used in comparisons. Simultaneous measurements in both areas could help relate pit ventilation rate to other environmental variables.

### 6.5.3 Slurry Emission

The slurry  $pH$  levels were low compared to reported  $pH_S$  levels in many other studies and the surface  $pH_S$  measurements were lower than the mixed slurry measurements in many instances as shown in table 6.6. In some cases, the surface  $pH_S$  varied by as much as 0.4 points across the length of the slurry channel. Only one composite sample was analyzed for  $TAN_S$  and mixed  $pH_S$  so the variation in these two measurements over the length of the pen is not clear.

In this study the slurry emission rate was less than 5% of the total emission rate for the room. The low level of slurry emission was linked to the slurry properties by the  $f_S$ -equation used. Aarnink and Elzing (1998) estimated 70% of the total emission was from the slurry channel based on their model. Again, the input slurry  $pH$  used in the simulations by Aarnink and Elzing (1998) was 7.5, which, when used in the ACES model would also estimate a much higher slurry emission (fig. 6.8). As stated in the Model Calibration section, it is possible that a  $K_a$  factor greater than 2.5 or a simplified  $f_S$ -equation similar to that developed in Chapter 5 for concentrated slurry samples may be more appropriate. Further development of the slurry fraction calculation is needed at a wider range of  $pH_S$  levels under more carefully controlled conditions than those that can be achieved in a full-scale barn.

### 6.5.4 Pit Ventilation Rate

In this study the low calculated slurry emission resulted in a low estimated pit ventilation rate. Expressing the pit ventilation rate as 4% of the room ventilation rate is low compared to Monteny and Overbeek (1997) where  $Q_H$  was approximately 25% of  $Q_R$ . However, when the pit ventilation rate is expressed on an airchange per hour basis the ratio of pit ventilation rate to room ventilation rate is 0.86 for the results from

Monteny and Overbeek (1997) and 0.76 for the results from this study. The maximum pit to room ventilation rate ratio (on an air change per hour basis) reported by Yu et al. (1991) was 0.21.

Development of a method to measure pit ventilation rate for various barn configurations and airflow patterns will help to further the application of this model, as well as the measurement of slurry emission separate from floor emission.

#### **6.5.5 Puddle Emission**

Puddle emission accounted for over 95% of the total emission in this study. In the model calculations, the fouled floor area and potential urease activity of the floor surface were the most important input factors contributing to the total puddle emission. It is also important to note that the model predicted the total floor emissions to come from urine puddles remaining on the top of the slatted floor surface in the pens when the solid floor portion of the pens was observed "clean".

In the ACES model the  $r$ -value impacts the puddle emission process by determining the number of possible urination locations, which is also based on the estimated puddle area, and therefore the rate that a new puddle replaces an old puddle rendering the old puddle non-existent. Incorporating the evaporation rate also affects the life-cycle of a urine puddle. The model by Aarnink and Elzing (1998) set a limit of 11 h for a puddle to continue emitting ammonia. In the ACES model, a typical urine puddle lasted less than 3 h.

The ACES model uses potential urease activity levels suggested in the literature. The sensitivity analysis of the puddle emission rate to urease activity showed that the levels used in the model were low enough that changes to the urease activity significantly impacted the puddle emission rate. Urease activity does become a non-limiting factor to

the puddle emission at high enough levels. This non-limiting level is for floor surfaces in swine barns has not been directly tested.

Mechanistic models such as the ACES model consider only the breakdown of urea. In the future, it may be a better option to measure the wetted floor area in a pen and treat the wetted area as one puddle for two reasons. First, the growth or change in composition of one puddle would be easier to measure and model provided the chemical and physical composition of the puddle is relatively consistent throughout the puddle. Second, if in the future wetted fecal material is deemed an important source of ammonia emissions, total wetted floor area would incorporate this emission site as well.

#### **6.5.6 Model Accuracy**

The ACES model was tested using data collected over a 12-week period in two different rooms. The validation data sets were separate from those used in the calibration process and there were more validation data sets than calibration data sets. This type of extreme or cross-validation (Ni et al., 2000c) helps to enhance the results of the validation by showing a greater range of applicability. However, this type of validation is more likely to have less accurate simulations than simulations using the same input data for calibration and validation.

The slurry emission, room concentration and pit headspace concentration are linked. Errors in the calculation of one variable can compound in the calculation of another variables. For example, the simulated room concentration provides the background ammonia concentration level in the slurry pit headspace, similar to the ambient concentration ( $C_A$ ) providing the background concentration to  $C_R$ . A high room concentration can result in a higher slurry pit headspace concentration and thus also diminish the slurry emission rate by lowering the concentration gradient within the

convective mass transfer equation. By estimating the slurry emission and puddle emission rates separately during the model calibration process, this compounding effect was lessened, but not removed.

The ACES model simulated the average room and headspace concentration levels to within 0.1 and 1.3 ppm, respectively. The model tended to over-predict the low concentration levels measured in the SBP room. At the higher concentration levels in the room and pit headspace of the Control room the model was more accurate. The average difference between measured and simulated room concentration levels was within  $\pm 2$  ppm for 15 of the 20 data-sets, and within  $\pm 5$  ppm for all the data sets. The simulated pit headspace concentration was dependent on the accuracy of the room concentration and slurry emission simulation so the accuracy was lower but the simulations were still within  $\pm 5$  ppm for all but 3 data-sets. The errors between measured and simulated slurry emission values could be attributed to small variation in the slurry surface *pH* measurement for most cases.

Using multiple evaluation parameters to evaluate the model performance helped to uncover where the model was performing well and where improvements could be made. Overall, the model simulated the desired variables well for this room design and production practices. Further testing with different barn designs or production practices such as different manure removal strategies will help to validate the applicability of the model to more barns.

## **6.6 Summary**

The ACES model was designed to simulate ammonia concentration within and ammonia emission from swine barns on an hourly basis. As well, the model was designed to simulate the ammonia concentration in the slurry channel headspace. This

mechanistic model incorporates sub-models that are also mechanistic in nature to describe the processes and factors that contribute to ammonia production within a barn. The sub-models are the Urination Frequency and Location Sub-Model, the Urine Puddle Emission Sub-Model and the Slurry Emission Sub-Model. The mechanistic nature of the model identifies the source and mechanisms for ammonia production that in the future can be used to identify potential ammonia reduction methods.

The ACES model was tested using extensive data from two rooms collected over one grow-finish cycle. The two rooms were identical in design, and similar in environmental control and production practices such as manure removal. The two rooms were fed diets differing in crude protein and sugar-beet pulp content. The differences between pit headspace and room concentration and in slurry properties point to differences in slurry emission based on diet.

Four different models for simulating the volatile fraction of *TAN* were tested. The model chosen assumes that the acid dissociation constant for ammonia in slurry at *pH* levels less than 7.5 is 2.5 times the acid dissociation constant for ammonium in water. Using this model, the pit ventilation rate was 4% of the room ventilation rate and over 95% of the total emission from each room was produced by urine puddles on the floor.

The model was validated using separate data from that used in the calibration process and several parameters were used to evaluate the model performance. Overall, the model simulated the average room and pit concentration levels to within 1% and 10% of average measured concentration values, respectively. The average nominal difference between room concentration measurements and simulations was less than 2 ppm for the majority



of data-sets tested and within 5 ppm when comparing measured and simulated slurry pit headspace concentrations.

The ACES model was able to accurately simulate a variety of conditions making it an important tool in future simulations of ammonia production in swine buildings.

### **Acknowledgments**

Thank you to Michel Payeur and Rob Fengler for their assistance in data collection. The Natural Sciences and Engineering Research Council of Canada provided funding for this project. Core funding for the Prairie Swine Centre is provided by the Saskatchewan Pork Development Board, Manitoba Pork, Alberta Pork and the Saskatchewan Agriculture and Food Development Fund.

## CHAPTER 7

### EVALUATING THE IMPACT OF FACTORS ON THE AMMONIA EMISSION RATE FROM SWINE BARNS

#### **Synopsis**

The ammonia concentration and emission simulation model that was developed in Chapter 6 is a valuable tool for evaluating the ammonia production within barns under various conditions. In this chapter, a series of simulations were performed to see the model predictions of how the ammonia emission rate would change for variation in some of the input variables. Three scenarios outlining possible ammonia reduction techniques are described and tested.

## 7.1 Introduction

Reviews of ammonia emission rates from confined swine operations by Groot Koerkamp et al. (1998) and Arogo et al. (2003a) demonstrate that there is high variability in ammonia production levels depending on animal size and type, barn design, manure storage and management and climate. Groot Koerkamp et al. (1998) showed that the average ammonia concentration within the various swine barns tested ranged from 4 to 18 ppm, with the maximum reported ammonia concentration level reaching 60 ppm. Lim et al. (2004) found ammonia concentrations varied between 5 and 17 ppm for similar rooms with different manure removal strategies. These emission and concentration levels show that ammonia is a prevalent gas within and around most swine barns and that there are many factors related to the variation, thus making it difficult to identify and test methods to reduce production rates.

Within swine barns the two main sources of ammonia are the urine puddles on the floor and stored slurry within the room. For both sources, ammonia production is a function of the amount of ammonia within each type of solution, and the rate of convective mass transfer from each solution to the air. It is possible to measure ammonia emission from individual sources in smaller-scale studies or the cumulative emission from both sources in a room situation, but it is difficult to measure the contribution of each site to the total ammonia produced within a swine barn. This makes it difficult to understand the contribution of source-specific factors on production rates. Considering all the factors involved in emission from urine puddles and slurry, the number of potential emission sites, and the interactions between all sites, mathematical models provide a time and cost-effective method to understand the various ammonia production methods, to

develop reduction methods based on the understood principles or processes, and quantify the potential impact of ammonia reduction techniques or technologies.

The objectives of this study are: (1) to run a series of simulations using the Ammonia Concentration and Emission Simulation (ACES) model developed in Chapter 6 with varying input factors and evaluate the impact of those factors on the ammonia emission rate; and (2) to demonstrate how the ACES model can be applied to test combinations of factors by simulating three theoretical ammonia reduction techniques on the indoor and surrounding environment.

## **7.2 Calculation Procedure**

The evaluation of factors related to ammonia production and the potential impact of various reduction techniques depends on the model used and the mean values used in the simulations. The following section provides a brief description of the model used, a description of the simulated conditions, and the procedure used to run and analyze various simulations.

### **7.2.1 ACES Model**

The effect of various factors on the ammonia production and emission process was evaluated using the ACES Model that was developed, calibrated and validated in Chapter 6. The ACES model is applicable to mechanically-ventilated grower-finisher barns with partially slatted floors. A summary of the model as it was used in the following analyses and testing is shown here while a more detailed explanation for various components was demonstrated in preceding chapters.

There are two main aspects of the ACES model that differentiates this model from previous room models. First, in the ACES model the room and slurry pit headspace are

considered two separate control volumes linked by the air exchange rate through the slatted floor ( $Q_R$ ) (fig. 7.1).

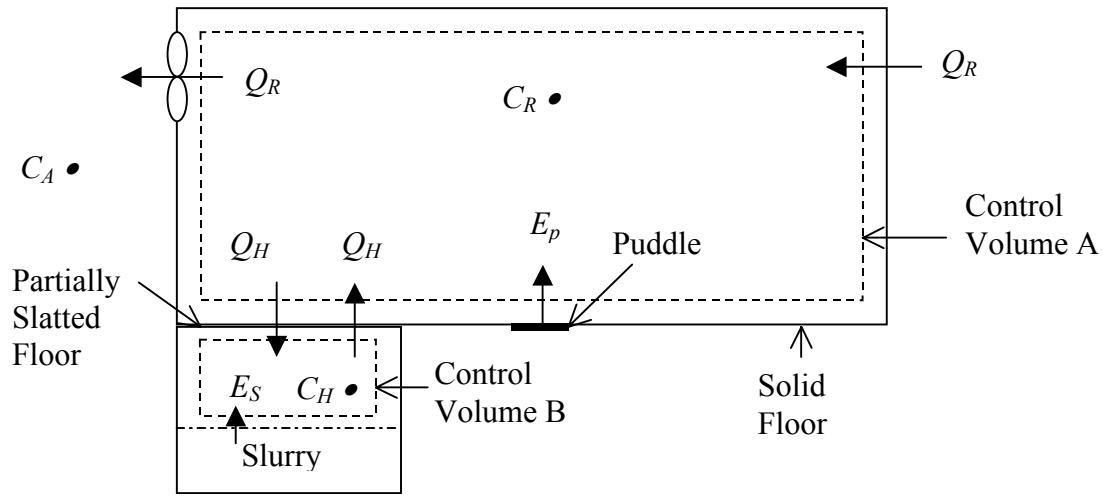


**Figure 7.1. Cross-sectional view of a partially-slatted floor room in a swine barn, with bold arrows representing ammonia addition and removal sites to the ammonia contained within Control Volume A (Room airspace) and Control Volume B (Slurry Pit Headspace).**

The basis of the model is the solution of equations 7.1 and 7.2 to determine the room and slurry channel headspace concentration, respectively, and using the resulting room concentration and ventilation rate to calculate the room emission rate (eq. 7.3).

$$\frac{dC_R}{dt} = \frac{Q_R \cdot (C_A - C_R)}{V_R} + \frac{Q_H \cdot (C_H - C_R)}{V_R} + \frac{E_{p,T}}{V_R \cdot 1000} \quad (7.1)$$

$$\frac{dC_H}{dt} = \frac{Q_H \cdot (C_R - C_H)}{V_H} + \frac{E_S}{V_H \cdot 1000} \quad (7.2)$$

$$E_R = Q_R \cdot 1000 \cdot (C_R - C_A) \quad (7.3)$$

The total emission rate from the floor surface is the sum of emissions from all existing urine puddles on the solid and slatted floor surfaces. Within equations 7.1 to 7.3 the emission rate values require units of  $\text{mol s}^{-1}$ . Emission rates can also be expressed in

units of  $\text{g } NH_3\text{-N d}^{-1} \text{ AU}^{-1}$  with some unit conversion ( $1 \text{ mol } NH_3 = 14 \text{ g } NH_3\text{-N}$ ;  $1 \text{ AU} = 500 \text{ kg live animal mass}$ ).

The second unique aspect of the ACES model is that in determining the emission rate from individual urine puddles ( $E_P$ ) and the slurry ( $E_S$ ), the ammonia concentration of the surrounding air for each emission site is included in the convective mass transfer calculations. Previous models, with the exception of Ni et al. (2000c), have neglected the bulk air concentration in the concentration gradient. The full explanation of how  $E_P$ ,  $E_{P,T}$  and  $E_S$  are calculated is explained in detail in Chapter 6.

Aside from the bulk air concentration for each site, the input factors affecting the ammonia emission rate for individual urine puddles, the total floor surface and the slurry are described in table 7.1. In the ACES model calculation of ammonia emission from individual urine puddles, the simultaneous processes of evaporation, urea degradation, changing puddle  $pH$  and convective mass transfer are considered. The floor surface emission rate is a function of the number of puddles on the floor at a given time and the current state of each puddle. The slurry emission rate is the rate of convective mass transfer of ammonia at the slurry surface to the surrounding air. The ACES model is not designed to simulate ammonia generation within the slurry, thus the surface conditions (total ammoniacal nitrogen concentration ( $TAN_S$ ) and  $pH_S$ ) are input values to the model in order to determine the emission rate.

**Table 7.1. The input factors that directly impact the ammonia emission rate calculations for different production sites in a swine barn.**

<b>Input factors affecting the ammonia emission rate calculation</b>		
<i>Individual urine puddle emission rate</i>	<i>Floor surface emission rate</i>	<i>Slurry emission rate</i>
<ul style="list-style-type: none"> <li>• Puddle surface area</li> <li>• Air velocity over the puddle surface</li> <li>• Room air temperature</li> <li>• Initial urea concentration</li> <li>• Urease activity of the floor surface</li> <li>• Puddle depth → Puddle volume → Urease activity</li> <li>• Relative humidity</li> </ul>	<ul style="list-style-type: none"> <li>• Fouled floor area</li> <li>• Slatted/Solid floor area</li> <li>• Puddle surface area</li> </ul>	<ul style="list-style-type: none"> <li>• Slatted floor area → Slurry surface area</li> <li>• Air velocity over the slurry surface</li> <li>• Slurry/pit headspace temperature</li> <li>• Total ammoniacal nitrogen (<math>TAN_S</math>) concentration</li> <li>• Slurry surface <math>pH</math></li> </ul>

Within the ACES model, several input factors were calculated based on relationships found in the literature. For example, the air velocity over the floor surface and over the slurry channel were linked to the room ventilation rate, and the puddle area on the slatted and solid floor surfaces were correlated to the animal weight and puddle volume, respectively. For the following analysis, these input variables were set to constant levels so that they could be studied independently from other variables. Under normal operating conditions, a lower relative humidity level is expected in summer compared to winter because of the difference in the ventilation rate, but relative humidity was also set to constant levels so the effect of this variable could be studied.

The ACES model is able to incorporate random number generators to increase the variation in the predicted number and location of urinations. During the following analysis, the number of urinations was based solely on the urination frequency equation described in Cortus et al. (2005) and location of urine puddles was distributed in a fixed

pattern. For test scenarios, the random number generators as described in Chapter 6 were used for simulation of the number and location of urinations.

### 7.2.2 Common Test Conditions

All simulations are based on the following facility description:

- One room in a grower-finisher swine facility
- Twelve pens per room
  - Pen dimensions: 4.2 m by 2.0 m
  - Variable percentage of slatted floor area per pen
- Slurry storage under the slatted floor area of each pen
  - Slurry pit depth: 1.0 m
  - Slurry depth: 0.3 m
- Twelve 50-kg pigs per pen
- All-in all-out operation
- Mechanical ventilation with variable levels of ventilation
- The facility is located in Western Canada

It was assumed that all incoming air entered the room through planned openings and had a negligible ammonia concentration ( $C_A = 0 \text{ mol L}^{-1}$ ).

For an all-in all-out system, the minimum ventilation requirement for 60-kg pigs is  $1.8 \text{ L s}^{-1} \text{ pig}^{-1}$  and summer ventilation requirement is  $54 \text{ L s}^{-1} \text{ pig}^{-1}$  (Zhang, 1994). These ventilation levels were used to create winter and summer test conditions. It is recognized that temperature, relative humidity and airflow conditions in swine barns are also different between seasons, but these variables were left constant between seasons so that the impact of each could be studied separately. The mean values for the remaining input variables are shown in table 7.2. It was assumed that the solid floor area in all pens was clean, and 25% of the slatted floor area was fouled. The mean average air velocity over the floor surface, air velocity over the slurry surface, puddle area on the solid/slatted floor puddle depth on the solid/slatted floor are based on average calculated values using the prediction calculations shown in Chapter 6.



**Table 7.2. Mean input values used in simulations with the ACES Model**

Factor	Units	Mean Input Value
Room temperature	°C	16
Air velocity over the floor surface	m s <sup>-1</sup>	0.6
Puddle area on the slatted floor	m <sup>2</sup>	0.06
Puddle depth on the slatted floor	m	0.0016
Puddle area on the solid floor*	m <sup>2</sup>	0.15
Puddle depth on the solid floor*	m	0.0006
Relative humidity	%	50
Initial urea concentration	mol L <sup>-1</sup>	0.3
Urease activity of the floor surface	g NH <sub>3</sub> m <sup>-2</sup> h <sup>-1</sup>	5
Fouled slatted floor area	%	25
Fouled solid floor area	%	0
Slurry/pit headspace temperature	°C	16
Air velocity over the slurry surface	m s <sup>-1</sup>	0.1
Slurry surface <i>pH</i>		7
Slurry <i>TAN</i>	mol L <sup>-1</sup>	0.3
Slatted floor area (in relation to total pen area)	%	30

\* Mean input variables only used as the solid floor area becomes fouled.

### 7.2.3 Reduction Techniques

Using the ACES model, three scenarios were evaluated for their potential effectiveness at reducing the ammonia concentration at the worker (room) level and the total ammonia emission rate. The mean input values shown in Table 7.2 were used with the exception of the factors shown for each scenario.

The scenarios tested here were based on estimated input values and the input factors should not be considered applicable for every barn; further testing and analysis to what is shown here is recommended before incorporating any ammonia reduction technique or technology.

#### 7.2.3.1 Scenario 1: Altered diet composition

There is a wide range of diet compositions that could be used to alter the nitrogen excretion patterns in swine, thus altering the factors for urine and slurry that affect the

ammonia emission rate. For the purposes of this study, a diet with lowered crude protein level (2 percentage units) and sugar-beet pulp inclusion (15%) was tested.

Smith et al. (2004) measured the nitrogen excretion patterns for grower-finisher pigs fed diets with high and low levels of crude protein with and without 15% sugar-beet pulp inclusion. With the low level of crude protein and sugar-beet pulp inclusion the nitrogen in the urine of grower pigs was significantly reduced from 39.3 to 27.9 g N d<sup>-1</sup> compared to a diet with 2% higher protein and no sugar-beet pulp. Translating the reduction in urine nitrogen to the initial urea concentration, this type of diet could result in a 29% reduction in the initial urea concentration. The total nitrogen excretion was reduced from 51.3 to 39.4 g N d<sup>-1</sup> using the same diet compared to the control diet. If the reduction in the nitrogen excretion patterns is applied to the *TAN* concentration of the slurry, the *TAN* concentration could be reduced by 23%. Canh et al. (1998a) found a 0.3 unit reduction in the slurry *pH* for animals fed a diet with 2% lower crude protein content, and Canh et al. (1998c) measured a 0.12 unit decrease in slurry *pH* for every 100-g increase in dietary non-starch polysaccharides (which includes sugar-beet pulp) in the animal's diet. Assuming no interaction between crude protein content and sugar-beet pulp inclusion, the low protein sugar-beet pulp diet tested in Smith et al. (2004) could result in a 0.7 unit decrease in the slurry *pH*.

The resulting input variables that were tested for this scenario were:

1. initial urea concentration: 0.21 mol L<sup>-1</sup>
2. slurry *TAN*: 0.23 mol L<sup>-1</sup>
3. slurry *pH*: 6.3

### 7.2.3.2 Scenario 2: Specific dunging area

Pigs are clean animals and prefer to keep their dunging area separate from their sleeping and feeding area (Watson, 1985). With little or no training, pigs will urinate and defecate over the slatted floor area and keep the solid floor clean in a partially-slatted floor pen. This scenario tested the possible effects of further reducing the slatted floor area per pen by 50% and assuming that there was frequent and complete manure removal beneath the slatted floor area (basically a toilet-type system per pen). The fouled floor area was increased to 50% of the slatted floor area. In order to simulate no slurry emission the model required a negligible mass transfer coefficient that was achieved by setting the air velocity over the slurry to  $0 \text{ m s}^{-1}$ . The resulting combination of input variables that was tested was:

1. slatted floor area: 10% of the total pen area
2.  $r_{slat}$ : 50%
3. air velocity over the slurry:  $0 \text{ m s}^{-1}$

### 7.2.3.3 Scenario 3: Oil layer on the slurry surface

In existing barns it is often difficult to retro-fit a manure removal system. An alternative to a manure removal system is a solution that can be applied on the slurry that inhibits ammonia diffusion to the surface gas phase. Derikx and Aarnink (1993) and Pahl et al. (Pahl et al., 2000) showed that the application of an oil layer on the slurry surface reduced the ammonia emission rate from slurry by 50% to 95% depending on the thickness and disturbance of the oil film. It is assumed that there was a significant decrease in the surface  $TAN_S$  concentration using this technique but this was not measured. The ACES model was not designed to simulate the ammonia concentration of

the slurry at different depths, so the model can only simulate the effect of a given surface concentration. The surface layer is assumed to be a neutral solution with a  $pH_s$  of 7.

The input variable used in the simulations for this scenario was:

1. slurry  $TAN$ :  $0.05 \text{ mol L}^{-1}$ .

#### **7.2.4 Method**

Similar to a sensitivity analysis, a series of simulations were completed where individual factors were varied while the other input variables remained constant at their mean value specified in table 7.2. Two tests spanning 48-h each were run using winter and summer ventilation rates, respectively. The average total puddle emission rate, slurry emission rate, total room emission rate ( $\text{g } NH_3\text{-N d}^{-1} \text{ AU}^{-1}$ ) and room concentration (ppm) for the second day in the simulations was reported. The first day in each simulation was ignored because during this time the number of urinations on the floor surface was being established.

For each of the three scenarios, three simulations were completed for both summer and winter conditions with each simulation spanning 48 h. Again, only data simulated in the last 24-h were used to calculate the average puddle emission rate, slurry emission rate, total emission rate and room concentration. The average emission and concentration values of three simulations were compared to the average values from three simulations using the mean values from table 7.2.

### **7.3 Results**

#### **7.3.1 Mean Simulated Values**

Figure 7.2 demonstrates the emission and room concentration simulations using the mean values from table 7.2. Under isothermal conditions, the variation in the

concentration and emission simulations is a result of the varying puddle emission. The peak in puddle emission occurs over night when urination frequency is low. Based on the model development explained in greater detail in Chapter 6, when there were fewer urinations the existing puddles were replaced on a less frequent basis, allowing  $TAN_P$  to build to higher levels within individual puddles and thus increase emission.

With the impact of ventilation rate removed from the air velocity predictions over the floor and over the slurry, the ventilation rate only impacts the floor and slurry emission rates by reducing the concentration gradient for convective mass transfer. This effect has a large impact in the slurry emission rate calculations between winter and summer. The ACES model predicts the slurry emission will be a very low percentage of the total emission in the winter (3%) compared to the summer (17%).

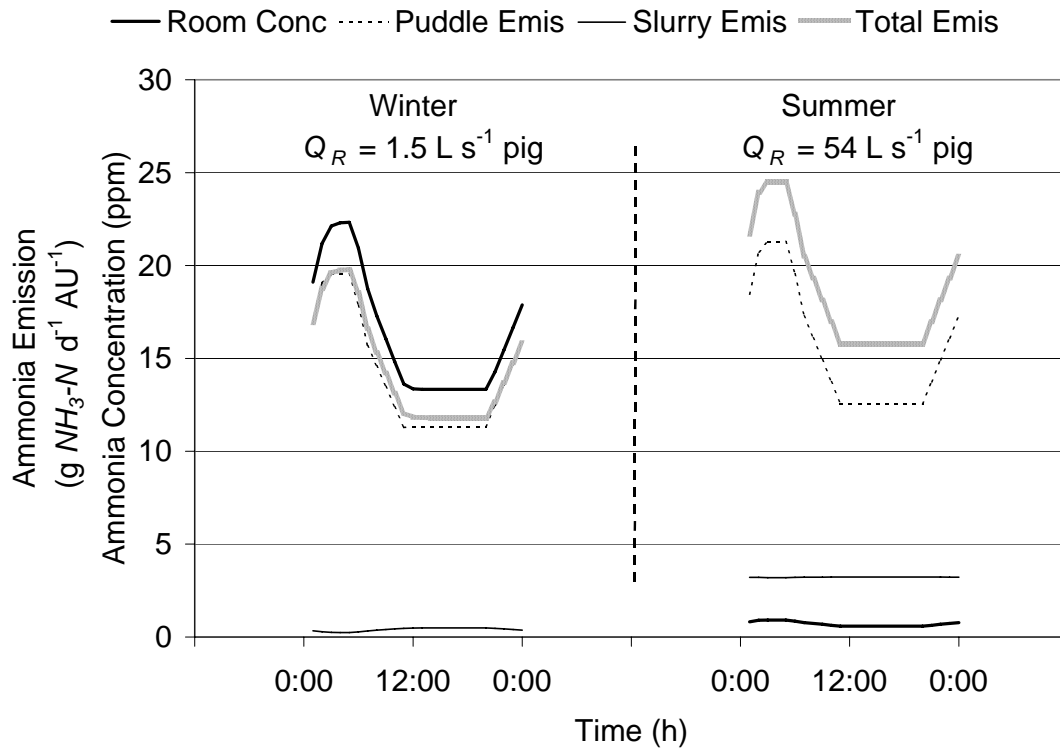


**Figure 7.2. Simulated room concentration and emission levels under low and high ventilation rate situations.**

### **7.3.2 Impact of Input Factors**

The impact of each input factor on the emission rates and room concentration is shown in Table 7.3 for winter conditions and Table 7.4 for summer conditions. The simulated room concentration for all simulations was very low for summer ventilation conditions. Room concentration levels for winter conditions are higher. The maximum simulated room concentration was 63 ppm when the slatted floor area was 100% of the total pen area.

The ACES model incorporates the surrounding room and pit headspace concentration in the concentration gradient for puddle and slurry emission calculations, respectively. This aspect of the ACES model has some important consequences that are shown in Table 7.3. For example, when the simulated puddle emission rate increased from increasing the air velocity over the floor surface, there was a decrease in the slurry emission rate because of an increased level of ammonia in the air surrounding the slurry. Similarly, an increase in the slurry and pit headspace temperatures increased the slurry emission rate and decreased the puddle emission rate. The lower concentration levels in the summer conditions (Table 7.4) reduced the impact of increased puddle emission affecting the slurry emission and vice versa.

**Table 7.3. Simulated emission rates and concentration levels for varying input factors under winter ventilation conditions.**

Factor and input values	Emission Rate (g $NH_3$ -N d <sup>-1</sup> AU <sup>-1</sup> )			Concentration (ppm) Room
	Floor	Slurry	Total	
<i>Mean conditions</i>	14.2	0.4	14.5	16.4
Room temperature (°C)				
14	11.7	0.5	12.1	13.7
18	17.2	0.3	17.5	19.8
Air velocity over the floor surface (m s <sup>-1</sup> )				
0.2	9.2	0.6	9.7	11.0
1	17.0	0.3	17.3	19.5
Puddle area on the slatted floor (m <sup>2</sup> )				
0.02	21.8	0.2	21.9	24.8
0.10	10.2	0.5	10.7	12.1
Puddle depth on the slatted floor (m)				
0.001	18.1	0.3	18.4	20.8
0.002	12.3	0.5	12.7	14.4
Relative humidity (%)				
20	14.4	0.4	14.8	16.7
80	14.0	0.4	14.4	16.2
Initial urea concentration (mol L <sup>-1</sup> )				
0.2	13.8	0.4	14.2	16.1
0.6	14.2	0.4	14.6	16.5
Urease activity (g $NH_3$ m <sup>-2</sup> h <sup>-1</sup> )				
1.2	4.0	0.7	4.7	5.3
12.2	25.6	0.1	25.6	29.0
Fouled slatted floor area (%)				
25	30.6	-0.1	30.5	34.5
50	42.2	-0.4	41.8	47.2
Slurry/pit headspace temperature (°C)				
6	14.2	-0.2	14.0	15.8
26	14.0	2.4	16.4	18.5
Air velocity over the slurry surface (m s <sup>-1</sup> )				
0.02	14.2	0.3	14.5	16.3
0.2	14.2	0.4	14.6	16.5
Slurry pH				
6	14.2	-0.3	13.9	15.7
8	13.5	7.3	20.8	23.5
Slurry TAN (mol L <sup>-1</sup> )				
0.1	14.2	-0.1	14.1	15.9
0.5	14.1	1.0	15.0	17.0
Slatted floor area (%)				
25	10.4	0.5	10.9	12.3
50	25.3	0.1	25.4	28.6
100	56.9	-1.0	56.0	63.2

**Table 7.4. Simulated emission rates and concentration levels for varying input factors under summer ventilation conditions.**

Factor and input values	Emission Rate (g $NH_3$ -N d <sup>-1</sup> AU <sup>-1</sup> )			Concentration (ppm) Room
	Floor	Slurry	Total	
<i>Mean conditions</i>	15.6	3.2	18.8	0.7
Room temperature (°C)				
14	12.9	3.2	16.1	0.6
18	18.8	3.2	22.0	0.8
Air velocity over the floor surface (m s <sup>-1</sup> )				
0.2	9.8	3.2	13.0	0.5
1	18.9	3.2	22.1	0.8
Puddle area on the slatted floor (m <sup>2</sup> )				
0.02	23.1	3.2	26.3	1.0
0.10	11.1	3.2	14.4	0.5
Puddle depth on the slatted floor (m)				
0.001	19.6	3.2	22.8	0.9
0.002	13.6	3.2	16.8	0.6
Relative humidity (%)				
20	15.8	3.2	19.0	0.7
80	15.4	3.2	18.6	0.7
Initial urea concentration (mol L <sup>-1</sup> )				
0.2	15.2	3.2	18.4	0.7
0.6	15.6	3.2	18.9	0.7
Urease activity (g $NH_3$ m <sup>-2</sup> h <sup>-1</sup> )				
1.2	4.4	3.3	7.6	0.3
12.2	28.1	3.2	31.3	1.2
Fouled solid floor area (%)				
25	33.9	3.2	37.0	1.4
50	46.0	3.1	49.1	1.8
Slurry/pit headspace temperature (°C)				
6	15.6	0.8	16.4	0.6
26	15.6	11.5	27.0	1.0
Air velocity over the slurry surface (m s <sup>-1</sup> )				
0.02	15.6	1.5	17.1	0.6
0.2	15.6	4.4	20.0	0.8
Slurry pH				
6	15.6	0.3	15.9	0.6
8	15.5	30.8	46.2	1.7
Slurry TAN (mol L <sup>-1</sup> )				
0.1	15.6	1.0	16.6	0.6
0.5	15.6	5.4	21.0	0.8
Slatted floor area (%)				
25	11.3	2.9	14.2	0.5
50	28.7	3.9	32.6	1.2
100	66.8	5.0	71.8	2.7



Increases in room temperature, air velocity over the floor surface, initial urea concentration and urease activity resulted in increased floor emission rates, and this can be attributed to the impact of each factor on the puddle emission rate from individual puddles. Increasing the fouled floor area and the slatted floor area in a pen also increased the floor emission rate by increasing the number of existing puddles. Increasing the puddle area resulted in a lower floor emission rate, which is opposite to the expected effect on the emission rate from an individual urine puddle. The increase in area resulted in a lower number of urinations co-existing on the fouled floor surface at a time and this impact was greater than the increase in emission per puddle. Increasing the puddle depth decreased the urease activity within the puddle, thus lowering the floor emission rate even though the puddle volume was slightly increased. Increasing relative humidity had a small and negative impact on the floor emission rate showing that the impact of puddle evaporation was small for the simulated conditions.

Based on the range of expected values for each input factor that was tested, urease activity, puddle area, puddle depth and air velocity over the floor surface had the largest impacts on the floor emission rate. Because the average floor emission rate was over 97% of the total emission rate in the winter and 83% in the summer, these factors had a large impact on the overall emission rate as well.

Increasing the slurry/pit headspace temperature, the air velocity over the slurry, the slurry *pH* or the slurry *TAN* resulted in increased slurry emission rates. The effect was more pronounced under summer ventilation conditions. Slurry *pH* had a very significant impact. In summer conditions an increase of 2 units in the slurry *pH* increased the slurry

emission rate by  $28 \text{ g NH}_3\text{-N d}^{-1} \text{ AU}^{-1}$  and the slurry emission rate was over 66% of the total emission rate.

### 7.3.3 Scenarios

Incorporating the random number generators in the ACES model, three simulations were run for the control conditions and each of the three scenarios in both winter and summer conditions. The average emission rate of three simulations for each scenario was calculated and is shown in figure 7.3. The emission rates from both the floor and the slurry for each scenario increased between winter and summer. There was no slurry emission in Scenario 2 because of the frequent manure removal stipulation.

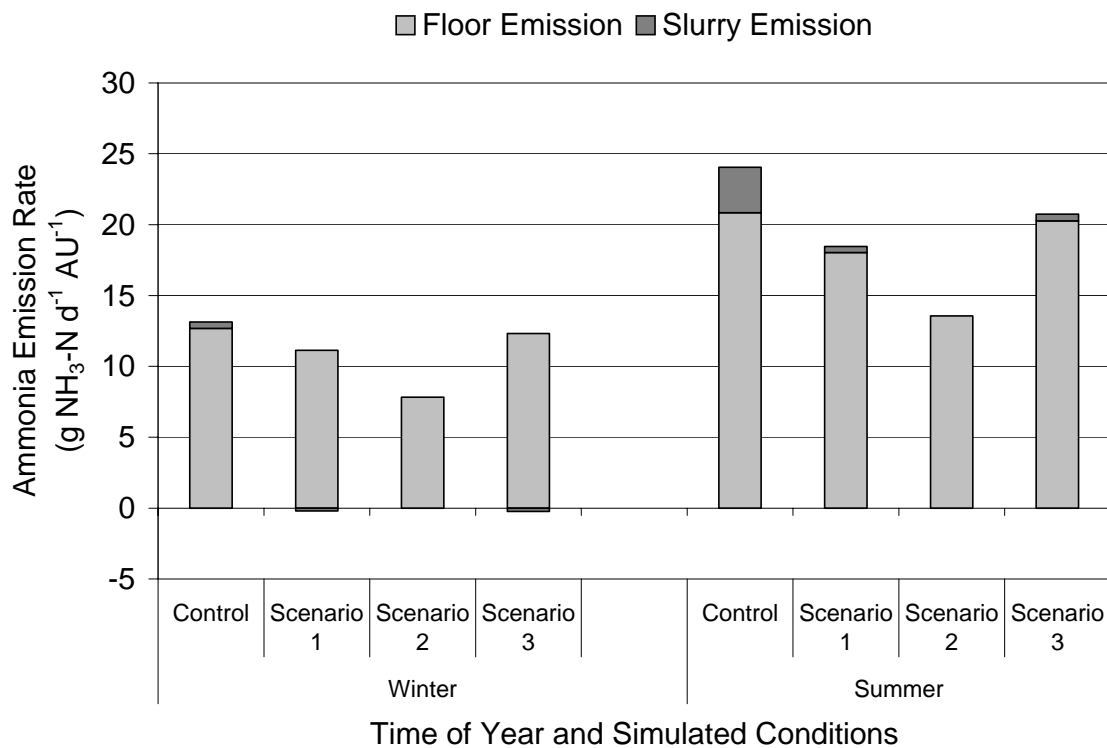


**Figure 7.3. Average floor emission and slurry emission rates for the four sets of conditions tested in winter and summer conditions.**

The percent reduction in total emission under winter conditions was 17% with Scenario 1, 40% with Scenario 2 and 8% with Scenario 3 compared to the Control.

Under summer conditions, the percent reduction levels were slightly higher with 23%, 44% and 14% reduction for Scenarios 1, 2 and 3, respectively. The average room concentrations during the winter conditions mirror the effect of the scenarios on the total emission rates. The average room concentration levels were 14.7 ppm (SD 2.5 ppm) for the Control conditions, 12.4 ppm (SD 1.7 ppm) for Scenario 1, 8.8 ppm (SD 1.8 ppm) for Scenario 2 and 13.6 ppm (SD 2.3 ppm) for Scenario 3. The average room concentrations in summer conditions were less than 1 ppm for all scenarios.

Scenario 2 resulted in the lowest reduction in ammonia emission by reducing the fouled-floor area and thus the puddle emission. Reducing the initial urea concentration of the urine puddles reduced the puddle emission rate to a lesser extent in Scenario 1.

Scenarios 1 and 3 were designed to reduce the slurry emission rate by lowering the  $TAN$  concentration of the slurry. Under summer conditions the average slurry emission rate was reduced 86% and 85% for Scenarios 1 and 3, respectively. The impact of reducing the  $TAN_s$  concentration below  $0.23 \text{ mol L}^{-1}$  appears minimal. In winter conditions, the slurry absorbed ammonia from the surrounding air resulting in negative slurry emission rates for Scenarios 1 and 3.

## **7.4 Discussion**

### **7.4.1 Factors Affecting Ammonia Emission**

There are numerous input variables for the ACES model, and each input variable has some variation associated with it. The simulations shown in this chapter examined how the ACES model was impacted by this variation in individual factors, and the simulated results can be validated to some extent by data from the literature. The strong impact of the puddle emission rate on the total emission rate results in a large impact of puddle emission factors on the total emission rate compared to slurry emission rate factors.

Aarnink and Elzing (1998) simulated on average 70% of the ammonia emission emanated from the slurry, thus the slurry emission factors were shown to have a larger impact in that model.

The factors affecting the emission rate from individual urine puddles such as room temperature, relative humidity and air velocity over the floor surface showed similar results compared to the Model Application Section in Chapter 4 with a few exceptions. The negative correlation between puddle area and floor emission rate was a result of the reduction in the number of emitting puddles. Similarly, increasing puddle depth increased the individual puddle volume but at the same time decreased the urease activity reducing the amount of urea converted to ammonia. Urease activity was not linked to puddle depth in the experimental work of Chapter 4.

A decreasing initial urea concentration had a stronger impact on the floor emission rate than increasing the initial urea concentration did. This is attributed to urine puddles being replaced with new puddles before all the urea was converted to ammonia. Theoretically, higher levels of initial urea concentration therefore only resulted in more urea being left on the floor, a phenomenon that has not been tested or incorporated in the ACES model. Decreasing the urea concentration of the urine from dairy cows has been shown to reduce ammonia emissions from dairy barns but in this study there was an impact of the urea concentration on the slurry concentration as well (Monteny et al., 2002).

Ni et al. (1999c) found a correlation ( $R^2 = 0.723$ ) between the ammonia emission rate and floor contamination for fattening pig houses. The ammonia emission rate increased 113% and 226% for 25% and 50% solid floor contamination. Under summer conditions,

the ACES model estimated the total emission rate would increase 97% and 161% for 25% and 50% fouled solid floor area.

Urease activity of the floor surface is an important factor in estimating the floor emission rate. Braam et al. (1997a) only found an impact of urease activity on the ammonia emission rate from a cubicle house for dairy cows when the urease activity was less than  $2 \text{ g } NH_3 \text{ m}^{-2} \text{ h}^{-1}$ . Model simulations shown here and in Chapter 6 show that urease activity continues to impact the simulated floor emission rate to levels above  $5 \text{ g } NH_3 \text{ m}^{-2} \text{ h}^{-1}$ . The levels at which urease activity becomes non-limiting to ammonia emission are not well understood, and likely depend on the environmental conditions as much as the measured urease activities.

A change in slurry temperature has the potential to dramatically change the slurry emission rate. The ACES model simulated a 26% increase in the slurry emission rate for every  $1.0^\circ\text{C}$  increase in slurry/pit headspace temperature (summer conditions). This translated to a 4% increase in the room emission rate given the small impact of slurry emission on the total simulated emission rate. Aarnink et al. (1996) measured a 10% change in total ammonia emission rate from a grower-finisher barn for a  $1.0^\circ\text{C}$  change in slurry temperature.

Other authors have reported a similarly strong relationship between simulated slurry emission rates increasing  $pH_s$ . Aarnink and Elzing (1998) calculated a 0.1 unit increase in slurry  $pH$  would result in a 9% increase in total emission. Under summer conditions, the ACES model simulated a 15% increase in total emission with a 0.1 unit increase in slurry  $pH$ .

#### 7.4.2 Ammonia Reduction Techniques

In tables 7.3 and 7.4 only one factor was varied at a time, with the remaining factors set to mean values. Often, ammonia reduction techniques or technologies impact more than one variable and models such as ACES help to evaluate the cumulative effect. Three scenarios were tested to demonstrate the potential impact of changing multiple variables at a time, or setting a variable such as slurry *TAN* outside of the normal expected range.

In Scenario 1, the lower total emission rate was the result of a decrease in both the slurry and floor emission rates. The slurry emission rate was reduced 146% in winter and 86% in summer, but because the slurry represented only a small portion of the total emission rate under the control conditions, the total emission rate and room concentration were only reduced by 17% and 23% in winter and summer, respectively. The lower initial urea concentration level in Scenario 1 reduced the puddle emission rate by 12% in winter and 13% in summer.

The strong impact of the diet on the slurry emission rate for Scenario 1 was mainly attributed to the 0.7 unit reduction in slurry *pH*. Other authors have reported significant decreases in ammonia emission levels for low protein and/or sugar-beet pulp based diets. Canh et al. (1998a) measured a 50% decrease in total ammonia emissions from grower-finisher pig rooms when the protein content of the diet was reduced from 16.5% to 12.5%. Canh et al. (1998b) found a 52% decrease in ammonia emissions from the manure collected from pigs fed a sugar-beet pulp based diet compared to a control barley-wheat based diet. In both studies (Canh et al., 1998a, 1998b), the *pH* of the slurry from the pigs fed the test diets was 0.6 to 0.8 units lower than the control slurry. Payeur (2003) found a 42% decrease in total ammonia emissions from grower-finisher rooms

where the pigs were fed a low protein diet with sugar-beet pulp added compared to rooms where the pigs were fed a control diet with higher protein content and no sugar-beet pulp added. The general impact of the diet on slurry composition was not reported. The literature suggests that changes in diet that result in changes in the slurry composition can have a significant impact on total emission rates from grower-finisher barns, but the impact will depend on the slurry contribution to the overall emission rate. There is often a prohibitive cost associated with adding sugar-beet pulp to a diet and replacing the crude protein with amino acids. If the sole purpose of the change in diet composition is to reduce the ammonia production within the room, further analysis should be done to ensure the ammonia reduction is significant enough to warrant increased feed costs.

Scenario 2 showed the largest reduction in total emission rate and room concentration level compared to the control conditions. The reduction can be mainly associated with the decrease in fouled floor area although the complete removal of slurry emissions could be very significant under different control conditions.

For this scenario to be implemented, animal-training methods using some form of motivation could be developed to promote both a smaller dunging area and even a controlled urination frequency. If the idea of a pig toilet is to be further developed, different methods of handling the slurry can also be incorporated. Stewart (2004) found both washing gutters and a conveyer belt system were able to remove the manure on a frequent basis from a pen and substantially lower ammonia emissions on a per-pig basis, but did not result in "zero" air contamination by manure. If the slurry is to remain in the room for significant periods of time, potential slurry emission should be re-incorporated in the simulations.

Scenario 3 showed only an 8% reduction in the total emission rate and room concentration level in the winter and 11% reduction in the summer. Despite large reductions in the slurry emission rate of 152% (winter) and 85% (summer), the slurry represented such a small portion of the total emission that the impact of reducing the  $TAN$  concentration was reduced at the room level. Under laboratory conditions, Derikx and Aarnink (1993) and Pahl et al. (2000) found oil layers reduced slurry emissions over 90%. There was no report of ammonia absorption by the slurry, such as the simulated winter slurry emission rate suggests, but the idea of a negligible ammonia concentration at the slurry surface appears to be supported. There have been reported difficulties in applying oil surface layers in barn-scale studies. Pahl et al. (2000) found the oil layer was compromised in one experiment by fecal material and urine accumulating on top of the oil layer. Aarnink and Wagemans (1997) suggested that sawdust in the pens of their experimental study may have compromised the oil layer on the slurry surface resulting in only a 31% decrease in ammonia emissions.

In Scenario 3 the assumption was made that the  $TAN_s$  concentration of the surface layer would remain the same throughout the simulation. In winter conditions, the negative slurry emission rate alluded to the slurry absorbing ammonia from the surrounding air in the manure channel. It is unlikely that the ammonia would diffuse down through the layer to the slurry with where the ammonia concentration is higher. However, the concept of the slurry (or any solution) absorbing ammonia shows another direction for ammonia reduction technologies to follow. In the past the focus has been to "block" ammonia from transferring to the surface gas phase either by trapping the ammonia under an oil layer, or trapping the ammonia in an acidic solution (Jensen,



2002). Perhaps the focus should be creating optimal conditions to "attract" ammonia from the room and pit headspace air.

### **7.5 Summary**

The impact of the ACES model input factors was evaluated for both summer and winter ventilation conditions. The number of emitting puddles on the floor surface had a strong impact on the floor emission rate, and the number of emitting puddles is a function of the fouled floor area and the area of individual urine puddles. The urease activity of the floor surface under the puddles also had a strong impact on the emission rate from individual puddles. The slurry *pH* was the slurry emission rate factor that had the largest impact on the total emission rate. The impact of factors related to floor or slurry emission on the total emission rate is dependent on the average simulated proportion of emission coming from each source, and increases in emission from one source can decrease the rate of emission from the other source.

Three scenarios were tested as possible technologies or techniques to reduce the ammonia emission rates and room concentration levels within grower-finisher barns. In Scenario 1, the impact of a low protein diet with sugar beet pulp added was simulated and resulted in a 17% to 23% reduction in the total ammonia emission rate. In Scenario 2, a reduction in the slatted floor area and thus the urine-fouled floor area in a pen along with frequent manure removal resulted in a 40% to 44% reduction in total ammonia emission rate. In Scenario 3, the impact of adding a surface layer of the slurry to reduce the *TAN* concentration of the slurry surface only showed an 8% to 11% reduction in total emission rate.

**Acknowledgements**

Project funding was provided by Natural Sciences and Engineering Research Council of Canada. Strategic funding for the Prairie Swine Centre is provided by the Saskatchewan Pork Development Board, Manitoba Pork, Alberta Pork and Saskatchewan Agriculture Development Fund.

## CHAPTER 8

### GENERAL DISCUSSION

#### **Synopsis**

The impact of the research conducted in the preceding chapters is discussed here in relation to how the research impacts our understanding of the ammonia production and emission mechanisms, and how future work in some areas will help provide more concrete answers to the "ammonia problem".

## 8.1 Introduction

Ammonia production within swine barns affects the sustainability of the swine industry. This problem has been recognized for many years now, but the following typical questions still remain:

- *Where does the ammonia in a barn originate?*
- *How much of the ammonia is coming from the slurry channel? From the floor surface?*
- *How can the ammonia production and emission rates be reduced?*

Unfortunately, there still is not one single easy answer to any of these questions. There are a lot of variables to take into consideration related to the barn design, production practices, environmental conditions, and of course cost. However, tools such as the Ammonia Concentration and Emission Simulation (ACES) model that combine the impact of many of these variables in the simulation of the ammonia production and emission within swine barns take us further than before. As the understanding of ammonia production mechanisms within barns further increases, the research may help provide more concrete solutions to the ammonia problem.

The objective of this chapter is to discuss the implications of the research presented in the preceding chapters to try and answer the above questions, and to suggest potential work that could be done in future studies of ammonia production, emission and abatement. The discussion is divided into five sections dealing with ammonia production and emission at the floor surface, ammonia emission from the slurry pit, modelling ammonia production and emission in swine barns, promising ammonia reduction

techniques and technologies, and future work. General conclusions are presented at the end of this chapter.

## **8.2 Ammonia Production and Emission at the Floor Surface**

The rate of ammonia production at the floor surface is generally not given as much emphasis as the rate of ammonia emission from slurry in swine barns. One reason may be because, visually, the fouled floor surface area does not appear as large or as foreboding as the slurry in the slurry channel. Often, floor contamination is hard to estimate because the bulk of the urine and feces fall through the openings in the slatted floor into the slurry channel below. However, there is increasing evidence that even with slatted floors, the floor surface will still produce a significant amount of ammonia.

The model simulations by Aarnink and Elzing (1998) estimated that an average of  $1.96 \text{ g NH}_3 \text{ d}^{-1} \text{ pig}^{-1}$  originated from urine puddles on the floor surface, representing 30% of the total simulated emission rate of  $6.36 \text{ g NH}_3 \text{ d}^{-1} \text{ pig}^{-1}$  for the described room conditions. In Chapter 6, the Ammonia Concentration and Emission Simulation (ACES) model simulated 95% of the total emission originated from the floor surface for the room conditions tested. At first it appears that there are dramatic differences between the ACES model and the model of Aarnink and Elzing (1998). However, it is important to remember that model simulations depend on the model used *and* on the room and slurry conditions in question. When the nominal floor emission rates are compared between models, the average value of  $11.5 \text{ g NH}_3\text{-N d}^{-1} \text{ AU}^{-1}$  (assuming 70-kg animals) from Aarnink and Elzing (1998) is comparable to the average estimate of  $23 \text{ g NH}_3\text{-N d}^{-1} \text{ AU}^{-1}$  (for 70-kg pigs) in Chapter 6. When these floor surface emission rates are compared to total emission rates of 4.7 to  $120 \text{ g NH}_3\text{-N d}^{-1} \text{ AU}^{-1}$  for barns across the mid-western

United States (Arogo et al., 2003a), it is evident that the floor surface should not be ignored when considering the ammonia production sites within a barn.

Animal behaviour, urease activity and environmental conditions all contribute to the ammonia production and emission rates from individual puddles and from the entire fouled floor area. There is also the potential for ammonia production by fecal material on the floor and ammonia absorbed into building materials, factors that have not been included in the ACES model or previous room models. These factors affecting ammonia production and emission from the floor surface are discussed in more detail in the following sections.

### **8.2.1 Animal Behaviour**

Two aspects of animal behaviour play important roles in the floor surface ammonia emission rate. Urination frequency behaviour and urination location are the two main factors that impact the number of emitting urine puddles on the floor surface as simulated by the ACES model. However, the randomness and variability associated with behaviour patterns affects the ability to model these processes.

While urination behaviour of farm animals may seem random, a urination frequency pattern was recognized for grower-finisher swine (Chapter 2). The development of this urination frequency model provides the important estimation of the number of urine puddles produced based on the time of day and reduces the need for time-consuming behaviour measurements. The CIGR (2002) sinusoidal dromedary (single-peak) model for diurnal variation in animal activity was used as the base model for this behaviour and from personal observations it seemed a logical choice. During night-time observations, the majority of animals were sleeping, but when an animal was moving around a pen the animal generally engaged in feeding, drinking and dunging activities. The link between

urination frequency and animal activity raises some important aspects that could be helpful for future research. First, there is the potential for other behaviours (such as drinking and feeding behaviour) to be linked together with urinating behaviour. Second, there is the potential to measure urination frequency using measurement systems designed for other behaviours. There are currently systems developed to measure animal activity (Pedersen and Pedersen, 1995). If in the future drinking behaviour provides a measure of urination frequency, water meter readings could also be an indication of urinating behaviour. If more specific links can be developed between different behaviours, the need for behaviour measurements will be further decreased and measurement systems easier to implement.

Animal dunging behaviour will affect the fouled floor areas on both the solid and slatted floor regions of a pen. Bate et al. (1988) and Ni et al. (1999c) correlated the fouled floor surface area to animal weight and indoor air temperature, but the fouled floor surface area remained an input value to the ACES model. Despite being an input value and not a modelled variable, there are still some important implications in how this behaviour was interpreted for this study. From personal observations, when the solid floor area of a partially-slatted floor pen is clean, the slatted floor area, the pen partitions and the animals themselves are also cleaner. Animal dunging patterns appear to remain stable and only a small portion of the slatted floor is used. As the percentage of fouled solid floor increases, everything in the pen appears dirtier, including the slatted floor area. Thus, the input values to the ACES model for percentage of fouled floor surface for both the solid and slatted floors were increased simultaneously with increased fouling reported for a pen.

From this study and the literature (Aarnink et al., 1996; Ni et al., 1999c) it is clear that the fouled floor area will impact the total emission rate and should be included as a measured value in any type of future study regarding ammonia emissions or abatement, not just as an input variable for modelling purposes. Estimating where urinations occur on solid floor surfaces is not very difficult (there is usually some evidence of misbehaviour), but on the slatted floor, the gaps in the floor surface make this type of estimation more difficult. What is important though, is that the fouled slatted floor area is not over-looked.

### **8.2.2 Urease Activity**

After urine is deposited on the floor, the enzyme urease is required to catalyze the conversion of urea to ammonia. Unfortunately, enzyme activity at the floor surface of swine barns is difficult to measure as was shown in Chapter 3. Enzyme activity measurement depends on the ability to measure either a decrease in reactant or an increase in product (Shuler and Kargi, 2002). The measurements from Chapter 3 were not able to give definitive urease activity levels for a swine barn because there was an unknown source of contamination affecting the two measurement techniques tried. Correlation between urease activity and the amount of "source material" is not a real possibility either because there may be many sources at the floor surface as urease activity has been linked to bacteria, yeasts, filamentous fungi and algae in the environment (Mobley and Hausinger, 1989).

Without accurate measurement of the urease activity levels for the specific floor surfaces used in the model simulations of Chapter 6, it was necessary to rely on reported urease activity measurements in the literature. The majority of the literature values originated from studies conducted in dairy cow houses in the Netherlands measuring



urease activity on different floor surfaces and for different manure removal strategies (Braam et al., 1997a; Braam et al., 1997b; Braam and Swierstra, 1999). Overall, urease activity levels were lowest on recently cleaned floors, especially when the floor surface was also treated with an acid wash. With an increasing amount of time where the floor surfaces were in contact with animals, their excrement, or both, it makes sense that the amount of bacteria on the floor surface would increase, and that the amount of urease would depend on the floor surface characteristics and cleanliness. Increased urease activity for increased surface roughness and water penetration depth is supported by the work of De Foy et al. (2004) who found manure soaked materials with higher water absorption ability and surface roughness showed increased levels of bacterial colonization. Surface roughness and water absorption appear to be the best predictors of urease activity and should be included as measurements in future studies of urease activity.

There are also temperature and *pH* impacts on enzyme activity. The impact of temperature and *pH* on urease activity from bovine feces was measured by Muck (Muck, 1982) and also seen in the experimental work in Chapter 4 when using Jack Bean Urease. On a larger scale, Braam et al. (1997a) found a slower rate of urease build-up on the floors of dairy-cow houses when the average daily temperature was at or below 10°C. The temperature-dependency of urease activity was modelled using an Arrhenius equation in all three studies. The importance of temperature and *pH* impacts on urease activity of floor surfaces in swine barns is not currently known and therefore was not included in the ACES model.

Urease activity is often expressed on a per area ( $\text{m}^2$ ) basis with some important consequences. First, it is easier to translate measurements to different floor surfaces and puddles with varying volume and depth. However, the second consequence is the urease activity value becomes a function of puddle depth, another difficult and variable measurement. In the ACES model, urease activity, puddle area, puddle depth and puddle volume were all estimated values based on information from the literature. Together, the estimated values worked well together based on the model validation. If more accurate urease activity measurements are available in the future, it may be necessary to re-visit the estimates of puddle area, depth and volume.

Braam et al. (1997a) found urease activity significantly impacted the ammonia emission from a dairy-cow house only up to levels around  $2 \text{ g NH}_3 \text{ m}^{-2} \text{ h}^{-1}$ , but the suggestion in Chapter 3 was to use a value of  $5 \text{ g NH}_3 \text{ m}^{-2} \text{ h}^{-1}$  for fouled floor surfaces in swine barns. Simulations using the ACES model showed that up to  $5 \text{ g NH}_3 \text{ m}^{-2} \text{ h}^{-1}$ , urease activity still impacted the simulated puddle emission rate and for the first two weeks of animal activity in the simulated rooms, lower urease activity levels resulted in better simulated puddle emission rates. The maximum level of  $5 \text{ g NH}_3 \text{ m}^{-2} \text{ h}^{-1}$  used in the simulations was not indicative of the non-limiting urease activity level though; higher urease activity levels resulted in higher simulated ammonia emissions. What the non-limiting level is for floor surfaces in swine barns remains to be fully tested, but the non-limiting levels will rely on the puddle area, depth and volume characteristics as well.

### **8.2.3 Environmental Conditions and Airflow Patterns**

Chapter 4 showed the important environmental variables related to the puddle emission process under experimental conditions. The most important result was the link between evaporation and ammonia emission. It was found that any factor that increased

the rate of evaporation would also increase the ammonia emission rate, either by affecting the simulated mass transfer coefficient or by increasing the amount of ammonia in solution relative to the water volume, thus increasing the concentration and emission. As long as there was still a urine puddle there was ammonia emission because of the continual dissociation of ammonia.

The dissociation of ammonia into ammonia and ammonium forms appeared to be continuous throughout the life of the simulated puddles tested in Chapter 4 and all of the ammonia formed within the puddle was emitted before the puddle completely evaporated. The total amount of ammonia emitted from a single puddle therefore depended on the rate and amount of urea that was broken down. While the evaporation rates of the puddles tested in Chapter 4 were not high enough to test the theory, it does seem possible that some urea will be left unconverted in a urine puddle on the floor surface if the puddle evaporates before the urea degradation process is complete.

The bench-scale study of ammonia emission from urine puddles allowed the impacts of temperature, air velocity and puddle size to be modelled and quantified, and also validated the application of the boundary layer theory approximation for the convective mass transfer coefficient. The transfer of these measurements to the real-life situation of a pig barn required many estimates though, notably in the air speed approximations. Airflow measurements within a swine barn were omitted from the experimental procedure in Chapter 6 with the exception of the ventilation rate measurement. Extensive work by various authors (Randall, 1980; Jin and Ogilvie, 1992; Deurloo et al., 1991; Ogilvie et al., 1990; Nicks et al., 1991) has shown there is a lot of variation in airflow patterns in the animal-occupied zone of a room depending on the inlet design, room

design and temperature conditions. The measured air speed levels at animal level were generally below  $1 \text{ m s}^{-1}$ , similar to levels simulated using the regression equations provided by Ogilvie et al. (1990). It was assumed that the air speed at animal level was the bulk air speed appropriate for the mass transfer coefficient and that animal movement within a pen did not affect the air speed either. Further measurements are possible, but there may be alternatives to this sensitive type of measurement. One possibility at the room level is to monitor the rate of puddle disappearance (by convection only) in order to estimate the evaporation rate, and relate the evaporation rate back to the mass transfer coefficient. Based on the Boundary Layer Theory for the convective mass transfer coefficient used throughout this thesis, estimation for the mass transfer coefficient for one substance (such as water) in air can be related to the estimation for another substance (such as ammonia).

The ACES model incorporated the estimates of puddle area within the fouled floor area. For a given fouled floor area, a smaller puddle was less likely to be replaced compared to a larger puddle. For this reason, the ACES model simulated a higher emission rate for smaller puddle areas. As stated before with regards to urease activity, the combination of the estimates for puddle area, puddle depth and urease activity appeared to work well within the ACES model. If measurements are undertaken in the future to better model puddle area and depth, the difference between male and female urination mechanisms should be addressed. Another option is to move towards summing the wetted floor area, and this is discussed in the Future Work section.

#### **8.2.4 Fecal Matter and Building Materials**

Emission by fecal material was neglected in the ACES model, as it has been in urine puddle emission models by Elzing and Monteny (1997b), Muck and Steenhuis (1981)

and room models by Aarnink and Elzing (1998), Monteny et al. (1998) and Ni et al. (2000c). No literature has been found to show the rate of breakdown of fecal material into volatile ammonia when dry or when combined with urine. In the urine puddle emission experiments by Elzing and Monteny (1997b), simulated ammonia emission measurements were well-matched to measured emission levels by assuming urea was the only ammonia source. However, to achieve this agreement a higher urease activity level was used in the simulations compared to the urease activity level that had been measured in a separate laboratory analysis. The excess ammonia in solution that the lower urease activity level did not account for could have potentially originated from the fecal material, but there is not enough information to draw any further conclusions or estimates.

There is also a general neglect of ammonia absorption, adsorption and desorption by the building materials in a barn and by the animals in ammonia emission modelling for barns. When discussing the impact of the surroundings, the components that are frequently covered in manure should be separated from those that are only subjected to the ammonia in the air. Pelletier et al. (2005) found that after being submerged in manure for 72-h and having the excess manure wiped off, 30 MPa concrete emitted up to  $175 \text{ g NH}_3 \text{ m}^{-2} \text{ h}^{-1}$  in the following 24 h. Other assorted building materials (plywood, cast iron, polyvinyl chloride, ect.) also emitted some ammonia after a similar manure treatment. This type of emission rate is significant, but it cannot be incorporated into ammonia models yet. What these results show is that when covered in manure, ammonia and related matter can absorb into the pores of the material but still be emitted over time. What will help the modelling process more is an understanding of how the absorption

into the concrete affects the emission rate, or if ammonia, urea or other nitrogenous compounds will be trapped in the concrete and what triggers their release. For materials that are not covered in manure, such as the walls and ceiling of a building, the building materials will probably absorb some ammonia gas into the pores of the material and this will be linked to the porosity. When a room is used over many cycles, it is assumed that the rate of absorption will be low because the material will be saturated, and thus, presently seems a negligible source to include in ammonia production models like ACES.

### **8.3 Ammonia Emission from the Slurry Pit**

Based on the results of the model simulations in Chapter 6, slurry emission was a very small part of the total emission rate from the grow-finish swine barn simulated. As stated before in the discussion about the floor surface emission rate, proportional estimates of slurry emission to total emission depend both on the model used and the conditions simulated by the model. With small changes in one factor, slurry surface *pH* for example, the estimated proportion of emission from the slurry channel under similar conditions could have been very different (Figure 8.1).

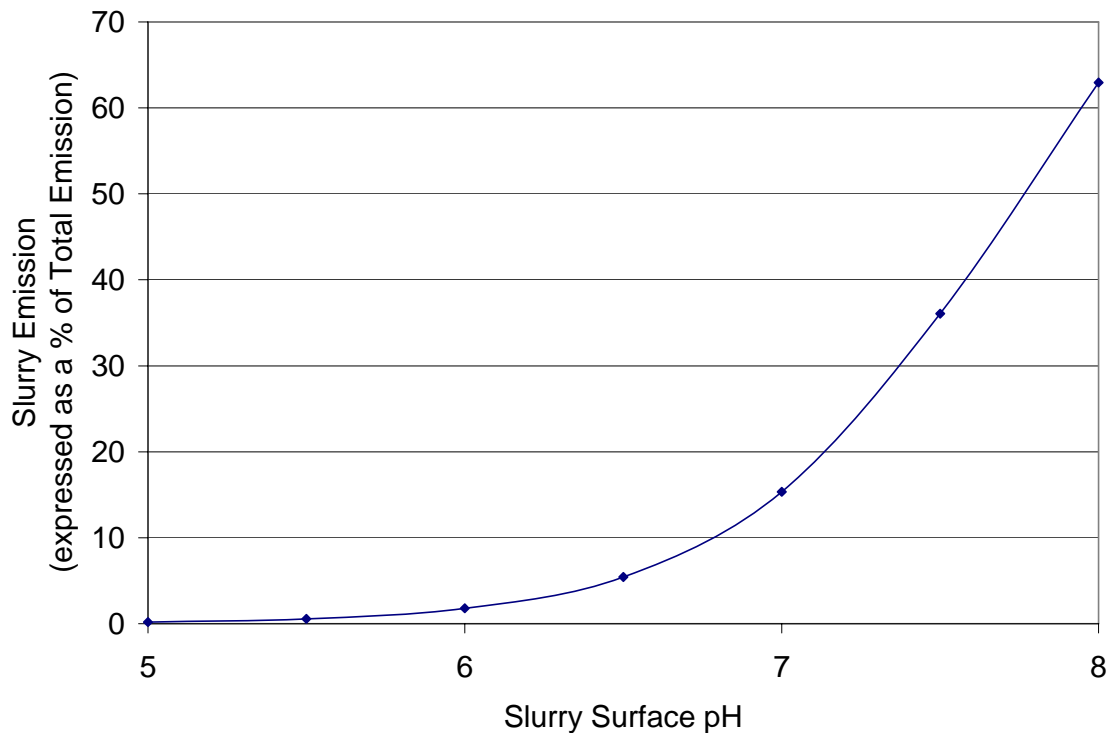


**Figure 8.1. An example graph showing the change in slurry emission (as a proportion of total emission) for varying levels of slurry *pH* assuming all other variables constant. (Total puddle emission = 23 g  $\text{NH}_3\text{-N d}^{-1} \text{ AU}^{-1}$ ).**

Nevertheless, the negative slurry emission rates measured occasionally as part of the Chapter 6 Experimental Results (based on the average difference between the room and slurry pit headspace concentrations) do show an interesting phenomenon that has not been shown before. It appears as though the slurry can absorb ammonia from the surrounding air, provided the ammonia concentration of the gas film at the slurry surface is lower than the bulk air concentration.

The ACES model did not simulate the rate of ammonia generation and transport within the slurry channel. Instead, the ACES model used constant input values for surface conditions of slurry *TAN* and *pH* over the 3-day simulated period. For constant surface conditions to occur, the rate of ammonia emission from the slurry surface must be

equal to the rate of ammonia diffusion within the slurry to the surface. Also, the relative concentrations of *TAN* and other components in the slurry must remain consistent. Ni et al. (2000b) suggested that the slurry surface *pH* would increase following a step-increase in ventilation because of different release rates of ammonia and carbon dioxide from the slurry surface, but there was not sufficient information to incorporate this theory in the ACES model. For example, it was not clear what would happen following a step-decrease in ventilation. The slurry composition measurements for the two rooms measured in Chapter 6 showed that there was a difference between the surface *pH* and the mixed *pH*, but the change in either of these variables was a maximum of 0.1 units per day.

Without consideration of the ammonia generation and transport rate within the slurry channel, the ACES model simulated the slurry emission rate as basically a static process, with the only changes in emission rate linked to changes in temperature, air velocity and the surrounding air concentration. In the following sections, the impact of slurry composition and environmental conditions and airflow patterns within the slurry channel are discussed.

### **8.3.1 Slurry Composition**

Slurry composition is highly variable in solids content, nutrient content and microbe populations. The largest error in modelling ammonia emission from slurry probably results from assuming the chemistry of all types of slurry is alike. To model the slurry emission rate, the method has been to start with water-based equations and make adaptations for slurry. This method is in particular used in determining the amount of *TAN* that is in ammonia form, and thus volatile.



With the current understanding of how to determine the fraction ( $f$ ) of  $TAN$  in ammonia form, the acid ionization constant or dissociation constant ( $K_a$ ) for ammonium and the slurry  $pH$  are important components. The limitations of applying the  $K_a$  value for ammonium in water has been noted by Hashimoto and Ludington (1971), Zhang et al. (1994), Liang et al. (2002) and Arogo et al. (2003b), and the result is a range of factors from 0.17 to 0.95 combined with the  $K_a$  value to express the dissociation of ammonium in slurry. The factors have been experimentally determined based on the relative emission rates of slurry at  $pH$  levels above 9. With all other factors being equal, the difference in emission rates was assumed related to  $f$ , which was in turn related back to the  $K_a$  value. Ionic strength of the solution can impact the dissociation constant (Sawyer and McCarty, 1978), but no specific link has been made between the  $K_a$  factor and any chemical or physical slurry properties.

Sommer and Husted (1995) measured and simulated the buffering capacity for 17 slurry samples from various sources, including seven samples of swine slurry. The change in  $pH$  of these slurry samples as acid or base was added to them revealed that most of the slurry samples had elevated buffering capacities between  $pH$  levels of 5 and 7, and between 8 and 11. A buffer is a solution that can resist changes in  $pH$  when small amounts of acid or base are added to the solution. Theoretically, between  $pH$  levels of 5 and 7, more ammonia (a base) could be added to the solution and buffered by the carbonate or volatile fatty acid components of the slurry without affecting the  $pH$ , thus skewing the prediction of volatile ammonia based on the  $K_a$  factor and  $pH$  alone. Between  $pH$  levels of 8 and 11, the  $TAN$  content of the slurry may provide the buffering

capacity as more acidic components are produced, consuming some of the available ammonia and resulting in lower fraction levels than expected.

When estimating the slurry emission rate, it appears that measurements of *TAN* and *pH* only are probably not sufficient, but it is unclear what other measurements are required. In the meantime, the best start may be use the model of Sommer and Husted (1995) and the concentrations of *TAN*, total inorganic carbon and volatile fatty acids in order to model the effective  $K_a$ , and to continue to use the relationship between  $f$ ,  $K_a$  and *pH*.

### **8.3.2 Airflow Patterns**

The airflow patterns through the slatted floor and inside the slurry channel are relatively unknown, but there has been some research to support the patterns and control volumes used in the development of the ACES model. Hoff (2000) discussed some observations of airflow patterns through slatted floors when exhaust fans were located in the pit headspace. Even with the exhaust fans "pulling" the room air into the pit headspace, some back-drafting of the slurry channel headspace air into the room airspace was observed. The general airflow patterns over the slurry surface were directional to the pen length, which was the assumption made in the ACES model. Ni et al. (2000a) reported elevated ammonia concentration levels in the pit headspaces of a deep-pit barn compared to room levels when the exhaust fans were located in the room airspace. These references support the ideas of air moving both downwards and upwards through the slatted floor between the room and pit headspace air volumes, and that different concentration levels are likely to develop in the two control volumes.

In Chapter 6, the air exchange rate through the slatted floor could only be estimated based on the simulated slurry emission rate. A relationship with ventilation rate was

logical because there were only small temperature differences between the room, pit headspace and slurry, and airflow over the slatted floor region of the pen is also correlated to the ventilation rate (Ogilvie et al., 1990). A ratio of 4% between the pit and room air exchange rates also makes sense because the ratio of pit volume to room volume was approximately 5%, depending on the slurry depth. Further measurements of the airflow through the slatted floor of swine barns would be beneficial to barns designs with and with slurry pit exhaust fans. First, it provides the important link between the room airspace and the slurry pit headspace. Second, as shown in Chapter 6, with a measure of room and pit headspace concentration the slurry emission rate can be estimated with knowledge of the pit ventilation rate, making comparisons of slurry treatment systems (additives, surface covers, ect.) more meaningful and accurate. Third, further measurement of the pit ventilation rate would support or deny air speed measurements over the slurry surface. Tracer gas measurement methods have been used in the past both for model-scale (Yu et al., 1991) and barn-scale measurements (Monteny and Overbeek, 1997). There is also the potential to develop the carbon dioxide mass balance method to estimate the air exchange rate through the slatted floor. This is discussed in greater detail in the Future Work section.

There are many potential factors related to the airspeed over the slurry surface including the slurry depth, the surface roughness, the temperature patterns and the airflow rate through the slatted floor. The ACES model incorporated a regression equation from Aarnink and Elzing (1998) to relate the airspeed over the slurry based on the ventilation rate per floor area. The simulated airspeed levels for the conditions tested in Chapter 6 were lower than the floor airspeed values which seemed reasonable. Monteny and

Lamaker (1997) measured air velocities between 0 and  $0.25 \text{ m s}^{-1}$  in the slurry channel of a cubicle-dairy-cow house, and related the airspeed measurements to a combination of effects by the ventilation rate, air entry location and temperature difference between the incoming air and top layer of slurry. Part of the difficulty in measuring the air velocity was capturing the true direction of the airflow and finding equipment sensitive enough to capture the low airspeeds (Monteny and Lamaker, 1997). Even though measurements of the slurry surface airspeed will provide more accurate measurements for use in models such as ACES, it seems more prudent to focus on the impact of slurry composition and the air exchange rate between the pit headspace and the room airspace first.

The use of exhaust fans in the slurry channel was not incorporated in the development of the ACES model, but given their prevalence in the industry it is worthwhile to mention their impact in relation to ammonia emissions. It has been shown that using exhaust fans in the slurry channel can decrease the ammonia concentration levels in the room airspace (Lavoie et al., 1997; Wilhelm and McKinney, 2001) by removing the higher-concentration air above the slurry before it enters the room airspace. There is the suggestion that exhaust fans in the pit headspace actually increase ammonia emission rates though. By reducing the pit headspace concentration the concentration gradient for slurry emission is increased, as is the potential for increasing air speed over the slurry surface. With a few changes to the core model equations of the ACES model, an air removal site could be added to the slurry pit headspace control volume. Consideration would also need to be given to ensure the air speed approximations and air exchange rate between the room and pit headspace area reflected the new airflow patterns.

## 8.4 Modelling Ammonia Production and Emission

Many models were developed throughout this project with the goals of: (1) understanding the mechanisms behind the ammonia production and emission processes; and (2) putting these processes into equations so that a range and combination of conditions could be tested. The ammonia production and emission processes were modelled using mechanistic models where possible, however, some empirical equations were developed where there was either a lack of information, or a lack of fit using mechanistic equations. Empirical models were developed to describe the volatile fraction of *TAN* in concentrated slurry samples, the airflow rate between the room and slurry pit headspace, and the change in the *pH* of urine puddles with time, demonstrating that the understanding of these mechanisms is currently lacking.

Chapters 4 and 5 described bench-scale experimental set-ups to test the ammonia emission rate factors for urine puddles and slurry, respectively. The benefit of these small-scale tests was that the important variables to the respective ammonia production and emission processes could be measured. This was especially beneficial for the urine puddle emission model, where the literature showed a lack of measurements where the emission from urine puddles was separated from potential ammonia production by fecal material or from concrete floor surfaces. Slurry emission models still require some more work because the variability in swine manure composition makes mechanistic models designed for dilute solutions difficult to apply in all cases.

Throughout this thesis, model simulations were evaluated using the Standard Guide for Statistical Evaluation of Indoor Air Quality Models (ASTM, 2003). This standard was designed for use with pollutant concentration measurements characteristic to the pollutant that may be gas, particulate matter or microbial populations. The six statistical

tests and the corresponding evaluation limits helped to evaluate each model in more ways than with just a regression or correlation. Using the six statistical tests suggested (Appendix A) helped to demonstrate the accuracy of the models in either simulating the average conditions, or the measurements over time. This was very important when evaluating the ACES model where more variables were estimated and the variability in measurements was higher.

ASTM (2003) suggests that indoor air quality model developers and users could, with continued use, further develop limits to qualitatively describe model performance as excellent, good, marginal or unsatisfactory, for example. For models such as the ACES model, it would be helpful to develop limits to describe the ability for a model to simulate the dynamic change in concentration (or emission) over time, and to simulate the average concentration over a period of a couple of days. Also, the error values associated with the model simulations should be evaluated in comparison to how accurate the contaminant can be measured, and both the expected and dangerous levels associated with the gas. Under the conditions simulated, the ACES model was able to simulate hourly concentration levels within 2.2 ppm, and pit headspace concentration levels within 4.3 ppm. Over 3-days, the average room and pit headspace concentration levels were within 1.6 and 2.9 ppm of the measured averages. In Chapter 6, the ammonia concentration measurement instrument had an accuracy of  $\pm 2$  ppm. Furthermore, the 8-h average exposure limit for humans to ammonia gas is 25 ppm. With these considerations in mind, the ability to predict the ammonia concentration levels to within 2.2 ppm was considered good.

### **8.5 Promising Ammonia Reduction Techniques and Technologies**

Despite extensive research into the mechanisms behind ammonia production and emission and testing of different reduction techniques, ammonia still exists in many barns. Therefore, more work in this area is still needed to be able to design ammonia reduction systems that work and are cost-effective. The ability to adapt new technologies in existing barns will also impact the rate of adoption.

The ACES model provides a tool to test potential ammonia reduction techniques and technologies. Simulations were carried out in Chapter 7 to show the predicted impact of three specific reduction techniques/technologies. For any potential ammonia reduction technique/technology, numerous simulations are suggested using as many site-specific and dynamic measurements as possible over the expected range of environmental and production parameters. The first step should be to identify the main source of emissions. The impact of reduction methods will depend on the amount of ammonia coming from the floor surface and from the slurry pit. Even without model simulations, estimates of fouled floor area and slurry composition would provide a start in determining the importance of each site.

What is discussed in the remainder of this section is a more general look at the starting points for identifying and developing potential reduction techniques. This discussion is not meant to list all possible reduction methods, but rather the factors shown to be important by the ACES model. Because ammonia generation was not modelled as part of the overall research project, the ammonia reduction techniques/technologies related to the slurry are only associated with impacts on slurry surface conditions.

Animal behaviour may be the best weapon to reduce the ammonia emission from the floor surface if this behaviour can be controlled. As shown in Chapter 6, by Ni et al.

(1999c), and Aarnink et al. (1996), ammonia concentration and emission levels increase with increased fouled floor area. This in itself should provide impetus to barn managers and workers to try and incorporate practices that promote dunging on the slatted floor area. A potential technique discussed in Chapter 7 involved setting aside a smaller percentage of the pen area for dunging behaviour, and removing the excrement immediately. The first step in implementing this technique would be to train the animals to dung in a certain area, and possibly at prescribed time intervals. Lemay et al. (2000) incorporated drinkers and water sprinklers in an enclosed dunging area design to discourage sleeping in the dunging area. Training techniques used for other livestock may work as well. For example, horses were trained using feed-motivation to dung at specified locations in an equine barn where they collect pregnant mare urine (personal communication with Jon Watts, Western College of Veterinary Medicine, August 2006). Even for fully-slatted floors, certain areas of pens could be made more attractive to dunging behaviour. Aarnink et al. (1997) spaced 50-mm high studs with 32-mm diameters at 200-mm intervals on part of the slatted floor portion of a pen, and these studs were found to discourage laying behaviour and increased the percentage of pigs who used the area for excretory behaviour.

Conveyer belts and washing gutters have the potential to remove excrement immediately from a room. Hoeksma et al. (1992) found a 70% maximum reduction in ammonia emissions when fresh slurry was diluted and removed from the pig house 1 to 4 times a day. Lim et al. (2004) found that more frequent manure removal resulted in reduced ammonia emissions, and the reduction was significantly increased when secondary lagoon effluent was used to recharge the pits after emptying. Predicala et al.



(2006) found that removing manure from a room on a daily basis with an under-floor manure scraper did impact hydrogen sulphide concentrations, but there was no significant impact on ammonia concentrations or emissions compared to a pull-plug system. Stewart (2004) tested both types of manure handling systems in an experimental facility and found that both reduced ammonia emissions in general, but did not totally eliminate air contamination by manure. The impact of these technologies would be better understood if the proportion of ammonia from the manure in the control and test rooms were better known.

When the urease activity of floor surfaces is better understood, there is the potential to test methods that reduce the urease activity of the floor surfaces in a barn, reducing the amount of floor surface emission. Though the measurements in Chapter 3 were not definitive, it appeared as though the floor surface under the drinker had the lowest urease activity/ammonia production rate because of frequent washing by spilled water. Water sprinkling on the slatted floor areas designated for dunging may help remove or dilute any excrement on the floor surface, reduce the existing urease activity, dilute the slurry under the slatted floor and encourage dunging in the wetted location (Lemay et al., 2000) at the same time. The water usage required for extra washing would need to be considered though.

Reducing the slurry *pH* still seems to be the most effective reduction method for slurry emission because a little change can have a large impact. Slurry *pH* could be changed in a number of ways. Jensen (2002) added sulfuric acid to slurry to maintain the slurry *pH* below 5.5, and in doing so, showed that there was a reduction of ammonia concentration levels, an increase in slurry nitrogen, and an improvement in pig performance. Jensen

(2002) noted a monitoring system for hydrogen sulphide was also installed to protect workers and animals from hydrogen sulphide exposure. Acid waste from other industries may be an effective spray treatment to apply to slurry, but corrosion of the building structure materials also needs to be considered. Changes in feed composition can reduce slurry *pH* and slurry *TAN* concentration (Canh et al., 1997, 1998a, 1998b, 1998c) but often represents a significantly higher feed cost that would exist as long as the animals keep eating. A simple sprinkling system that can be used only when required (i.e. when slurry *pH* levels are high) seems the most practical, the easiest to implement, and theoretically would provide the most consistent results.

Surface layers have been highly effective at reducing ammonia emissions from slurry in bench-scale studies, but the impact has been decreased with room-scale measurements. The reduction in impact may be attributed to the proportion of emissions originating from the slurry channel, or the way in which fecal material and urine are added to the slurry. For example, Pahl et al. (2000) found that while ammonia emission rates greater than 90% were achieved in laboratory-scale studies of oil layers on slurry, the ammonia emission reduction in the barn-scale study was either negligible because slurry built up in a layer on top of the oil, or only significant for a short time period because the oil film deteriorated. Pahl et al. (2000) noted that the cost and the potential for increased anaerobic decomposition in stored slurry under the oil film are also drawbacks to this type of method. As other industries look to use their waste material, new surface-cover materials will likely evolve. If any of these materials can be shown to absorb ammonia from the surrounding air, the benefit of increased nitrogen in the slurry may help offset the cost of implementing the technology or technique.

## 8.6 Future Work

Throughout the thesis and the preceding discussion, different areas have been suggested where more research would promote the understanding of ammonia production and emission. The following list summarizes the areas of research that currently appear most important, and where possible, a suggestion is made as to the direction the research can take.

- *Ammonia emission from fecal material*

A bench-scale study similar to that described in Chapter 4, except with fecal material in place of urine, will provide the important and missing proof that fecal material is not a major contributor to ammonia emissions. A variety of environmental conditions and water contents will help determine at what point in time, if any, fecal material begins to break down and whether or not this rate of decomposition should be included in ammonia emission modelling.

- *Wetted floor area*

Modelling the floor surface emission rate can potentially be made easier by considering the total wetted floor area of a pen as one puddle. This idea is based on the observation that when pens become increasingly fouled, the solid floor surface often begins to mirror the surface of the slurry channel. Measurements of the manure composition throughout this "floor slurry" will indicate whether this simplification is valid. If valid, puddle evaporation will become less significant, fecal material breakdown will be incorporated, and individual puddle dimensions and sizes will not be required.

- *Method for measuring the air exchange rate through the slatted floor*

There is the potential to measure (or at least better estimate) the air exchange rate through the slatted floor using the carbon dioxide mass balance method. The development of this type of method would allow researchers to use gas measurement systems already extensively utilized that collect multiple gas readings from each measured location, and in some instances would allow researchers to use data already collected. Ni et al. (1999b, 1999d) have studied carbon dioxide production by animals and by manure, and this research could provide some initial input values to the two-control volume mass balances for carbon dioxide, similar to the core equations of the ACES model (Chapter 6).

- *Method for measuring urease activity of barn floor surfaces*

There are a variety of urease activity measurement methods available, but very few have been used for barn floor surfaces. Any measurement method that relies on measuring the change in concentration of urea or ammonia for solutions that are in contact with barn floor surfaces can be contaminated with nitrogenous compounds that already exist on the floor. By using a marked solution, such as  $^{15}\text{N}$ -labelled urea, the urea that is added as part of the measurement method would be separated from the compounds pre-existing on the floor surface. Using labelled compounds may also reveal the amount of solution absorbed into concrete, and the amount, if any, of nitrogenous compounds released from the floor when the floor is wetted. Urease activity measurements will be further validated if concentration changes over variable time-periods and with variable initial urea concentrations are monitored.

## 8.7 Final Conclusions

The conclusions to this research project are as follows:

1. The urination frequency of swine follows a diurnal pattern that is linked to the lighted period in a room. A grow-finish pig between 51 and 78 kg will urinate on average 0.62 times per hour with a variation of 0.58 urinations per pig per hour.
2. Urease activity of the floor surface can be an important factor to the ammonia emission from the floor surface, especially after cleaning. More definitive measurements of the presence of urease on floor surfaces in swine barns are required.
3. Urine puddle emission is a function of water evaporation, urea degradation, change in total ammonia concentration within the puddle and changes in the puddle *pH* occurring simultaneously. Water evaporation is a new and important inclusion to modelling urine puddle emission, given that urine puddles can potentially evaporate before all the urea in a puddle has been converted to ammonia. The urine puddle emission model developed accurately simulated the puddle volume, puddle *pH*, *TAN* concentration and total emission from individual simulated urine puddles.
4. Slurry emission was modelled as a convective mass transfer process occurring within the slurry storage channel. The emission rate depended on the amount of ammonia at the gas surface and the concentration gradient between the surface and the surrounding pit headspace. The slurry emission model was able to predict the slurry pit headspace concentration in bench-scale slurry pits to within  $\pm 25\%$  of the measured concentration for the majority of concentrated

manure samples. More work is required to accurately model the proportion of total ammoniacal nitrogen in slurry that is volatile.

5. A dynamic, mechanistic model to simulate the hourly ammonia concentration levels in the room and slurry pit headspace areas of grower-finisher swine barns was developed, calibrated and validated. The ACES model simulated the hourly room concentration levels with an accuracy of  $\pm 2.2$  ppm and the hourly pit headspace concentration levels with an accuracy of  $\pm 4.3$  ppm, and thus was considered an accurate model to perform simulations for similar barn designs and conditions with. Use of a two-airspace model not only showed the concentration differences that can exist between two areas in a barn, but also helped to separate out measurements of slurry emission from floor emission.
6. The floor surface is an important contributor to the overall ammonia emission rate for a barn and should not be overlooked when designing ammonia reduction techniques or technologies. There are significant ammonia emissions from fouled areas on the solid and slatted floor areas.
7. Ammonia reduction methods that show the greatest impact on reducing ammonia production and emissions are reducing the urine-fouled floor area, either by developing animal training procedures or regular washing, and by reducing the slurry *pH*, either through spray additives or diet manipulation.

## REFERENCES

- Aarnink, A.J.A. 1997. Ammonia emission from houses for growing pigs as affected by pen design, indoor climate and behaviour. Ph.D. diss. Wageningen, Netherlands: Agricultural University Wageningen, Wageningen Institute of Animal Sciences and the Department of Agricultural Engineering and Physics.
- Aarnink, A.J.A. and A. Elzing. 1998. Dynamic model for ammonia volatilization in housing with partially slatted floors, for fattening pigs. *Livestock Production Science*. 53: 153-169.
- Aarnink, A.J.A. and M.J.M. Wagemans. 1997. Ammonia volatilization and dust concentration as affected by ventilation systems in houses for fattening pigs. *Transactions of the ASAE*. 40(4): 1161-1170.
- Aarnink, A.J.A., A. Keen, J.H.M. Metz, L. Speelman, and M. Verstegen. 1995. Ammonia emission patterns during the growing periods of pigs housed on partially slatted floors. *Journal of Agricultural Engineering Research*. 62: 105-116.
- Aarnink, A.J.A., A.J. van den Berg, A. Keen, P. Hoeksma, and M.W.A. Verstegen. 1996. Effect of slatted floor area on ammonia emission and on the excretory and lying behaviour of growing pigs. *Journal of Agricultural Engineering Research*. 64: 299-310.
- Aarnink, A.J.A., D. Swierstra, A.J. van den Berg, and L. Speelman. 1997. Effect of type of slatted floor and degree of fouling of solid floor on ammonia emission rates from fattening piggeries. *Journal of Agricultural Engineering Research*. 66: 93-102.
- ACGIH. 2000. *2000 TLVs and BEIs*. Cincinnati, OH: American Conference of Governmental Industrial Hygienists.
- Agriculture and Agri-Food Canada. 1998. The health of our air: Toward sustainable agriculture in Canada. Ottawa, ON: Agriculture and Agri-Food Canada.
- Albright, L.D. 1990. *Environmental Control for Animals and Plants*. St. Joseph, MI: ASAE.
- Anderson, G.A., R.J. Smith, D.S. Bundy, and E.G. Hammond. 1987. Model to predict gaseous contaminants in swine confinement buildings. *Journal of Agricultural Engineering Research*. 37: 235-253.
- Aneja, V.P., P.A. Roelle, G.C. Murray, J. Southerland, J.W. Erisman, D. Fowler, W.A.H. Asman, and N. Patni. 2001. Atmospheric nitrogen compounds II: emissions, transport, transformation, deposition and assessment. *Atmospheric Environment*. 35: 1903-1911.

- Arogo, J., P.W. Westerman, and A. Heber. 2003a. A review of ammonia emissions from confined swine feeding operations. *Transactions of the ASAE*. 46(3): 805-817.
- Arogo, J., P.W. Westerman, and Z.S. Liang. 2003b. Comparing ammonium ion dissociation constants in swine anaerobic lagoon liquid and deionized water. *Transactions of the ASAE*. 46(5): 1415-1419.
- ASTM. 2003. Standard guide for statistical evaluation of indoor air quality models. D5157-97 (Reapproved 2003). West Conshohocken, PA: ASTM International.
- Bate, L.A., R.R. Hacker and P.A. Phillips. 1988. Effect of growth on porcine defecation patterns. *Canadian Agricultural Engineering*. 30: 191-192.
- Baxter, M.R. 1982. Environmental determinants of excretory and lying areas in domestic swine. *Applied Animal Ethology*. 9: 195.
- Braam, C.R. and C.J. van den Hoorn. 1996. Concrete floors for animal houses with low ammonia emission: Results of experimental and applied research (In Dutch). Report 96-12. Wageningen, The Netherlands: IMAG-DLO.
- Braam, C.R. and D. Swierstra. 1999. Volatilization of ammonia from dairy housing floors with different surface characteristics. *Journal of Agricultural Engineering Research*. 72: 59-69.
- Braam, C.R., J.J.H.M. Ketelaars, and M.C. Smits. 1997a. Effects of floor design and floor cleanliness on ammonia emission from cubicle houses for dairy cows. *Netherlands Journal of Agricultural Engineering*. 45: 49-64.
- Braam, C.R., M.C. Smits, H. Gunnink, and D. Swierstra. 1997b. Ammonia emission from a double-sloped solid floor in a cubicle house for dairy cows. *Journal of Agricultural Engineering Research*. 68: 375-386.
- Canh, T.T., A.J.A. Aarnink, J.B. Schutte, A.L. Sutton, D.J. Langhout, and M. Verstegen. 1998a. Dietary protein affects nitrogen excretion and ammonia emission from slurry of growing-finishing pigs. *Livestock Production Science*. 56: 181-191.
- Canh, T.T., A.J.A. Aarnink, M.W.A. Verstegen, and J.W. Schrama. 1998b. Influence of dietary factors on the pH and ammonia emission of slurry from growing-finishing pigs. *Journal of Animal Science*. 76: 1123-1130.
- Canh, T.T., A.L. Sutton, A.J.A. Aarnink, M.W.A. Verstegen, J.W. Schrama, and G.C.M. Bakker. 1998c. Dietary carbohydrates alter the fecal composition and pH and the ammonia emission from slurry of growing pigs. *Journal of Animal Science*. 76: 1887-1895.
- Canh, T.T., M.W.A. Verstegen, A.J.A. Aarnink, and J.W. Schrama. 1997. Influence of dietary factors on nitrogen partitioning and composition of urine and feces of fattening pigs. *Journal of Animal Science*. 75: 700-706.



- Chang, R. 1998. *Chemistry*. 6th ed. New York, NY: WCB McGraw-Hill.
- CHEMINFO. 2000. CHEMINFO Record No. 48 (Ammonia gas). CHEMINFO Database. Canadian Centre for Occupational Health and Safety. Available at: <http://www.ccohs.ca/products/databases/cheminfo.html>. Accessed 2 January 2001.
- CIGR. 2002. Climatization of animal houses. Fourth report of working group. Horsens, Denmark: Research Centre Bygholm, Danish Institute of Agricultural Sciences.
- Cortus, E.L., H.W. Gonyou, S.P. Lemay and E.M. Barber. 2005. Measuring and simulating the urination frequency of grower-finisher pigs. *Canadian Journal of Animal Science*. 85: 537-539.
- CPC. 2006. Description of Canadian Hog Farms. Canadian Pork Council. Available at: [www.cpc-ccp.com/stats.html](http://www.cpc-ccp.com/stats.html). Accessed 8 May 2006.
- De Foy, C., P. Bégué, R. Hogue, A. Marquis, S. Godbout, and R. Gagné. 2004. Selection of interior finish materials to improve sanitary status in swine buildings: Relations between odor emissions, material physical characteristics and bacterial retention on the surfaces. ASAE Paper No. 044090. St. Joseph, MI: ASAE.
- Derikx, P.J.L. and A.J.A. Aarnink. 1993. Reduction of ammonia emission from slurry by application of liquid top layers. In *Proceedings of the 1st International Nitrogen Flow in Pig Production and Environmental Consequences Symposium*. EAAP Publication No. 69. 344-349. Wageningen, The Netherlands: Pudoc Scientific Publishers.
- Deurloo, J.A., J.J.R. Feddes, J.J. Leonard, and D.E. Darby. 1991. Effect of recirculated air on air speeds at animal level: commercial-scale swine barn tests. *Canadian Agricultural Engineering*. 33(1): 179-83.
- Donham, K.J. 1991. Association of environmental air contaminants with disease and productivity in swine. *American Journal of Veterinary Research*. 52(10): 1723-1730.
- Donham, K.J. 2000. The concentration of swine production: Effects on swine health, productivity, human health and environment. *Veterinary Clinics of North America: Food Animal Practice*. 16(3): 559-597.
- Donham, K.J., S.J. Reynolds, P. Whitten, J.A. Merchant, L. Burmeister and W.J. Popendorf. 1995. Respiratory dysfunction in swine production facility workers: Dose-response relationships of environmental exposures and pulmonary functions. *American Journal of Industrial Medicine*. 27: 405-418.
- Elzing, A. and G.J. Monteny. 1997a. Ammonia emission in a scale model of a dairy-cow house. *Transactions of the ASAE*. 40(3): 713-720.

- Elzing, A. and G.J. Monteny. 1997b. Modeling and experimental determination of ammonia emission rates from a scale model dairy-cow house. *Transactions of the ASAE*. 40(3): 721-726.
- France, J. 1988. Mathematical modelling in agricultural science. *Weed Research*. 28: 419-423.
- Groot Koerkamp, P.W.G., J.H.M. Metz, G.H. Uenk, V.R. Phillips, M.R. Holden, R.W. Sneath, J.L. Short, R.P. White, J. Hartung, J. Seedorf, M. Schroder, K.H. Linkert, S. Pedersen, H. Takai, J.O. Johnsen, and C.M. Wathes. 1998. Concentrations and emissions of ammonia in livestock buildings in Northern Europe. *Journal of Agricultural Engineering Research*. 70(1): 79-95.
- Hammond, E.G., C. Fedler, and G. Junk. 1979. Identification of dust-borne odors in swine confinement facilities. *Transactions of the ASAE*. 22(5): 1186-1189, 1192.
- Hammond, E.G., C. Fedler, and R.J. Smith. 1981. Analysis of particle-borne swine house odors. *Agriculture and Environment*. 6(4): 395-401.
- Harper, L.A., R.R. Sharpe, and T.B. Parkin. 2000. Gaseous nitrogen emissions from anaerobic swine lagoons: Ammonia, nitrous oxide, and dinitrogen gas. *Journal of Environmental Quality*. 29(4): 1356-1365.
- Hashimoto, A.G. and D.C. Ludington. 1971. Ammonia desorption from concentrated chicken manure slurries. In *Proceedings of the International Livestock Waste Management and Pollution Abatement Symposium*. 117-121. St. Joseph, MI: ASAE.
- Haslam, R.T., R.L. Hershey, and R.H. Keen. 1924. Effect of gas velocity and temperature on rate of absorption. *Industrial and Engineering Chemistry*. 16(12): 1224-1230.
- Hendriks, J., D. Berckmans, and C. Vinckier. 1998. Field tests of bio-additives to reduce ammonia emission from an ammonia concentration in pig houses. *ASHRAE Transactions*. 104: 1699-1706.
- Hoeksma, P., N. Verdoes, J. Oosthoek, and J.A.M. Voermans. 1992. Reduction of ammonia volatilization from pig houses using aerated slurry as recirculation liquid. *Livestock Production Science*. 31: 121-32.
- Hoff, S.J. 2000. Evaluating pit-ventilation effectiveness. In *Proceedings of the First International Swine Housing Symposium*. 227-234. St. Joseph, MI: ASAE.
- Incropera, F.P. and D.P. DeWitt. 1996. *Fundamentals of Heat and Mass Transfer*. 4th ed. New York, NY: John Wiley & Sons.
- Jayaweera, G.R. and D.S. Mikkelsen. 1990. Ammonia volatilization from flooded soil systems: A computer model. I. Theoretical aspects. *Soil Science Society of America Journal*. 54: 1447-1455.

- Jensen, A.O. 2002. Changing the environment in swine buildings using sulfuric acid. *Transactions of the ASAE*. 45(1): 223-227.
- Jin, Y. and J.R. Ogilvie. 1992. Airflow characteristics in the floor region of a slot ventilated room (isothermal). *Transactions of the American Society of Agricultural Engineers*. 35(2): 695-702.
- Jones, J.B., C.M. Wathes, and A.J.F. Webster. 1997. Behavioural responses of pigs to atmospheric ammonia. In *Proceedings of the 5th International Livestock Environment Symposium*. 875-882. St. Joseph, MI: ASAE.
- Krupa, S.V. 2003. Effects of atmospheric ammonia (NH<sub>3</sub>) on terrestrial vegetation: A review. *Environmental Pollution*. 124: 179-221.
- Lavoie, J., G. Marchand and G. Gingras. 1997. Pit ventilation in pig-housing facilities. *Canadian Agricultural Engineering*. 39(4): 317-326.
- Lemay, S.P., H.W. Gonyou, J. Feddes, E.M. Barber, and R. Coleman. 2000. Two airspace building design to reduce odour and gas emissions from pig farms. In *Proceedings of the First International Swine Housing Symposium*. 219-226. St. Joseph, MI: ASAE.
- Lewis, A.J. and L.L. Southern. 2001. *Swine Nutrition*. 2nd ed. New York, NY: CRC Press.
- Lewis, W.K. and W.G. Whitman. 1924. Principles of gas absorption. *Industrial and Engineering Chemistry*. 16(12): 1215-1220.
- Liang, Z.S., P.W. Westerman and J. Arogo. 2002. Modeling ammonia emission from anaerobic swine manure. *Transactions of the ASAE*. 45: 787-798.
- Lim, T.T., A.J. Heber, J.Q. Ni, D.C. Kendall and B.T. Richert. 2004. Effects of manure removal strategies on odor and gas emission from swine finishing. *Transactions of the ASAE*. 47(6): 2041-2050.
- Liss, P.S. and P.G. Slater. 1974. Flux of gases across the air-sea interface. *Nature*. 247(5464): 181-184.
- Mackie, R.I., P.G. Stroot, and V.H. Varel. 1998. Biochemical identification and biological origin of key odor components in livestock waste. *Journal of Animal Science*. 76(5): 1331-1342.
- Martin, P. and P. Bateson. 1993. *Measuring Behaviour: An Introductory Guide*. 2nd ed. New York, NY: Cambridge University Press.
- Merck. 1983. *The Merck Index*. 10th Ed. Rahway, NJ: Merck and Co. Inc.

- Mobley, H.L.T. and R.P. Hausinger. 1989. Microbial ureases: Significance, regulation and molecular characterization. *Microbiological Reviews*. 53(1): 85-108.
- Monteny, G.J. and J.P.E. Overbeek. 1997. Air exchange in and ammonia emission from slurry storage in cubicle dairy-cow houses. ASAE Paper No. 974014. St. Joseph, MI: ASAE.
- Monteny, G.J., D.D. Schulte, A. Elzing, and E.J.J. Lamaker. 1998. A conceptual mechanistic model for the ammonia emissions from free stall cubicle dairy cow houses. *Transactions of the ASAE*. 41(1): 193-201.
- Monteny, G.J., M.C.J. Smits, G. van Duinkerken, H. Mollenhorst, and I.J.M. de Boer. 2002. Prediction of ammonia emission from dairy barns using feed characteristics. Part II: Relation between urinary urea concentration and ammonia emission. *Journal of Dairy Science*. 85(12): 3389-3894.
- Muck, R.E. 1982. Urease activity in bovine feces. *Journal of Dairy Science*. 65: 2157-2163.
- Muck, R.E. and T.S. Steenhuis. 1981. Nitrogen losses in free stall dairy barns. In *Proceedings of the Fourth International Symposium on Livestock Wastes*, 406-409. St. Joseph, MI: ASAE.
- National Research Council. 1998. *Nutrient Requirements of Swine*. 10<sup>th</sup> ed. Washington, DC: National Academy Press.
- Ni, J.Q. 1999. Mechanistic models of ammonia release from liquid manure. *Journal of Agricultural Engineering Research*. 72: 1-17.
- Ni, J.Q., A.J. Heber, C.A. Diehl, and T.T. Lim. 2000a. Ammonia, hydrogen sulphide and carbon dioxide release from pig manure in under-floor deep pits. *Journal of Agricultural Engineering Research*. 77(1): 53-66.
- Ni, J.Q., A.J. Heber, T.T. Lim, C.A. Diehl, A.L. Sutton, R.K. Duggirala, B.L. Haymore, and V.I. Adamchuk. 1999a. Effect of a manure additive on the reduction of ammonia emission from large swine finishing buildings. ASAE Paper No. 994032. St. Joseph, MI: ASAE.
- Ni, J.Q., J. Hendriks, J. Coenegrachts, and C. Vinckier. 1999b. Production of carbon dioxide in a fattening pig house under field conditions. I. Exhalation by pigs. *Atmospheric Environment*. 33: 3691-3696.
- Ni, J.Q., J. Hendriks, C. Vinckier, and J. Coenegrachts. 2000b. A new concept of carbon dioxide accelerated ammonia release from liquid manure in pig house. *Environment International*. 26: 97-104.

- Ni, J.Q., J. Hendriks, C. Vinckier, and J. Coenegrachts. 2000c. Development and validation of a dynamic mathematical model of ammonia release in pig house. *Environment International*. 26: 105-115.
- Ni, J.Q., C. Vinckier, J. Coenegrachts, and J. Hendriks. 1999c. Effect of manure on ammonia emission from a fattening pig house with partly slatted floor. *Livestock Production Science*. 59: 25-31.
- Ni, J.Q., C. Vinckier, J. Hendriks, and J. Coenegrachts. 1999d. Production of carbon dioxide in a fattening pig house under field conditions. II. Release from the manure. *Atmospheric Environment*. 33: 3697-3703.
- Nicks, B., P. Debliquy, B. Canart, B. Buzitu, and A. Dewaele. 1991. Study of microclimate and ventilation in a fattening pig house. *23es Journees de la Recherche Porcine en France*. 23: 21-6.
- Ogilvie, J.R., E.M. Barber, and J.M. Randall. 1990. Floor air speeds and inlet design in swine ventilation systems. *Transactions in Agriculture*. 33(1): 255-259.
- Pahl, O., A.G. Williams, R.W. Sneath, J. Goodman, L. Taylor, R.J. Godwin, and M.J. Hann. 2000. Reducing ammonia emissions from pig production - experiences with oil and foam as a cover material for slurry under slats. In *Proceedings of the 2nd International Air Pollution from Agricultural Operations Conference*. 100-107. St. Joseph, MI: ASAE.
- Paul, J.W. and E.G. Beauchamp. 1989. Relationship between volatile fatty acids, total ammonia and pH in manure slurries. *Biological Wastes*. 29: 313-318.
- Payeur, M. 2003. Canola oil sprinkling combined with a low protein diet for reducing ammonia, dust and odour emissions of swine buildings. M.Sc. thesis. Saskatoon, SK: University of Saskatchewan, Department of Agricultural and Bioresource Engineering.
- Pedersen, S. and C.B. Pedersen. 1995. Animal activity measured by infrared detectors. *Journal of Agricultural Engineering Research*. 61: 239-246.
- Pedersen, S. and H. Takai. 1997. Diurnal variation in animal heat production in relation to animal activity. In *Proceedings of the 5th International Livestock Environment Symposium*. 664-671. St. Joseph, MI: ASAE.
- Pelletier, F., A. Marquis, S. Godbout, R. Joncas, J.P. Larouche, D. Massé, and P. Bégué. 2005. Gas and odor emissions from swine building materials. *Transactions of the ASAE*. 48(2): 721-728.
- Pond, W.G. and K.A. Houpt. 1978. *The Biology of the Pig*. Ithaca, NY: Cornell University Press.

- Pond, W.G., D.C. Church, and K.R. Pond. 1990. Proteins and amino acids. In *Basic Animal Nutrition and Feeding*. Toronto, ON: John Wiley & Sons.
- Predicala, B.Z. E.L. Cortus, S.P. Lemay and C. Laguë. 2006. Effectiveness of a manure scraper for reducing concentrations of hydrogen sulphide in a swine grower-finisher room. Submitted to *Journal of Agricultural Safety and Health*. (under review)
- Randall, J.M. 1975. The prediction of airflow patterns in livestock buildings. *Journal of Agricultural Engineering Research*. 20: 199-215.
- Randall, J.M. 1980. Selection of piggery ventilation systems and penning layouts based on the cooling effects of air speed and temperature. *Journal of Agricultural Engineering Research*. 25(2): 169-187.
- Rao, S.S. 2002. *Applied Numerical Methods for Engineers and Scientists*. Upper Saddle River, NJ: Prentice Hall.
- Ritter, W.F. 1989. Odor control of livestock wastes: State-of-the-art in North America. *Journal of Agricultural Engineering Research*. 42: 51-62.
- Ruckdeschel, F.R. 1981. *BASIC Scientific Subroutines Volume I*. Peterborough, NH: Byte/McGraw-Hill.
- Sawyer, C.N. and P.L. McCarty. 1978. *Chemistry for Environmental Engineering*. 3rd ed. Toronto, ON: McGraw-Hill Book Company.
- Schiffman, S.S. 1998. Livestock odors: implications for human health and well-being. *Journal of Animal Science*. 76(5): 1343-1355.
- Schlichting, H. and K. Gersten. 2000. *Boundary Layer Theory*. 8th ed. New York, NY: Springer.
- Searle, P.L. 1984. The Berthelot or indophenol reaction and its use in the analytical chemistry of nitrogen. *Analyst*. 109: 549-568.
- Shaw, M.I. 2003. Effect of diet composition on water utilisation in growing pigs. M.Sc. Thesis. Saskatoon, SK: University of Saskatchewan, Department of Animal and Poultry Science.
- Shuler, M. L. and F. Kargi. 2002. *Bioprocess Engineering: Basic Concepts*. 2nd ed. Upper Saddle River, NJ: Prentice Hall PTR.
- Smith, L.F., S.P. Lemay, J.F. Patience, and R.T. Zijlstra. 2004. Effects of dietary crude protein level and sugar beet pulp inclusion on nitrogen excretion patterns in grower and finisher pigs. *Canadian Journal of Animal Science*. 84(4): 717-720.

- Sommer, S.G. and S. Husted. 1995. A simple model of pH in slurry. *Journal of Agricultural Science*. 124: 447-453.
- Stewart, K. 2004. Experimental manure handling systems for reducing airborne contamination. M.Sc. Thesis. Saskatoon, SK: University of Saskatchewan, Department of Agricultural and Bioresource Engineering.
- Stinson, R., S.P. Lemay, E.M. Barber, and T. Fonstad. 1999. Effectiveness of three manure pit additives in commercial scale manure channels and simulated outdoor storage. ASAE Paper No. 994150. St. Joseph, MI: ASAE.
- Sutton, M.A., C.E.R. Pitcairn, and D. Fowler. 1993. The exchange of ammonia between the atmosphere and plant communities. *Advances in Ecological Research*. 24: 301-393.
- Svennerstedt, B. 1999. Drainage properties and ammonia emissions in slatted floor systems for animal buildings. *Journal of Agricultural Engineering Research*. 72(1): 19-25.
- Technicon. 1974. Ammonia determination. Technicon Industrial Method No. 325-74W. Tarrytown, NY: Technicon Industrial Systems.
- Thu, K., K. Donham, R. Ziegenhorn, S. Reynolds, P.S. Thorne, P. Subramanian, P. Whitten and J. Stookesberry. 1997. A control study of the physical and mental health of residents living near a large-scale confined swine operation. *Journal of Agricultural Safety and Health*. 3(1): 13-26.
- Treybal, R.E. 1980. *Mass-Transfer Operations*. 3rd ed. Toronto, ON: McGraw-Hill Book Company.
- Turner, S. P., A.G. Sinclair, and S.A. Edwards. 2000. The interaction of liveweight and the degree of competition on drinking behaviour in growing pigs at different group sizes. *Applied Animal Behaviour Science*. 67: 321-334.
- Webster, A.J.F. 2001. Farm animal welfare: the five freedoms and the free market. *The Veterinary Journal*. 161: 229-237.
- Welty, J.R., C.E. Wicks and R.E. Wilson. 1984. *Fundamentals of Momentum, Heat and Mass Transfer*. 3rd ed. Toronto, ON: John Wiley & Sons.
- Watson, T.S. 1985. Development of eliminative behaviour in piglets. *Applied Animal Behaviour Science*. 14(4): 365-377.
- Wilhelm, L.R. and D.B. McKinney. 2001. Environmental measurements in production swine facilities. *Applied Engineering in Agriculture*. 17(5): 669-675.
- Worthington. 1995. Assay of urease (URC). Test Method #3889. Lakewood, NJ: Worthington Biochemical Corporation.

- Yu, L., C. Zhang, and E.M. Barber. 1991. Measuring air exchange through slotted floors. ASAE Paper No. 914550. St. Joseph, MI: ASAE.
- Zhang, R.H., D.L. Day, L.L. Christianson, and W.P. Jepson. 1994. A computer model for predicting ammonia release rates from swine manure pits. *Journal of Agricultural Engineering Research*. 58: 223-229.
- Zhang, Y. 1994. *Swine Building Ventilation: A Guide for Confinement Swine Housing in Cold Climates*. Saskatoon, SK: Prairie Swine Centre Inc.
- Zhu, J., D.S. Bundy, X. Li, and N. Rashid. 1997. Swine manure odor control using pit additives - A review. In *Proceedings of the 5th International Livestock Environment Symposium*. 295-302. St. Joseph, MI: ASAE.



## APPENDIX A

### MODEL EVALUATION PARAMETERS

The model evaluation method used throughout the thesis is based on the ASTM D 5157-97 Standard, "Standard Guide for Statistical Evaluation of Indoor Air Quality Models" (2003). Model evaluation parameters are based on  $n$  corresponding pairs of measured ( $C_o$ ) and predicted ( $C_p$ ) values, and the mean measured ( $\overline{C_o}$ ) and mean predicted value ( $\overline{C_p}$ ).

Evaluation Parameter	Equation	Suggested Evaluation limit
<b>General Agreement</b>		
Correlation Coefficient ( $R$ )	$R = \frac{\sum_{i=1}^n [(C_{oi} - \overline{C_o}) \cdot (C_{pi} - \overline{C_p})]}{\sqrt{\sum_{i=1}^n [(C_{oi} - \overline{C_o})^2] \cdot \sum_{i=1}^n [(C_{pi} - \overline{C_p})^2]}}$	$R > 0.9$
Regression Slope ( $b$ )	$b = \frac{\sum_{i=1}^n [(C_{oi} - \overline{C_o}) \cdot (C_{pi} - \overline{C_p})]}{\sum_{i=1}^n [(C_{oi} - \overline{C_o})^2]}$	$0.75 < b < 1.25$
Regression Intercept ( $a$ )	$a = \overline{C_p} - (b \cdot \overline{C_o})$	$a < 0.25 \cdot \overline{C_o}$
Normalized Mean Square Error ( $NMSE$ )	$NMSE = \frac{\sum_{i=1}^n (C_{pi} - C_{oi})^2}{n} \cdot \frac{1}{\overline{C_o} \cdot \overline{C_p}}$	$NMSE < 0.25$
<b>Bias</b>		
Fractional Bias ( $FB$ )	$FB = \frac{2 \cdot (\overline{C_p} - \overline{C_o})}{(\overline{C_p} + \overline{C_o})}$	$-0.25 < FB < 0.25$
Variance Bias ( $FS$ )	$FS = \frac{2 \cdot (\sigma_{C_p}^2 - \sigma_{C_o}^2)}{(\sigma_{C_p}^2 + \sigma_{C_o}^2)}$	$-0.5 < FS < 0.5$

## APPENDIX B

### USER MANUAL FOR ACES PROGRAM

#### **Scope**

The ACES program was developed by E. Cortus as a tool to simulate the ammonia concentration within grower-finisher swine rooms, both in the room and in the slurry channel headspace, as well as the ammonia emission rates from the floor surface, from the slurry channel to the room airspace, and from the room to the surroundings. The following program was developed and tested with the Prairie Swine Centre Floral barn as the model of a typical partially-slatted floor room. Variations in room design, diet composition and environmental conditions are expected when this program is used for other facilities. While input parameters to the model are designed to handle some of these differences, not all input conditions will be possible. As well, the model has not been verified with different barn designs.

The program is designed as a simulation tool to see the quantity of ammonia produced at different locations within a swine barn, and to investigate ammonia mitigation techniques. However, accurate measurements will always take precedence over model simulations.

#### **Computer Requirements**

The computer program code is written in Visual Basic 6.0 programming language. An executable (.exe) file has been created which will allow the program to be run on any computer that operates on Microsoft Windows. The user will only be able to input certain parameters and view the results; the user will not be able to make any changes to the program or see the underlying code.

The computing time for this program will depend on the time interval chosen, the complexity of the input variables and the iteration interval. However, unless an error is created, the program will take less than a few minutes to complete the computations for a four-day period.

Some problems or "bugs" in running the program have been identified, and more are inevitable. A list of identified bugs has been started and these bugs are listed in the last section "Problems Associated with the ACES Program".

## Basic Model

The majority of the ACES model is "hidden" from the user. The user is only involved in setting the input variables and viewing the results (fig. B.1).

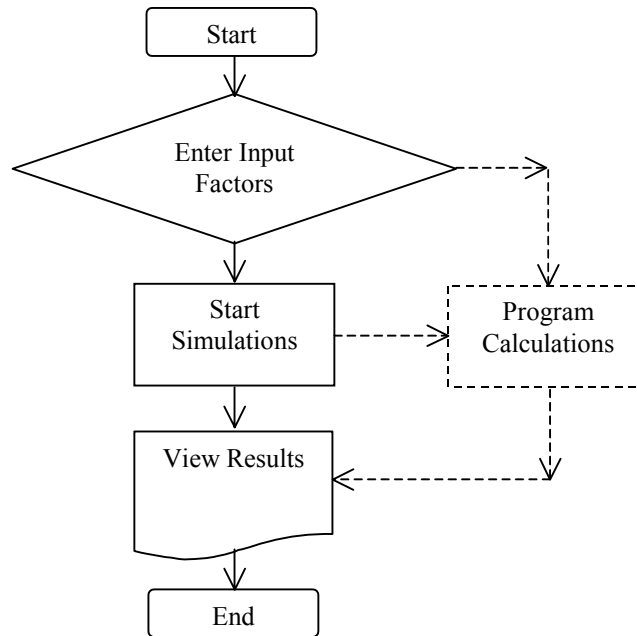


**Figure B.1. Simplified flowchart showing the parts of the program visible to the user in solid lines, and the program parts visible only to the designer in dashed lines.**

The "hidden" portion of the ACES model contains the computation process, outlined in figure B.2.

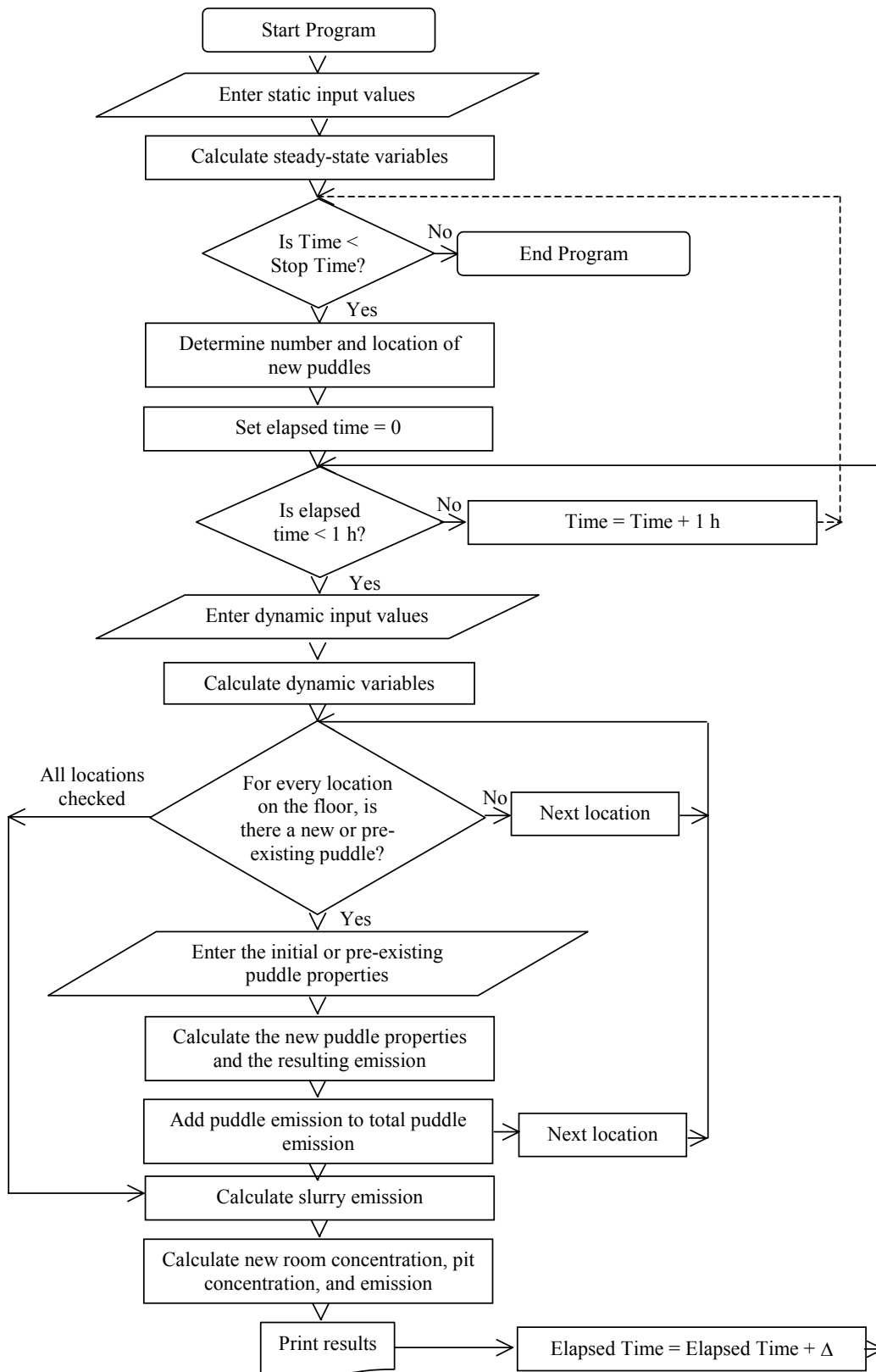


**Figure B.2. Program calculations within the ACES computer program.**

## Program Operation

### *Starting the Program*

Open the program, ACES.exe, and the main page (fig. B.3) will appear.

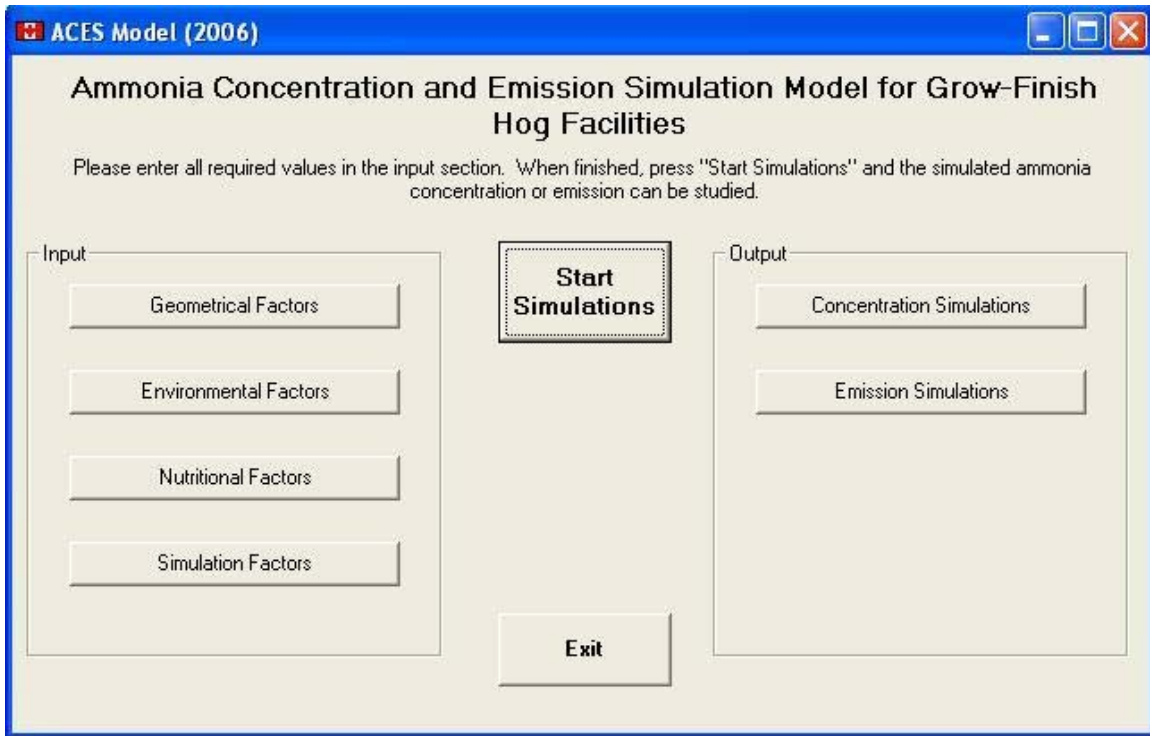


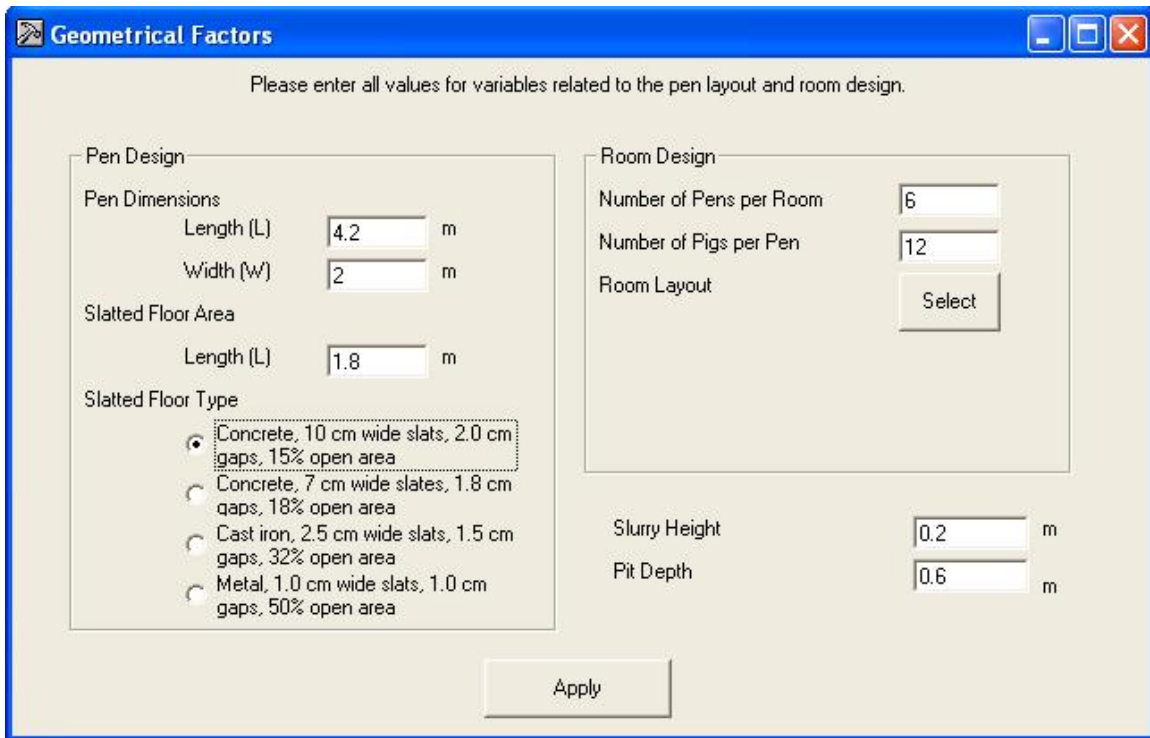
**Figure B.3. Main page of the ACES model.**

The main page is the central interface for the user. From the starting point of this form, the user enters the input data related to building design, environmental conditions, urine and slurry composition and the time interval tested. Each input section must be opened for the program to work properly, but the order that they are opened in is not important.

### *Entering the Input Data*

Following the instructions on the main page, enter the required information in each of the input sections.

Click on the command button labelled "Geometrical Factors" and the Geometrical Factors Form (fig. B.4) will appear. On this page, enter the required information. If the default values are suitable, no changes are necessary.



**Geometrical Factors**

Please enter all values for variables related to the pen layout and room design.

**Pen Design**

Pen Dimensions

Length (L)  m

Width (W)  m

Slatted Floor Area

Length (L)  m

Slatted Floor Type

- ☒ Concrete, 10 cm wide slats, 2.0 cm gaps, 15% open area
- ☐ Concrete, 7 cm wide slats, 1.8 cm gaps, 18% open area
- ☐ Cast iron, 2.5 cm wide slats, 1.5 cm gaps, 32% open area
- ☐ Metal, 1.0 cm wide slats, 1.0 cm gaps, 50% open area

**Room Design**

Number of Pens per Room

Number of Pigs per Pen

Room Layout

Slurry Height  m

Pit Depth  m

**Figure B.4. Geometrical Factors input form.**

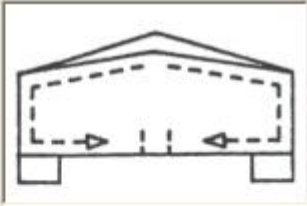
The selection of slatted floor type determines the area of urine puddles on the slatted floor.

By clicking the "Select" command button beside ventilation design/room layout, a separate form (fig. B.5) will appear that describes different ventilation set-ups, with a corresponding drawing. All descriptions and pictures are from Ogilvie et al. (1990). Once the appropriate ventilation design is selected, click the command button "OK" to return to the Geometrical Factors form.

**Ventilation Design**

Please select the design that most closely resembles the layout of the inlets with respect to the pens.

- ☐ Recirculation air bag in center of room, horizontal flow
- ☒ Center-inlet, horizontal flow, bar penning in centre of room
- ☐ Center-inlet, horizontal flow, solid penning at side of room
- ☐ Center-inlet, downward flow, bar penning in center of room
- ☐ Center-inlet, downward flow, solid penning in center of room
- ☐ Center-inlet, downward flow, bar penning at side of room
- ☐ Center-inlet, downward flow, solid penning at side of room
- ☐ Slot inlet, horizontal flow, bar penning in center of room
- ☐ Eave inlet, horizontal flow, solid penning in center of room
- ☐ Eave inlet, horizontal flow, bar penning at side of room



OK

*Source: J.R. Ogilvie, E.M. Barber, J.M. Randall, Transactions in Agriculture 33(1): 255-259*

**Figure B.5. Ventilation and room design selection form.**

**NOTE:**

General assumptions regarding the geometrical factors that are built in the program are:

- The room volume calculation within the model assumes the width of the room is 15% larger than the total width of all pens, the room length is 20% longer than the total length of all pens, and the room height is 3 m.

By clicking "Apply" on the Geometrical Factors form, the main page will reappear.

Click on the command button labelled "Environmental Factors", and the Environmental Factors form (fig. B.6) will appear. On this page, first select whether you want to enter steady state environmental conditions by selecting "Static Environmental Factors", or, if you have a data sheet available with time-based measurements, select "Dynamic Environmental Factors".

**Figure B.6. Environmental Factors input form.**

If "Static Environmental Factors" was selected, enter the required information in the measurement units displayed.

If "Dynamic Environmental Factors " was selected, the data you wish to import into the program must be formatted in a certain way. The ACES program recognizes data in comma-separated value (.csv) files containing the datenumber, room temperature.... data, in this **specific** order. The variable datenumber refers to the number Microsoft Excel (and Visual Basic) assigns to a date and time. Within the program calculations, the ACES program uses the data in the future. Once the time in the program has passed the time in the current line of the data file, the next line of data is read and used in the calculations. An example data file is included in the program called "AmmMod-Room128-ELW-0703.csv".

By clicking "Apply" on the Environmental Factors form, the main page will reappear.

Click on the command button labelled "Nutritional Factors" and the Nutritional Factors Form (fig. B.7) will appear. On this page, the user selects whether to enter the urine data manually, or the user can use the MESPRO program, developed by Aarnink et al. (1992) to determine the initial urea concentration.



**Nutritional Factors**

Please select whether you want to input the nutritional factors manually or use MESPRO (Aarnink and Elzing, 1998) to calculate the nutritional factors based on the diet. The slurry factors must be input.

☒ Manual

Urine Volume: 2.5 kg d<sup>-1</sup>

Initial Urea Concentration: 0.46 mol l<sup>-1</sup>

Average Pig Weight: 56.6 kg

Slurry TAN: 0.300 mol l<sup>-1</sup>

Slurry pH: 7

☐ MESPRO

Animal Weight: 56.6 kg

Water Intake: 6.6 kg d<sup>-1</sup>

Feed Intake: 2.184 kg d<sup>-1</sup>

Nitrogen Retention: 30 % of N Intake

Average Temperature: 24.45 °C

Crude Protein: 20.7 %

Digestible Energy: 3.48 Mcal kg<sup>-1</sup> feed

Nitrogen Intake: 0.0724 kg d<sup>-1</sup>

Ash Intake: 4.196 %

Crude Fat Intake: 1.4 %

Apply

**Figure B.7. Nutritional Factors input form.**

If "Manual" or "MESPRO" was selected, enter the required information in the measurement units displayed. The user must enter the slurry properties in either case.

By clicking "Apply", if "MESPRO" was selected, a sub-model will perform the necessary calculations to determine the urine volume and initial urea concentration; in either case the main page will reappear.

Click on the command button labelled "Simulation Factors" and the Simulations Factors Form (fig. B.8) will appear.

**Simulation Factors**

Please enter the values for variables related to the simulation interval and enter the ".csv" filename where you would like the simulations saved.

NOTE: If you have chosen to use dynamic temperature, ventilation and humidity data, the simulations will start at the first date and time in the file or at the specified start time, whichever occurs last. Ensure the data file contains data past until at least the stop time. The maximum recommended simulation period is one week.

Start Time  
 Date: September 21, 2001  
 Time: 0 hr

Stop Time  
 Date: September 24, 2001  
 Time: 0 hr

Iteration Interval: 15 min

Save to File: C:\Documents and Settings\Erin Cortus\My Documents\Current Work Projects\ACES Model Preliminary Testing\test 3.csv

Do you want to save the puddle data? ☐ (Puddle data will be saved on the C-drive, labelled with the current date and time in number format)

Initial Conditions  
 Room Concentration: 0 ppm  
 Pit Concentration: 0 ppm

Pen Cleanliness - % Covered in wet manure (0 - Clean to 100 - Completely Covered)  
 Slatted Floor: 20  
 Solid: 20  
 Number of Dirty Pens: 6

Apply

**Figure B.8. Simulation Factors input form.**

The user must enter the start date and time and stop date and time in the units shown. The iteration interval chosen will dictate the frequency that the output variables will be calculated. The iteration interval must be between 3 min and 1 h, and should evenly divide into 1 h.

The initial conditions for room and pit concentration can be added in units of ppm (if known).

Pen cleanliness of both the slatted and solid floor areas can be assessed a cleanliness score from 0 to 100, with 0 being very clean, and 100 being completely covered in wet manure. Values between 0 and 100 are interpreted as the percentage of floor area that is used for fouling behaviour. The ACES program will override a pen cleanliness score for the slatted floor less than 25, and set the value at 25. This is for situations where animals are moved into a freshly washed room. The ACES program assumes that the animals will dung over at least 25% of the slatted floor space. A score of 0 is possible for the solid floor.

By clicking on "..." the user is instructed to create a file where the output data will be saved. The file will automatically be saved as a .csv file.

The user can also choose to save the urine puddle data for the solid and slatted floor areas. By clicking the check box beside "Do you want to save the puddle data?", two files will be created on the C:Drive labelled with the floor area and current date and time in number format.

By clicking "Apply" on the Simulation Factors form, the main page will reappear.

Once back at the main page, click "Start Simulations" to start the calculation process. The progress bar will alert you when the calculations have stopped. Refer to figure B.2 to understand what calculation processes have occurred. See the section "Viewing the results" to see the results in the various forms and files available.

### ***Viewing the results***

If you would like to see a graphical representation of the concentration data and/or the emission simulations, click "Concentration Simulations" or "Emission Simulations" and figures B.9 and B.10 will appear, respectively.

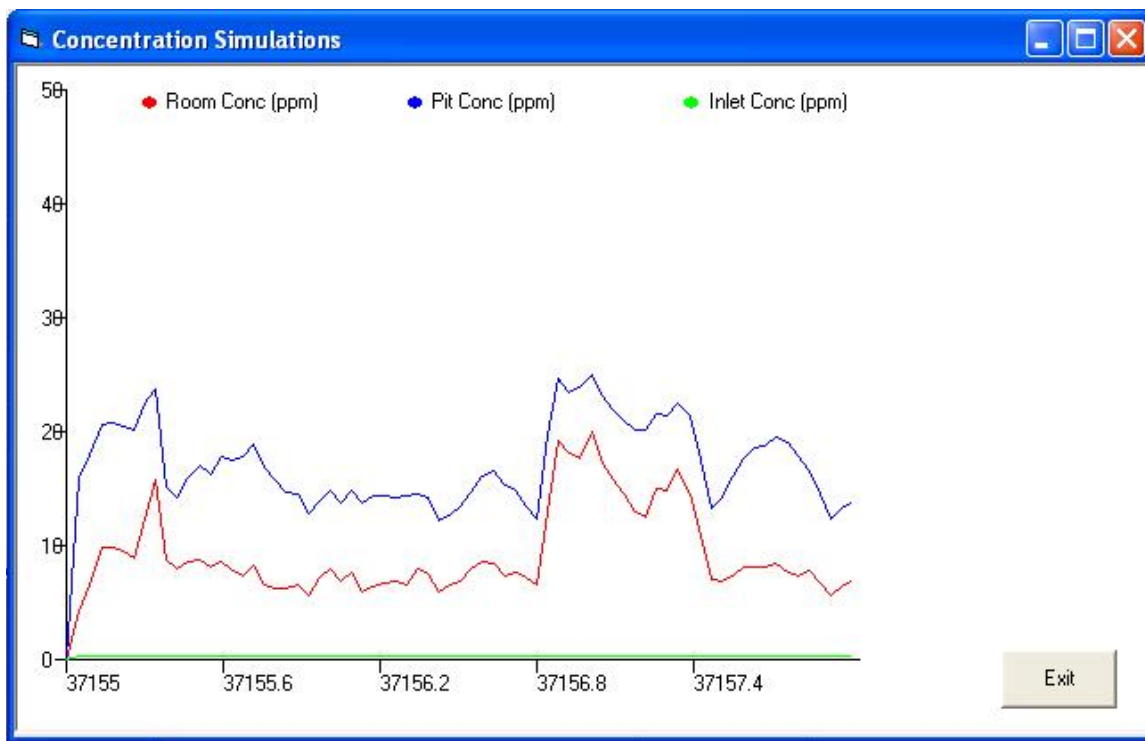


**Figure B.9. Concentration Simulations output form.**

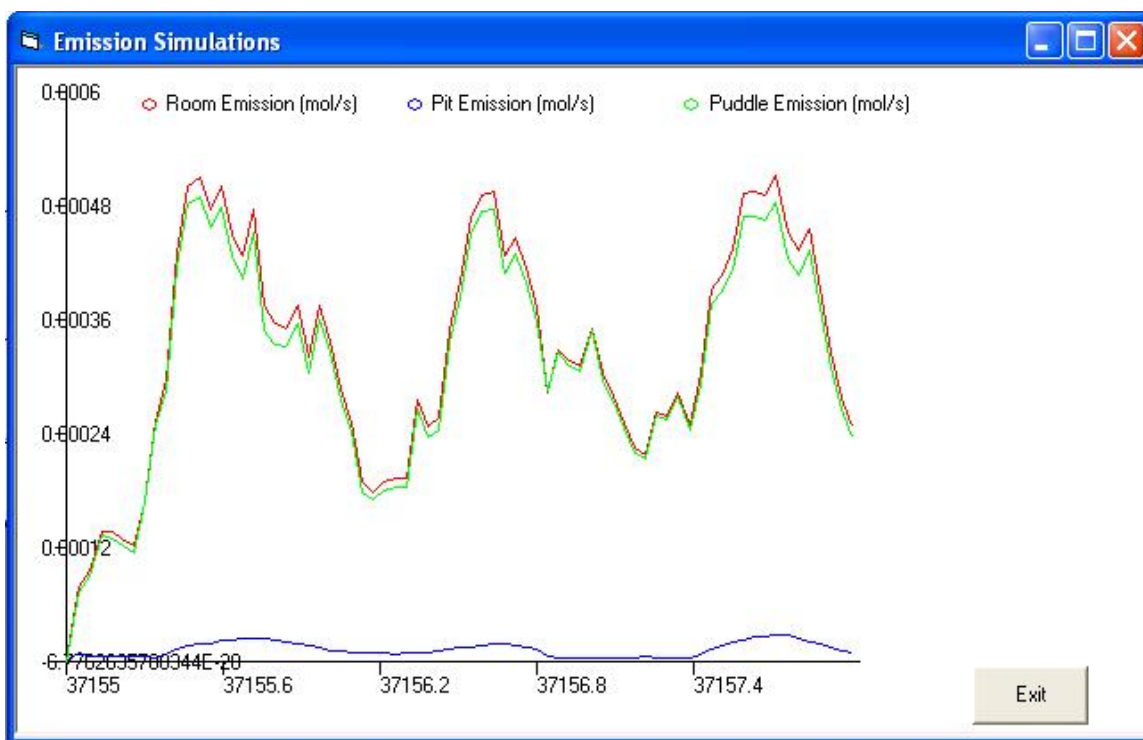


**Figure B.10. Emission Simulation output form.**

The axes on the concentration and emission graph are currently fixed. If a simulated value is greater than the axis allows the calculated value will not be visible.

Click "Exit" on either output form to return to the main page. The program can be closed by clicking "Exit" on the main page. If the user wants to run another simulation or change certain parameters, the program must be restarted.

The concentration and emission data from every simulation is also saved in a comma-separated data file specified by the user in the simulation factors input section. To view the file in MSExcel, simply open the saved file from within MSExcel. Provisions have been made within the ACES program so that when opened in MSExcel, the data will be separated in the appropriate columns.

If the user chose to save the puddle data, the user can locate these .csv files on the C:drive. Again, provisions have been made within the ACES program so that when opened in MSExcel, the data will be separated in the appropriate columns. However, the puddle data files can be sorted for easier interpretation. The suggested method for sorting the data is to select all columns with data, and using the Sort function of MSExcel, sort the rows by "Location" and then "Date and Time" columns. When sorted this way, the user can see what has occurred in every puddle location over the simulation period.

## Problems Associated with the ACES Program

As with the development of any new program, certain "bugs" are inevitable. The user is encouraged to keep track of errors that occur when running the program, and conditions that were input to the model if possible, so that the problems can be addressed in future versions.

The following "bugs" have been noted thus far, and the user is encouraged to keep these in mind when using the program.

- All input forms must be opened, in no particular order. It is not necessary, however, for the user to change all input variables from the default value if a change is not warranted.
- The user must select a ventilation/design layout by clicking the "Select" button on the Geometrical Factors form.
- The user must enter a new file name when creating a file to save the data each time the program is running.
- On the Concentration Simulation and Emission Simulation Output forms, the date and time along the x-axis is described in number format (number of days since Dec 31, 1899).

Please note that there are some "random" number generators incorporated in the ACES program to add variability in the number of urinations and the location of urinations calculations. Therefore, it is likely that two simulations using the same input variables may result in slightly different end results.

## References

- Aarnink, A.J.A., E.N.J. van Ouwerkerk and M.W.A. Verstegen. 1992. A mathematical model for estimating the amount and composition of slurry from fattening pigs. *Livestock Production Science* 31: 133-147.
- Ogilvie, J.R., E.M. Barber, and J.M. Randall. 1990. Floor air speeds and inlet design in swine ventilation systems. *Transactions in Agriculture*. 33(1): 255-9.